FHWA/NJ 89-006-7702

NEW JERSEY EXPERIMENTAL PAVEMENT PROJECT

ROUTE I-80 & I-95

A FINAL REPORT
JULY 1988

BY
ROBERT F. BAKER
PRINCIPAL ENGINEER, RESEARCH
AND
JOHN J. QUINN
PROJECT ENGINEER, RESEARCH

Prepared By:

New Jersey Department of Transportation
Division of Research and Demonstration
Bureau of Transportation Structures Research
In Cooperation With the
U.S. Department of Transportation
Federal Highway Administration

NJ
TE
212
B3
1988
C.1

NOTICE

This publication is disseminated in the interest of information exchange. The opinions, findings and conclusions expressed in the publication are those of the author and not necessarily those of the New Jersey Department of Transportation or the Federal Highway Administration.

This report does not constitute a standard, specification or regulation.

NJ
TE
212
B3
1988
c.1

Technical Report Documentation Page

1. Report No.	2. Government Accession No.	3. Recipient's Catalog No.
FHWA/NJ 89-006		

4. Title and Subtitle	5. Report Date
New Jersey Experimental Pavement Project Route I-80 and I-95	July, 1988
	6. Performing Organization Code
7. Author(s) Robert F. Baker and John J. Quinn	8. Performing Organization Report No. 89-006-7702
9. Performing Organization Name and Address New Jersey Department of Transportation Division of Research and Demonstration 1035 Parkway Avenue Trenton, NJ 08625	10. Work Unit No. (TRAIS)
	11. Contract or Grant No.
12. Sponsoring Agency Name and Address U.S Department of Transportation Federal Highway Administration 25 Scotch Road Trenton, NJ 08628	13. Type of Report and Period Covered Final Report
	14. Sponsoring Agency Code

15. Supplementary Notes

16. Abstract

See attached.

17. Key Words	18. Distribution Statement
Pavement Design, Elastic layer theory	Anyone interested.

19. Security Classif. (of this report)	20. Security Classif. (of this page)	21. No. of Pages	22. Price
Unclassified	Unclassified		

Form DOT F 1700.7 (8-72) Reproduction of completed page authorized

Abstract

This report documents the twenty-year performance of an AASHO satellite experimental pavement project which consisted of nine test sections of various base course materials and two surface courses.

The objectives in undertaking the experimental pavement project were:

1) to determine the relative performance of various types of New Jersey base course materials,
2) to compare the relative performance of these base courses to the material used in the AASHO road test,
3) to determine the performance of a composite pavement,
4) to determine the performance of a medium aggregate to fine aggregate surface course, and
5) to derive a structural layer coefficient for each type of base course.

A secondary emphasis of the study was to model pavement behavior by a state-of-the-art mechanistic computer program. The specific computer model was the VESYS IIIA computer program which was developed by the Federal Highway Administration.

Since construction of the nine test sections in 1964, annual monitoring data has included Benkelman beam deflections, rut depths, roughness data, cracking surveys and traffic data. Using this annual data, historical trends shows relationships with the calculated equivalent 18 kip loads. Based on a PSI failure of 2.5, the terminal 18 kip loads are determined for each test section to calculate AASHO structural layer coefficients for each base course material.

The limited number of non-replicated test sections and the relatively short length of the test sections adversely affected the data analysis. Also, inherent errors in the roughness data adversely affected the terminal PSI. Due to the change in mix design (Marshall Tests), a change to AC-20 asphalt cement, and the discontinued use of some materials, the results of the study have a limited application to present pavement design.

However, the cement treated base and the bituminous stabilized base show the greatest number of 18 kip loads to failure (PSI = 2.5) and the best overall performance.

Due to the absences of laboratory modulus of elasticity data for all materials, the mechanistic analysis was unable to develop accurate predictions for rutting, cracking and PSI.

Implementation Statement

The experimental pavement information developed during the course of this study has provided the New Jersey Department of Transportation with documentation of the relative performance of five different base courses and two different surface course mixtures. Although this study does not provide specific implementable designs or materials improvements, it does confirm and demonstrate that the bituminous stabilized base and cement treated base (similar to lime fly ash concrete) are suitable base courses for high volume pavements. It also demonstrates that unbound bases, such as densely graded stone, asphalt penetration macadam and drybound macadam are not suitable for high volume pavements.

The experimental pavement computer modeling provided initial experience with the VESYS IIIA computer program. Undoubtedly, the VESYS IIIA computer program is a valuable research tool for analysis of pavement sections.

PREFACE

The real value of the experimental pavement project is the 20 years of practical experience with pavement performance and the five years experience and countless hours of research and reading of hundreds of reports on the subject of the elastic layer theory and the mechanistic design procedure. Although practical experience cannot be measured in dollar amounts, the specific knowledge related to rutting and cracking add a great amount of knowledge that is required for pavement design. The practical experience with the VESYS IIIA computer program and mechanistic design system will save many hours of investigation into concepts and mechanisms of the system.

The experimental pavement research provides a foundation for future research into rut resistant pavements, cracking and the mechanistic design procedures, which will probably be adopted eventually by the AASHTO pavement design committee. New Jersey's initial experience with the mechanistic design procedures began with the experimental pavement project.

TABLE OF CONTENTS

		PAGE
	Abstract	iii
	Implementation Statement	vi
	Preface	vii
	Table of Contents	viii
	Figures	x
	Tables	
	Summary and Conclusions	1
	Analysis Based on the Relative Performance Data	1
	Analysis Based on the Mechanistic Procedures of the VESYS IIIA Computer Program	9
	Recommendations	10
1.0	Introduction	12
	1.1 Research Objectives	12
	1.2 Background	12
	1.3 Design of Experiment	14
	1.4 Analysis Approach	14
2.0	Performance Analysis	19
	2.1 Introduction	19
	2.2 AASHO Serviceability Concept	19
	2.2 Performance Data	21
	2.3.1 Roughness	21

2.3.1.1 Data 22
2.3.1.2 Discussion 26
2.3.2 Rutting 29
2.3.2.1 Data 29
2.3.2.2 Discussion 32
2.3.3 Cracking 35
2.3.3.1 Data 36
2.4 PSI-Pavement Failure 39
2.5 Traffic Data 46
2.6 Deflection Analysis 50
2.6.1. Deflection Data 51
2.6.2 Deflection Basin Data 53
2.7 Structural Layer Coefficients 60
2.7.1 Research Studies 60
2.7.2 Analysis of Structural Layer Coefficients 60
2.7.3 Discussion 68
3.0 Elastic Layer Analysis 70
3.1 Introduction 71
3.2 VESYS III Computer Program 75
3.2.1 Introduction 75
3.2.2 Verification and Sensitivity Analysis of VESYS 77
3.2.3 Input Variables 81
3.2.3.1 Tire Pressure and Contact Area 81
3.2.3.2. Material Characterizations 83
3.2.3.3. Poisson's Ratio 83
3.2.3.4. Permanent Deformation Characteristics 88
3.2.3.5. Fatigue 88
3.2.3.6. Pavement Temperature 91
3.2.3.7. Traffic Analysis 93
3.2.4 Predicted Response 93
3.2.4.1. Rutting 95
3.2.4.2. Roughness 95
3.2.4.3. Fatigue Cracking 95
3.2.4.4. Deflections 95
3.2.4.5. Performance 97
REFERENCES 98

FIGURES

		PAGE
1.1	Location Map	15
1.2	Test Section Design	16
2.1	Relationship Between NJ Roughometer and the Percent Defective Length	24
2.2	Relationship Between BPR Roughometer and NJ Roughometer	25
2.3	Statistical Test of Variability	28
2.4	Rut Depth Measurement Procedure	30
2.5	Bar Chart of 1984 Mean Rut Depth Data	34
2.6	Crack Survey	40
2.7	Rebound Basin Procedure	52
2.8	Mean Rebound Data	54
2.9	Utah Rebound Basic Criteria	56
2.10	Rebound Basins	57
2.11	Graph of AASHO Road Test Performance Equation	63
3.1	Multilayered Elastic System	72
3.2	Stress Directions	73
3.3	Modulus of Resilience Data	85
3.4	Asphalt Concrete Pavement Deformation Characteristics	89
3.5	Permanent Deformation Characteristics of Granular Materials	90
3.6	Temperature Relationships	94

TABLES

		PAGE
1.1	Experimental Design	17
2.1	Severity Levels of Rutting	31
2.2	Equivalent 18,000 Pound Loads to 1/2 Inch Rutting Criteria	33
2.3	Cracking	37
2.4	PSI-Pavement Failure	45
2.5	1984 Average Annual Daily Traffic	47
2.6	Accumulated Equivalent 18 Kip Pount Loadings	48
2.7	Thickness Eqivalency Values	61
2.8	Penn State Structural Layer Coefficients	61
2.9	NDJOT Structural Layer Coefficients	65
2.10	Base Course Structural Coefficients	66
3.1	Modulus of Resilience Values	84
3.2	Base Course Modulus of Reslience Values	86
3.3	Poissons Ratio	87
3.4	Temperature Data	92
3.5	VESYS Predicted Deflection	96

APPENDICES PAGE

A. Material Gradations 101
B. Roughness Data, Figure B1 through B16 104
C. Rut Depth Data, Figures C1 through C16 120
D. PSI vs. Traffic, Figures D1 through D16 136
E. Deflection Histories, Figures E1 through E8 152
F. VESYS III A Rut Depth Predictions, Figures F1 through F9 168

Summary and Conclusions

The Experimental Pavement Project was initiated as an AASHO Road Test follow-up study. The intent of the project was to compare the relative performance of six base course materials (drybound macadam, bituminous stabilized base-gravel and stone mix, asphalt penetration macadam, densely graded stone, and cement treated base) and to determine AASHO structural coefficients for these materials. Since construction of the nine test sections in 1964, annual monitoring data has included Benkelman beam deflections, rut depths, roughness data, cracking surveys and traffic data. The study was modified in 1983 to include an analysis of the test sections with the mechanistic analysis of the elastic layer theory and the VESYS predictive computer program.

Analysis Based on Relative Performance Data

The relative roughness, rutting and cracking data were analyzed with the equivalent 18 kip load traffic data to compare the relative historical trends of the base course in each test section. In the first six test sections, a comparison can be made between different base course materials of the same thickness with similar subbase, top course materials and thicknesses. Also, a comparison is made between a six-inch thick and a four-inch thick bituminous stabilized base course with the same subbase, top course materials and thicknesses. In the last three test sections, a cement treated base course is compared to the then standard design section and a fine aggregate surface course is compared to a medium aggregate surface course.

Roughness

Using standard linear regression techniques, the roughness data were analyzed with the 18 kip load data to show historical trends. The accuracy

of this analysis was adversely affect by the large scatter of data point. However, the regression analysis showed that the bituminous stabilized base (Test Section 2E & 2W) and cement treated base (Test Section 7E & 7W) have the least roughness after 9 million 18 kip loads. The MA-BC and FA-BC-Bituminous Stabilized base, drybound macadam base courses (Test Section 8 & 9) have the greatest roughness after 9 million 18 kip loads.

The problems with the roughness data are related to the poor initial roughness and the large scatter of subsequent data. The initial roughness from all test sections were rated fair to poor by the then current Bureau of Public Roads criteria and were relatively high (rough) compared to later measurements. This large variation in data is attributed to:

1. Five different roughness measurement devices which were used for data collection.
2. The extrapolation of measured roughness from the short test sections (500 feet) to inches per mile units of the roughness data,
3. The construction of New Jersey bituminous pavements which in general, were characterized in 1963-64 by an average 10 to 60 percent greater roughness than similar pavements surveyed in other Northeastern states.

Rutting

Using the standard regression techniques, the rutting was analyzed with the 18 kip loads to show historical trends. Applying the FHWA criteria for medium severity rutting (1/2 inch to 1 inch) to the regression as an indicator, the 18 kip loads required for a section to rut significantly was determined. The 1/2 inch criteria was achieved by the stabilized base courses before the drybound macadam, asphalt penetration

macadam, densely graded stone and cement treated base. In essence, the bituminous stabilized base ruts to the 1/2 inch criteria with fewer 18 kip loads.

The first contributing factor to the severe rutting on the bituminous base course is that in 1963-64, the NJDOT did not have Marshall stability or voids requirements for top course, and binder course materials. Essentially, the bituminous mixes were made by the contractor according to NJDOT specifications and gradations without the benefit of Marshall test for quality acceptance. The second contributing factor is that the then used 85-100 penetration grade asphalt cement was softer than the current AC-20 grade asphalt cement. Indeed, the soft asphalt cement is a major contributor to bituminous pavement rutting. In addition, the rounded gravel in the bituminous stabilized base was a major cause of rutting in that test section.

Cracking

Detailed annual crack surveys were made on the experimental pavement test sections. In 1973 non-connecting and connecting (fatigue type) cracks began to appear in the outside lane of the asphalt penetration macadam and the densely graded stone base courses. The cracking was attributed to heavy truck traffic in that lane. Earlier cracking had occurred in the above sections in the inside lane where no heavy truck traffic is experienced. The inside lane cracking was attributed to moisture in the subbase and an age hardening of the bituminous top course.

Generally, the most severe cracking occurred on the base courses with the highest Benkelman beam deflections, i.e., drybound macadam, asphalt penetration macadam, and densely graded stone. The least percentage of cracking occurred on the bituminous stabilized base course where

deflections were low and the 85-100 penetration asphalt cement permitted the cracks to close during the summer months. The cement treated base course has a few fine transverse cracks which are considered to be insignificant.

Present Serviceability

The performance of the experimental pavement test sections was expressed in terms of the AASHO present serviceability index. The PSI for each test section was obtained from measurements of roughness, cracking, and rutting. In estimating the PSI and terminal serviceability (2.5), roughness is the dominate factor. Being highly dependent on the roughness, the estimate of the PSI is extremely variable. As such, its value for determination of accurate performance for these test sections is questionable. Indeed, in recent years, the AASHO present serviceability index equation's applicability to NJDOT pavement conditions has been questioned.

As in the AASHO Road Test, the PSI values were analyzed with the equivalent 18 kip axle load traffic data to compare the relative historical trends of the base courses in each test section. Since this is highly dependent on the roughness, any conclusion of the relative PSI between base courses is largely judgment. However, the cement treated base course shows the greatest number of 18 kip loads to failure (PSI = 2.5) with a small percentage of cracking, low rutting and low deflections. The bituminous stabilized base stone mix shows the next greatest number of 18 kip loads to failure (PSI = 2.5) with little or no cracking, low deflections but high rutting. The drybound macadam, asphalt penetration macadam and densely graded stone base show the lowest 18 kip loads to failure (PSI = 2.5) with significant cracking, less severe rutting and high deflections.

Comparisons of Relative Magnitude

An overall comparison of the relative magnitude of the base course materials ranking is shown in Table A. This table summarizes the "best" to "worst" base courses as represented by the roughness, rutting and cracking after 20 years of service. The comparison is based on Roughness (Figures B1-B16), Mean Rut Depth (Figure 2.5) and Crack Survey (Figure 2.6).

Since the past and present costs of the base courses are not available, this simplistic ranking of the relative magnitude does not imply that the ""worst" ranked base course should not be used in a pavement. The difference in costs may justify the use of one type of material over another in certain traffic conditions. For example, the use of a densely graded stone is justified by the low cost on a low-volume road where it would provide adequate service life. However, a bituminous stabilized base which has higher costs than the densely graded stone, may be more than adequate (over designed) for the same location.

In Table A, the cement-treated base performs "best" in areas of relative roughness and second "best" in the area of rutting. In the area of cracking, it is ranked fourth. However, this ranking is not significant because the cracks are fine cracks which do not adversely affect the pavement service. The cement-treated base provides the "best" overall performance ranking. The bituminous stabilized base performs "best" in the area of relative cracking and second "best" in the area of relative roughness.

With the bituminous stabilized base, these advantages are trade-offs for the decrease in the rut resistance where the moldability or deformation characteristics of the material can be seen from the data. The FA-BC/drybound macadam base performed "best" in the area of rutting.

Table A

COMPARISON OF RELATIVE PERFORMANCE

Combined Eastbound & Westbound

Ranking	Roughness	Rutting	Cracking
1. (Best)	Cement Treated Base (Test Section 7E & 7W)	FA-BC/Bit. Stab. Base/Drybound Macadam (Test Section 9W)	Bituminous Stab. Base (Test Section 2E & 2W)
2.	Bituminous Stab. Base 6" (Test Sections 2E & 2W)	Cement Treated Base (Test Section 7E & 7W)	MA-BC/Bit. Stab. Base Drybound Macadam (Test Section 8)
3.	Bituminous Stab. Base 4" (Test Section 3E & 3W)	MA-BC/Bit. Stab. Base/Drybound Macadam (Test Section 8)	Bituminous Stab. Base (Test Section 3E & 3W)
4.	Drybound Macadam (Test Section 1E & 1W)	Drybound Macadam (Test Sections 1E & 1W)	Cement Treated Base (Test Section 7E & 7W)
5.	Densely Graded Stone (Test Section 6E & 6W)	Densely Graded Stone (Test Sections 6E & 6W)	FA-BC/Bit. Stab. Base Dry-bound Macadam (Test Section 9W)
6.	Asphalt Penetration Macadam (Test Sections 5E & 5W)	Asphalt Penetration Macadam (Test Sections 5E & 5W)	Bituminous Stab. Base-Gravel (Test Sections 4E & 4W)
7.	Bituminous Stab. Base (Gravel) (Test Sections 4E & 4W)	Bituminous Stab. Base 4" (Test Sections 3E & 3W	Asphalt Penetration macadam (Test Sections 5E 7 5W)
8.	MA-BC/Bit. Stab. Base/Drybound Macadam (Test Section 8)	Bituminous Stab. Base 6" (Test Sections 2E & 2W)	Densely graded stone (Test Sections 6E & 6W)
9.(Worst)	FA-BC/Bit. Stab. Base/Drybound Macadam (Test Section 9W)	Bituminous Stab. Base 4" (Test Section 3E & 3W)	Drybound macadam (Test Section 1E & 1W)

However, the MA-BC/drybound macadam base performed third "best" in the area of rutting. The relationship of rutting between the FA-BC and MA-BC surface is contrary to the expectations which were that the MA-BC would provide better rut resistance. Essentially, the average rut depth difference between the FA-BC (0.51 inches) and MA-BC (0.57 inches) is small, i.e. 0.06 inches. The difference could be the result of the small sample size, i.e. one test section of each top course, and it is probably the result of an interpretation of the measurement error.

As a general rule, the drybound macadam, densely graded stone and the asphalt penetration macadam perform better in the area of rutting than the bituminous stabilized base, but worse in the areas of roughness and cracking than the bituminous stabilized base. This is due to the greater resilience of the unbound material. However, a greater flexibility (resilience) yields fatigue cracking.

Structural Layer Coefficients

The structural coefficients for the base course materials were calculated with the AASHO Road Test equation and the PSI data from the experimental pavement test sections. The highly variable roughness data and resulting PSI values reduce the significance of the calculated coefficients. Confidence in the coefficients as a function of materials type and properties is very low. Indeed, no justification can be presented to utilize these coefficients in place of the currently used coefficients in New Jersey pavement design.

The following base course structural coefficients were calculated in this study:

Base Course	Direction		Currently-Used Design Structural Coefficient
	Eastbound	Westbound	
Drybound Macadam	.28	.37	.20
Bituminous Stabilized Base (6")	.38	.37	.44
Bituminous Stabilized Base (4")	.50	.48	.44
Bit. Stab. Base (Gravel Mix)	.23	.34	.34
Asphalt Penetration Macadam	.30	.30	.30
Densely Graded Stone	.32	.20	.14
Cement Treated Base	.23	.15	.30

Other research studies as well as the AASHO Road Test have shown that the structural layer coefficients vary with respect to layer thickness and the material location in the pavement system. The coefficients are not constant based on the material type but were average values adopted by the AASHO Interim Guide to facilitate pavement design.

In addition to the roughness problems, which are discussed above, and the constraints which are discussed in the above paragraph, the comparison of the experimental pavement data to the AASHO Road Test empirical equations is restricted by the single foundation soil of the AASHO test pavements, the short duration of the tests, inadequate thickness of many AASHO pavements, and traffic application at the Road Test which did not reflect normal traffic patterns. Furthermore, the climactic conditions of the AASHO tests differ significantly from that of the NJDOT experimental test sections.

Analysis Based on Mechanistic Procedures of VESYS IIIA Computer Program

In an attempt to correct the deficiencies of the AASHO analysis of the NJDOT experimental pavement, the mechanistic procedures of the VESYS IIIA computer program were adopted to model the experimental pavement for the development of terminal serviceability of the base course materials. The VESYS IIIA computer program is based on the mechanistic structural subsystem which operates by evaluating a given pavement design for its elastic layer response to expected loading and environmental conditions. Using various input data, the computer program predicts rutting, roughness, cracking, and PSI response.

The VESYS program uses thirty different pieces of input data which are inter-related. The program input is not simple plug-in type data. Input data for the experimental pavement modeling was obtained from laboratory tests and literature values which were suggested by the FHWA and Penn State University.

The computer predictions of rutting were compared to the measured data from each test section. Due to the questionable application of literature input data and modulus of elasticity material characterizations which used AC-20 asphalt cement instead of the 85-100 penetration grade asphalt cement of the test sections, the computer program over estimated the drybound macadam, asphalt penetration macadam and densely graded stone base course rut depth. The computer program underestimated the bituminous stabilized base rut depths. Additional research is necessary to identify typical tire contact areas, tire contact pressures, load durations, and permanent deformation properties of bituminous mixes for New Jersey materials and conditions. The time constraints of this project did not permit a thorough evaluation of these input variables.

The roughness prediction were not compared to the experimental pavement data due to the erroneous roughness data of the test sections.

The cracking predictions were not analyzed due to the inability to perform fatigue laboratory tests or to find an appropriate fatigue relationship for New Jersey bituminous mixes. Laboratory fatigue tests are essential for the evaluation of fatigue cracking.

The comparison of predicted fall deflections with the measured Benkelman beam deflections showed reasonable agreement. However, additional resilient modulus tests are required to characterize the bituminous mixes for various temperatures.

The VESYS IIIA computer program is a complex mechanistic predictive program which requires complex data input. Various research studies have shown that VESYS is a sensitive research tool for material and pavement analysis. Given sufficient time and laboratory input data, the program could become a valuable research tool for NJDOT pavement research.

RECOMMENDATIONS

1. The use of the current AASHO structural layer coefficients should be continued for the NJDOT pavement design. Since inaccurate roughness data prohibited a thorough analysis of the experimental pavement data with the AASHO Road Test equations, structural coefficients of the experimental pavement base course materials could not be made with sufficient confidence. In addition, current bituminous mixes differ significantly from those used in the experimental pavement and other base course materials such as drybound macadam, asphalt penetration macadam, and densely graded stone, are no longer used by the Department

2. The VESYS computer program should be thoroughly analyzed for its potential as a mechanistic pavement design research tool. With

accurate laboratory input data, the program can calculate stresses, strains, and deflections for a given multi-layer pavement design and predict rutting, roughness, cracking, and PSI pavement failure.

3. Although the severe rutting on the experimental test section can be attributed to the soft 85-100 penetration grade asphalt cement and the lack of a Marshall stability acceptance criteria in the top course, the rutting data suggests that rutting can be attributed to the bituminous stabilized base-gravel and stone mix. Since recent evidence suggests that rutting of bituminous mixes is serious throughout the state, the rutting characteristics of the current AC-20 grade asphalt cement bituminous should be investigated with the intent of improving the Marshall stability and permanent deformation characteristics.

4. The cement treated base course, (composite pavement section) was the overall best section of the experimental pavement. Although cement treated base is not commonly used in New Jersey, lime fly ash stabilized base course is used on a limited basis. The lime fly ash has similar characteristics to cement treated base. The use of composite pavements with lime fly ash should be evaluated for an alternate pavement type.

1.0 INTRODUCTION

1.1 Research Objectives

The principal objectives of this study were:

1. To determine the relative performance of the various types of base course materials used in New Jersey;
2. To compare the performance of the base course material used in the AASHO Road Test with that of the base course materials commonly used in New Jersey;
3. To assess the performance of a composite pavement (bituminous surface over a rigid base course) incorporating a cement-treated, crushed stone base course relative to that of a bituminous pavement constructed over a conventional stone base courses.
4. To derive an equivalent thickness factor for each type of base course as determined by its 20-year performance that will serve as an aid in future pavement design;
5. To determine the relative stability, performance and appearance of Medium Aggregate Bituminous Concrete (MABC) surfacing as compared with Fine Aggregate Bituminous Concrete (FABC) surfacing;

1.2 Background

The major stimulus for initiating the experimental pavement project was the findings of the 1958-1960 AASHO Road Test at Ottowa, Illinois.

The American Association of State Highway Officials (AASHO) Road Test was a scientitically-designed, factorial experiment that included hundreds of bituminous pavement test sections. The principal findings were

empirical relationships between pavement performance (as measured by trends in Present Serviceability Index), and pavement thickness, and traffic load applications.

The relationships developed at the Road Test, of course, reflected the specific physical environment of the project, to the particular materials used in the pavements, and to the range of thicknesses and number of load applications in the experiment. The AASHO Road Test relationships were used to develop the AASHTO "Interim Guide for Design of Pavement Structures", which presents the design method used to determine the required thickness of a pavement structure necessary to withstand a given number of axle load applications before the performance of the pavement reaches a terminal serviceability index. The Road Test researchers recognized that, in subsequent applications, the developed relationship -- structural layer coefficients -- should reflect the specific materials used.

In order to provide these necessary verifications of the structural coefficients for each state's specific conditions (materials, climate and traffic) and to develop performance relationships based on these coefficients, the researchers recommended the follow-up (satellite) experiments be constructed. This basic end -- tailoring the AASHO Road Test findings to New Jersey conditions was the impetus for undertaking the New Jersey Experimental Pavement Project.

1.3. Design of Experiment

The New Jersey experimental pavement was constructed between June and October 1964 on an urban section of Route I-80, Ridgefield Park and Route I-95, Fort Lee. The construction site is a rock cut with stable foundation and essentially uniform bearing capacity. The rock cut consists of interbedded shales and sandstone.

Eight experimental test sections were constructed in the eastbound and westbound local lanes of Route I-80 and one experimental test section in the eastbound local lanes of Route I-95. The location map is shown in Figure 1.1

The design cross sections of experimental test section design is shown in Figure 1.2. Material gradations are given in Appendix A.

The nine test sections were designed to compare the performance of New Jersey base course materials to the AASHO Road Test base course and to compare the performance of the composite pavement to the then conventional New Jersey bituminous pavement. To permit these comparisons to be made, identical subbases and top course thickness were used throughout the base course experiment. A tabulation of the specific comparisons made between test sections is presented in Table 1.1. In addition, two test sections compare the performance of the FABC surfacing with the MABC surfacing. Two similar test sections compare a 4 inch bituminous stabilized base to a 6 inch bitiminous stabilized base.

1.4 Analysis Approach

As originally conceived, the primary emphasis in this study was to be given to the substitution of data into the empirical equations of the AASHO Road Test Define equations. These equations are the basis for comparisons of test section performance and the determination of pavement structural

FIGURE I.1

LOCATION MAP OF ROUTE I-80 & I-95 EXPERIMENTAL PAVEMENT PROJECT

FIGURE 1.2

CROSS SECTIONS OF EXPERIMENTAL PAVEMENT TEST SECTIONS

Test Section 1

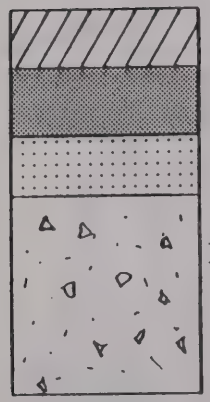

Test Section 2

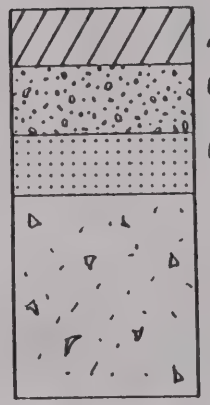

Test Section 3

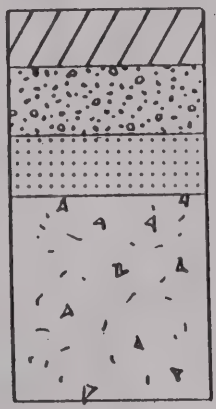

Test Section 4

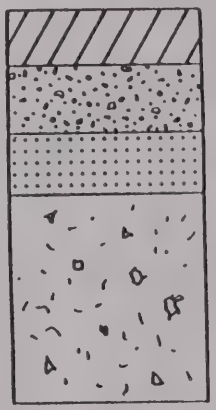

Test Section 5

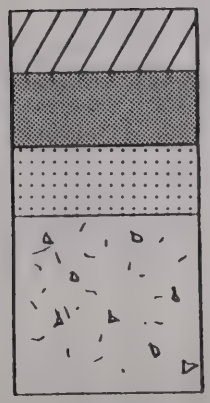

Test Section 6

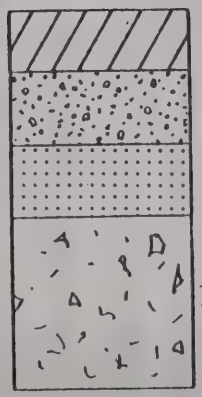

Test Section 7

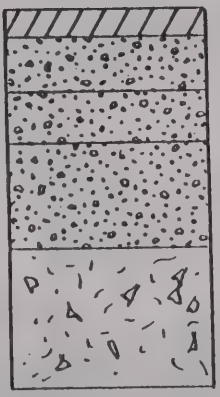

Test Sections 8 & 9

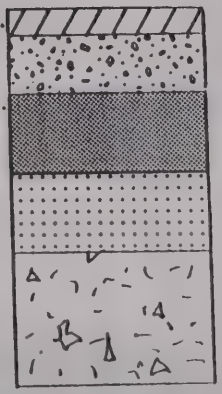

*Test Sections 8 & 9 are identical with the exception that Section 8 has an MABC top course and Section 9 has an FABC top course.

Table 1.1

Experimental Design

Comparison of Experimental Test Sections

Base Course Design	Thickness Design	Cement Treated Base Design	Surface Course Design
Comparison of Base Course Materials (all 6 inches thick)	Comparison of Bit. Base Course Thickness (4 and 6 inches thick)	Comparison of Cement Treated Base Design to 1962 Standard Pavement Section	Comparison of FABC surface to MABC surface
Test Section 1E & 1W Drybound Macadam	Test Sections 2E & 2W 6 inches Bituminous Stabilized Base Stone Mix.	Test Sections 7E & 7W Cement Treated Base Course Base Course	Test Section 9E & 9W FABC Surface
Test Sections 4E & 4W Bitumnous Stabilized Base - Gravel Mix	Test Sections 3E & 3W 4 inches Bituminous Stabilized Base Stone Mix	Test Section 9E & 9W Bit. Stab. Base, Drybound Mac. Quarry Processed.	Test Section 8E MABC Surface
Test Sections 5E & 5W Asphalt Penetration Macadam			
Test Sections 6E & 6W Densely Graded Stone			

numbers. For the most part, least squares regression techniques were used to determine the best fit curve for the data.

The choice of procedures for determining structural coefficients for NJDOT experimental pavements will be greately influenced by the character of the data. The project is a non-factorial study consisting of nine experimental test sections of different base course materials. As previously stated, the AASHO Road Test was constructed as a factorial experiment of 468 sections of mostly one type of base course material. That large number of data points permitted an extensive interdependent regression analysis of the SN equation and terminal traffic load applications. Given the small number of test sections in the NJDOT analysis, an AASHO Road Test regression is not practical.

Since the inception of this project in 1964, significant improvements in state-of-the-art structural pavement design procedures and computer technology advances have occurred which provide comprehensive computer programs for the analysis of pavement data. The procedures consist of a mechanistic theory to calculate stresses, strains, and deflections, and predictive models for fatigue cracking, rutting, and pavement serviceability. These modals will provide improved knowledge of the experimental design.

As a secondary emphasis in this study, the need to model pavement behavior by state-of-the-art computer programs was necessitated by an insufficient number of test sections. The mechanistic pavement model will be compared to the regression equations from the empirical procedure. The specific computer model is the VESYS (Viscoelastic System) IIIA computer program which was developed by the Federal Highway Administration.

2.0 PERFORMANCE ANALYSIS

2.1 Introduction

In this section, the performance analysis is discussed with the intent to develop a pavement failure criteria which is based on the Present Serviceability Index failure criteria of the AASHO Road Test. The main objective of the pavement analysis is to evaluate the base courses of the test sections using the AASHO Road Test performance relationships. The evaluation will compare the distress manifested by the experimental pavements (rutting, deflection, cracking and roughness) with the performance equations of the Road Test.

2.2 AASHO Serviceability Concept

One of the major accomplishments at the AASHO Road Test was the development of a working definition of pavement "performance" (Present Serviceability Concept) (PSI) and a pavement failure (terminal Serviceability Index. As developed at the Road Test, performance was defined as the trend of the pavements' ability to serve traffic. It was found at the Road Test that the serviceability of a pavement was primarily dependent on its roughness (longitudinal profile deformation), rut depths, and the extent of cracking and patching. Based on the Road Test correlation study, equations relating these variables to serviceability were developed and a numerical definition of pavement failure (i.e., Terminal Serviceability Index) was established to be 2.5 for heavy traffic highways

The PSI equation used to analyze the performance of the New Jersey experimental pavement is given by:

$$PSI = 11.29 - 4.11 \text{ Log } RI - 0.01\sqrt{(C+P)} - 1.23\ RD^2 \qquad \text{Equation \#1}$$

where:

RI = Roughness Index (BPR inches per mile)
RD = Mean rut depth (inches)
C+P = Cracking and patching per 1000 square feet.

The above equation will be used to define serviceability on the experimental pavements. The equation (Ref.2) is a generalized formula resulting from experience with eight BPR-type roughometers over a considerable number of test sections at the AASHO Road Test and Purdue University Test Sections.

The Road Test serviceability concept permits the determination of relationships between traffic loadings, pavement thickness, and type of materials (the latter is expressed in terms of a structural layer coefficient). The structural number (SN), which is a measure of a pavement's overall load carrying capability, is calculated by multiplying the thickness of each pavement layer by the structural layer coefficient for that layer and summing as:

$$SN = a_1d_1 + a_2d_2 + a_3d_3 \qquad \text{Equation \#2}$$

where:

SN = Structural Number

a_1, a_2, a_3, = Structural coefficient for each layer.

d_1, d_2, d_3, = thickness of each layer

The structural coefficients for each layer of material at the Road Test were determined empirically by using the different layer thicknesses as independent variables to predict the structural number. Simultaneous equations were used to solve for the structural numbers. The resulting regression equation coefficients were then considered representative of the materials. The regression equation developed different material structural coefficients for different thicknesses. This problem was solved by taking

the average of the coefficients for each group of experimental test sections at the Road Test.

In place of a regression analysis to determine structural coefficients in the NJDOT experimental pavement, two approaches can be used to reasonably estimate the coefficients. First, the estimated structural numbers and structural coefficients of the NJDOT experimental pavements can be substituted into the AASHO Road Test equations. The estimate is made by substituting the 18 kip loadings, PSI and cracking data into the AASHO equations. Then, the equations are solved for the structural coefficients. The result, although only one point for each test section, will show a relationship between the estimated structural coefficient (see Section 2.7) of the experimental pavement and the structural coefficient of the AASHO Road Test. (This approach is discussed in detail in Sections belows). Second, the test section's materials and performance can be modeled by the VESYS IIIA computer program. The estimate of the structural coefficients is made by inputting material properties into the program to estimate rutting, cracking, terminal PSI and traffic. These results are substituted into the AASHO equation, which is solved for structrual coefficents.

2.3 Performance Data

The basic assumptions in the behavior of the experimental pavement are that the pavement will withstand a number of load applications before it reaches a terminal serviceability, and that this failure can reasonably be defined by Equation #1. This equation uses three forms of distress to define failure:

2.3.1 Roughness

Roughness is defined as pavement surface irregularities which adversely effect the riding quality. Surface irregularities consist of

random waves across the pavement surface and may be related to the subbase, base and/or surface course. These irregularities can either be built into the pavement during construction or they can develop after construction due to traffic loading.

2.3.1.1 Data

The roughness data of the experimental pavement was effected by built-in surface irregularities which adversely effected the normal increase in roughness, various roughness devices, statistical errors with data correlations, and roughness variations across the pavement.

In 1963-64, New Jersey bituminous pavements were characterized by an average of 10 to 60 percent greater relative roughness than flexible pavements surveyed in three other northeastern states (Massachusetts, New Hampshire and Vermont). The experimental pavement data shows a high initial roughness which was a characteristic of pavement construction at that time. Essentially, if roughness begins high, the pavement has nearly reached the point of its maximum roughness. At this point, roughness will increase at a slower rate than at the lower roughness. In this discussion of PSI, it will be shown that this effects the PSI by decreasing the PSI at a slower rate.

The roughness data of the experimental pavement were obtained over 20 years with five different roughness devices:

1. Bureau of Public Roads Roughometer (1964, 1965, 1967 and 1972);
2. The New York-New Jersey Port Authority BPR Type Roughometer, (1966);
3. New Jersey Roughometer (1968 through 1971);

4. First New Jersey rolling straightedge (1973);

5. Second New Jersey rolling straightedge 1974-1984

All data were taken in the outside lane in both wheelpaths. The data are shown in Appendix B in figures B1 through B16.

The rolling straightedge data expressed as the summary statistic, (Percent Deflective Length, L_D) were converted to New Jersey roughness units (inches per mile) using a correlation which was developed by Croteau (Ref.3). All data in New Jersey roughness units were then converted to BPR roughness units using another correlation presented in Reference 3. These relationships are shown in Figures 2.1 and 2.2.

In any correlation of data, inherent error in each data point and error in lack of fit exists in the estimation of the regression line between the two variables. In the case of the step wise process described above, i.e. estimating the N.J. roughness units from rolling straightedge data and then estimating the BPR roughness from N.J. roughness units, the error is cumulative. This error is added to the error associated with the individual measurements that are extrapolated from the 500 test sections to the inches-per-mile data of N.J. roughness data and the percent defective length measurements of the rolling straightedge data. Indeed, the roughness measurements on the 500 foot section must be multiplied by ten to obtain inches per mile.

It is recognized that errors are introduced in each step of that stage transformation and that inherent errors exist in each data point. Since the precision is not quantifiable for that reason, the data must be used with extreme caution.

FIGURE 2.1

Relationship Between New Jersey Roughometer Readings And The Percent Defective Length

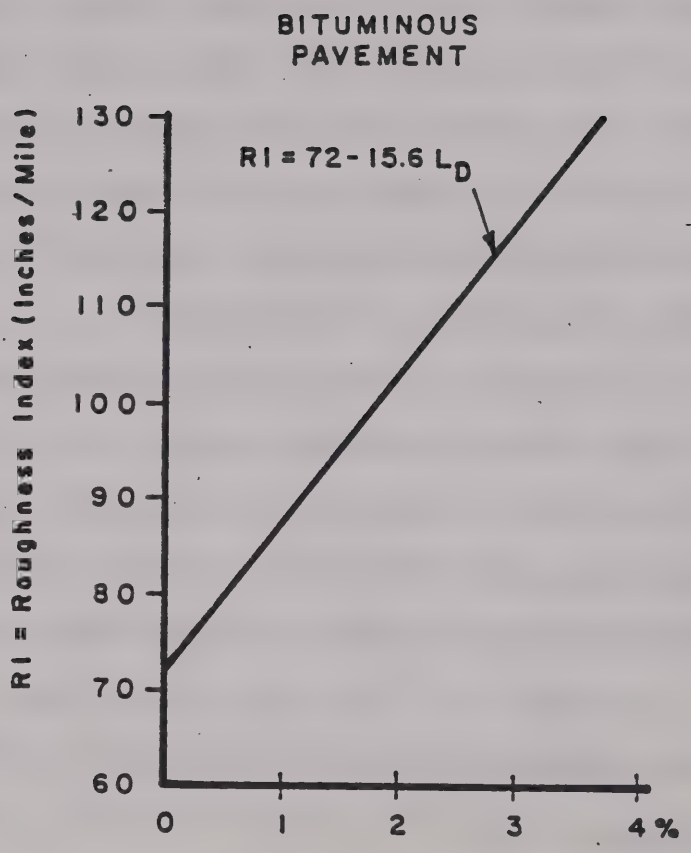

L_D = Percent Defective Length

FIGURE 2.2

Relationship Between Bureau Of Public Road Rough — ometer And New Jersey Roughometer

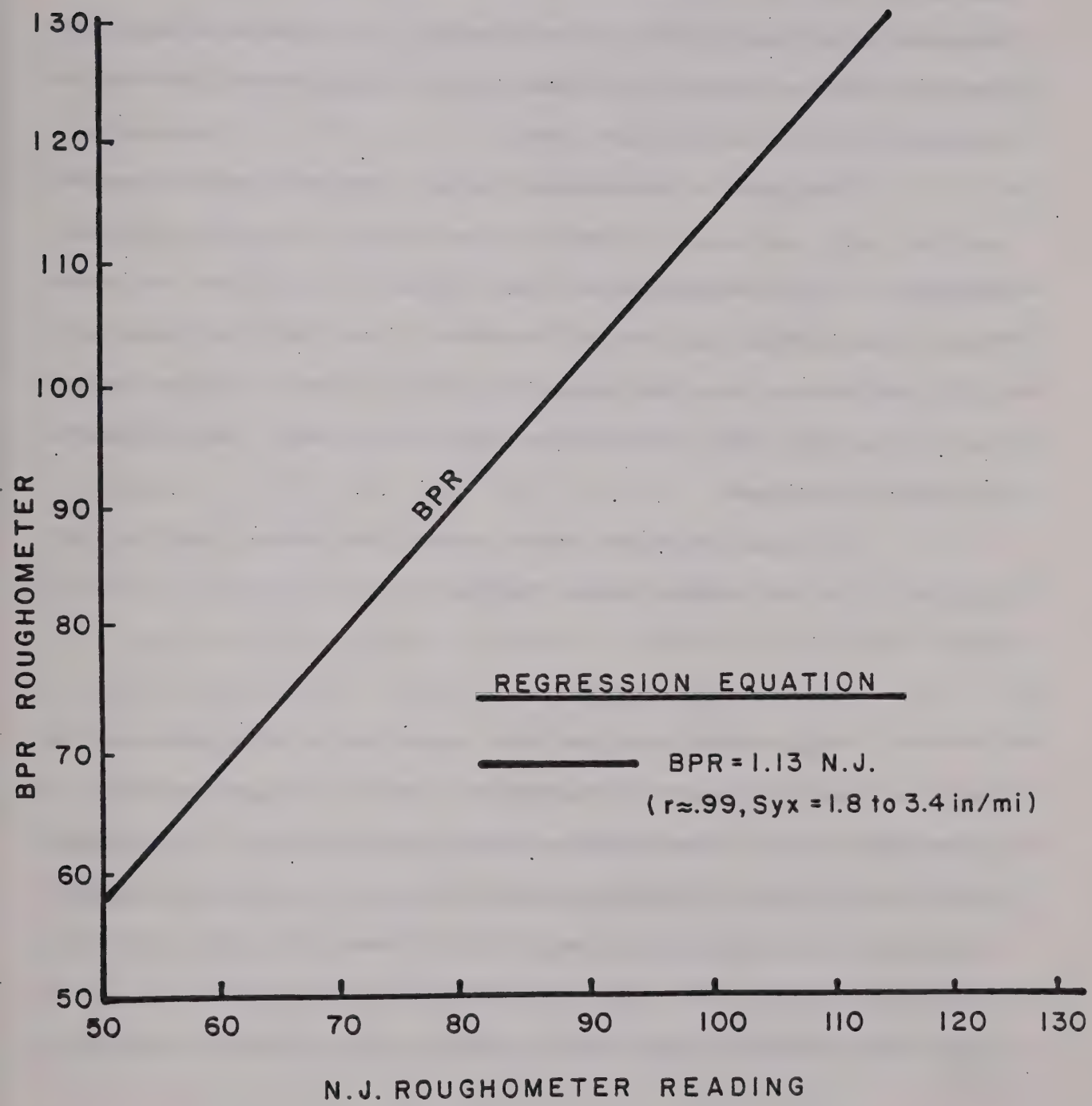

In figure B1 through B16 in Appendix B, all initial roughness measurements were high relative to other measurements and were rated fair (82-102) or poor (above 102) by 1967 Bureau of Public Roads criteria which was based on their experience with their roughometer. The initially high roughness measurements were attributed to the extrapolation of data from the short sections (500 feet) to inches per mile, and pavement construction techniques at the time of construction.

In Figures B1 through B16, the data does indicate that the test sections with the least roughness after 20 years are those with the bituminous stabilized base course (Test Section 2E & 2W) and the cement treated base course (Test Section 7E & 7W). It is very difficult to say which test sections have the greatest roughness. However, it appears that most of the other test sections have very high roughness (over 200 inches per mile of roughness).

A linear regression line on the form of $y = mx + b$ was generated from the roughness data. The line shows the general trend of the data.

2.3.1.2 Discussion

Since the beginning of data collection in 1964, plots of the data as shown in Figures B1 through B16 show a wide scatter which is attributed in part, to the causes which are discussed above. A statistical test of data variability was performed to determine the amount of roughness variation across the outside lane. Six-one foot wide paths were marked across the outside lane. The area of one and one-half foot wide in the center and two feet on each side at the inner and at the outer edge were

not measured for the test. The rolling straightedge was run within each of the six paths to measure the percent defective length. This data is shown in Figure 2.3.

In Figure 2.3 a large variation is shown for the rolling straightedge data. The roughness of the six paths varies from 2.3% to 10.3% deflective length. The statistical variation indicated possible measurements of 0.8% to 11.6% (95% probability) defective length. In essence, this statistical test indicates that a large variability exists for the rolling straightedge measurements.

The New Jersey Department of Transportation (Ref. 4) conducted a panel rating of present serviceability of N.J. pavements. The present serviceability rating (PSR) was correlated to the Mays roughness measurements. The panel rating established a PSR of 2.0 at the Mays roughness of 240 inches per mile at which 50% of the panel rating determined an overlay or rehabilitation was needed.

In order to determine a ball-park estimate of the significance of the experimental pavement roughness in relation to the panel rutting, the relationship in reference 5 between Mays roughness and rolling straightedge defective length were used to determine the corresponding defective length criteria. The Mays roughness of 240 per mile is roughly equivalent to 20% defective length. All defective length measurements on the experimental pavement test sections are below the 20% defective length associated with the need for overlay or rehabilitation.

Errors are Inherent errors in estimating the relationships between Mays roughness and rolling straight edge defective length influence

FIGURE 2.3

Statistical of Variability

Rolling Straightedge Data

	Inside Wheelpath Path Number			Outside Wheelpath Path Number		
	1	2	3	1	2	3
Percent Defective Length	10.3	5.9	7.9	2.3	5.5	5.3

Distribution of Data

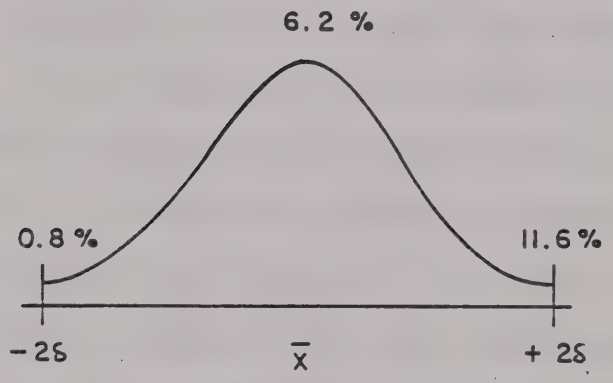

N = 6

$\bar{x}$ = 6.2 %

δ = 2.7 %

the selection of the 20% defective length criteria. The relationships may not be valid for the high defective length values. However, the intent is to show that the experimental pavement test sections would probably not be rated as failed on the basis of roughness for an overlay or pavement rehabilitation.

2.3.2 Rutting

Wheelpath rutting is defined as a surface depression caused by permanent deformation in any or all of the pavement layers or subgrade. The permanent deformation is caused by consolidation or lateral movement of the materials due to traffic loads. Significant rutting has the potential for contributing to vehicle hydroplaning and can be an indication of pavement deterioration.

2.3.2.1 Data

Rut depth measurements were made annually on each test section at 25-foot increments. The measurements were made by placing a ten foot straightedge across the wheelpath as shown in Figure 2.4. The rut depth is the distance from the lower edge of the straightedge to the pavement surface as measured with a 1/16 inch graduated scale. The annual mean rut depth data for each test section are shown in Appendix C Figures C1 through C16, in plots of the data versus the equivalent 18 Kip loads.

In the plots of the rut depth data, the regression line was generated by the standard regression techniques. The line represents the central tendency of the data with the line $y = C\sqrt{x}$ where C is a constant, x is the accumulated 18 Kip loads and y is the rut depth in inches. As the central tendency, the regression line will represent the data for evaluation criteria.

FIGURE 2.4

RUT DEPTH MEASUREMENT PROCEDURE

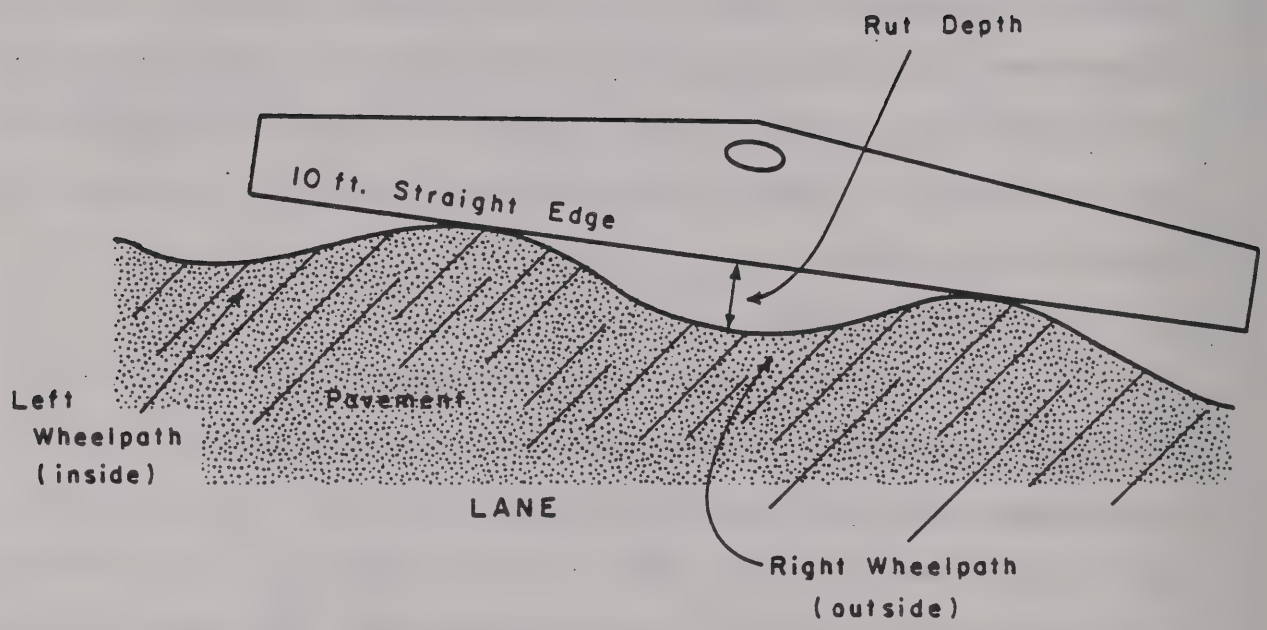

Table 2.1

Severity Levels of Rutting*

Severity	Mean Rut Depth Criteria
Low	1/4 - 1/2 inch (6-13 mm)
Medium	1/2 - 1 inch (13 m - 25 mm)
High	1 inch (25 mm)

* Highway Pavement Distress Identification Manual for Highway Condition and Quality of Highway Construction Safety," U.S. DOT/FHWA, March 1980.

Severity levels of rutting are shown in Table 2.1 as recommended by the Federal Highway Administration (Ref. 6). Severity is determined by the mean rut depth measurements.

Using an arbitrary 1/2 inch rutting criteria (low range of the medium severity), Table 2.2 shows the equivalent 18 Kip loads from the regression analysis in Figures C1 through C16 (Appendix C). The selection of the rutting criteria depends greatly on the pavement cross slope which provides drainage to prevent hydroplaning. The 1/2 inch criteria may be conservative and practical for most pavements.

2.3.2.2 Discussion

The 1984 rut depth data are shown graphically in Figure 2.5. After 20 years, the gravel mix bituminous stabilized base course (Test Section 4E & 4W) has the greatest rut depth. The large rutting (1 1/8 inches average) of both sections is attributed to the remolding characteristics of the relatively soft, temperature susceptible, 85-100 penetration grade asphalt cement, and the gravel aggregate which does not provide adequate interlock.

In Figure 2.5, the stone mix bituminous stabilized base course (Test Section 2E & 2W, 3E & 3W) has slightly higher rutting than other base courses of similar design. Although the crushed stone provides adequate aggregate interlock, the soft asphalt cement (as above) probably contributes to the slightly higher rutting.

The cement treated base (Test Section 7E & 7W), the MA-BC surface with drybound macadam-bituminous stabilized base course (Test Section 8), and the FA-BC surface with the drybound macadam-bituminous stabilized base course (Test Sections 9E & 9W) show the least rutting. The drybound macadam (Test Section 1E & 1W), the asphalt penetration macadam

Table 2.2

Equivalent 18 Kip Loads to ½ Inch Rutting Criteria

Based On Regression Analysis (Figure C1-C16)

Test Section and Base Course	Loads
1E Drybound Mac.	6,250,000
1W Drybound Mac.	4,940,000
2E Bit. Stab. (Stone	4,130,000
2W Bit. Stab. (Stone)	3,120,000
3E 4" Bit. Stab. (Stone)	4,850,000
3W 4" Bit. Stab. (Stone)	3,080,000
4E Bit. Stab. (Gravel)	1,220,000
4W Bit. Stabl. (Gravel)	1,990,000
5E Asphalt Pen. Mac.	5,160,000
5W Asphalt Pen. Mac.	4,100,000
6E Den. Gr. Stone	4,940,000
6W Den. Gr. Stone	4,940,000
7E Cement Treated	6,710,000
7W Cement Treated	4,380,000
8 Dry Mac. & Bit. Stab. (MABC)	6,130,000
9W Dry Mac. & Bit. Stab. (FABC)	6,640,000

FIGURE 2.5

BAR CHART OF 1984 MEAN RUT DEPTH

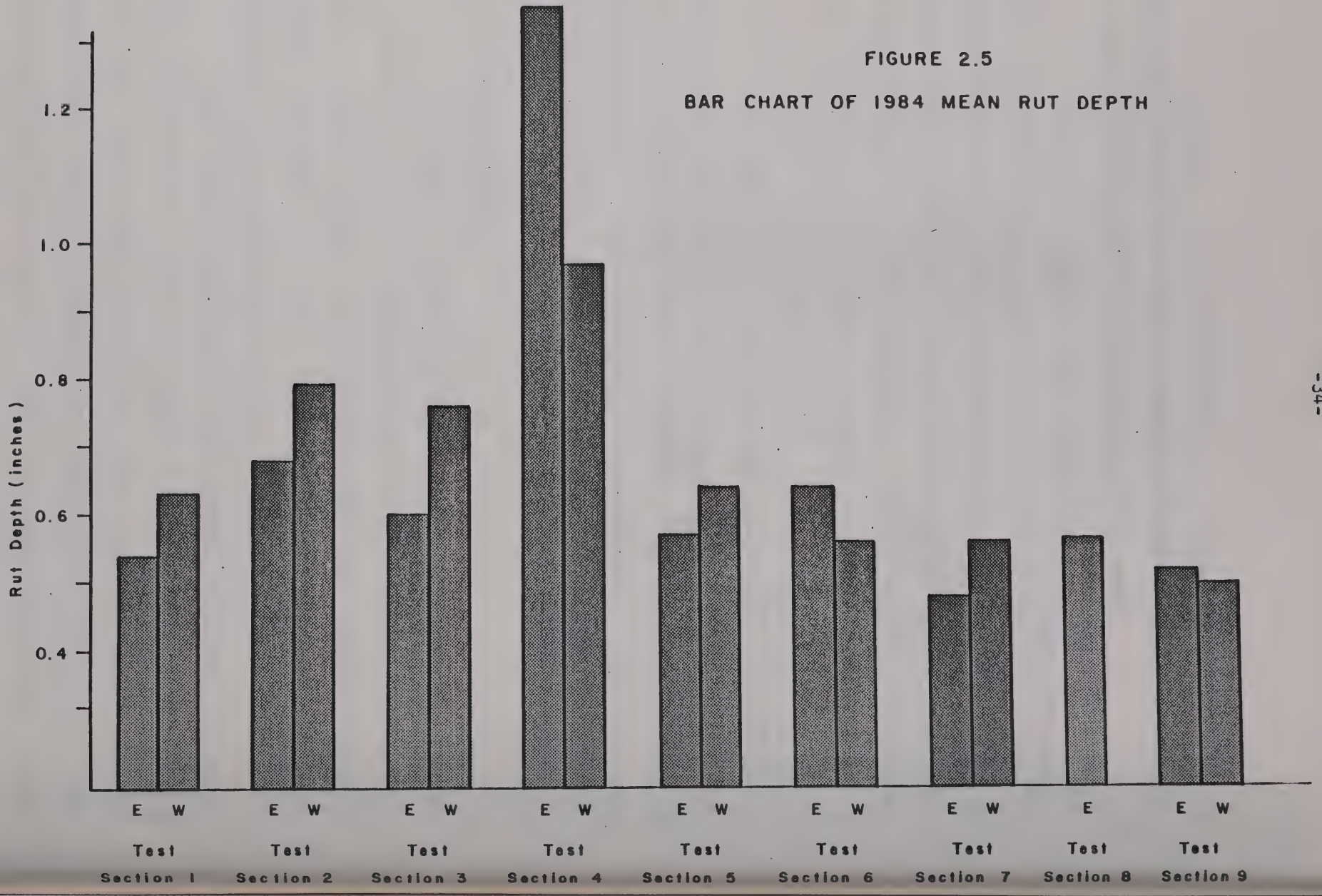

(Test Section 5E & 5W) and the densely graded stone (Test Section 6E & 6W) show slightly greater rutting than the above sections.

In Table 2.2, the bituminous stabilized base course-gravel mix (Test Sections 4E & 4W) shows the least equivalent 18,000 pound loads to the 1/2" criteria. The low equivalent loads reflect the high rate of rutting which is characteristic of the gravel mix remolding. The cement treated base (Test Section 7E), the dry-bound macadam base (Test Section 1E), drybound macadam-bituminous stabilized base (Test Section 9W) and the medium aggregate-bituminous concrete - drybound macadam base course (Test Section 3) show the greatest equivalent 18 Kip loads to the 1/2" criteria.

It may be that the analysis of the rutting criteria was adversely affected by the soft, 85-100 penetration grade asphalt cement in the bituminous stabilized base course and bituminous top and binder course. Since Marshall stability specification for bituminous top and binder course were not required at the time of construction, their absences contributed to the variation of rutting between test sections. In consideration of these facts, it is extremely difficult to make any conclusions regarding the rutting characteristics of the base course materials.

2.3.3 Cracking

The AASHO Road Test defines cracking in three classes:

1. Class #1 cracking is fine single non-connecting cracks usually in the wheelpaths,

2. Class #2 cracking is defined as cracks that have connected together to form a grid-type (alligator) pattern, and

3. Class #3 cracking is defined as cracks in which the bituminous surfacing segments become loose in a cracked grid-type pattern.

The Class #2 cracking, also called fatigue cracking, is caused by fatigue failure of the bituminous concrete surface source (or bituminous stabilized base course) under repeated traffic loadings. In most literature, it is assumed that cracking begins at the bottom of the bituminous layers where the greatest horizontal tensile stresses and strains are concentrated by heavy traffic loads. As discussed later in the text, cracks on the experimental pavement began at the top.

2.3.3.1 Data

A detailed annual crack survey was made on the experimental pavement test sections. The crack survey included mapping and measuring cracks during January of each year when the cracks were widest due to thermal shrinkage. Beginning in 1973 when significant interconnecting fatigue type cracking first appeared in the outside lane, Table 2.3 shows the percentage of cracking on each test section.

The percentage of cracking is based on the area of cracking as defined by the AASHO Road Test crack classification. Cracks on the test sections are classified by Class #1 and #2.

Non-connecting cracking appeared first (1970-71) in the westbound inside lane of the asphalt penetration macadam and densely graded stone base (Test Sections 5W & 6W); not shown in Table 2.3. This initial cracking was attributed to excessive moisture in the subbase and an premature age hardening of the bituminous surface course. The inside lane has very little heavy truck traffic. These two test sections are located in a low area where winter snows were piled in the median and rain water was not adequately drained away.

As reported in the 9th interim Report (Ref. 7), cores were taken in the cracked and uncracked areas and tested at the NJDOT laboratory

Table 2.3
Cracking Survey Outside Lane
Percent of All Cracking and Percent Fatigue Cracking

Section	Type of	1973	1974	1975	1976	1977	1978	1979	1980	1981	1982	1983	1984
1E	All	--	5	9	15	20	25	25	25	43	43	43	75
	Fatigue	--	2	2	10	10	10	15	15	20	25	24	48
1W	All	--	10	17	20	20	20	20	22	22	22	22	38
	Fatigue	--	2	2	5	5	5	10	10	10	15	15	20
2E	All	--	--	--	--	2	2	2	2	2	2	2	2
	Fatigue	None	--	--	--	--	--	--	--	--	--	--	--
2W	All	None	--	--	--	--	--	--	--	--	--	--	--
	Fatigue	None	--	--	--	--	--	--	--	--	--	--	--
3E	All	--	--	--	6	6	6	6	6	10	10	10	10
	Fatigue	None	--	--	--	--	--	--	--	--	--	--	--
3W	All	--	1	1	1	1	1	1	1	1	1	1	1
	Fatigue	None	--	--	--	--	--	--	--	--	--	--	--
4E	All	--	6	10	10	10	12	12	12	12	12	12	12
	Fatigue	None	--	--	--	--	--	--	--	--	--	--	
4W	All	--	8	10	14	24	25	25	25	25	25	25	26
	Fatigue	--	None	--	--	--	--	--	--	--	--	--	--
5W	All	--	10	12	15	20	20	20	20	20	20	20	27
	Fatigue	--	2	5	5	10	10	15	15	15	20	20	20
6E	All	--	10	12	12	12	12	12	17	17	35	45	57
	Fatigue	--	8	10	10	10	10	10	10	15	30	35	50
6W	All	10	12	15	15	15	15	15	17	17	17	17	37
	Fatigue	2	2	5	5	5	5	5	8	8	8	8	23
7E	All	--	--	--	1	1	1	1	1	1	1	1	1
	Fatigue	--	None	--	--	--	--	--	--	--	--	--	--
7W	All	--	--	--	5	6	6	6	7	7	7	7	7
	Fatigue	--	None	--	--	--	--	--	--	--	--	--	--
8	All	--	--	--	1	1	1	1	1	1	1	1	2
	Fatigue	--	None	--	--	--	--	--	--	--	--	--	--
9W	All	--	3	8	12	12	12	19	20	20	20	20	20
	Fatigue	--	None	--	--	--	--	--	--	--	--	--	--

for asphalt recovery which includes penetration tests. The average penetration of the top course recovered asphalt was 61 (.1 millimeters) for uncracked cores and 43 for the cracked cores. An examination of the cracked cores indicated that the cracks began at the top of the pavement surface and propagated downward. The low penetration of the cracked cores and the downward propagation are indicative of age hardening.

In Table 2.3, the percent of all cracking (class #1 & #2) and fatigue cracking (Class #2) is based on the area of cracking in the outside lane as defined by the AASHO Road Test (Ref. 1). In 1973, cracking (Class #1 & #2) began in the outside lanes of the asphalt penetration macadam (Test Section 5W) and densely graded stone (Test Section 6W.) Although the initial cracking which began in the inside lane in 1970-71 was attributed to age hardening, the cracking in the outside lane is attributed to asphalt fatigue and loads. In essence, early data showed little or no heavy truck traffic in the inside lane. Most heavy truck traffic was in the outside lane. Therefore when cracking occured in the inside lane it was not attributed to traffic loads. Cracking in the outside lane, where the heavy trucks are concentrated, is attributed to asphalt fatigue.

In Table 2.3, fatigue cracking (Class #2) is shown for the dry-bound macadam (Test Section 2E & 2W), asphalt penetration macadam (Test Section 5E & 5W), and the densely graded stone (Test Section 6E & 6W). No fatigue cracking is shown for the other test sections. Load related fatigue cracking occurs when the accumulated strain repetitions exceed the fatigue strength of the bituminous material. In comparison with Figure 2.8, the fatigue cracking has occured on the test sections which show the highest deflection measurements and where the accumulated loadings have probably exceeded fatigue strength of the bituminous course.

The 1984 cracking survey is shown graphically in Figure 2.6. This figure is presented to clarify the cracking comparison between test sections.

Crack patterns are shown in photo #1 through #4. Initial cracking is characterized by a single fine crack (Class #1) in the longitudinal direction and usually in the wheelpath as shown in photo #1. As cracking progressed, connecting cracks appeared as shown in photos #2 & #3.

Several small transverse cracks have appeared in the area between the lanes as shown in photo #4. These cracks are attributed to temperature changes and bituminous stiffness.

On the bituminous stabilized base courses (Test Sections 2E & 2W, 3E & 3W, and 4E & 4W), cracks are characterized by Photos #1 & #2. On the cement treated base course (Test Section 7E & 7W) cracks are characterized by Photo #1. In the drybound macadam (Test Section 1E & 1W), asphalt penetration (Test Section 5E & 5W), densely graded stone (Test Sections 6E & 6W) and the drybound macadam-bituminous stabilized base course (Test Sections 9E & 9W) cracks are characterized by Photos #2 & 3. The cracking which is shown in photo #4 is present to some degree in all test sections and is not characteristic of any one type of base course.

2.4 PSI-Pavement Failure

The performance of the experimental pavement test sections is expressed in terms of the present serviceability index (PSI) as discussed previously. The PSI is obtained from measurements of roughness, cracking, and rutting. Roughness is the dominant factor in estimating the PSI and the terminal serviceability. As previously described, the variation and scatter of the roughness data reduces significantly the confidence in the

FIGURE 2.6

CRACK SURVEY

1984

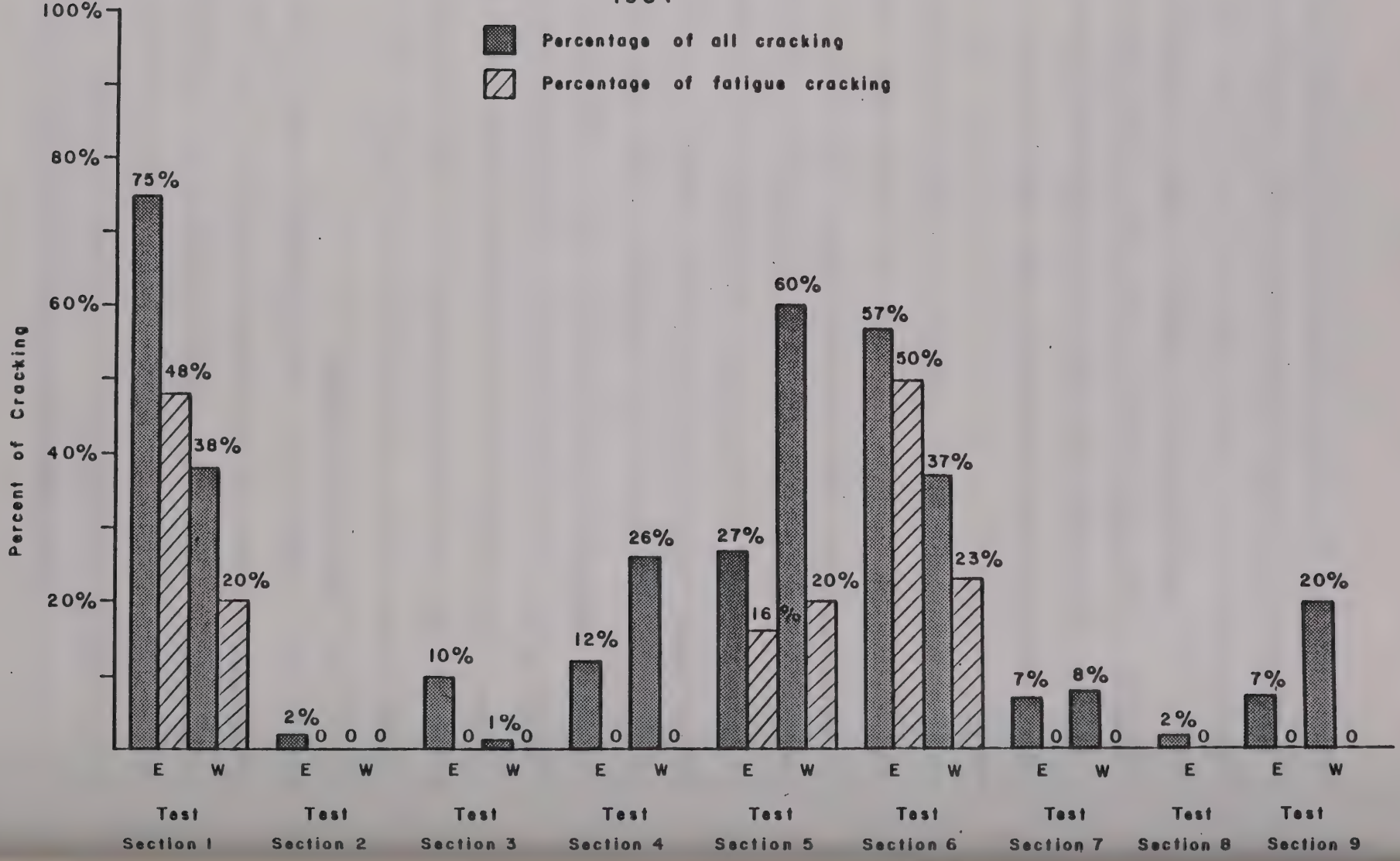

PHOTO #1

Single non-connecting crack (Class #1)

PHOTO #2

Connecting crack (Class #2)

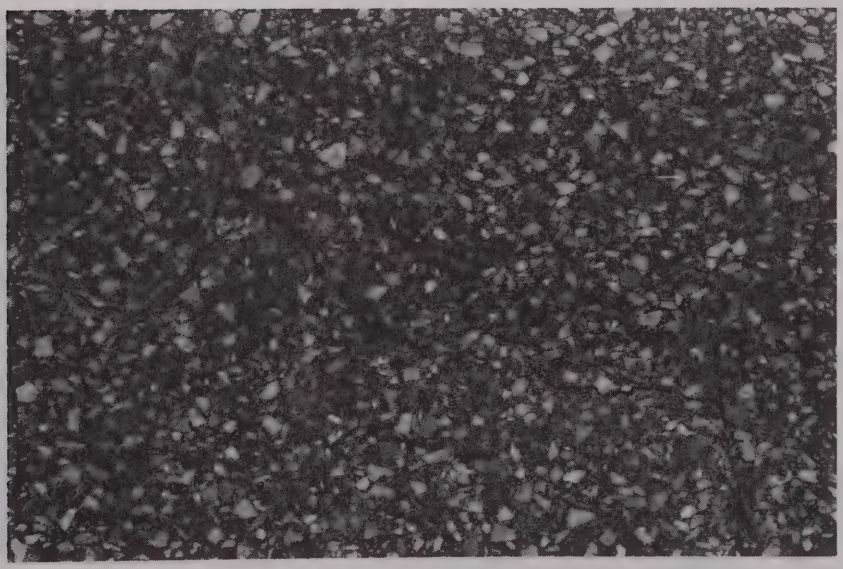

PHOTO #3

Connecting Cracks (Class #2)

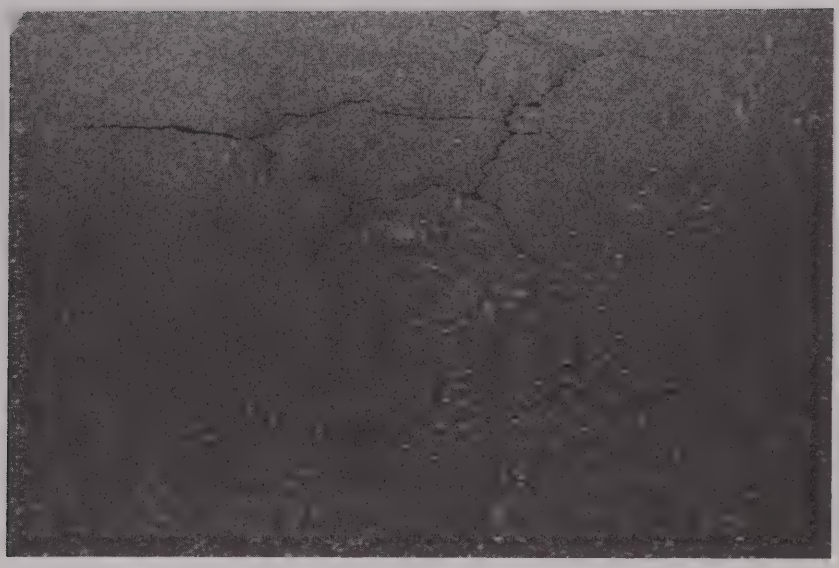

PHOTO #4

Small Transverse Cracks at the edge of the lane

PSI values. In consideration of the fact, a forgiving attitude must be allowed toward the statistically derived PSI regression equation if any results are to be determined.

Since roughness is an important factor in the PSI equation, the change in roughness data controls the change in PSI values and the prediction of pavement failure. In order to obtain a meaningful index of performance, the initial serviceability index should be at least one PSI value above the terminal value (2.5). In addition, a pavement that is constructed initially with a high PSI (4.5) will have a significantly longer life than one constructed to a lower PSI (4.0) (Ref. 8). A pavement with a low PSI will deteriorate at a quicker rate than one constructed with a high PSI.

The Washington State Department of Transportation (Ref. 9) recommends that a regression analysis is the initial approach employed in generating relationship between performance variables in the PSI equation and accumulated traffic loadings. For data that shows a large scatter, Washington recommends fitting a "typical" best fit curve through the points. This curve provides a central tendency and an averaging of the data. Each measured point is an estimate of the actual data. In this analysis, each point represents a large distribution of data.

Since the typical PSI curve is expected to be a downward (negative sloping) straight line, this typical best fit line was selected to represent the experimental pavement data (other model curves did not fit as well as the straight line):

$$y = m x + b \qquad \text{Equation 3}$$

where: y = PSI values
x = Accumulated traffic loads
m = Slope of the line
b = The y-intercept

The best fit regression line and the plot of the measured PSI values are shown in Appendix D Figures D1 through D16.

From these plots, it is possible to roughly estimate the terminal traffic loadings which are based on the terminal serviceability value of 2.5 as determined by the AASHO Road Test. The terminal traffic loading for each test section is shown in Table 2.4. The Table also shows the correlation coefficient for each best fit equation.

In Table 2.4, the cement treated base course (Test Section 7E) shows the largest number of traffic loadings to the terminal serviceability value of 2.5. However, the loads to failure of the other cement treated base course (Test Section 7W) are not consistent with test section 7E. Essentially, the low initial PSI value for the best fit curve and the measured value are below 3.0. The very low correlation coefficients for both best fit curves indicates that the curves do not adequately define the scatter of points. Although judgement suggests that these two sections are the "best" of all test section, the best fit curves of the regression analysis do not confirm or dispute this suspicion.

The bituminous stabilized base course (Test Section 2E) shows the next highest traffic loadings to failure. However, the other bituminous stabilized base course (Test Section 2W) indicates a terminal failure which is inconsistent with test section 2E. No apparent reason is obvious for this inconsistency. A reasonable judgement suggests that these two sections are the "second best" to the cement treated base course.

The bituminous stabilized base-gravel mix (Test Section 4E) and the densely graded stone mix (Test Section 6W) show the two lowest traffic loads to failure. Since the gravel mix has the highest rutting which effects the PSI value and the densely graded stone has a low structural

Table 2.4

PSI - Pavement failure

Terminal 18 Kip Loads to Failure

Model: $y = mx+b$

Test Section	Correlation Coefficient (r^2)	Total 18 Kip loads to PSI = 2.5
1E	.60	1,645,000
1W	.75	3,587,000
2E	.68	4,301,000
2W	.78	3,379,000
3E	.77	2,920,000
3W	.71	2,256,000
4E	.92	1,122,000
4W	.83	2,745,000
5E	.65	2,141,000
5W	.68	1,833,000
6E	.76	2,294,000
6W	.61	940,000
7E	.22	4,721,000
7W	.37	1,960,000
8	.91	1,430,000
9W	.75	1,096,000

strength, it is reasonable to expect low terminal serviceability traffic loadings.

The total accumulated 18 kip traffic loading to failure will be used in section 2.7 to develop the AASHO Road Test structural layer coefficients. However, at this point it is obvious that the low correlation coefficients and inconsistent estimates of traffic loadings between test sections reduces significantly the value of the structural coefficients.

2.5 Traffic Data

The annual traffic data for the experimental pavement were collected by the Bureau of Data Resources. The data includes traffic summary sheets, and truck weight information from W-2 and W-4 Tables which were furnished by the Federal Highway Administration.

The loadometer data and traffic counts were obtained at station 2-1-10 which is located on the experimental pavement in Ridgefield Park and Bogota Boroughs. The loadometer data were obtained annually until 1976 when the data was collected once every two years.

Table 2.5 shows the 1984 Average Annual Daily Traffic for the outside lanes of the eastbound and westbound local lanes of the test sections. The data is an actual 24 hour count of vehicles. This data shows the percent trucks in the outside lanes.

The total yearly traffic data were used to calculate the 18 kip loadings which were obtained by multiplying the days per month by the monthly average daily traffic and summed. The truck percentage is than multiplied by the total yearly vehicles for the total yearly trucks.

The accumulated equivalent 18 Kip axle loadings are shown in Table 2.6. The yearly 18 Kip loadings are obtained by multiplying the equivalent

Table 2.5

Average Annual Daily Traffic

Outside Lane

1984

Total	Eastbound	Westbound
Passenger Cars	6537	7170
Total Trucks	2559	2806
Total vehicles	9096	9976
Percent trucks	28%	28%

TABLE 2.6

ACCUMULATED 18 KIP AXLE REPETITIONS

EASTBOUND - OUTSIDE (RIGHT HAND) LANE

	Traffic		18 Kip Axle Equivalent Factors		Yearly 18 Kip Axle Equivalent Repetitions			Accumulated 18 Kip Axle Equivalent Repetition
Date	Passenger	Trucks	Passenger	Trucks	Passenger	Truck	Total	
1965	859,990	248,216	.0002	4279	171	106,212	106,383	106,383
1966	1,112,545	403,486	.0002	4635	223	214,733	214,956	321,339
1967	1,146,098	422,029	.0002	4222	228	179,500	179,728	501,067
1968	1,224,729	435,025	.0002	4266	244	185,427	185,671	686,738
1969	1,316,100	457,138	.0002	4090	263	187,583	187,846	874,584
1970	1,564,986	457,140	.0002	3844	313	150,179	150,492	1,025,076
1971	1,260,106	465,844	.0002	3597	254	167,556	167,810	1,192,886
1972	1,625,894	875,138	.0002	6397	325	559,823	560,148	1,753,034
1973	1,507,517	959,810	.0002	6928	302	664,956	665,258	2,418,292
1974	1,547,550	760,981	.0002	6254	309	475,918	476,227	2,894,519
1975	1,888,106	797,646	.0002	5662	377	451,627	452,004	3,346,523
1976	1,914,810	1,074,812	.0002	5662	383	608,558	608,941	3,955,464
1977	2,050,518	1,119,011	.0002	5878	410	704,779	705,189	4,660,653
1978	2,171,327	1,054,968	.0002	5878	434	620,110	620,544	5,281,197
1979	2,180,851	1,063,347	.0002	6524	436	693,975	694,163	5,975,360
1980	1,991,242	976,358	.0002	6524	398	636,975	637,373	6,612,733
1981	2,925,734	807,060	.0002	5371	585	433,471	434,057	7,046,847
1982	2,925,734	807,060	.0002	5371	585	433,471	434,057	7,480,487
1983	2,356,490	922,433	.0002	6481	471	597,828	598,300	8,079,147
1984	2,356,390	922,433	.0002	6481	471	597,828	598,300	8,677,447

TABLE 2.6 (CONTINUED)

ACCUMULATED 18 KIP AXLE REPETITIONS

EASTBOUND - OUTSIDE (RIGHT HAND) LANE

	Traffic		18 Kip Axle Equivalent Factors		Yearly 18 Kip Axle Equivalent Repetitions			Accumulated 18 Kip Axle Equivalent Repetition
Date	Passenger	Trucks	Passenger	Trucks	Passenger	Truck	Total	
1965	1,273,240	250,673	.0002	4279	254	107,263	107,517	107,517
1966	1,672,352	279,330	.0002	4635	324	174,875	175,199	282,716
1967	1,695,338	416,203	.0002	4222	329	177,031	177,360	460,076
1968	1,806,367	415,417	.0002	4266	361	177,061	177,422	637,498
1969	1,923,169	549,739	.0002	4090	385	225,425	225,810	863,308
1970	2,226,558	511,627	.0002	3844	490	196,664	197,154	1,060,462
1971	1,994,344	498,148	.0002	3597	397	179,182	179,579	1,239,644
1972	1,780,119	799,581	.0002	6397	356	511,487	511,843	1,751,887
1973	2,089,277	870,018	.0002	6928	418	602,748	603,166	2,355,053
1974	2,207,779	977,993	.0002	6254	442	611,637	612,079	2,967,132
1975	2,227,054	1,052,919	.0002	5662	445	596,163	596,608	3,563,740
1976	2,344,012	1,107,259	.0002	5662	468	626,930	627,313	4,191,138
1977	2,440,751	1,091,465	.0002	5878	488	641,563	642,051	4,833,189
1978	2,446,851	1,052,194	.0002	5878	493	618,479	618,972	5,452,161
1979	2,421,549	1,119,031	.0002	6524	482	730,055	730,537	6,182,698
1980	2,477,003	1,048,352	.0002	6524	495	683,945	684,440	6,867,138
1981	2,744,094	793,034	.0002	5371	549	425,938	426,487	7,293,625
1982	2,744,094	793,034	.0002	5371	549	425,938	426,487	7,720,112
1983	2,595,480	1,012,876	.0002	6481	519	656,445	656,964	8,377,076
1984	2,595,480	1,012,876	.0002	6481	519	656,445	656,964	9,034,040

18 Kip load factor from the W-4 tables by the total yearly trucks and passengers vehicles. It is accumulated in the far right column of Table 2.6.

The equivalent 18 Kip load factor converts mixed traffic load applications into 18 Kip single axle applications of the AASHO Road Test. It is based on an analysis of the total number of daily mixed load applications (W-4 Tables) that are carried on the pavement. The total number of mixed load applications are broken down into axle load groupings which are then resolved into equivalent 18 Kip single axle load applications. This is done by multiplying the number of applications in each weight category by an equivalence factor which was developed by the AASHO Road Test (Ref. 1).

2.6. Deflection Analysis

At the AASHO Road Test, the principal purpose for measuring deflections in bituminous pavement was to find relationship between deflections measured at a given time and the future performance of the pavement. The assumption was made that the deflection of a pavement under a given load would serve as a measure of the pavements ability to serve many applications of the load.

The magnitude of the surface deflections of a bituminous pavement under load is a indication of the number of load applications that the pavement can sustain prior to failure. In essence, the higher the deflections the lower the expected number of loads to failure. The elastic portion of the deflection which is called rebound, was established (Ref. 1) as the most accurate part of the deflection for performance relationships.

2.6.1 Deflection Data

The deflection data were obtained by the Benkelman beam rebound procedure using an 18 Kip axle load (9000 pound dual wheel load). Seven permanent stations on each test section (five stations are measured on Test Section 8) were measured annually in October or November. The fall measurement period was chosen because pavement moisture and temperature conditions are expected to be the most consistent in this period.

Prior to 1979 the measurement procedure consisted of placing the Benkelman beam probe through the dual tires to a point four feet ahead. The deflection measurement was made by slowly rolling the truck forward past the beam probe. In this procedure, the initial pavement deflection and pavement recovery (rebound) are measured as the trucks moves four feet beyond the probe. However, only the rebound measurement is utilized in the deflection analysis.

Beginning in 1979, the rebound basin procedure (Static Method) was initiated to further define deflection behavior. The procedure consists of marking the pavement at 20 inches and 40 inches ahead of the probe which is directly under the axle of the dual tires.

With the beam stationary, the deflection basin measurements are made as the truck rolls slowly forward over the marks. The procedure actually measures the rear portion of the deflection basin as shown in Figure 2.7.

The historical plots of the deflection (do) and equivalent 18 Kip load applications (traffic) are shown in Appendix E, Figure E1 through E16. In an overall perspective, the plots do not show a significant upward trend of data with the exception of the data for the years 1979 through 1984. The slight increase for that data is directly attributed to the static deflection procedure and not attributed to a real upward trend of data.

FIGURE 27

REBOUND BASIN PROCEDURE

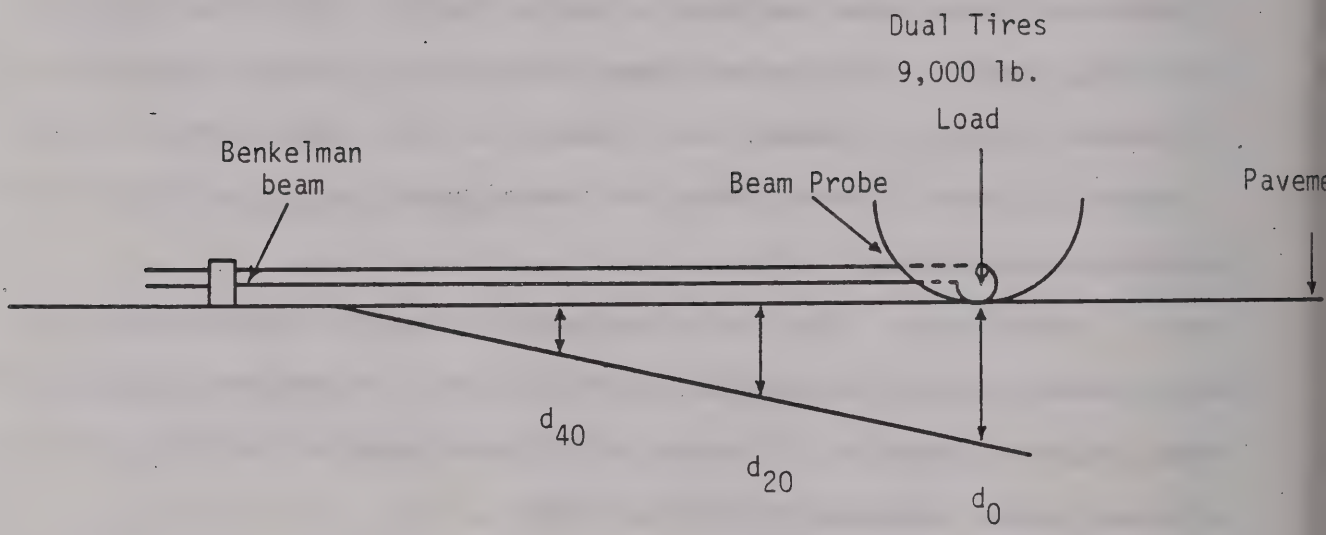

d_0 = maximum rebound - initial point (origin) of probe

d_{20} = rebound at 20 inches from d_0

d_{40} = rebound at 40 inches from d_0

Some normal variation is shown for a few data points. The variation is due to load conditions such as tire contact area, truck load, operator error, and variation in pavement temperature.

The mean rebound data for 1979 through 1984 are shown in figure 2.8. Since this data was obtained by the static procedure and indicates no upward or downward trend, the data was averaged to show the relative deflection performance between test sections.

In Figure 2.8, the greatest rebound data is shown for the densely graded stone (Test Sections 6E & 6W). The least mean rebound data is shown for the cement treated base (Test Sections 7E & 7W).

In an overall analysis of the six test sections which were constructed with similar base course thickness for direct comparison, the bituminous stabilized base courses (Test Section 2E & 2W, 3E & 3W and 4E & 4W) have lower mean rebounds than the crushed stone base courses (Test Section 1E & 1W, 5E & 5W, 6E & 6W).

As stated above, the AASHO Road Test measured deflections to find a relationship between deflections and future performance. Plotting the total 18 kip loads to PSI = 2.5 from Table 2.4 and the mean deflections from Figure 2.8, (not shown here) shows a wide scatter of data and no data trend. The scatter of points is due to the poor PSI data as described earlier. The New Jersey experimental pavement data does not show a relationship between deflections and future performance. Therefore, defections were not used in the analysis of the structural coefficients.

2.6.2 Deflection Basin Data

The Benkelmann beam rebound basin is an indicator of pavement structural adequacy. Utah (Ref. 10) reports that the rebound basin describes structural adequacy with the probable nature of failure being

FIGURE 2.8

MEAN REBOUND DATA

1979 – 1984

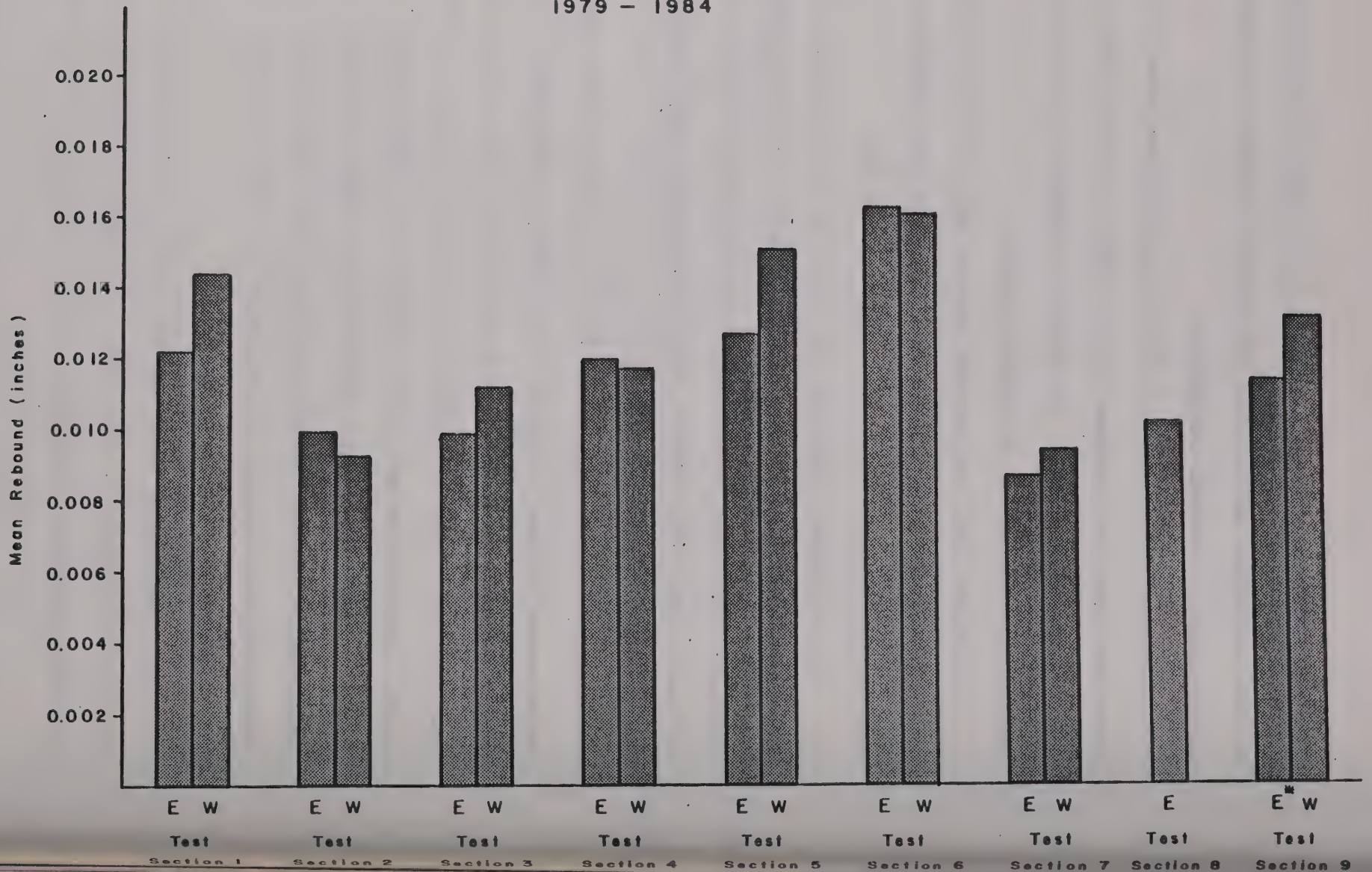

determined by the size and shape of the basin. The Utah basin shapes are shown in Figure 2.9.

From actual field experience, Utah determined that a pavement is performing adequately where the basin shape is defined by a gently downward sloping straight line (Figure 2.9, line segments d_{40}-d_{20}-d_0). A pavement is performing inadequately when the rebound basin is defined by a gently sloping line segment (d_{40}-d_{20}) and a steep downward sloping line segment (d_{20}-d0) indicates an adequately performing surface course and as inadequately performing base course or subbase. An analysis of the rebound basins of the experimental pavement will concern the relative basin shapes between the test sections.

The average rebound basins for the combined eastbound and westbound test sections are shown in Figure 2.10. From these basin shapes, it is possible to generalize regarding the Utah pavement structural conditions. The straight downward line of the bituminous stabilized base course (Test Section 2E & 2W) and cement treated base course (Test Section 7E & 7W) indicate that the base courses are providing adequate support. The steep sloping line segment (d_{20}-d_0) of the drybound macadam (Test Section 1E & 1W) and densely graded stone (Test Section 6E & 6W) indicate an adequately performing surface course and an inadequately performing base course, i.e. the base courses do not provide adequate load support. The other basin shapes (Test Section 3E & 3W, 4W & 4W, 5E & 5W, 8W, 9W) indicate a steeper line segmented (d_{20}-d_0) than the line segment (d_{40}-d_{20}). However, the degree of relative steepness between line segments is not dramatic and may not be significant. As with the plot of the defections and 18 kip loads to PSI = 2.5, the defection basin analysis did not really show an indication of the structural capacity of the test sections.

FIGURE 2.9

UTAH REBOUND BASIN CRITERIA

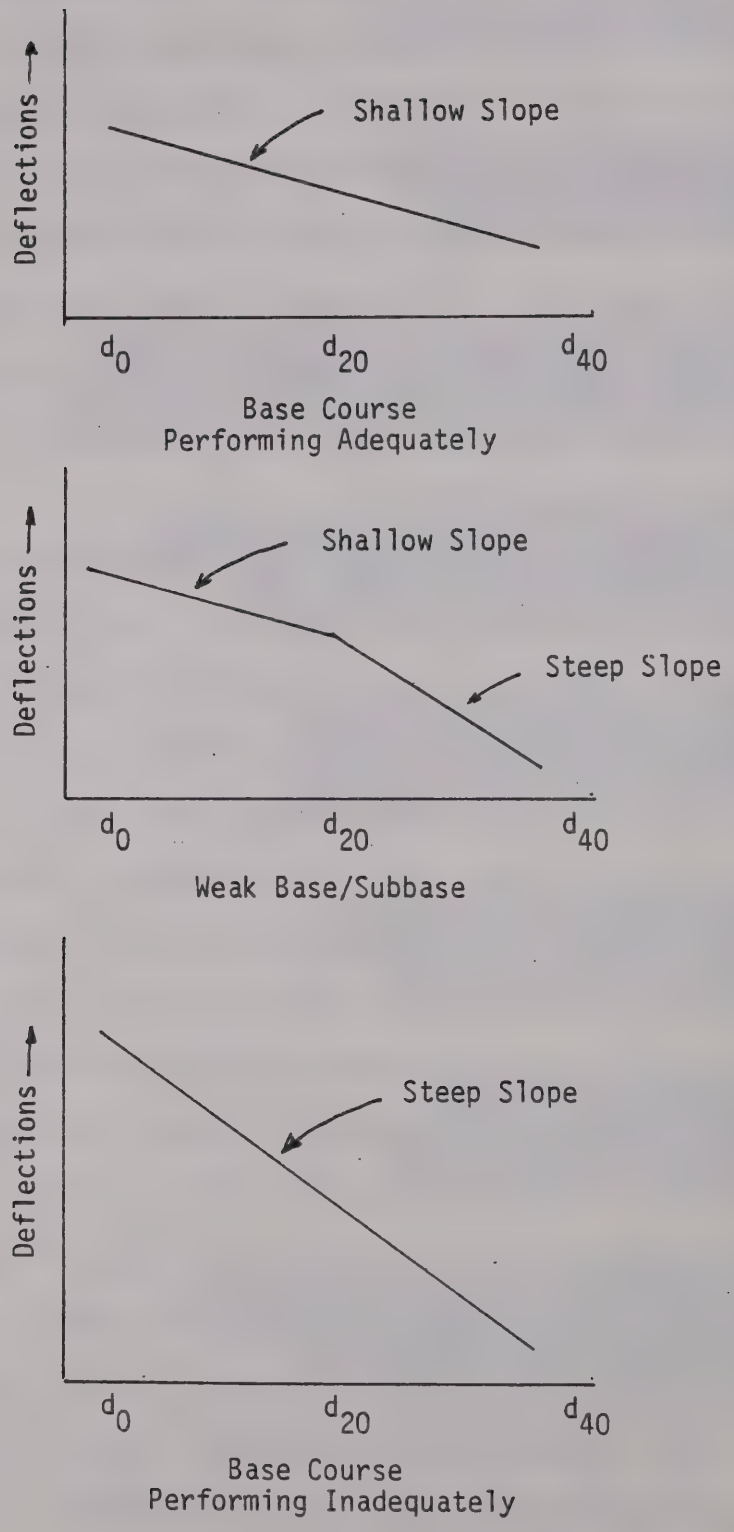

FIGURE 2.10

BENKELMAN BEAM REBOUND BASIN

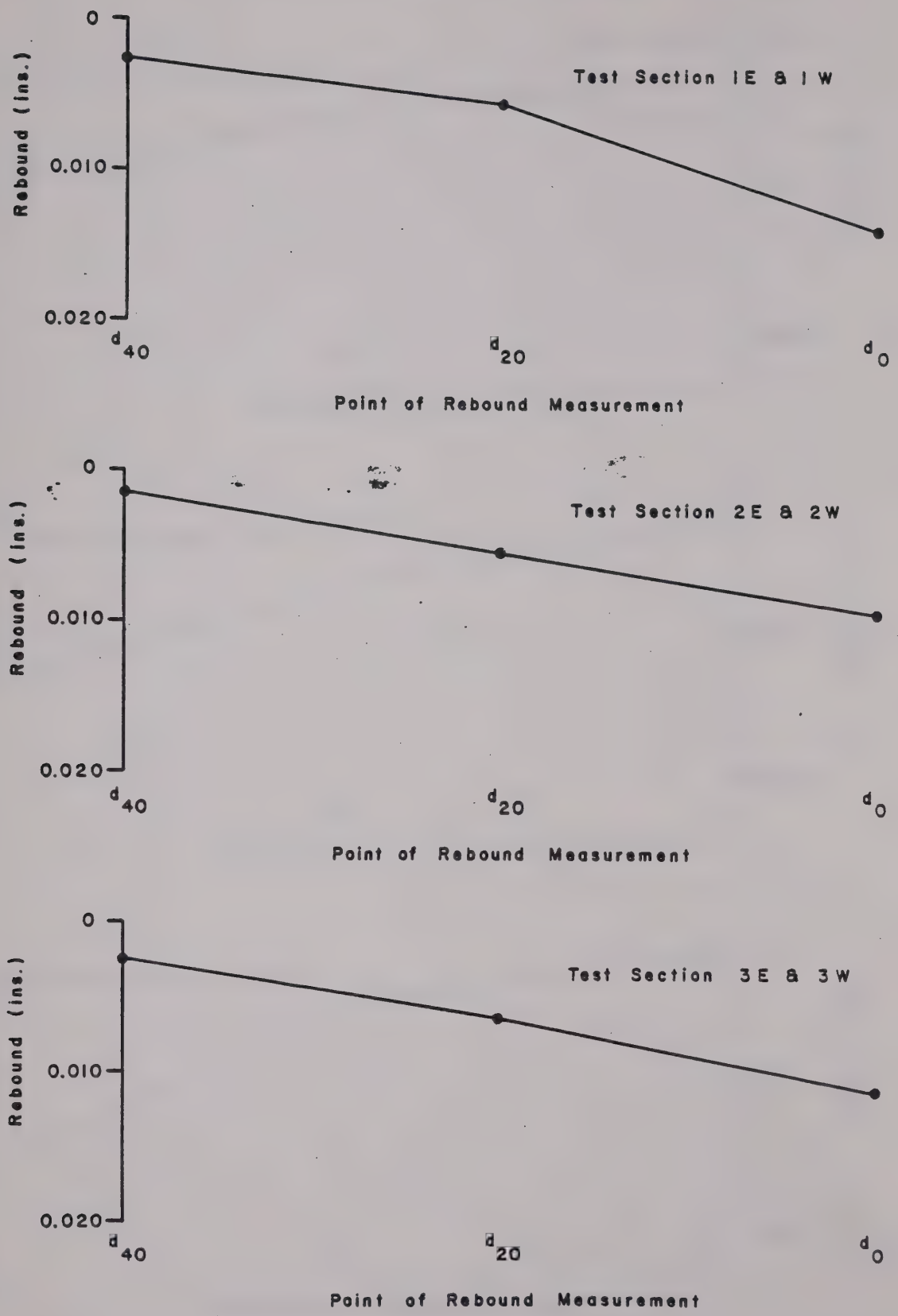

FIGURE 2.10 Continued

BENKELMAN BEAM REBOUND BASIN

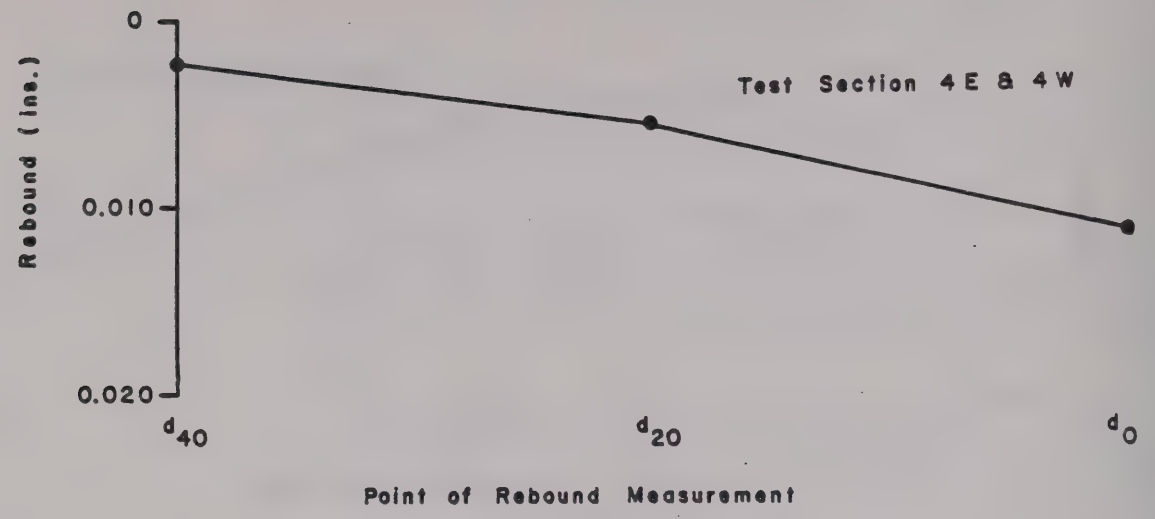

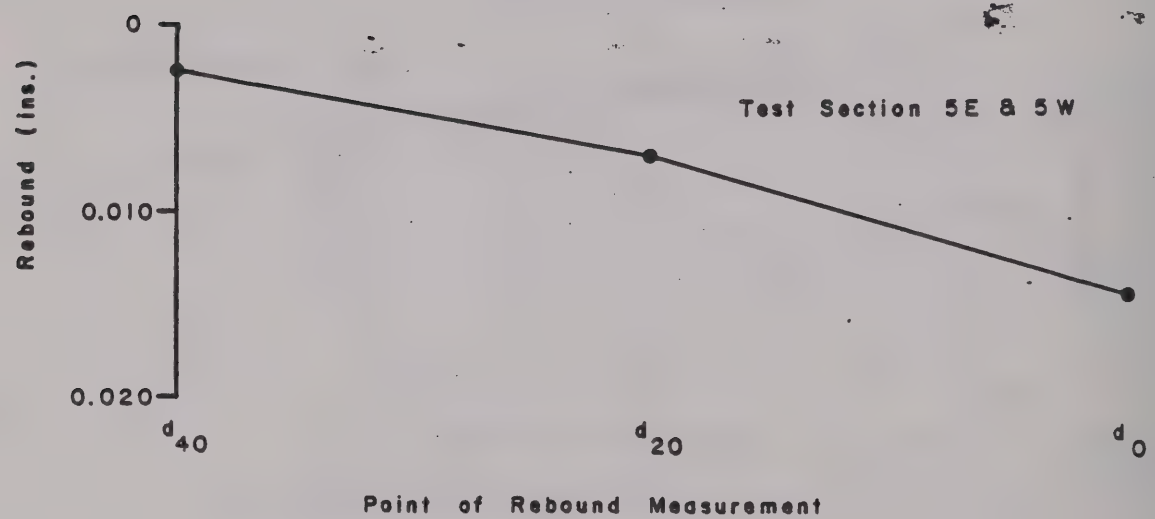

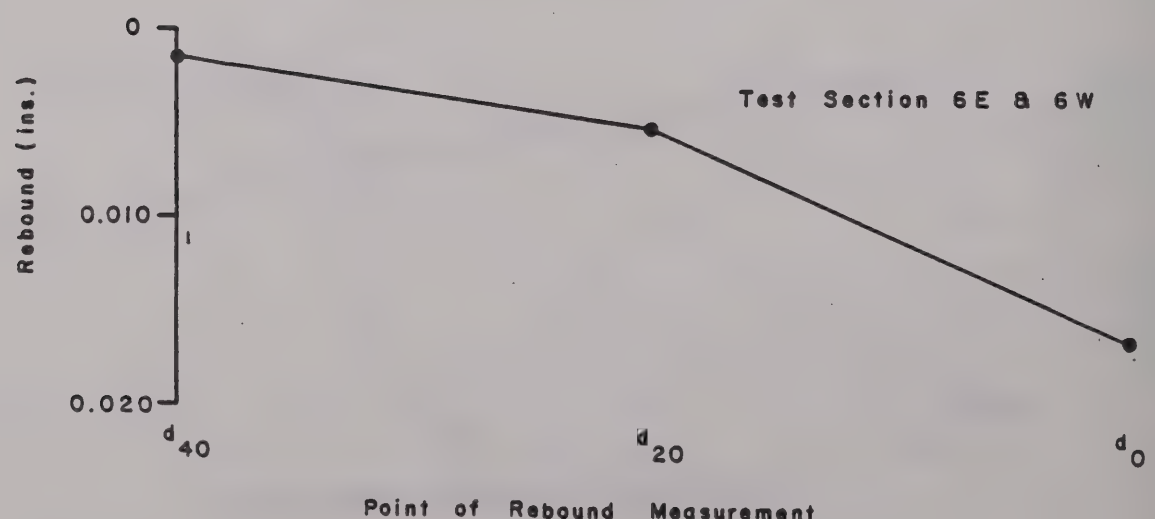

FIGURE 2.10 Continued

BENKELMAN BEAM REBOUND BASIN

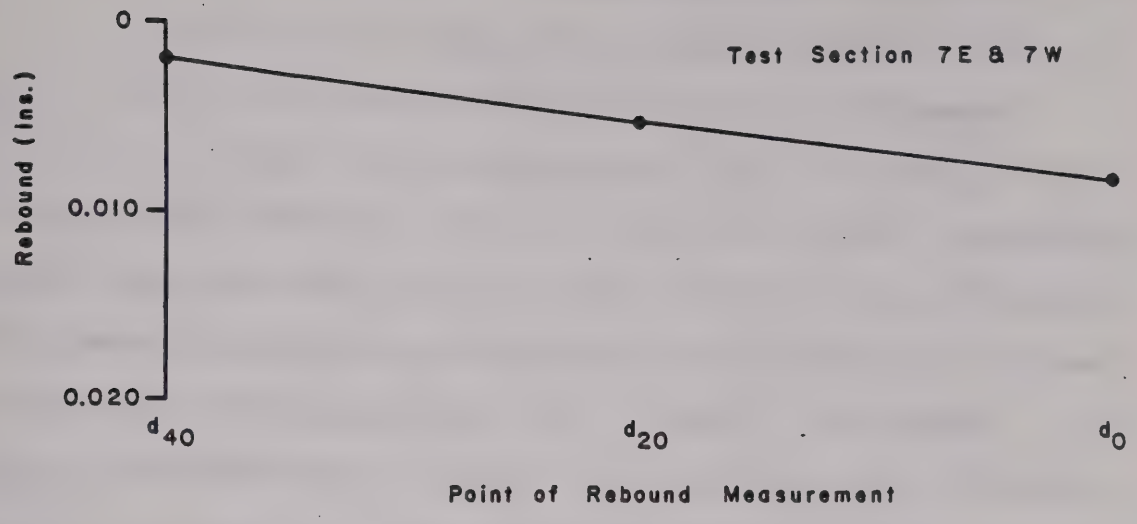

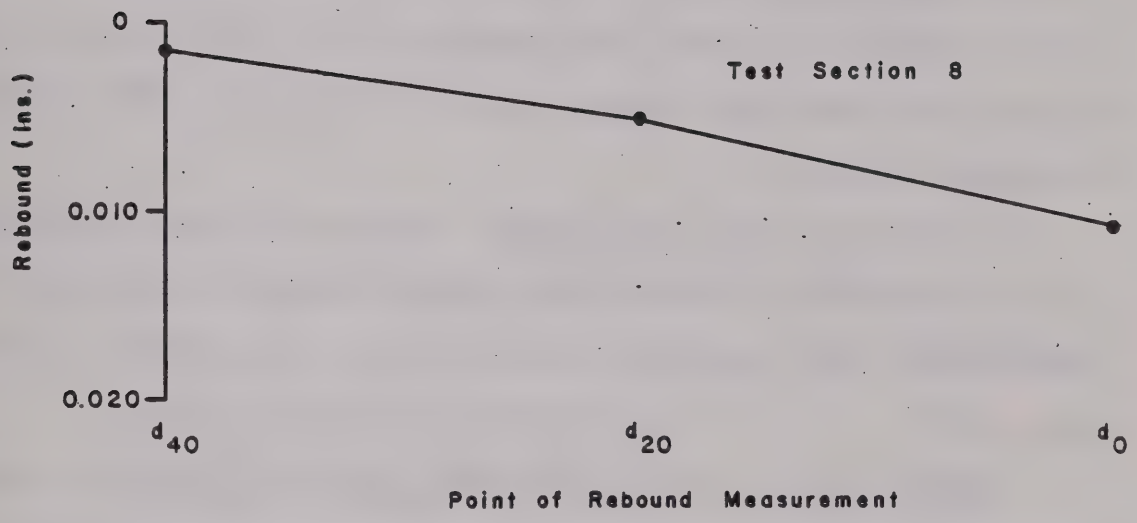

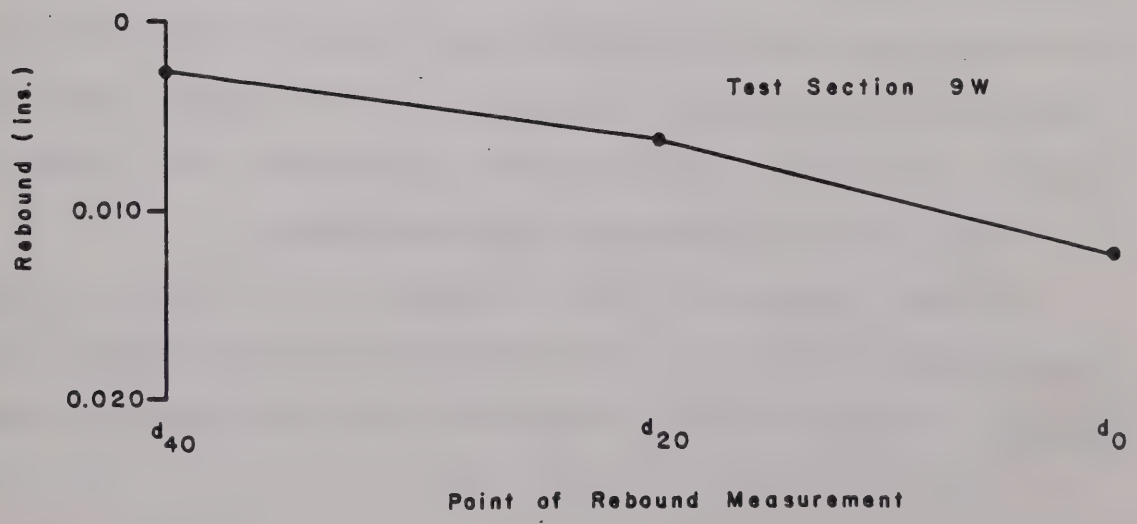

2.7 Structural Layer Coefficients

2.7.1 Research Studies

Vaswani (Ref. 11) developed thickness equivalency values of commonly used top course and base course materials in Virginia. The thickness equivalency values were used to develop structural coefficients with deflection data, modulus of resilience values and a regression analysis. Vaswani's equivalencies and corresponding coefficients are shown in Table 2.7. Essentially, Vaswani's data substantiated the development of structural layer coefficients for inclusion in the AASHO design equations.

The Pennsylvania State University (Ref. 12) conducted an extensive study to establish structural layer coefficients for base course materials. The Penn State researchers adopted a modified form of the AASHO Terminal 18 kip loading equation.

The Penn State test track terminal serviceability data was substitued into that equation to solve for the structural number and structural layer coefficients. The Penn State structural layer coefficients are shown in Table 2.8.

Although the conclusions of the Penn State study indicated that the structural layer coefficients of the bituminous concrete base course were not constant but vary with layer thickness, the study demonstrated that the substitution of performance data into the AASHO Terminal Serviceability equation was feasible for development of structural layer coefficients.

2.7.2 Analysis of Structural Layer Coefficients

A major objective of this research was to determine structural coefficients of the base course materials in the experimental pavement project. The base course materials are dry bound macadam, bituminous

Table 2.7

Thickness Equivalency Values of Materials in flexible Pavement System

Material	Equiv.	Coeff.
Asphalt Concrete (Surface & Base Course)	1.0	.44
Cement Treated Aggregate	1.0	.44
Dense graded aggregate	.35	.15
Soil Cement (Subbase)	.40	.18
Cement treated aggregates (Subbase)	.60	.26

Table 2.8
Penn State Structural Layer Coefficients

Base	Coefficients(a_2)
Aggregate Cement Base Course	0.55
Aggregate Lime Pozzolon Base Course	0.51
Bituminous Concrete Base Course	0.51
Aggregate Bituminous Base Course	0.49

stabilized base (stone mix), bituminous stabilized base (gravel mix), asphalt penetration macadam, densely graded stone, and cement treated base.

The primary input for the analysis of structural layer coefficients consists of the serviceability trends (PSI vs. Traffic loading Plots) as shown in Table 2.4. The field data which was used in the PSI calculation included pavement roughness, cracking and rutting.

The structural coefficients are calculated by substituting the serviceability trends and terminal traffic loadings into the AASHO performance equation. The equation was developed at the AASHO Road Test by correlating the terminal traffic loadings for particular levels of PSI and structural numbers. The following equation is the result of that correlation:

$$\text{Log } W_{t_1} = 5.93 + 9.36 \text{ Log } (SN + 1) - 4.79 \log (L_X + L_2) + 4.33 \text{ Log } L_2 + G_{t/B_x} \quad \text{Equation 4}$$

(AASHO Eq. C-15)

Where:

W_t = Number of applications of axle load L at the given PSI

SN = Structural number

L_X = magnitude of axle load in kips

L_2 = axle type, 1 for single and 2 for tandem

$$G_t = \text{Log } \frac{4.2 - P_t}{4.2 - 1.5}$$

$$B_X = .40 + \frac{0.081 \ (L_x + L)_2 3.23}{(SN + 1)^{5.19} L_2^{3.23}}$$

P_t = terminal PSI (i.e., failure criterion)

This equation is shown graphically in Figure 2.11

The NJDOT design structural numbers for the experimental pavement test sections were derived from current design structural coefficients. Knowing the values of W_1, L_x, L_2 and P_t from field data, the design

FIGURE 2.11

GRAPH OF AASHO ROAD TEST PERFORMANCE EQUATION

PSI = 2.5

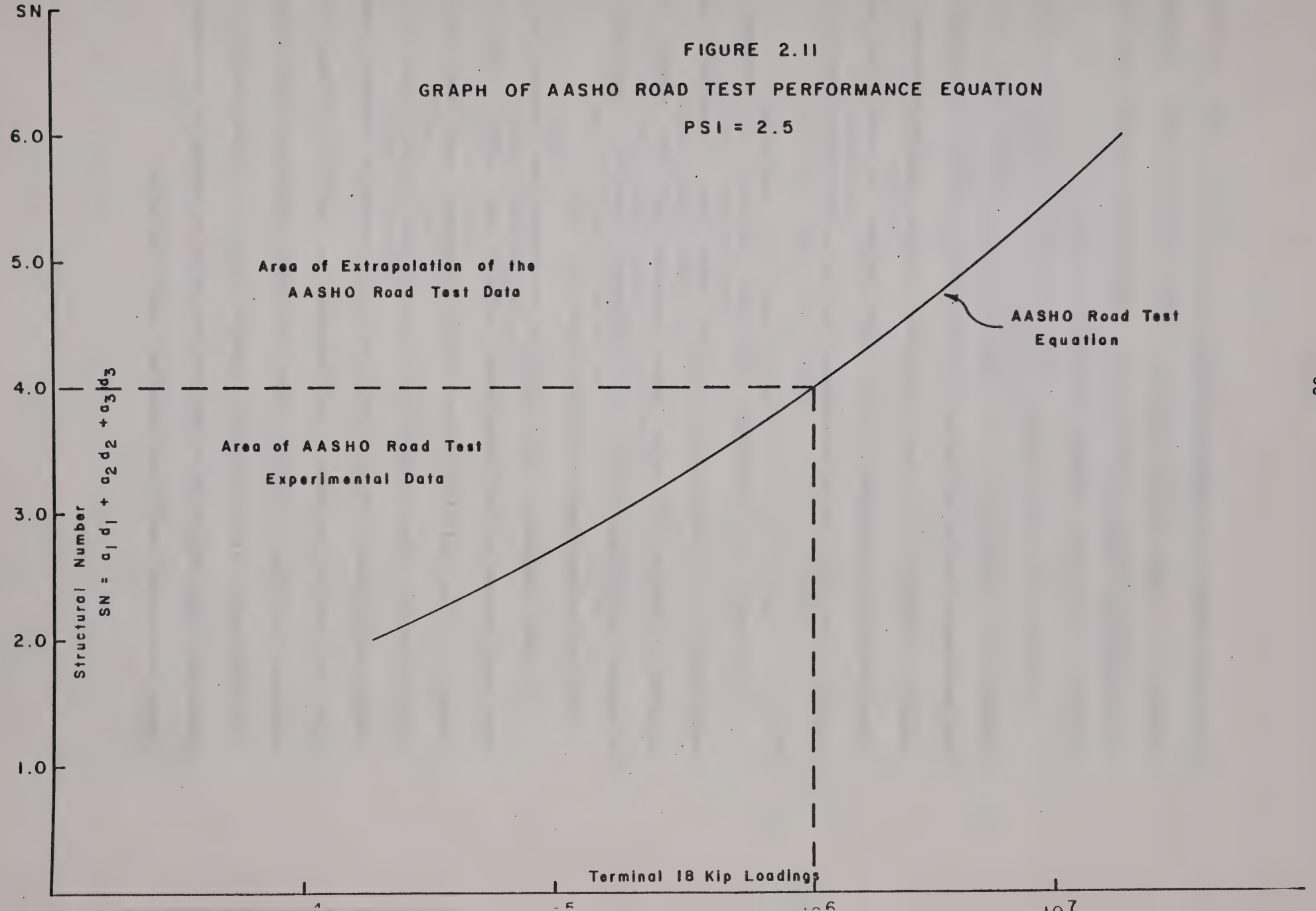

structural numbers were substituted into equation #4 to obtain the design terminal 18 kip traffic loadings. The current NJDOT structural coefficients are shown in Table 2.9. The design SN values and design terminal 18 kip traffic loadings are shown in Table 2.10.

In Table 2.10, the calculated (new) structural numbers (Col. 5) were obtained from substitution of the terminal 18 kip loadings (Col. 6) from the performance curves of the test sections (Table 2.4) into the graphical solution in Figure 2.9. The calculated structural number represents the actual effective thickness of each test section to obtain the actual terminal 18 kip loadings as determined from the performance curves at a PSI = 2.5

To obtain the structural coefficient of each base course, the calculated SN is substituted into the three layer structural number equation (Equation #2) with layer thickness and the current NJDOT structural coefficients (Table 2.9) of bituminous concrete - top course (a. = 0.44) and subbase quarry processed stone (a_3 = 0.14).

Drybound Macadam - The calculated structural coefficients (a_2) for each base course of the experimental pavement are shown in Table 2.10, Column 7. The calculated base course structural coefficient for the drybound macadam (Test Section 1E & 1W) are significantly higher than the design coefficients. This reflects the larger number of terminal loadings than the design loadings. As discussed in the PSI Pavement Failure section, the terminal loading reflect the errors associated with estimating the performance curves from the roughness data. In consideration of the relatively high deflection values and the large percentage of cracking, the larger structural coefficient does not seem reasonable.

Table 2.9

Current NJDOT Structural Coefficients

Pavement Component	Structural Coefficient		
	a_1	a_2	a_3
Surface Course			
Roadmix Course (low stability)	0.20		
FA-BC-Top	0.44		
-Binder	0.44		
MA-BC-Top	0.44		
-Binder	0.44		
Base Course			
Bituminous Stab. base (Stone)		0.44	
Bituminous Stab. base (Gravel)		0.34	
Densely graded stone		0.14	
Dry bound Macadam base		0.20	
Cement treated Base (Plant mixed)		0.30	
Asphalt Penetration Macadam		0.30	
Subbase			
Quarry Processed Stone (5A)			0.14
Type 1, Class A			0.11
Type 1, Class B			0.10
Type1 , Class C			0.08

Table 2.10
Base Course Structural Coefficients

Col. 1	Col. 2	Col. 3	Col. 4	Col. 5	Col. 6	Col.
Test Sec.	Des. SN	Design* Terminal Loading	Base Course Design (a_2) Str. Coeff.	SN	Calculated Terminal Loading	Str. Coe
1E	3.8	798,000	.20	4.3	1,645,000	.28
1W	3.8	798,000	.20	4.8	3,587,000	.37
2E	5.2	6,413,000	.44	4.9	4,301,000	.38
2W	5.2	6,413,000	.44	4.8	3,379,000	.37
3E	4.4	2,039,000	.44	4.6	2,920,000	.50
3W	4.4	2,039,000	.44	4.5	2,256,000	.48
4E	4.6	2,743,000	.34	4.0	1,122,000	.23
4W	4.6	2,743,000	.34	4.6	2,745,000	.34
5E	4.4	2,039,000	.30	4.4	2,141,000	.30
5W	4.4	2,039,000	.30	4.4	1,833,000	.30
6E	3.4	402,000	.14	4.5	2,294,000	.32
6W	3.4	402,000	.14	3.8	940,000	.20
7E	5.6	10,969,000	.30	5.0	4,721,000	.23
7W	5.6	10,969,000	.30	4.4	1,960,000	.15
8	4.7	3,172,000	.20	4.2	1,430,000	.11
9W	4.7	3,172,000	.20	4.0	1,096,000	.09

* The design terminal loading are based on the current NJDOT structural number in Table 2.9

Stabilized Base Course (Stone Mix) - The calculated base course structural coefficient for the bituminous stabilized base course stone mix (Test Sections 2E & 2W, and 3E & 3W) show coefficients that range from 0.37 to 0.50. In the AASHO Road Test, the regression coefficients for bituminous concrete ranged form 0.33 to 0.83 and were averaged to obtain a 0.44. If the calculated structural coefficients are averaged, the average coefficient is 0.43. However, the AASHO Road Test did not analyze bituminous concrete in the base course. Essentially, the AASHO Road Test coefficient of 0.44 was intended for use with top course.

Stabilized Base Course (Gravel Mix) - The calculated base course structural coefficient for the bituminous stabilized base course-gravel mix (Test Section 4E) is less than the design coefficient. This reflects the performance curve which was adversely affected by the large rutting. The bituminous stabilized base gravel mix in Test Section 4W is identical to the design structural coefficient. Indeed, considering the assumed errors in the performance curve, this is probably a chance occurrence

Pentration Macadam - The calculated base course structural coefficients for the asphalt penetration macadam (Test Section 5E & 5W) are also identical to design structural coefficients. In consideration of the assumed errors in the performance curves, this is also probably a chance occurence. However, in view of its rutting, cracking and deflection measurements relative to other sections, the structural coefficient may be reasonable. Since the NJDOT does not use this type of base course at the present, further discussion is not necessary.

Densely Graded Stone - The calculated base course structural coefficient for the densely graded stone (Test Section 6E & 6W) show higher calculated coefficients than the design coefficients. The design terminal

18 kip loadings appear low and the calculated terminal 18 kip loadings may not be reasonable because of error in the performance curves. The densely graded stone has relatively low rutting characteristics, but has high deflection and a high percentage of cracking. From the test section data, it is not possible to make any conclusions regarding these structural coefficients.

Cement-Treated Base - The calculated structural coefficient for the cement treated base (Test Section 7E & 7W) show lower calculated coefficients than the design coefficients. The estimated terminal 18 kip loadings are grossly inconsistent between Test Section 7E & 7W. The inconsistency is caused by the poor correlation between the performance curve and PSI data. Indeed, these two test sections have relatively low deflections, little or no cracking and relatively low rutting characteristics. The test sections are performing the "best" of all the experimental pavement sections.

Drybound Macadam (1962 Standard Section) - The calculated structural coefficient for the drybound macadam base course in Test Section 9W is lower than the design coefficient. Since the calculated structural coefficient is related to the performance curve, the low terminal 18 kip loading results in the low structural coefficient. However, an additional problem in the analysis is created when the bituminous concrete top course is assumed to have an equal coefficient to the bituminious stabilized base course which is above the drybound macadam. This misplaced layer may adversely effect the AASHO regression equation and adversely alter the structural coefficients.

2.7.3 Discussion of Results

The AASHO structural number equation (Equation #2) is a three layer regression relationship between layers. This three layer structural number equation was used to derive the structural coefficients of base course materials in the NJDOT experimental pavement project. Using this three layer equation, the layers of subbase material below the quarry processed stone and above the subgrade are ignored in the analysis of the NJDOT experimental pavement.

In the AASHTO design guides, which were a result of the AASHO Road Test, a regional factor and a soil support value were suggested to account for such difference from the original AASHO design concept. However, the use of the regional factor and soil support were never substantiated in the literature. The values are commonly used as safety factors in the pavement design. Essentially, to use these factors in an experimental pavement analysis would add significant statistical risk of error.

Factorial Experiment - In a factorial experiment such as the AASHO Road Test, numerous test section performance curves and resulting structural numbers would be averaged to obtain a single regression relationship for the structural coefficient. In the NJDOT experimental pavement, one non-factoral test section was available for the structural coefficient analysis. In essence, the results are hampered by this limitation.

Futhermore, research studies (Ref. 13) have demonstrated that structural layer coefficients vary with respect to the following factors:

1. Layer thickness
2. Layer location (A layer's location contributes to pavement life)

3. Traffic loadings

4. Material type and quality

5. Strain, stress and deflection of the pavement structure.

The layer coefficients are not constants, but were adopted by the AASHO Interim Guide as constants to facilitate pavement design.

Limitations of Data - Several additional limitations are evident in the NJDOT analysis of the AASHO Road Test structural number concepts. The single foundation soil of the test pavements in the AASHO regression analysis limits the application of the findings. The short duration of the AASHO test was not realistic for application to long term pavement design. The inadequate thickness of many AASHO pavements did not reflect realistic pavement layer combinations of the NJDOT experimental pavement. Most AASHO SN values were between 3 and 4, whereas NJDOT values are between 5 and 6. The single axle Load applications of the AASHO Road Test were different from the actual mixed traffic conditions of the NJDOT Experimental Pavement. Futhermore, the climatic conditions of the AASHO test differ from that of the NJDOT Experimental Pavement.

The purpose of the above discussion is to show the potential for errors in an analysis that attempts to fit experimental field data to a regression analysis with the above limitations. The overall aspects of the data from the NJDOT experimental pavement differ dramatically from the AASHO Road Test. Indeed, a high potential for a high risk of statistical error exists in the analysis of NJDOT experimental pavement data.

3.0 Elastic Layer Analysis

The purpose of this section is to describe the use of the elastic layer theory for the analysis of the NJDOT experimental pavement project

structural layer coefficients. At the suggestion of the Federal Highway Administration, the analysis uses the mechanistic procedures and computer modeling of the Viscoelastic Systems (VESYS).

3.1 Introduction

In the elastic layered theory, the pavement is represented as horizontal layers of uniform thickness and infinite extent in the horizontal plane as shown in Figure 3.1. The pavement rests on a subgrade layer which is infinite in the horizontal direction and semi-infinite in the vertical direction. The pavement layers are assumed to be isotropic, homogenous and to obey the in stress-strain relationship as represented by Hooke's Law. The load is uniformly distributed over a circular area. The layer material is characterized by the Modulus of Elasticity and Poission's Ratio.

For the uniformly loaded circular area shown in Figure 3.2, a cylindrical coordinate system is used to express the various equations for solution of stresses (Ref. 14). The cylindrical coordinates are described by the layered elastic computer programs as vertical (z), tangential (t) and radial (r).

In Figure 3.2, the element with faces parallel to the axial plane is used to describe the principal stresses. This element describes the nine stresses which exist as a result of the load and are comprised of three normal stresses (σ_z , σ_r , σ_a) acting perpendicular to the element face and six shearing stresses (τ_{ra} , τ_{ar} , τ_{rz}, τ_{za}, τ_{az}, τ_{za}) acting parallel to the faces. Under conditions of static equilibrium on the element, the shearing stresses become zero for vertical load conditions and the normal load conditions and the normal stresses are defined as principal stresses (Ref. 15).

Figure 3.1

Multilayered Elastic System

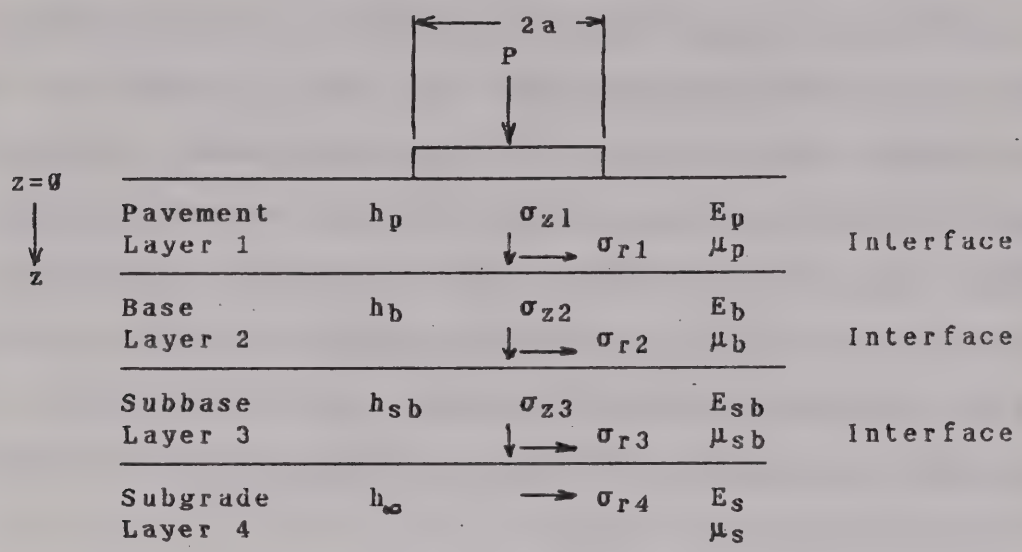

Where:

P	=	Load
2a	=	Diameter of loaded area
z	=	Vertical direction
r	=	Horizontal direction
h	=	Thickness of layer by subscript
E	=	Modulus of Elasticity
μ	=	Poisson's Ratio
σ_z	=	Vertical stress at layer subscript
σ_r	=	Horizontal (radial) stress at layer subscript

FIGURE 3.2

Uniformly Loaded Circular Area

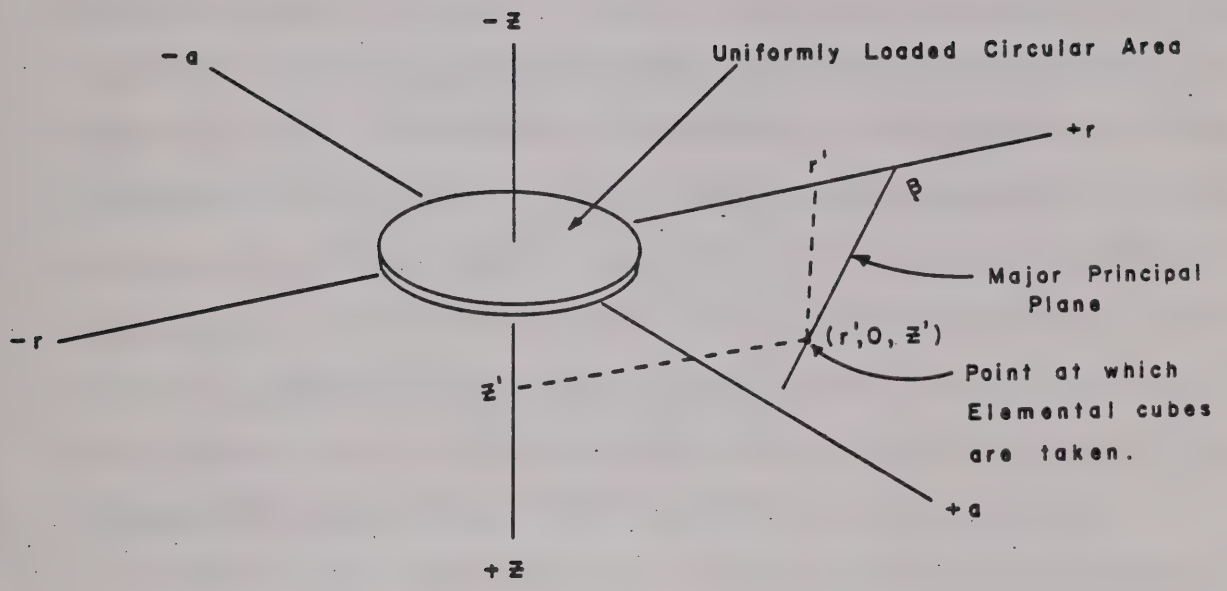

Stress on the Element

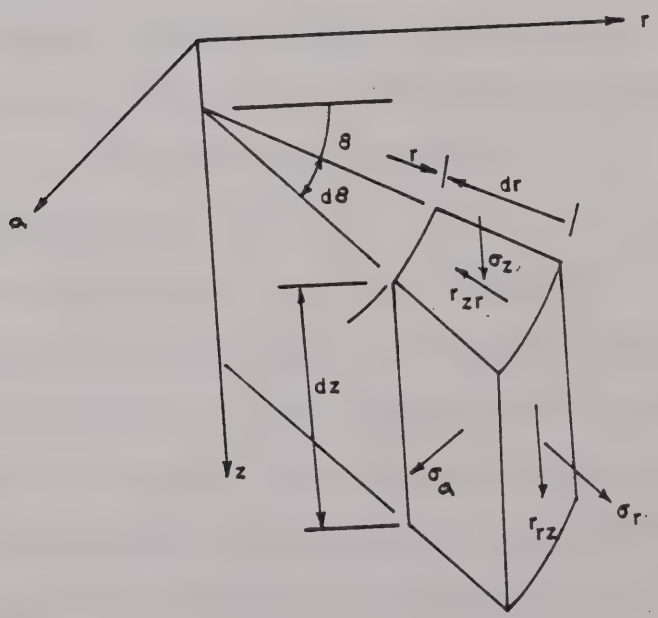

Figure 3.2 (continued)

Symbols and Signs for Stress Directions

r, a, z,	=	Cylindrical coordinates - positive to the right, outward and downward.
σ	=	Normal stress - positive for compression, letter subscript indicates axis parrallel to which the line of action of the stress.
τ	=	Shear stress - positive in positive quadrant and negative in mixed quadrant.
β	=	Angle of major principal plane

Donald M. Burmister (Ref. 16) presented the layered elastic theory to provide a basis for an understanding of the nature of the real phenomena of pavement response and to explain the fundamental relationship between the physical factors which control load-deflection relationships. The Burmister theory provides a working hypothesis regarding the basic functional form of the physical laws which control the stress-strain responses of the layered pavement system. This working hypothesis provides understanding and knowledge of the pavement response phenomena and provides the engineer with a competent scientific tool for interpreting, analyzing and evaluating stresses and strain in layered pavement systems. However, it must be realized that the very nature of such a working hypothesis can never become merely a routine matter, but must always be a matter of basic knowledge and understanding, and of common sense and judgement.

The Burmister equations explain the state of stresses and strains for the pavement system shown in Figure 3.1. The multi-layered equations are utilized in the VESYS computer program to define normal stresses. Due to space limitation, the equations are not reproduced here. However, M.G. Sharma (Ref. 17)shows the derivation of these equations.

3.2 VESYS Computer Program

The VESYS IIIA modeling of the New Jersey Experimental Pavement Project compared pavement response and damage-performance predictions to the observed historical deflections, rutting, cracking and PSI as discussed in the Performance Analysis section. The modeling techniques use the procedures of previous verification studies which are discussed in section 3.2.2 below. The modeling data are discussed in section 3.2.3.

3.2.1 Introduction

Developed by the Office of Research, Federal Highway Administration (FHWA), the VESYS pavement design procedure (Ref. 18) is based on the mechanistic structural subsystem. This procedure operates by evaluating a given design for its elastic layer response to expected loading and environment conditions.

The VESYS IIIA computer program predicts the performance of a pavement in terms of its Present Serviceability Index (PSI) as defined from the AASHO Road Test analysis. The computer program expresses the PSI in the form of roughness, cracking and rutting variables by using data from materials properties, geometry, traffic and environment.

The primary response model of the VESYS IIIA represents the pavement as a multi-layer system with the upper layers having a finite thickness and the bottom layer having semi-infinite depth. Each layer may be described by it elastic or viscoelastic properties. The materials in each layer are assumed isotropic and locally homogenous. The program assumes a single stationary circular loading at the pavement surface, complete shear (no slippage) at the interfaces and incompressibility of layer materials.

In the damage model, three closed-form probabilistic models represent the prediction for cracking, rutting and roughness. The fatigue cracking model assumes Miner's law for crack propagations. Miner's law postulates a linear accumulation of damage independent of the order in which loads are applied with no healing effects. The rutting model consists of a repeated loading deformation law that uses a built-in decay factor to determine the accumulated permanent strain. The rutting model uses deflection response which are calculated in the primary response model and permanent deformation characteristics which are inputed from laboratory tests. The roughness model predicts changes in longitudinal roughness in terms of

slope variance as defined by the AASHO Road Test. These changes are dependent on changes in the pavement's material properties (Modulus of Elasticity, permanent deformation characteristics) which are based on variations in temperature. The PSI performance model uses the AASHTO PSI equation to predict mean and variance of the PSI for selected periods.

3.2.2 Verification and Sensitivity Analysis of VESYS

The Vesys IIIA computer program is the result of eight predecessors which include VESYS IIM. The VESYS IIIA system was intended to correct the deficiencies noted by various researchers with the VESYS IIM discussed below. It is apparent from these studies that the VESYS pavement design system has definite potential for the analysis of flexible pavement systems and materials in that system. The verification and sensitivity studies indicate a fairly good agreement between observed data and VESYS pavement system. Since the VESYS IIIA computer program was revised to correct the deficiencies which are noted below, the use of VESYS IIIA computer program appears warranted for the New Jersey Experimental Pavement Project.

Rauhut, et al (Ref. 19) performed a comparison of VESYS IIM subsystem predictions to the results of the Brampton and AASHO Road Test performance. The comparison selected four sections from the Brampton Road Test and four overlayed sections from the AASHO Road Test. In the comparison with the results from the Brampton Road Test, the VESYS IIM predictions were good for the conventional pavement sections of crushed stone base and fair for the full-depth bituminous pavements. In the comparison with the results of the AASHO Road Tests, the predicted rut depths of the overlayed sections approximated the measured rut depth for three of the four sections. The PSI prediction appeared to perform rationally even though no definite conclusions were reached in the Rauhut study.

Another sensitivity analysis of the VESYS IIM program was conducted by Rauhut, O'Quinn and Hudson (Ref. 20). The analysis studied effects of fifteen independent input variables on the predicted performance of real pavements. The VESYS program contains a total thirty variables: preliminary screening eliminated fifteen of those variables Using a technique of "fractional factorials", the analysis developed interactions and main effects of the variables. The findings show that the fatigue life constants and factors controlling strain and traffic loadings are important to the prediction of cracking. The permanent deformation characteristics of the bituminous concrete and wheel loadings are very important in the predictions for rut depth, slope variance and pavement serviceability. Temperature was found to be fairly important to predict cracking, but not as important to predict rutting. In the VESYS IIIA, temperature becomes more important since the modeling of the permanent deformation coefficients are determined as a function of temperature.

The Utah Department of Transportation (Ref. 21) conducted a field verification and an implementation study of the VESYS IIM system. The study rationale was to develop a "rational" approach to pavement design that could give an indication of how new materials, mix designs (analysis of asphalt cements) and new procedures will perform in the field. The research approach was to use laboratory indirect tensile tests for the development of input variables in the VESYS predictive system and compare those results with yearly field data to provide an indication of the accuracy of the various predictive models.

The Utah DOT utilized an indirect tensile test apparatus similar to the device utilized by the NJDOT for resilient modulus testing of Marshall specimens. The advantage of using this test equipment is that input

variables such as modulus of elasticity values, permanent deformation characteristics and the fatigue tests can be simply and efficiently determined by using this method. With minor modifications in the testing procedure, all three variables can be obtained from the same sample; thus eliminating the costly use of beam samples for the fatigue testing.

The preliminary findings of the study indicate that the performance prediction models in the program appear adequate to predict field measurements. It was concluded that the predictions from VESYS were more accurate than those of Utah's modified AASHTO methods. Furthermore, it was concluded that the VESYS IIM program has potential for use in a design procedure in Utah.

Sharma, et al (Ref. 17) used VESYS IIM to relate the observed rutting, PSI and fatigue cracking at the Pennsylvania Test Track facility flexible pavements to corresponding values predicted by the computer program. The results indicated that the computer program did predict the relative magnitudes of these distress and performance indicators. However, it was recommended that modifications and improvements be made to the structural subsystem models for rutting, PSI and fatigue cracking. At the time of this report writing, Sharma's modification to these models have not been completed.

The Florida Department of Transportation (Ref. 23) conducted a verification and implementation study of the VESYS IIM computer program. The ultimate aim of the project was to generate information to calibrate and implement the VESYS program for the design of new pavements and analysis of new materials. The Chief-land Test Road Experiment was used for the comparison with the VESYS performance predictions. The experiment consisted of twenty-four pavement sections of varying base course materials

and thicknesses. Standard laboratory modulus of resilience and fatigue tests were conducted on test specimens. Field measurements included Benkelman beam deflections, PSI and traffic loadings.

In the Florida study, it was concluded that the VESYS IIM did predict cracking using the fabricated fatigue curves and modulus of elasticity values. The rut depth were fairly well predicted when compared with field observations. Pavement aging was found to be a significant factor in the prediction of performance since the fatigue potential of samples cut from the roadway was found to be much lower than the fatigue potential of laboratory fabricated beams.

The University of Nebraska-Lincoln conducted an evaluation and verification of the VESYS - IIIA computer program for two test sites in Nebraska (Ref. 24). (The VESYS IIM is indentical to the VESYS IIIA with the exception that materials are characterized by creep compliance in VESY IIM and by modulus of elasticity in VESYS IIIA). It was concluded that PSI prediction's were in good agreement with field measurements. Rut depth estimates from the model were lower than actual measurements but, essentially, were in agreement with field measurements. Cracking estimates were poor and underestimated measured fatigue cracking in the field.

Material characterizations (modulus of resilences) were performed by repeated load indirect tensile tests using Marshall test specimens. Fatigue characterizations were determined by indirect tensile tests. However, the tests greatly underestimated pavement fatigue life when compared to back calculated AASHO Road Test data.

The research studies of the VESYS computer program show that it has the ability to reasonably estimate rutting, deflections, cracking and PSI

for pavement design. However the program does require refinements as discussed above which are being incorporated into newer versions.

3.2.3 Input Variables

The input variables for the New Jersey VESYS IIIA computer program system are read from an input file. The variables are defined in the "Users Guide, August 30, 1980, Federal Highway Administration."

In the input subsystem of VESYS IIIA, the program integrates the n-layer primary response model of the previous VESYS G program with the expanded environmental characterization of the previous VESYS A program and inputs the layer modulus of elasticity by season.

The primary response model produces estimated values for stresses, strains and deflections in a n-layer viscoelastic system on the basis of input variables such as geometry, materials characteristics, and environment. The primary response model passes this information to the damage model where serviceability predictions are then made. The damage-performance values are fatigue cracking, rut depth predictions, roughness predictions and present serviceability index (performance) predictions.

3.2.3.1. Tire Pressures and Contract Area

As pressure on legislatures concentrates on increasing the gross vehicle weight, the associated increase in tire inflation pressures (loaded area of tire contact) are a concern of highway engineers who foresee the effects of these increases on pavement deterioration. Using tire models in pavement analysis, researchers (Ref. 24) have developed relationships that show a profound influence of these contact pressures on all aspects of tire and pavement performance.

These studies show that the effect of increased tire pressure was so great for weak base courses (such as densely graded stone and quarry processed stone) that the bituminous surface course was inable to carry the additional loads without significant short term deterioration. The only solution presented by the researchers was to increase thickness of stiffter surfacing to develop satisfactory fatigue lives.

The significance of this conclusion is that highway engineers must consider the increased tire pressure in pavement design. At the present, the AASHTO 18 Kip Load emperical design method does not account for the increase in contact pressure area. Being an emperical method, considerable road test research is necessary to accommodate this increase.

However, the VESYS computer program can accommodate the increase in tire pressures, and in VESYS IV (This is a latter version of VESYS IIIA), the various tire configuration and loading frequencies can be considered in the pavement design. In the VESYS IIIA computer modeling, the tire-pressure contact area is critical to accurate predictions.

The contact area of three sets of dual tires were measured during the Benkelman beam data collection. The areas varied from 112 to 128 square inches for 80 psi tires with an 18 kip axle load. The large variation of the contact area is attributed to the use of regular and radial tires.

In order to select the appropriate contact area and loading to model the AASHO Road Test 18 kip load with the VESYS program, Kenis (Ref. 18) suggests an average estimate of the radius of the circular loaded area of $r = 6.4$ inches and a load of 70 psi on the contact area. These values are consistent with measurements of 128 square inches for dual tires of an 18,000 pound load. The values are inputed into the VESYS computer program.

3.2.3.2 Material Characterizations

In the VESYS IIIA computer program pavement materials are characterized by the permanent deformation properties. The resilient modulus of bituminous materials depends on temperature, loading time, and mix characteristics. For input in the program, the resilient modulus of bituminous materials may be determined by indirect tensile tests. The resilient modulus of unbound granular materials may be determined by repeated load triaxial compression tests or predicted from conventional soil CBR tests.

Laboratory resilient modulus tests of the bituminous concrete mixes were made with the NJDOT resilient modulus device (Mark V) developed by Retsina Company. This data is shown in Table 3.1. Additional bituminous modulus data were obtained from extrapolated results of modulus of resilience tests by Penn State University. This data is shown in Figure 3.3

Unfortunately, funds were not available in this study to evaluate the dynamic properties of the granular base course materials. Therefore, it was necessary to use resilient modulus values of base course from previous NJDOT studies (Ref. 27) and modulus of resilience values which were calculated from CBR values by the relationship E = 1500 CBR (Ref. 28, 29). The values of the resilient modulus of the granular materials are shown in Table 3.2.

3.2.3.3 Poisson's Ratio

Poisson's ratio is the relationship of lateral strain (ϵ_z) to the axial strain (ϵ_x). It is experimentally derived from indirect tensile tests of bituminous mixes and triaxial compression tests of granular materials.

Table 3.1

NJDOT Resilient Modulus Values (Mr)*
(Pounds Per Square Inch)

	Stabilized Base	Binder Course	Bit. Top. Course	Bit. FABC Course
Sample #1	376,000	264,000	302,000	440,000
Sample #2	344,000	236,000	281,000	406,000
Sample #3	333,000	245,000	320,000	345,000
Average	351,000	248,000	301,000	397,000

*All data at room temperature 68° F.

FIGURE 3.3

MODULUS OF RESILIENCE DATA

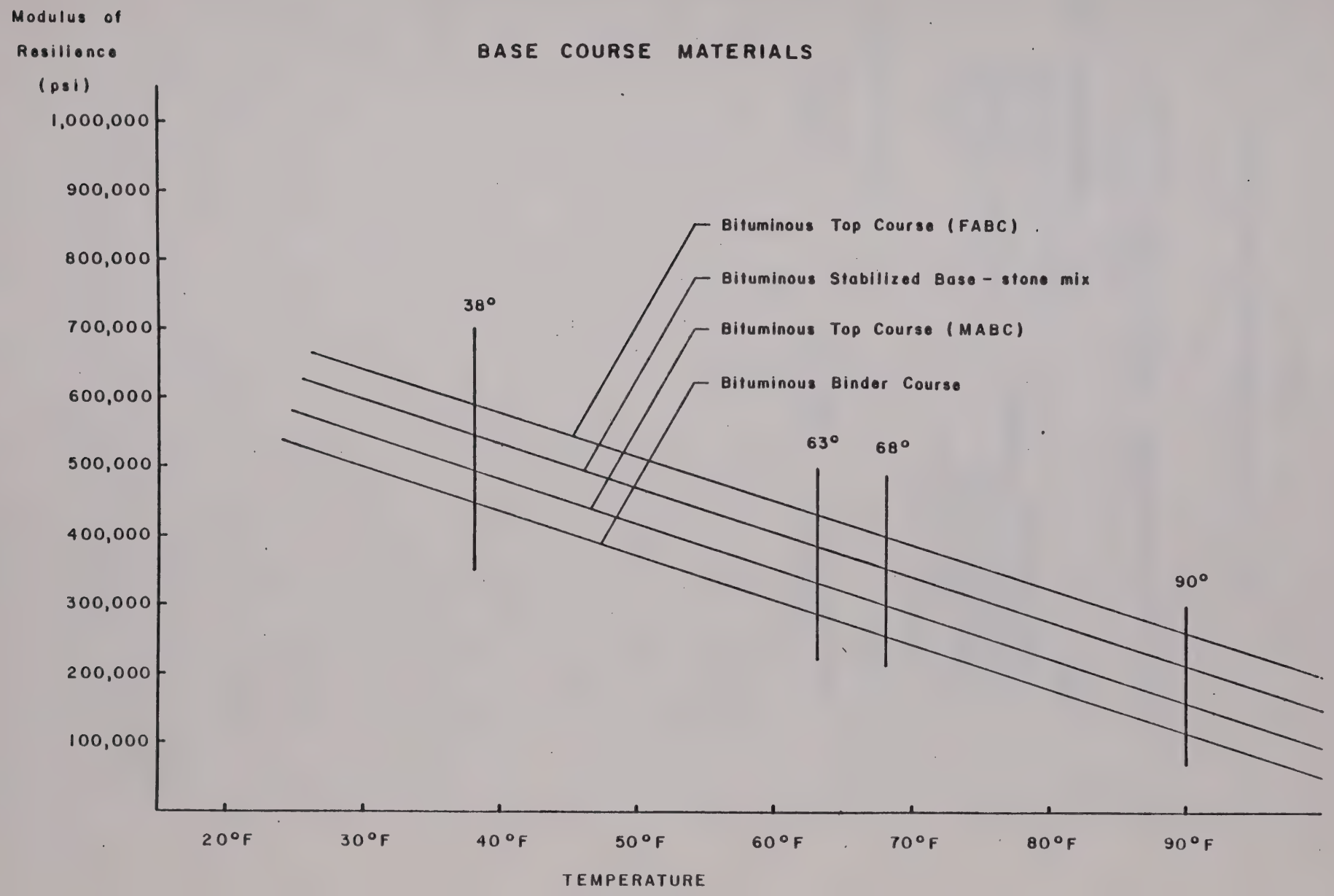

Table 3.2

Base Course Modulus of Resilient Values

for

Experimental Analysis of VESYS IIIA
(pounds per square inch)

Base		Suggest M_r. (Values)
Drybound Macadam		45,000
Asphalt Penetration Macadam		400,000
Densely Graded Stone		40,000
Cement Treated Base		2,000,000
Quarry Processed Stone		65,000
Average M_r. Value		
Subbase		(5) Average Values
NJDOT Spec. 1A	CBR = 49	73,500
Spec. 1C	CBR = 30	45,000

Table 3.3

Poisson's Ratio

Material	Poisson Ratio
Bituminous Concrete	.35
Unstabilized granular bases and subbases 5A, 1A, & 1C	.40
Cement Treated Base	.15

Experimentally derived Poisson's rato values were calculated by Barker (Ref. 27) to be 0.30 to 0.45 for NJDOT materials. However, the more conservative and widely used values (Ref. 30) of Table 3.3 will be used in this study.

For most pavement materials, the influence of Poisson's ratio for a given material is normally small. This allows for the use of typical assumed values for analysis rather than direct testing (Ref. 15).

3.2.3.4. Permanent Deformation Characteristics

Permanent deformation is defined as the plastic strain that is dependent on the state of stress and time loading. Permanent deformation properties are obtained with Incremental Static-Dynamic Tests (Ref. 18) which calculate the total permanent strain at the end of each unload increment and plots that strain versus the incremental time of loading. The best fit straight line through the points is constructed to determine the intersection with the vertical axis and the slope of the line. Permanent deformation characteristics are important input variable for the rut depth model and slope variance model (roughness).

The permanent deformation characteristics (Alpha & Gnu) were suggested by Sherwood (Ref. 29, 33) for the experimental pavement materials in the VESYS IIIA program. Graphs of these deformation characteristics are shown in Figures 3.4 & 3.5.

3.2.3.5. Fatigue

Fatigue is defined (Ref. 31) as a repetitive load-induced cracking in the bituminous surface layers due to a repeated strain below the ultimate strength of the material. The characterization of fatigue life for bituminous concrete pavements is developed by laboratory tests which employ simply supported small beams that are subjected to repetitive

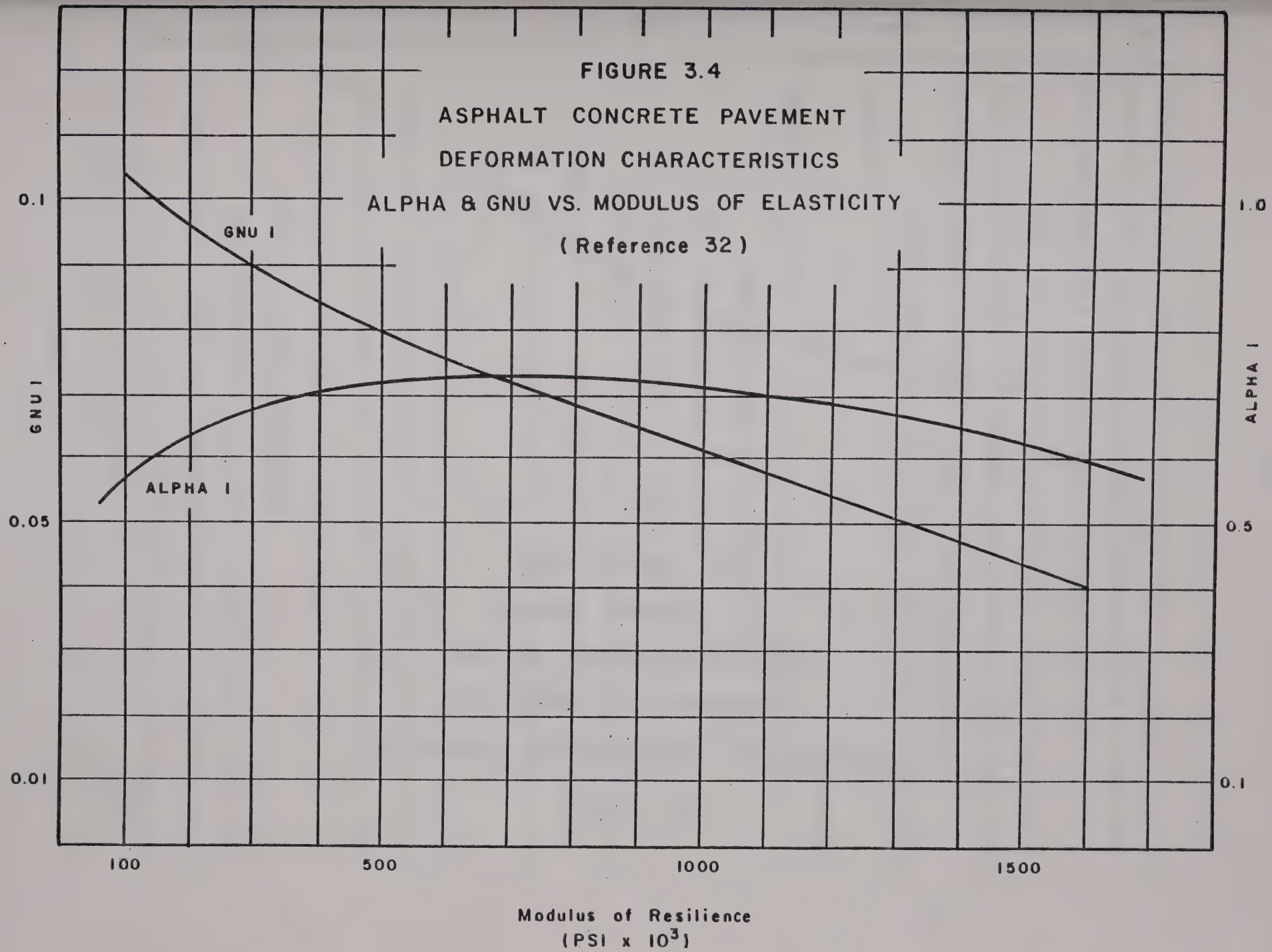
FIGURE 3.4
ASPHALT CONCRETE PAVEMENT
DEFORMATION CHARACTERISTICS
ALPHA & GNU VS. MODULUS OF ELASTICITY
(Reference 32)
GNU I
ALPHA I
0.1
0.05
0.01
1.0
0.5
0.1
100
500
1000
1500
Modulus of Resilience
(PSI x 10^3)

FIGURE 3.5

PERMANENT DEFORMATION COEFFICIENTS

OF GRANULAR MATERIALS

GNU VS. DEVIATOR STRESS

ASSUME ALPHA = .75

(REFERENCE 32)

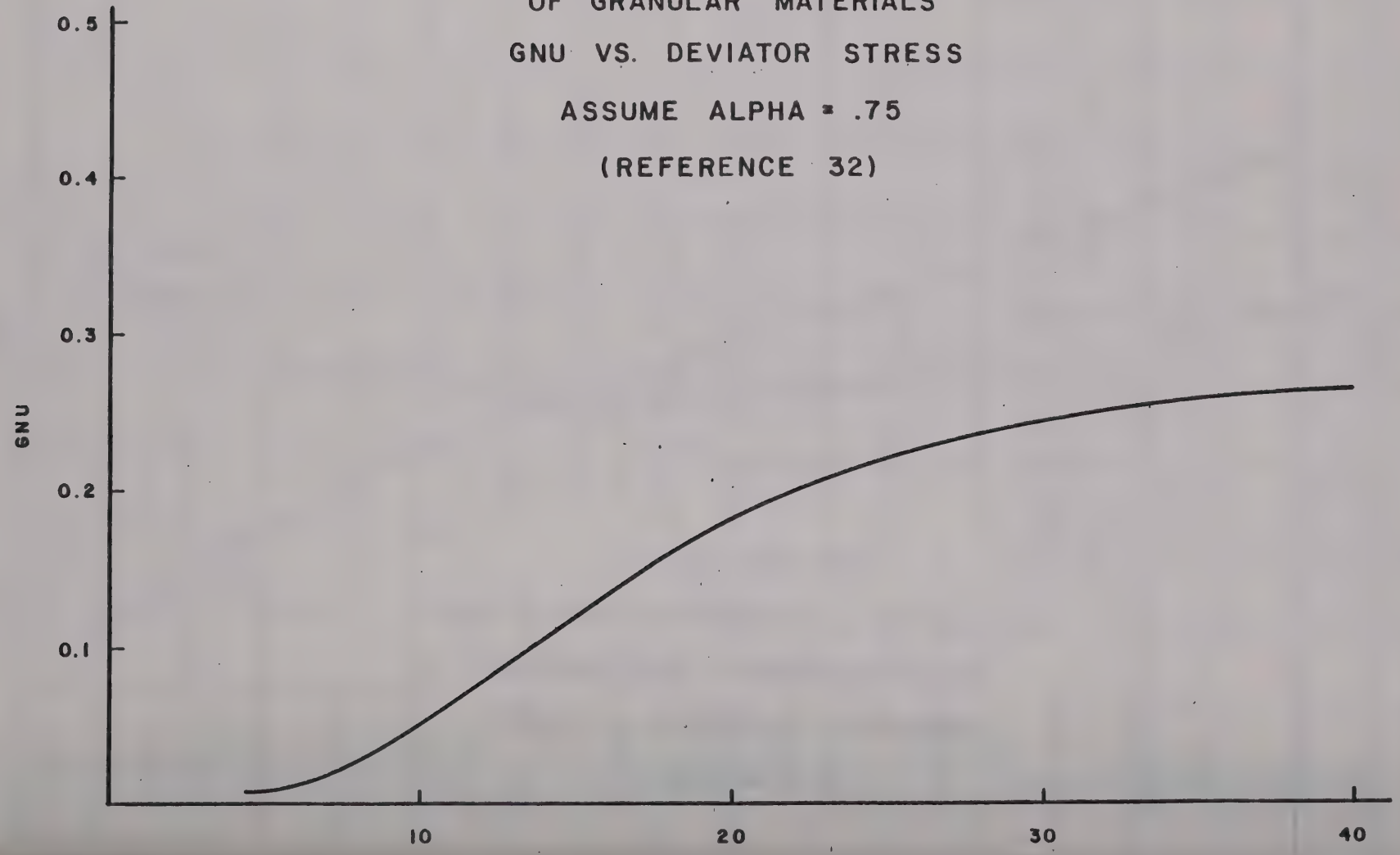

loading with either constant load or constant strain. A shortcoming of the laboratory beams tests is that frequently the tests do not simulate actual field conditions and a realistic crack propagation process.

The form of the fatigue relationships in the VESYS program is derived from a logarithmic relationship between strain at the bottom of the bituminous concrete layer and the number of load cycles to failure.

The following relationship is the general form of the fatigue equation:

$$N_f = K1 \ (1/\epsilon)^{K2} \qquad \text{Equation 5}$$

where: N_f = Number of load cycles to failure for a loading that results in a tensile strain (ϵ)

ϵ = Calculated strain under load

K1, K2 = experimentally derived constants

The constants of K1 and K2 depend primarily on material characteristics and temperature. It was suggested by Sherwood (Ref. 29) that K1 = 2.16×16^{13} and K2 = 4.995 for the experimental test Sections.

A sophisticated laboratory program is required to perform fatigue tests. However, Rauhut (Ref. 31) suggests that it is reasonable to select a fatigue relationship that is typical for bituminous concrete mixes and to modify that relationship on a rational basis.

3.2.3.6. Pavement Temperature

Since temperature is a major influence on the bituminous pavement response, VESYS inputs temperature changes in the top bituminous layer to a depth of two inches. Mean monthly pavement temperatures are inputed for the locality of the pavement.

Table 3.4

Mean Seasonal Temperatures

Newark, N.J.

(Mean of Typical 4 year period)

Winter		Spring		Summer		Fall	
Air	Pavement	Air	Pavement	Air	Pavement	Air	Pavement
32F	38F	53F	63F.	76F.	90F.	58F.	68.5 F.

Mean monthly air temperatures were obtained from Local Climatological Data from the National Weather Bureau Station at Newark, N.J. These temperatures are shown in Table 3.4.

The estimated mean monthly pavement temperature at a 2 inch depth was determined from a Pavement Temperature relationship developed by Witczak (Ref. 37) This relationship is shown in Figure 3.6.

3.2.3.7. Traffic Analysis

It is generally accepted that the AASHO Road Test equalivent load concept may not adequately define traffic volumes and axle weight distributions which significantly effect pavement life. Predictions of future traffic characteristics are extremely valuable to the pavement design engineer for the development of reliable designs. In the VESYS program, expected actual axle weight distributions can be inputed with mean traffic rate over a maximum 25 year period. Normal designs are for a 20 year period.

From W-4 Tables, which are supplied by the FHWA (not shown here), an estimate of the distribution of axle weights is obtained from an analysis of single and tandem axles. The mean of the axle weight distributions are calculated by relationships from Kenis (Ref. 18). The traffic rate specifies the average number of heavy truck axles per day for each incremental traffic and analysis period from the W-4 tables.

3.2.4 Predicted Response

Unfortunately, the predicted responses of the VESYS IIIA program with the limited experimental and literature generated input data did not successfully model the observed performance of the experimental pavement test sections with a any degree of confidence. Indeed, the observed performance of the test sections is questionable due to the erroneous

FIGURE 3.6

TEMPERATURE RELATIONSHIPS FOR SELECTED ASPHALT CONCRETE PAVEMENT THICKNESSES. (REFERANCE 31)

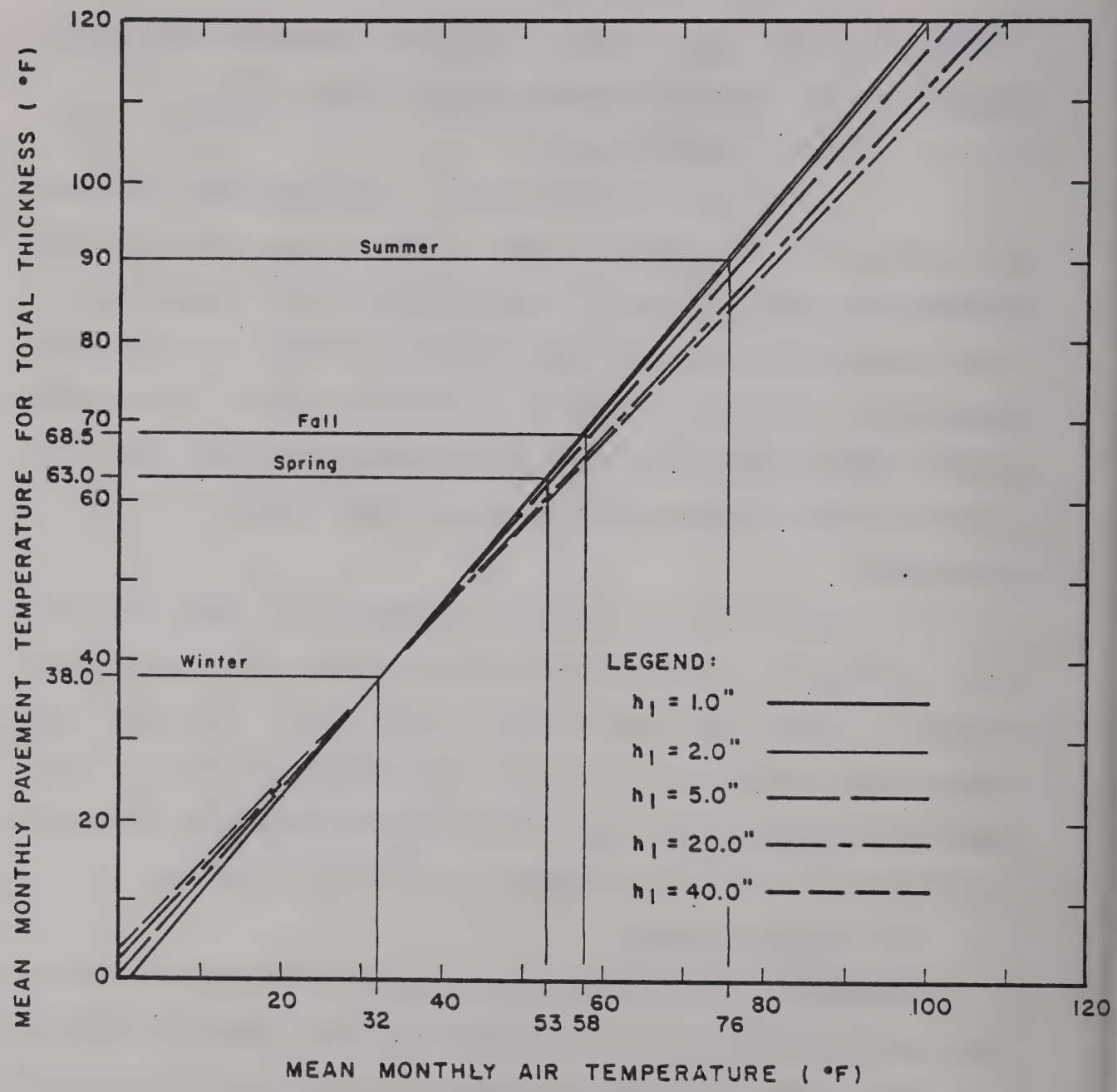

roughness data. It may well be that the VESYS program predicted reasonably close approximations to the expected pavement performance, but it was not possible with the given data to prove or disprove that hypothesis.

If the computer program had predicted the deflections and rutting with reasonable accuracy, the estimated values for modulus of resilience with permanent deformation characteristics could be reasonable. It would follow that the remaining roughness and PSI predictions could be reasonable.

3.2.4.1 Rutting

The predicted VESYS rutting are shown in Appendix F (Figures F1 through F9). The rutting predictions do not appear significantly similar to the observed values for a comparison.

3.2.4.2 Roughness

The predicted VESYS roughness was not compared with the experimental pavement data due to the erroneous nature of that field data as described previously.

3.2.4.3 Fatigue Cracking

The predicted VESYS fatigue cracking and cracking index were not compared to the experimental pavement data due to the inability to obtain a reasonable fatigue relationship from the literature or from experimental laboratory data.

3.2.4.4 Deflections

The predicted VESYS deflections are compared with the experimental pavement data in Table 3.5.

Sherwood (Ref. 29) suggests that the static deflection method which is used by the New Jersey Department of Transportation, will produce a higher deflection value by 0.002-0.003 inches than the VESYS predicted

Table 3.5

VESYS IIIA Predicted Deflections

	Test Section	Deflection from Figure 2.5 (inches) E'bd	W'bd	Predicted Fall
1.	Drybound Mac.	.0122	.0144	.0114
2.	6" Stab. base (Stone)	.0095	.0092	.0069
3.	4" Stab. base	.0095	.0112	.0078
4.	Slab. base (Gravel)	.0128	.0117	.0071
5.	Asph. Pene. Mac.	.0127	.0150	.0067
6.	Den. Grad. Stone	.0162	.0160	.0118
7.	Cement Treated base	.0086	.0094	.0062
8.	MA-BC Surface	.0102	----	.0097
9.	FABC - Surface	.0114	.0132	.0093

values. The difference is attributed to the VESYS deflection model which uses a haversine curve to model the load on the bituminous materials.

Due to the nature of the modulus of resilience data, confidence in the deflection prediction is low. However, the predictions for the drybound macadam, bituminous stabilized base, and cement treated base may be somewhat reasonable, which indicates that the modulus of resilience values are ballpark estimates. The deflection predictions for the other test sections indicates that the modulus of resilience values may not be reasonable estimates.

3.2.4.5 Performance

The predicted VESYS performance (PSI) is not compared to the experimental pavement data due to the misleading nature of the roughness data which has the greatest influence on the PSI value.

REFERENCES

1. "The AASHO Road Test, Report 5 - Pavement Research", Highway Research Board Special Report 61E, 1962.

2. Irich, P.E. and R. W. Hudson, "Guidelines for Satellite Studies of Pavement Performance", National Cooperative Highway Research Program Report 2A Highway Research Board, 1964.

3. Croteau, J. R., "Pavement Riding Quality", New Jersey Department of Transportation, Research Report 74-001-7713, April 1974.

4. Vitillo, N., Personal Correspondence, New Jersey Department of Transportation, April 1986.

5. Croteau, J. R., "Pavement Roughness Evaluations using a Mays Ride Meter", New Jersey Department of Transportation, Research Report 82-003-7776, June 1981.

6. Smith, R. E., and M. I., Darter, S. M. Herrin, "Highway Pavement Diskes Identification Manual for Highway Condition and Quality of Highway Construction Survey", Federal Highway Administration, March 1979.

7. Baker, R. F., and J., Quinn, "New Jersey Experimental Pavement Project - 9th Interim Report"., New Jersey Department of Transportation, 1971.

8. "Proposed AASHTO Guide for Design of Pavement Structures", NCHRP Project 20-7/24 National Cooperative Highway Research Program, March 15, 1985, pg. 1-12.

9. Nelson, T. L., and R. V., CeClerc, "Development and Implementation of Washington State's Pavement Management Systems", Washington State Department of Transportation, September 1982.

10. Liddle, W. J., and G. M., Jones, Peterson, D. E. Peterson, "Predicting Performance of Pavements by Deflection Measurements", Utah State Highway Department 1969.

11. Vaswani, N K., "Design of Flexible Pavements in Virginia Using AASHO Road Test Results", Highway Research Record 291, Transportation Research Board 1969,

12. Dunn, H. C., and E. S., Lindow, T. D. Larson, "Pavement Performance and Pavement Distress as Determinats of Base Course Structural Equivalences: Volumes 8", Pennsylvania Department of Transportation Project 71-7, October 1974.

13. Gomez, M., and M. R., Thompson, "Structural Coefficients and Thickness Equivalency Ratios", University of Illinois, Interim Report No. UILU-ENG-83-2009, June 1979.

14. Ahlvin, R. G., and H. H. Ulery, "Tabulation Values for the Determination of the Complete Pattern of Stresses, Strains and Deflections, Highway Research Board, HRB Bullentin 342, 1962.

15. Yoder, E. J. and M. W. Witczak, "Principles of Pavement Design", New York: John Wiley and Sons, Inc. 1975.

16. Burmister, D.M., "The General Theory of Stresses and Displacements in Layered Systems and Applications to the Design of Airport Runways", Proceedings of the Highway Research Board, Washington, D.C. Vol. 23, 1943.

17. Sharma, M. G., and E. S. Lindow, H. Recart, T. D. Larson, "An Evaluation of Pennsylvania's Flexible Pavement Design Methodology Volume 1: Flexible Highway Pavement Design - The State of the Art", Commonwealth of Pennsylvania, Department of Transportation Report PTI 7504, 1973, pages 86-95.

18. Kevis, W. J., "A Design Method for Flexible Pavements Using the VESYS Structural Subsystem", Fourth International Conference Structural Design of Asphalt Pavements", University of Michigan, Volume I, 1977.

19. Rauhut, J. B., and R. G. G. Hass, T. W. Kennedy, "Comparison of VESYS IIM Predictions to Trampton/AASHO Performance Measurements", Fourth International Conference Structural Design of Asphalt Pavements, University of Michigan, 1977.

20. Rauhut, J. B.and C. O'Quinn, W. R. Hudson, "Sensitivity Analysis of FHWA Structural Model VESYS IIM", Fourth International Conference Structural Design of Asphalt Pavements, University of Michigan, 1977.

21. Anderson, D. I, and J. C. McBride, D. E. Peterson, "Field Verification of the VESYS IIM Structural Subsystem in Utah", Fourth International Conference Structural Design of Asphalt Pavements, University of Michigan, 1977.

22. Sharma, M. G., and W., J., Kenis, T. D. Larson, W. L. Grambling, "Evaluation of Flexible Pavement Design Methodology Based on Field Obsevations at PSU Test Track", Fourth International Conference Structure Design of Asphalt Pavements, University of Michigan, 1977.

23. Sharma, J. and L. L. Smith, B. E. Ruth, "Implementation and verification of Flexible Pavement Design Methodology" Fourth International Conference Structural Design of Asphalt Pavements, University of Michigan, 1977.

24. Sneddon, R. U., "Evaluation and Verification of the VESYS IIIA Structural Design System for Two Test Sites in Nebraska", University of Nebraska - Lincoln, January 1986.

25. Roberts, F., and B. Rosson, "Effects of Higher Tire Pressures on Strain in Thin ACP Pavements", Texas Transportation Institute, 1985.

26. Sharma, M. G., Personal Communications, April 1986.

27. Barker, W. R., and R. C. Gunkel, "Improved Drainage and Frost ACtion Criteria for New Jersey Pavement Design, Phase III: Structural Strength of Pavment with Open Graded Bases", U.S. Army Engineer Waterways Experiment Station, Vicksburg, Missouri, 1979.

28. Huckelom, W. and C. R. Foster, "Dynamic Testing of Pavement", Proceedings, ASCE, Vole. 86, 1960.

29. Sherwood, J., Federal Highway Administration, Personal Communications.

30. Transportation Research Board, Special Report 162: "Test Procedure for Characterizing Dynamic Stree-Strain Properties of Pavement Materials", Washington, D.C. 1975.

31. Rauhut, J. B., and T. W. Kennedy, "Characterizing Fatigue Life for Asphalt Concrete Pavements", Brent Rauhut Engineering, Inc., Austin, Texas, 1981.

32. Witczak, M. W., "Design of Full Depth Asphalt Airfield Pavements, The Asphalt Institute, April 1972.

33. Sherwood, J., "Verification and Examples of Damage Predictions", FHWA.

Appendix A

Material Gradations

Quarry-processed stone* - conforming to the following gradation:

Sieve Size	% Passing
2"	100
3/4"	55-90
No. 4	25-60
No. 40	15-30
No. 200	5-12

Dry-bound Macadam - consists of large stone aggregate and stone screening conforming to the following gradation:

Stone Aggregate		Screenings	
Sieve Size	% Passing	Sieve Size	% Passing
3-1/2"	100	3/4"	100
3"	85-100	1/4"	40-100
2-1/4"	0-45	30	25-65
1-1/4"	0-5	200	5-20

Bituminous-stabilized base* - soil aggregate conforming to the following gradation:

Sieve Size	% Passing	
	Stone Mix	Gravel Mix
1-1/2"	100	100
3/4"	55-90	65-100
3/8"	---	50-90
No. 4	25-60	35-75
No. 10	20-50	25-60
No. 40	15-30	12-30
No. 80	---	6-20
No. 200	5-12	3-8
Bit.	4-7	4-7

Penetration macadam* - large aggregate is 2-1/2 inch size and the choke aggregate is 5/8 inch or 1/2 inch size. The bituminous binder is an asphalt cement, grade 85-100 or 100-120.

Sieve Size	% Passing
3-1/2"	100
3"	85-100
2-1/4"	0-45
1-1/4"	0-5

Densely-graded stone base - conforming to the AASHTO gradation shown below:

Sieve Size	% Passing
1-1/2"	100
1"	90
3/4"	80
1/3"	68
No. 4	50
No. 40	21
No. 200	11

FA-BC* - (fine aggregate bituminous concrete) - Top course conforms to the following gradation:

Sieve Size	% Passing
1"	90-100
1/2"	60-88
1/4"	58-80
No. 10	56-63
No. 30	39-52
No. 50	30-33
No. 80	13-37
No. 200	9-21
Bitumen Content	5.5-9

MA-BC* - (medium aggregate bituminous concrete) - Top course conforms to the following gradation:

Sieve Size	% Passing
1"	75-90
1/2"	65-80
1/4"	55-60
No. 10	46-53
No. 30	35-41
No. 50	23-31
No. 80	15-22
No. 200	11-14
Bitumen Content	5-8

Bottom* (Binder) is the second course of FA-BC-2 or MA-BC-2 conforming to the following gradation:

Sieve Size	% Passing
1-1/2"	65-100
1"	30-40
1/2"	20-30
1/4"	15-20
No. 10	9-14
No. 30	0-7
No. 50	0-7
No. 80	1-7
No. 200	1-2
Bitumen Content	4-6

*These specifications are from the "1961 - Standard Specification."

** AASHO Specification

FIGURE B1
Plot of Roughness and 18 Kip Loads
Test Section 1E

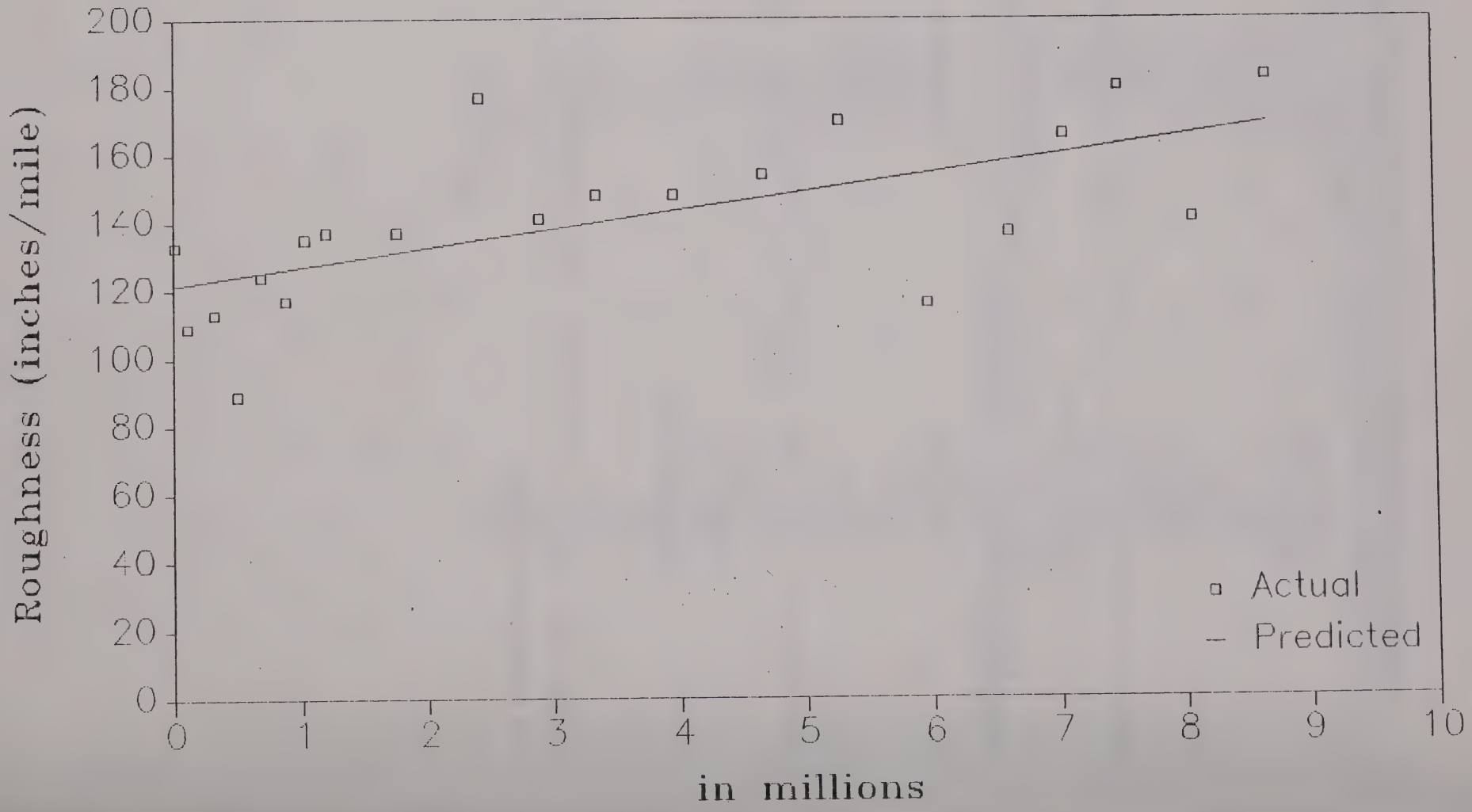

FIGURE B2
Plot of Roughness and 18 Kip Loads
Test Section 1W

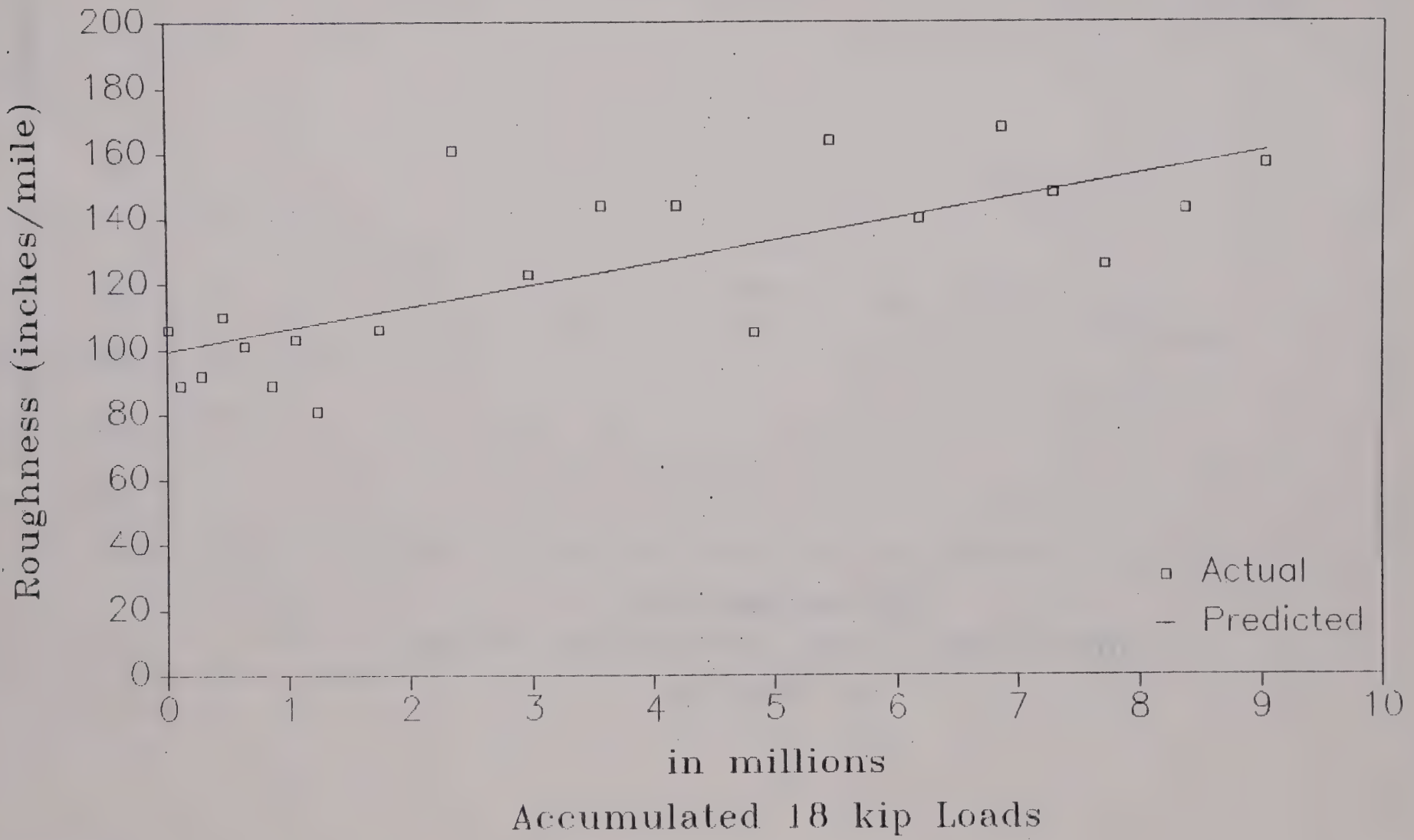

FIGURE B3
Plot of Roughness and 18 Kip Loads
Test Section 2E

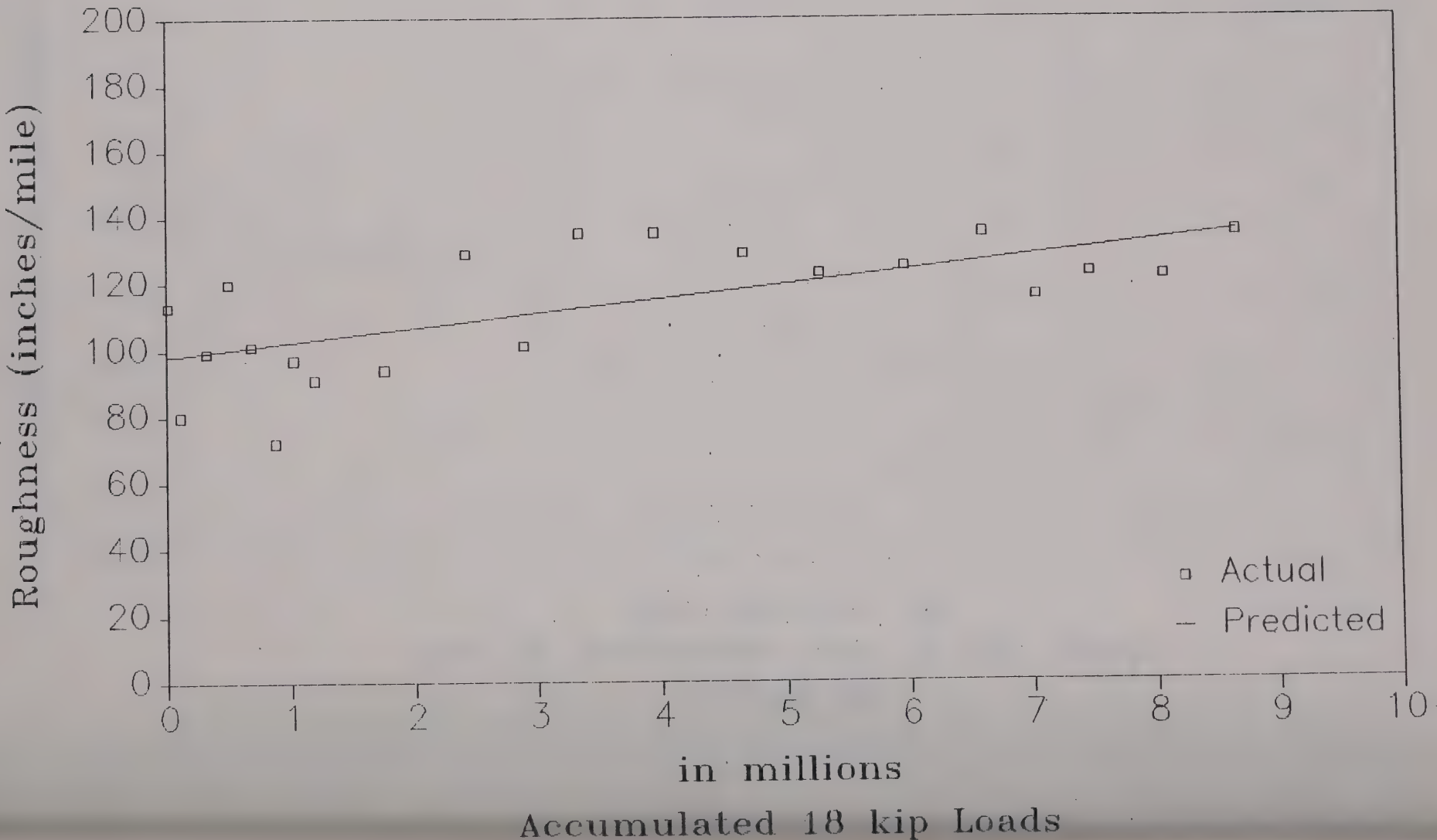

FIGURE B4
Plot of Roughness and 18 Kip Loads
Test Section 2W

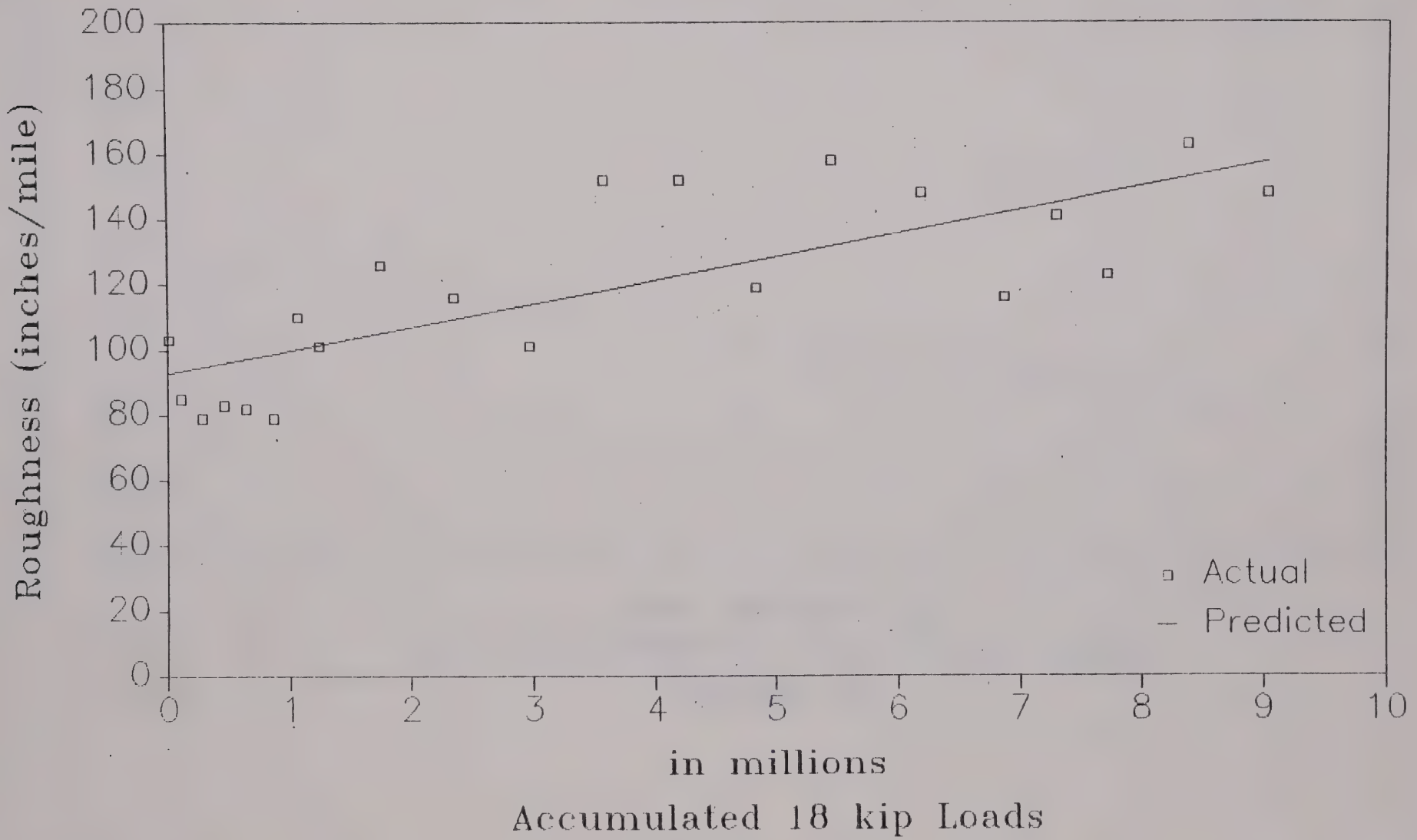

FIGURE B5
Plot of Roughness and 18 Kip Loads
Test Section 3E

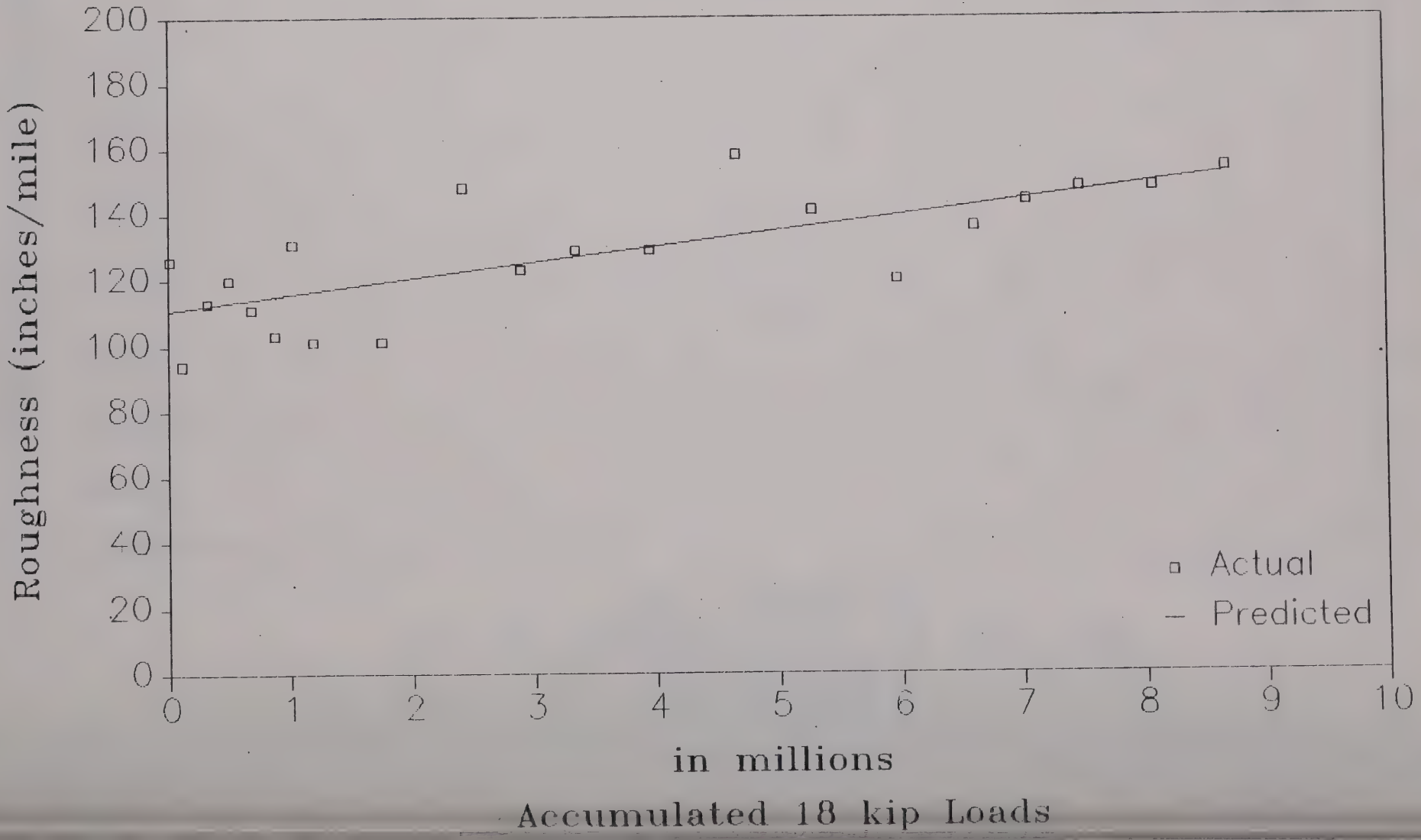

FIGURE B6
Plot of Roughness and 18 Kip Loads
Test Section 3W

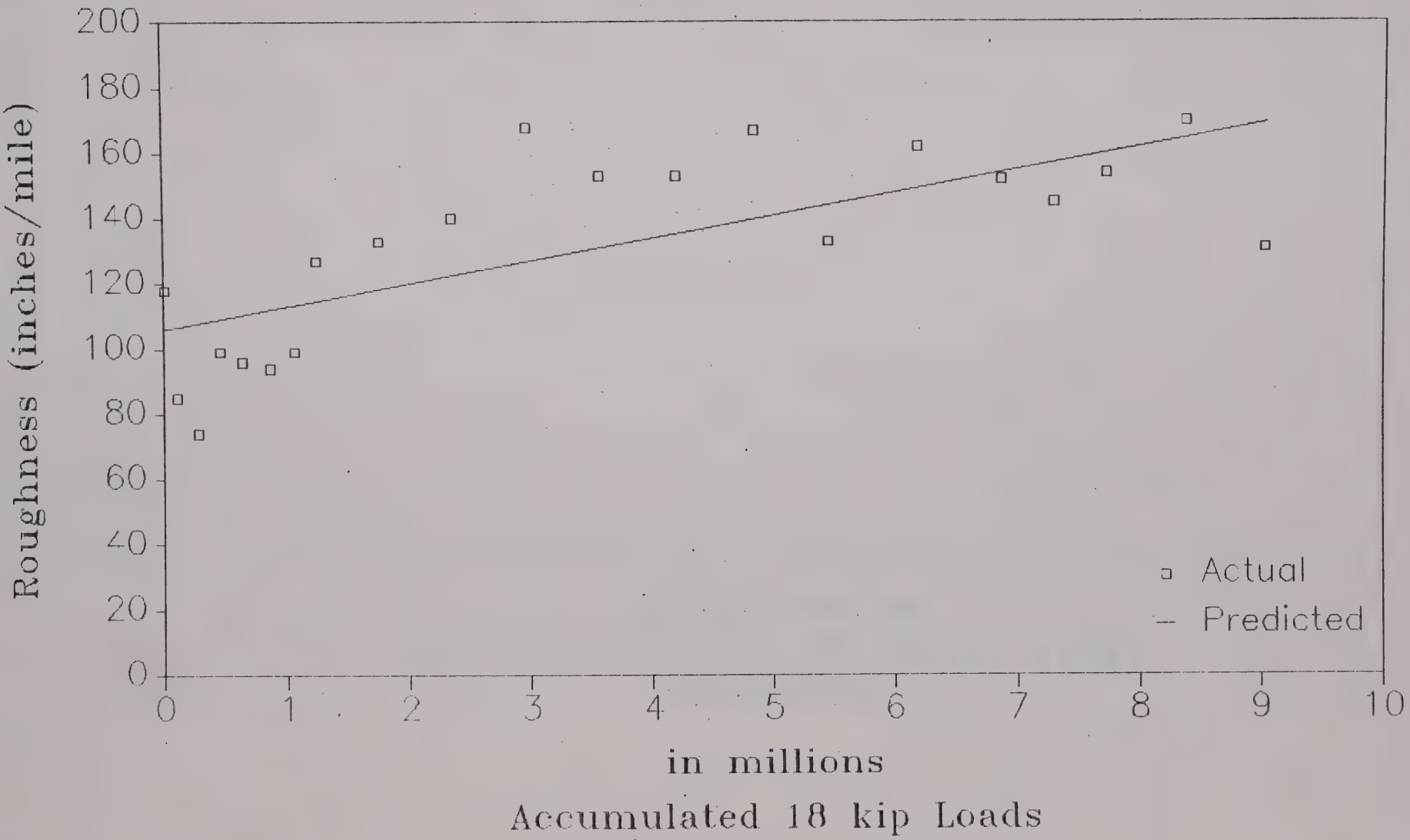

FIGURE B7
Plot of Roughness and 18 Kip Loads
Test Section 4E

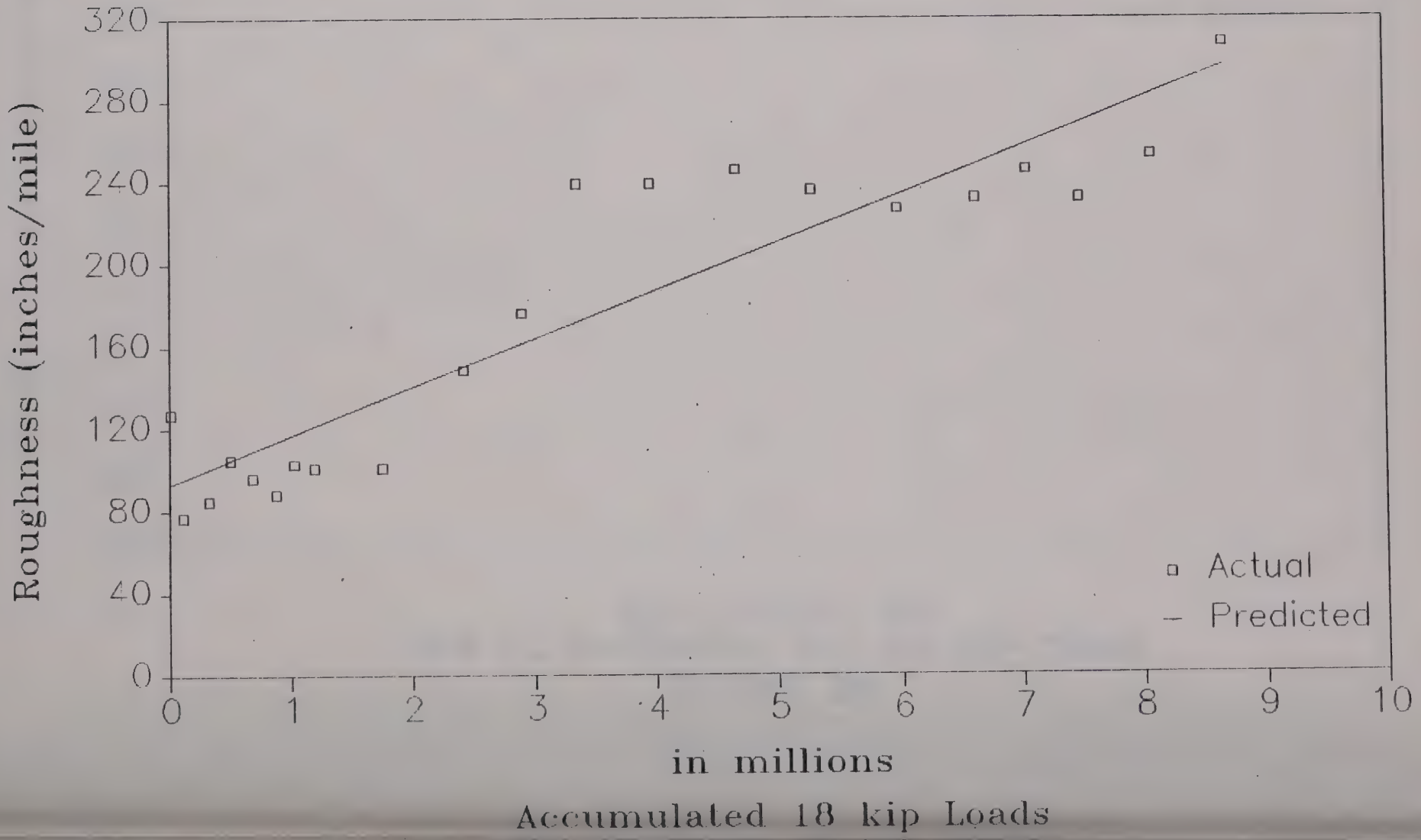

FIGURE B8
Plot of Roughness and 18 Kip Loads
Test Section 4W

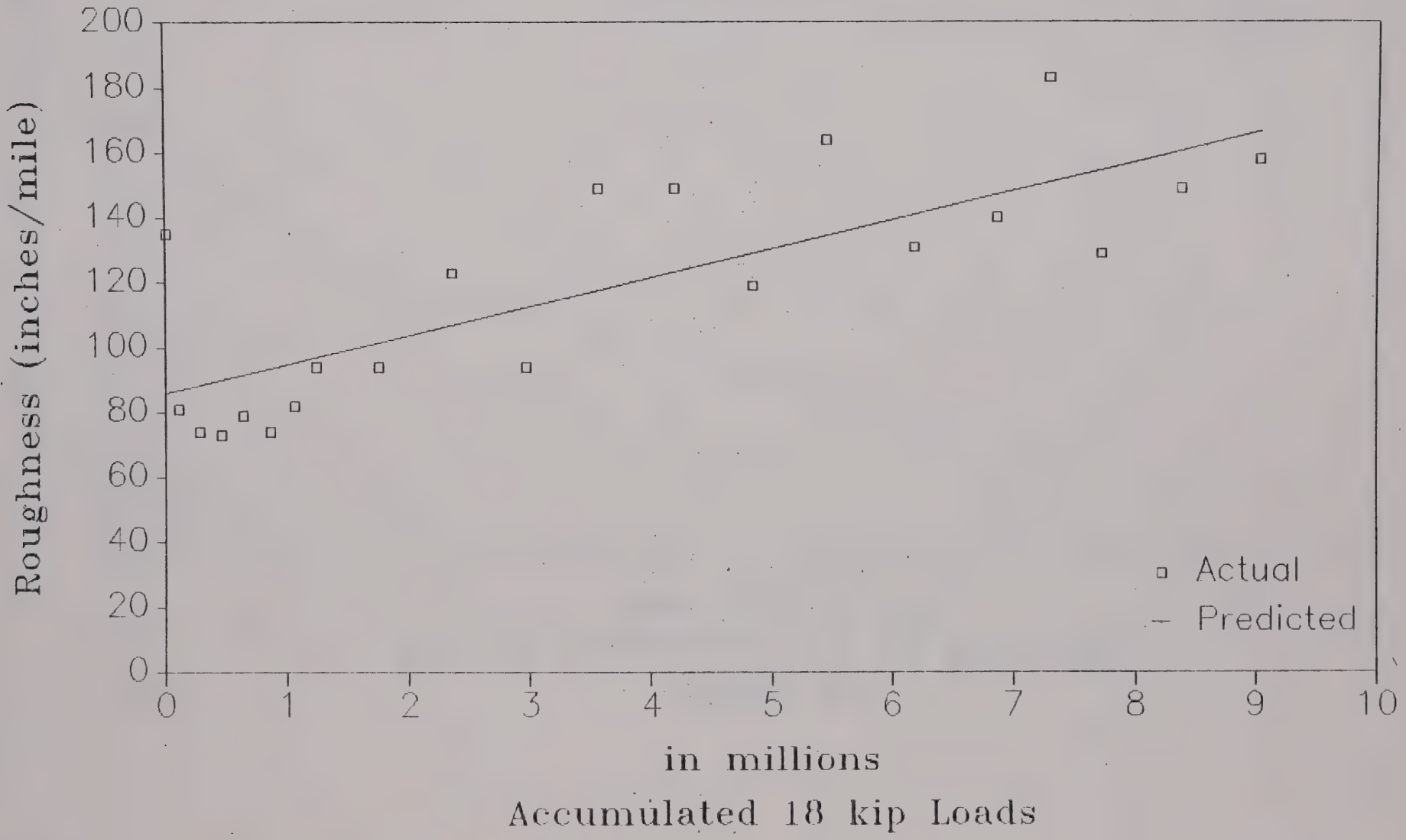

FIGURE B9
Plot of Roughness and 18 Kip Loads
Test Section 5E

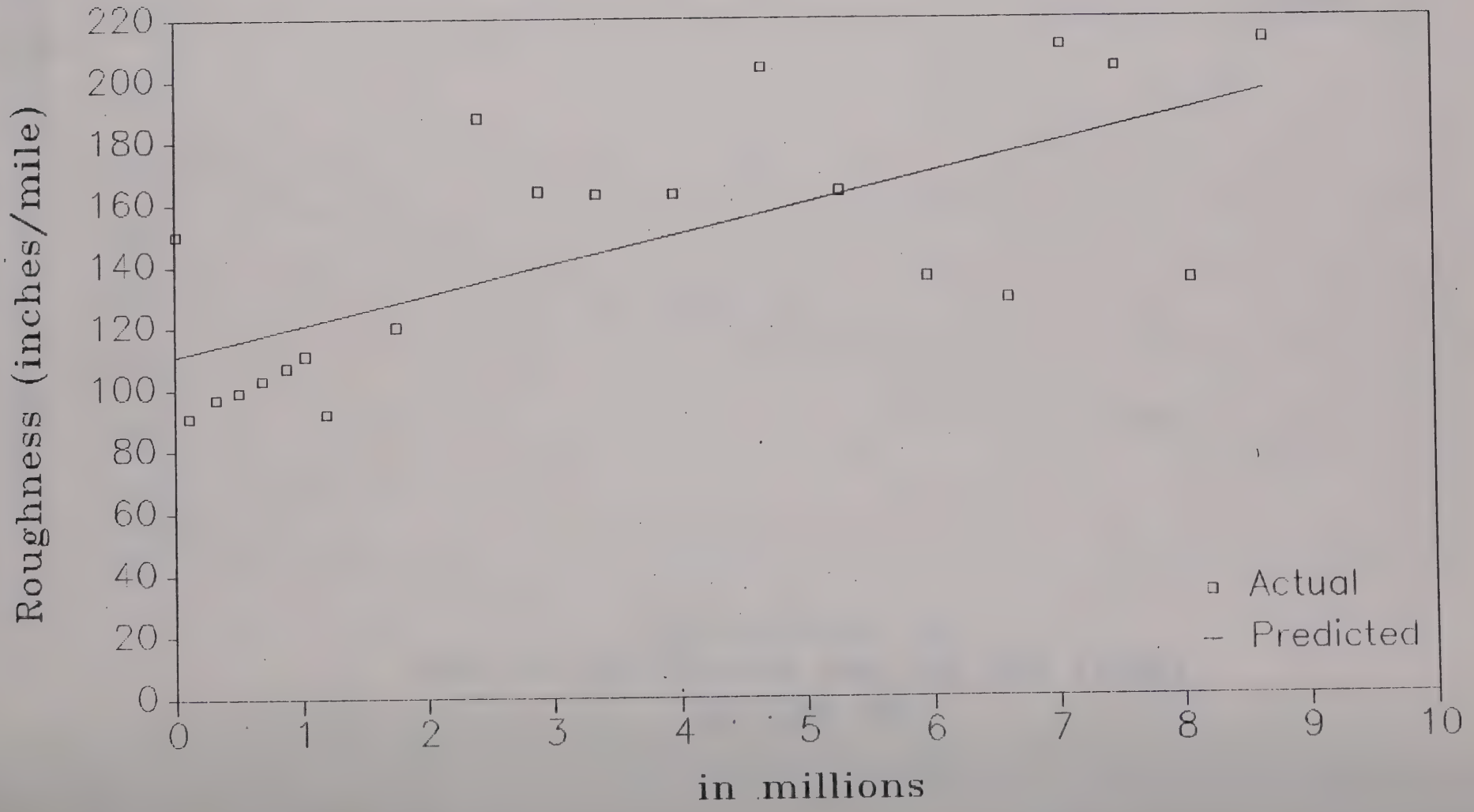

FIGURE B10
Plot of Roughness and 18 Kip Loads
Test Section 5W

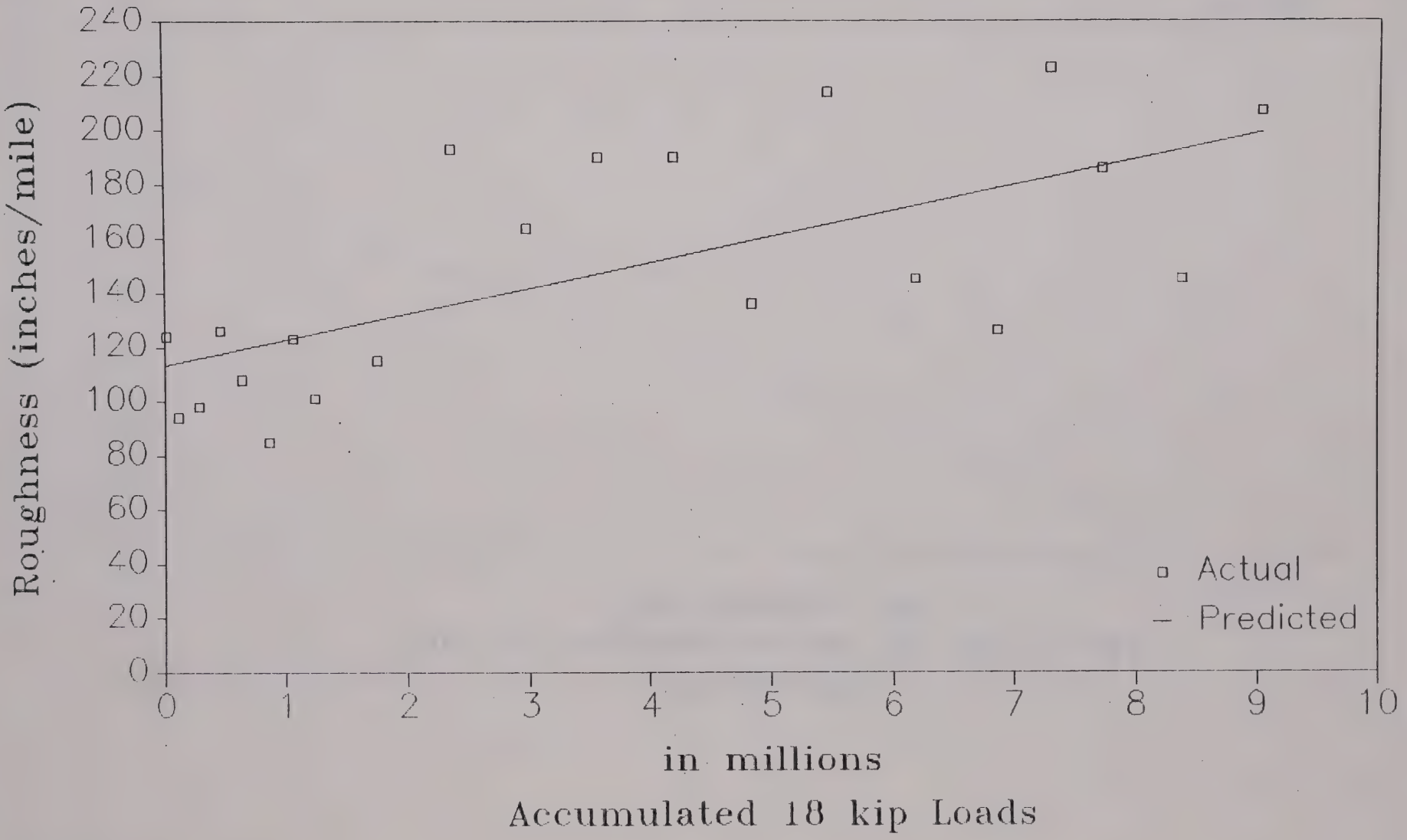

FIGURE B11
Plot of Roughness and 18 Kip Loads
Test Section 6E

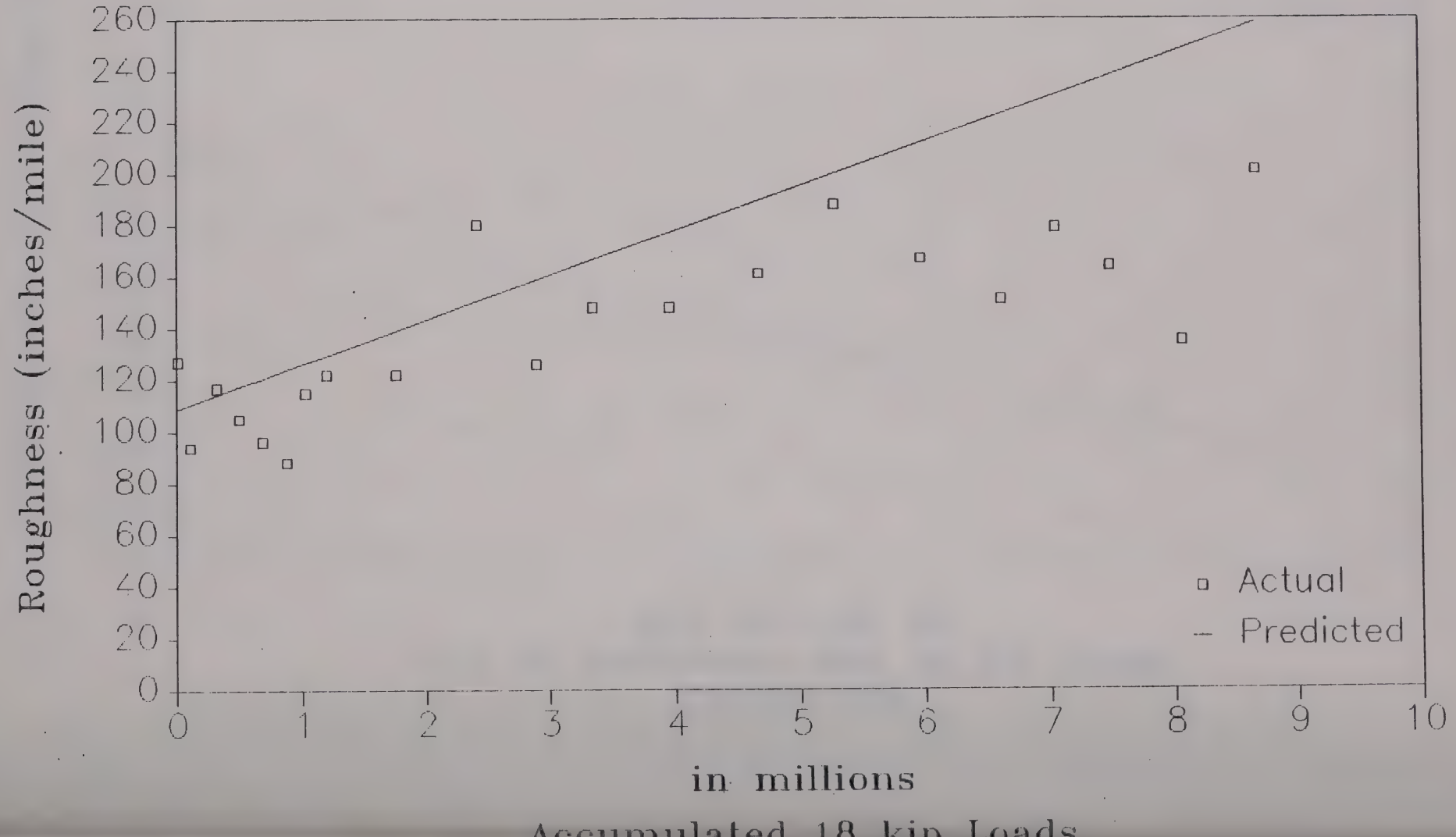

FIGURE B12
Plot of Roughness and 18 Kip Loads
Test Section 6W

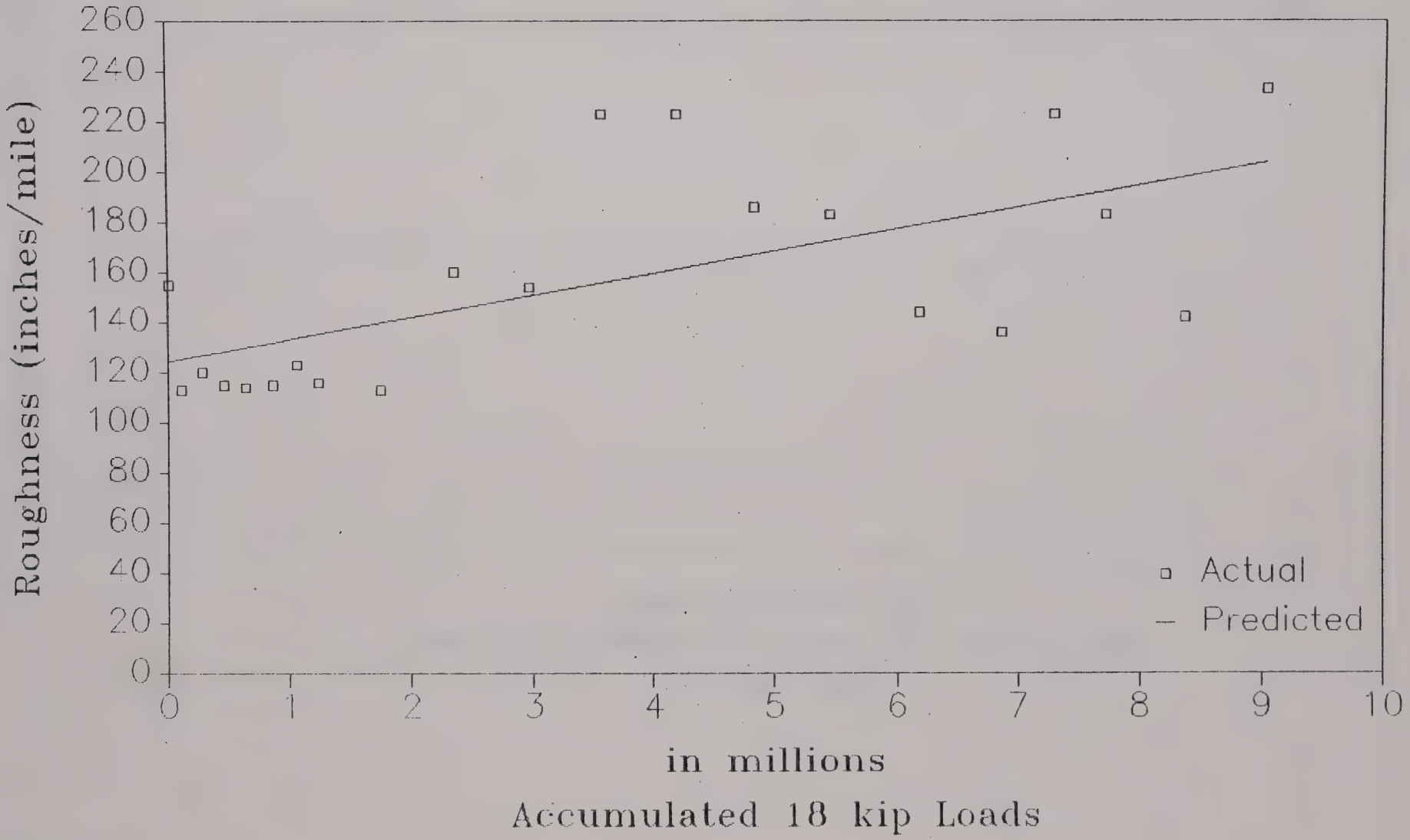

FIGURE B13
Plot of Roughness and 18 Kip Loads
Test Section 7E

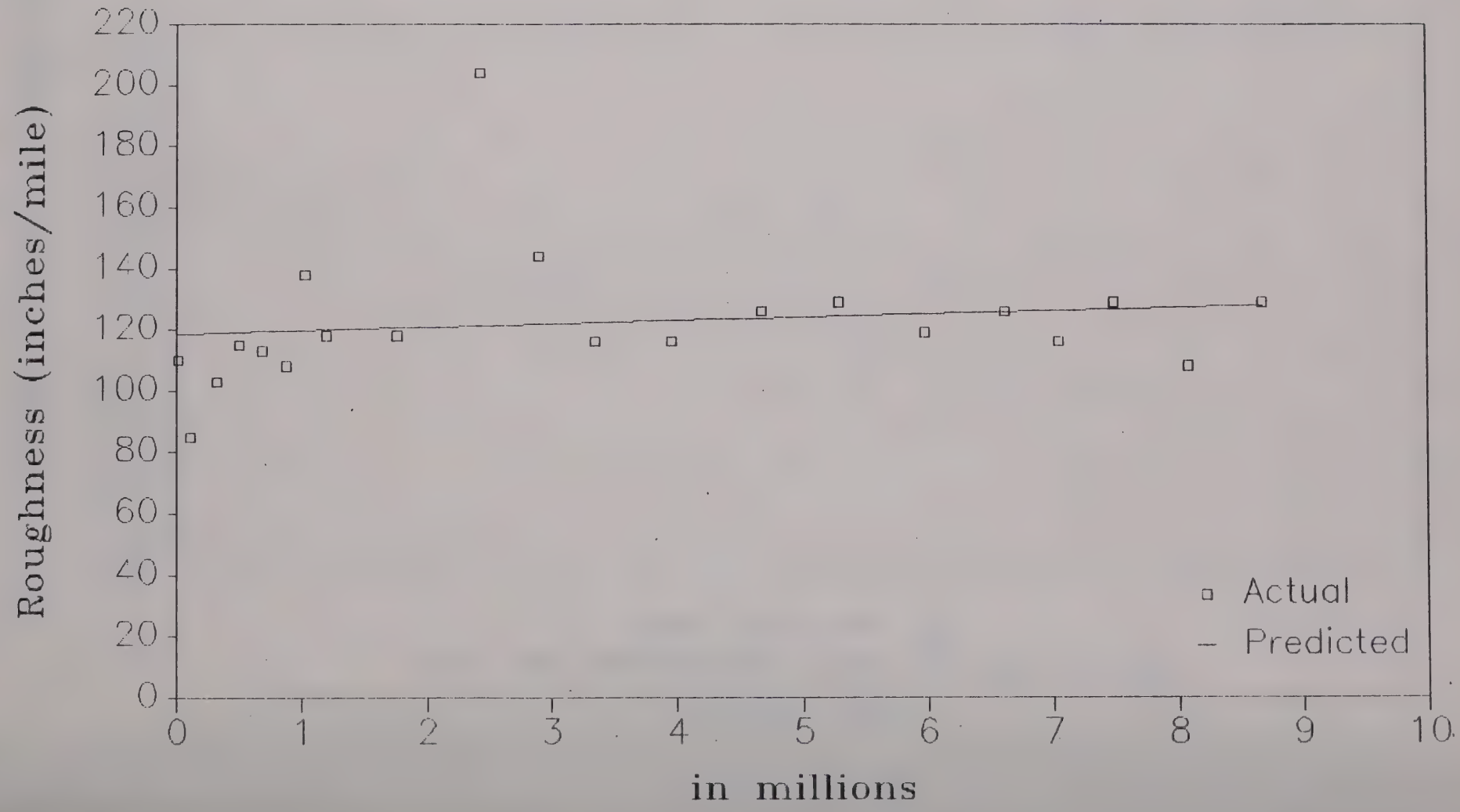

FIGURE B14
Plot of Roughness and 18 Kip Loads
Test Section 7W

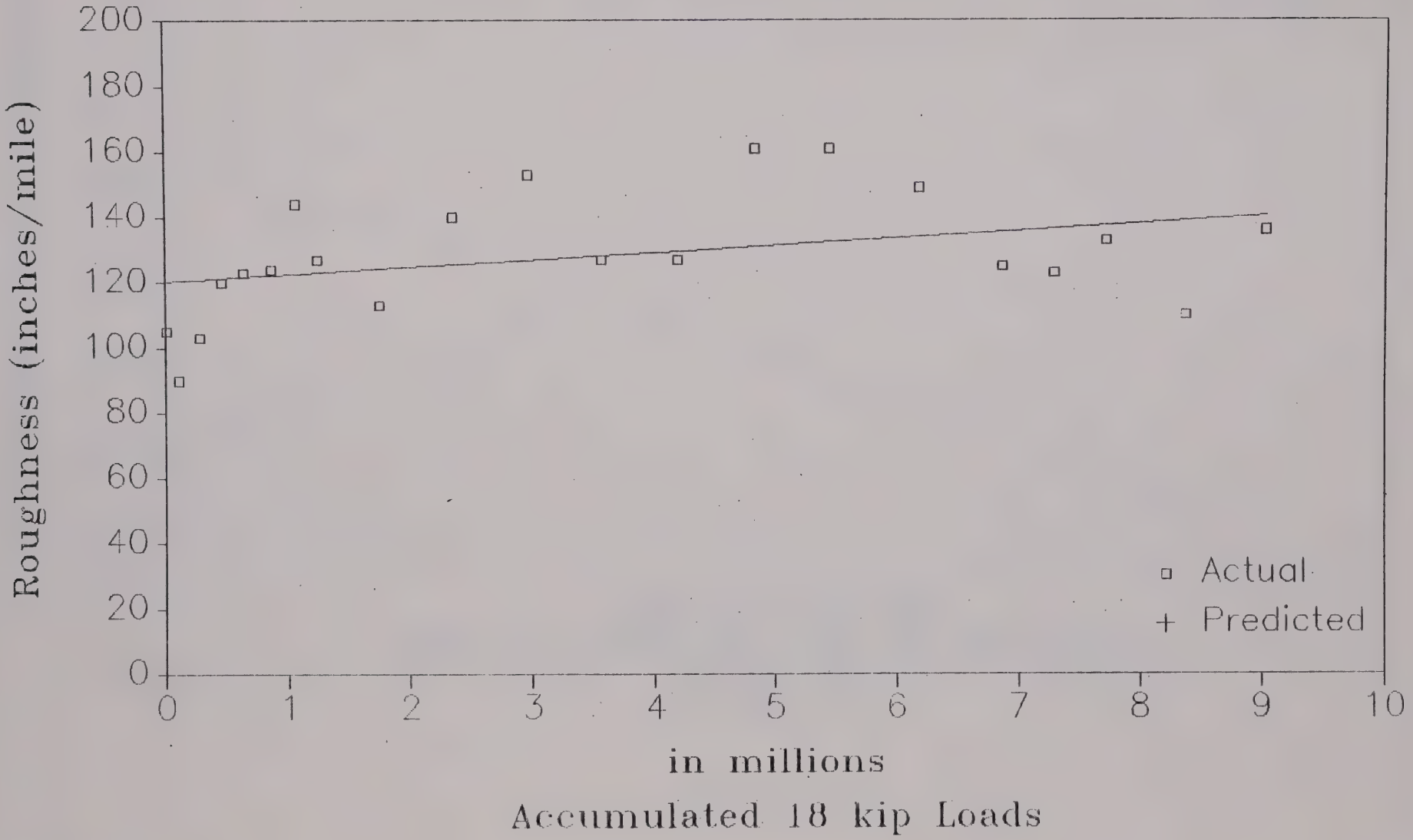

FIGURE B15
Plot of Roughness and 18 Kip Loads
Test Section 8E

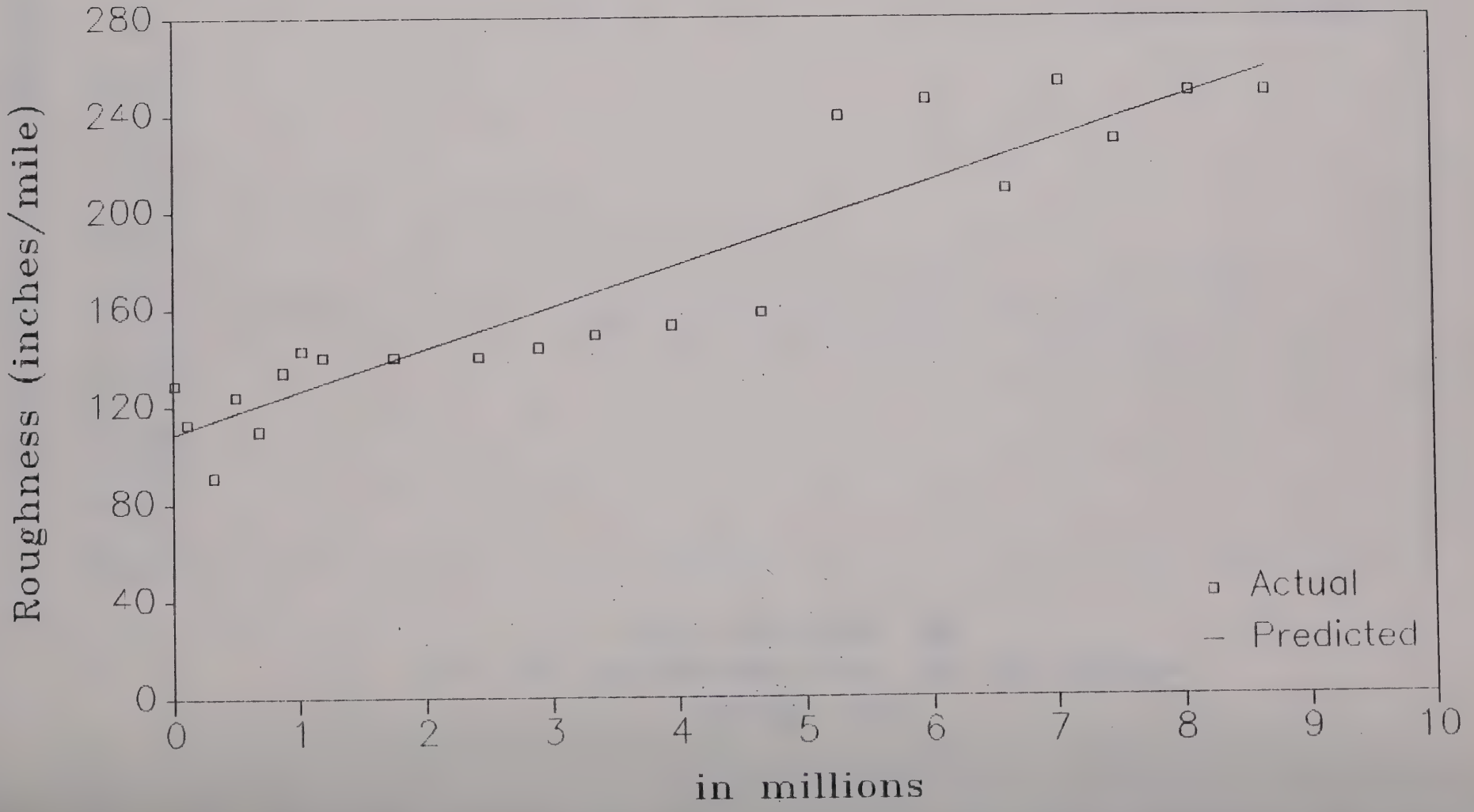

FIGURE B16
Plot of Roughness and 18 Kip Loads
Test Section 9W

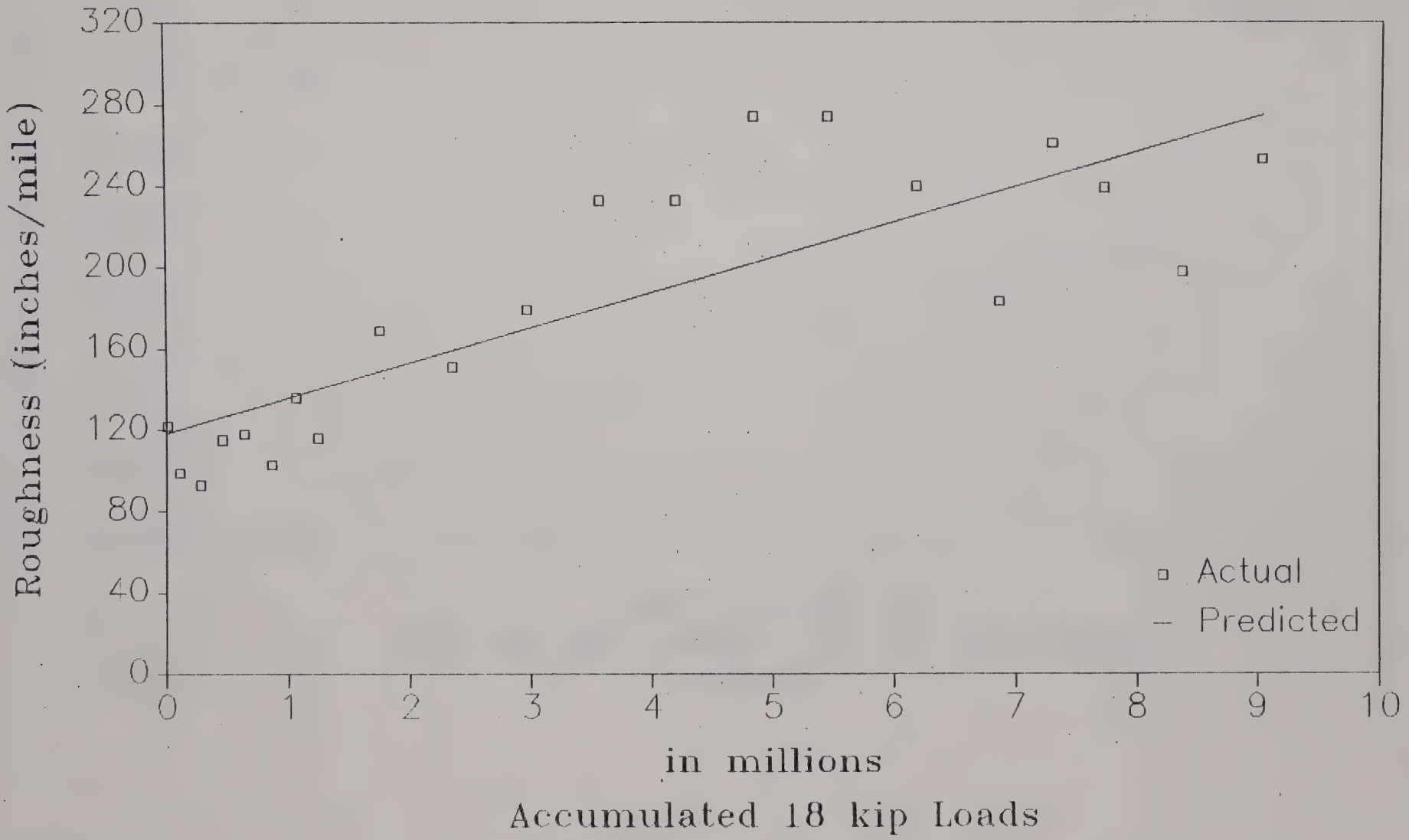

FIGURE C1
Plot of Rut Depths and 18 kip Loads
Test Section 1E

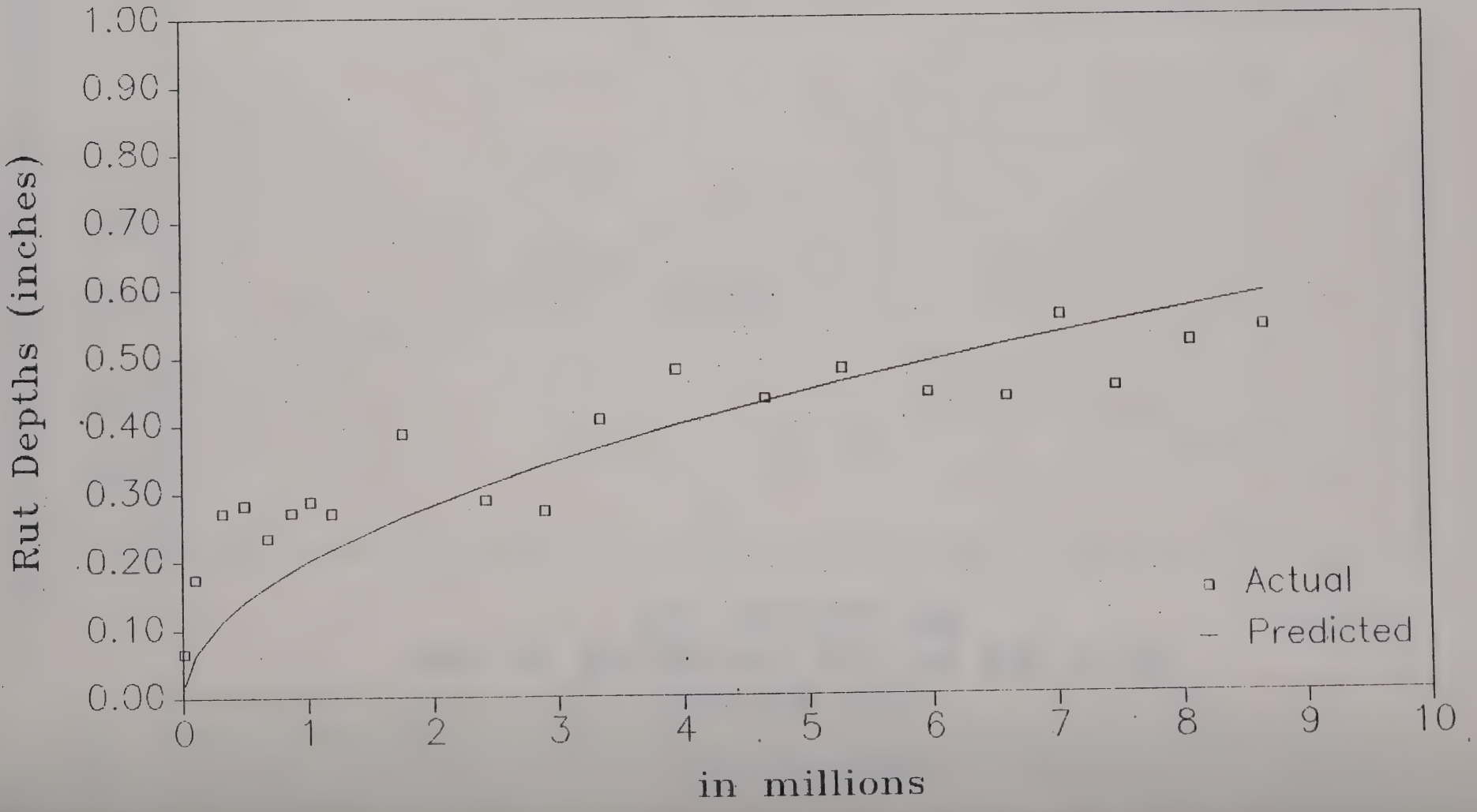

FIGURE C2
Plot of Rut Depths and 18 kip Loads
Test Section 1W

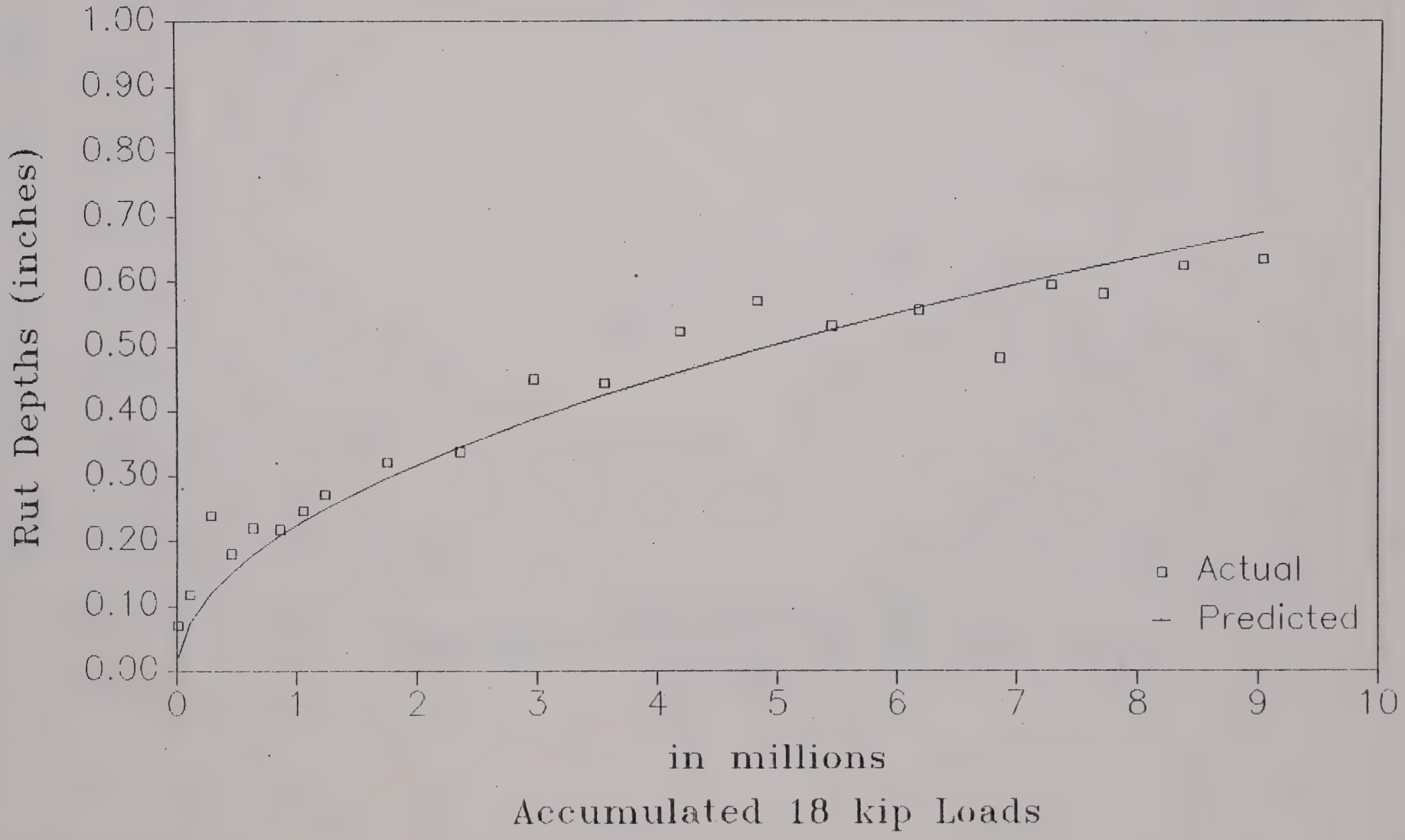

FIGURE C3
Plot of Rut Depths and 18 kip Loads
Test Section 2E

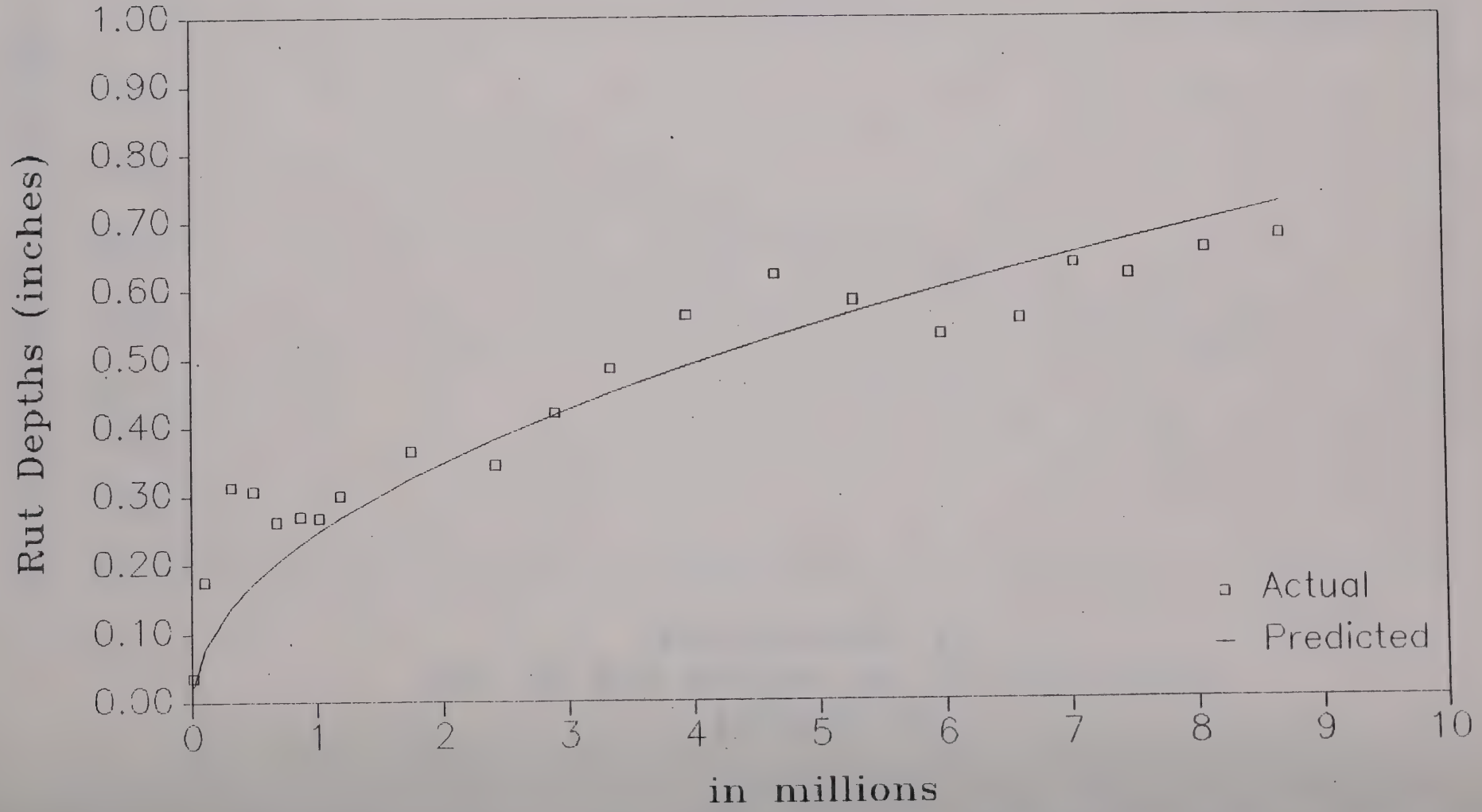

FIGURE C4
Plot of Rut Depths and 18 kip Loads
Test Section 2W

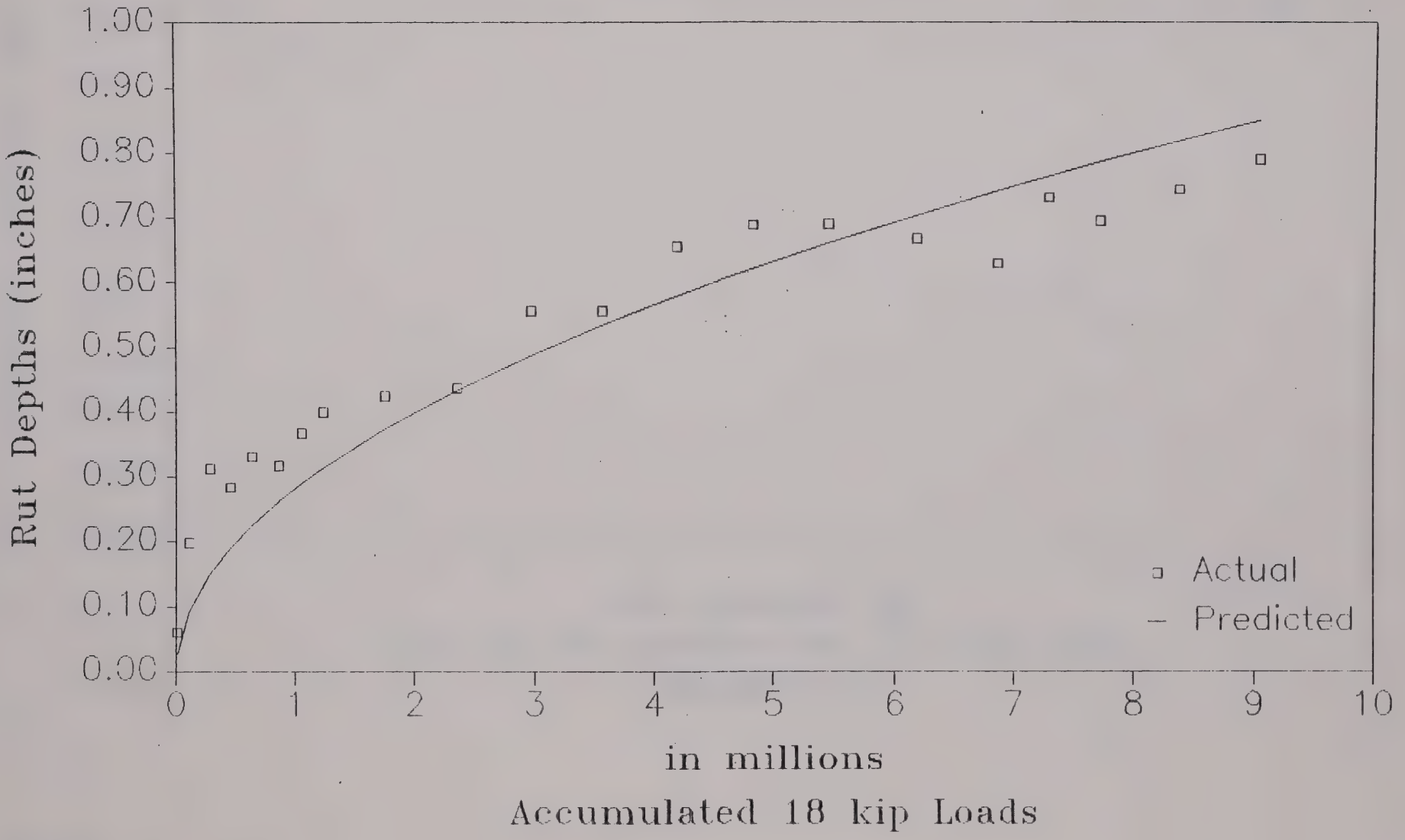

FIGURE C5
Plot of Rut Depths and 18 kip Loads
Test Section 3E

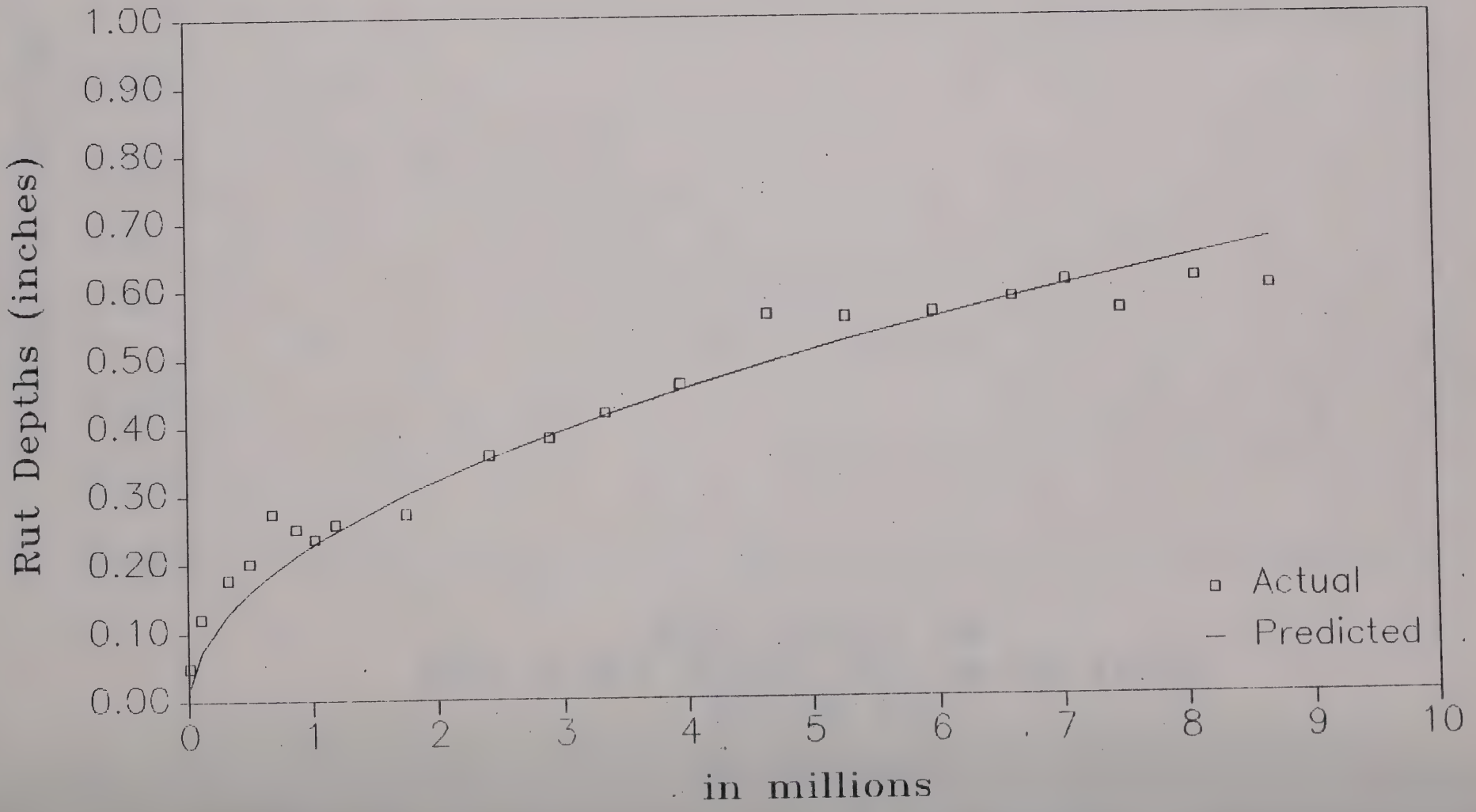

FIGURE C6
Plot of Rut Depths and 18 kip Loads
Test Section 3W

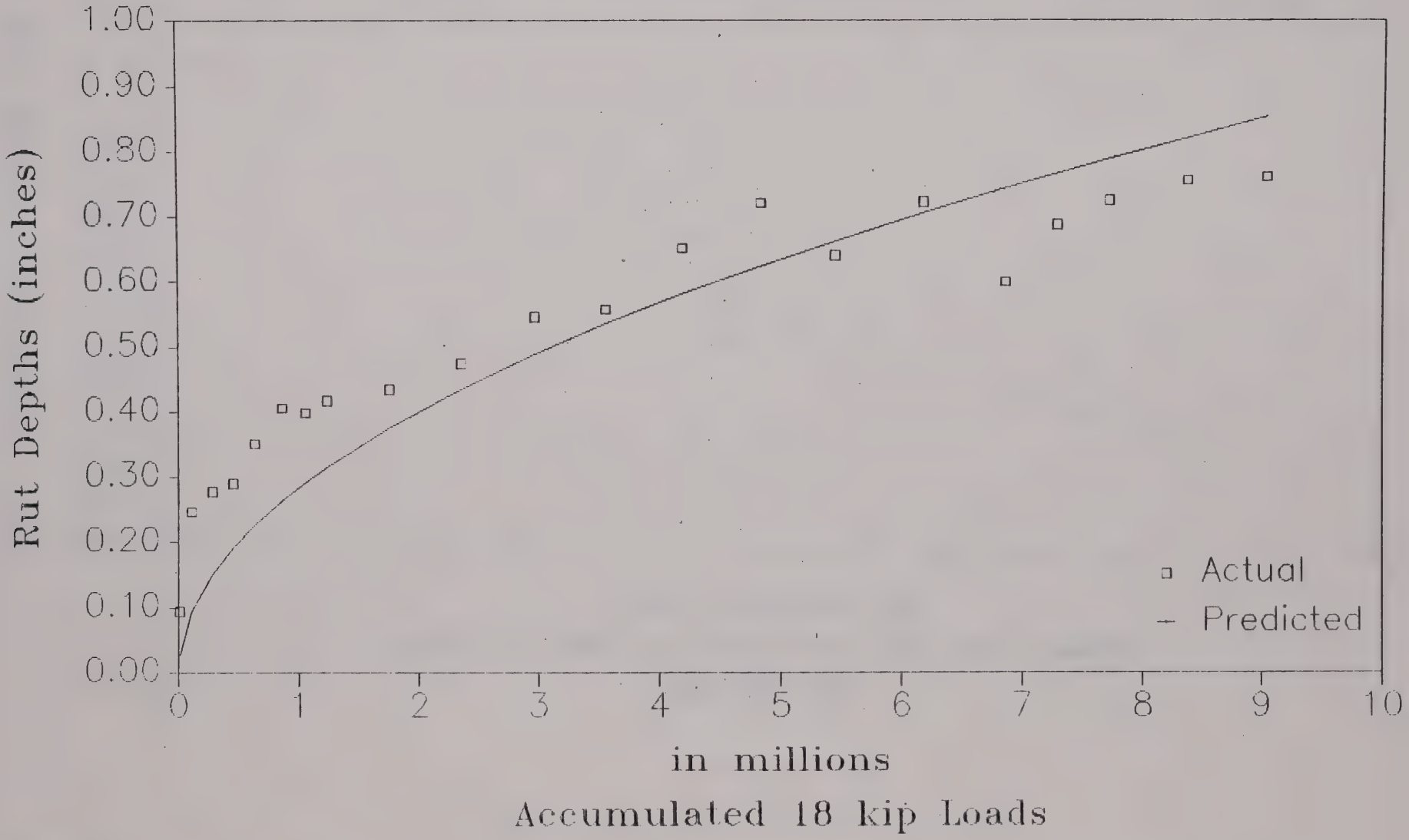

FIGURE C7
Plot of Rut Depths and 18 kip Loads
Test Section 4E

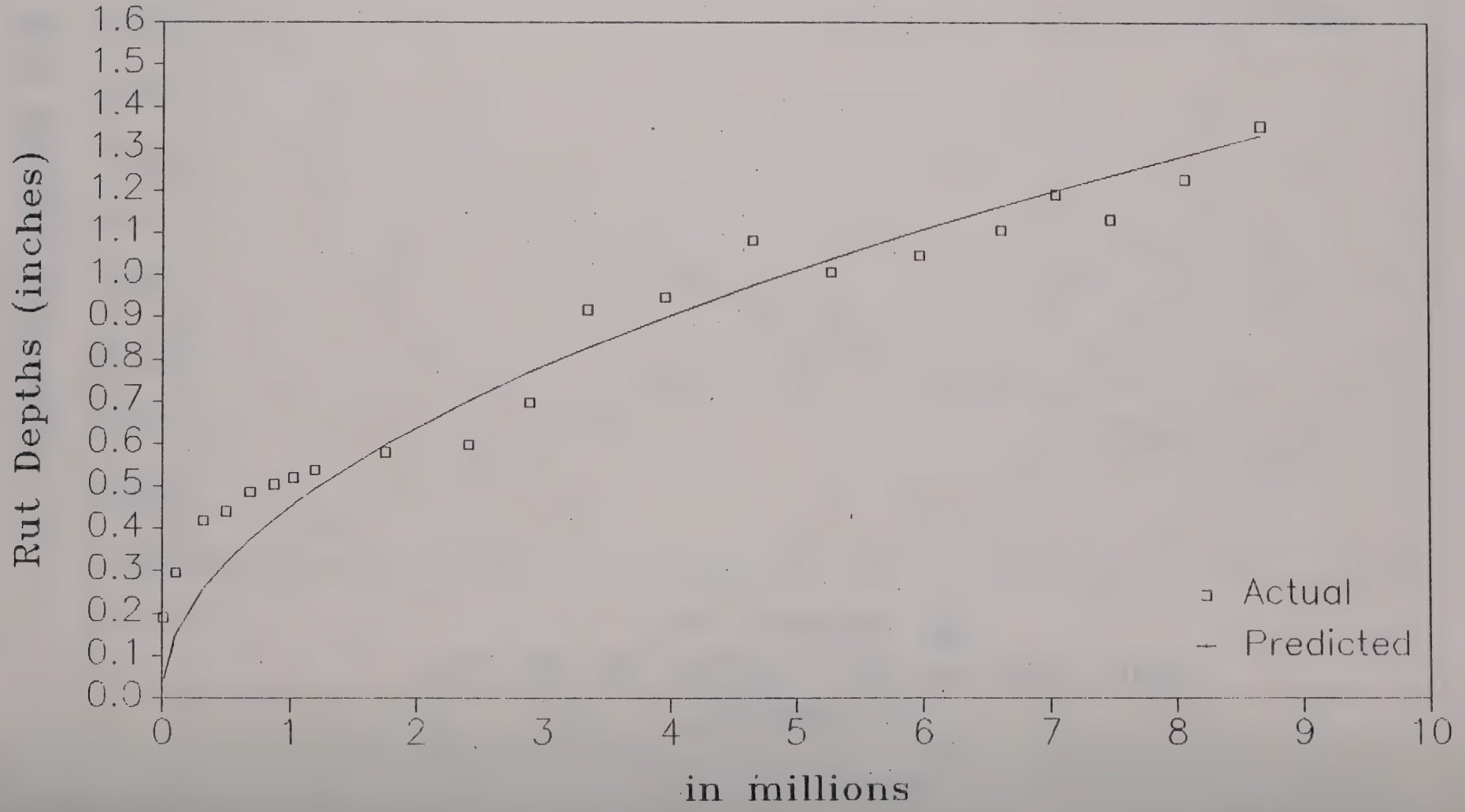

FIGURE C8
Plot of Rut Depths and 18 kip Loads
Test Section 4W

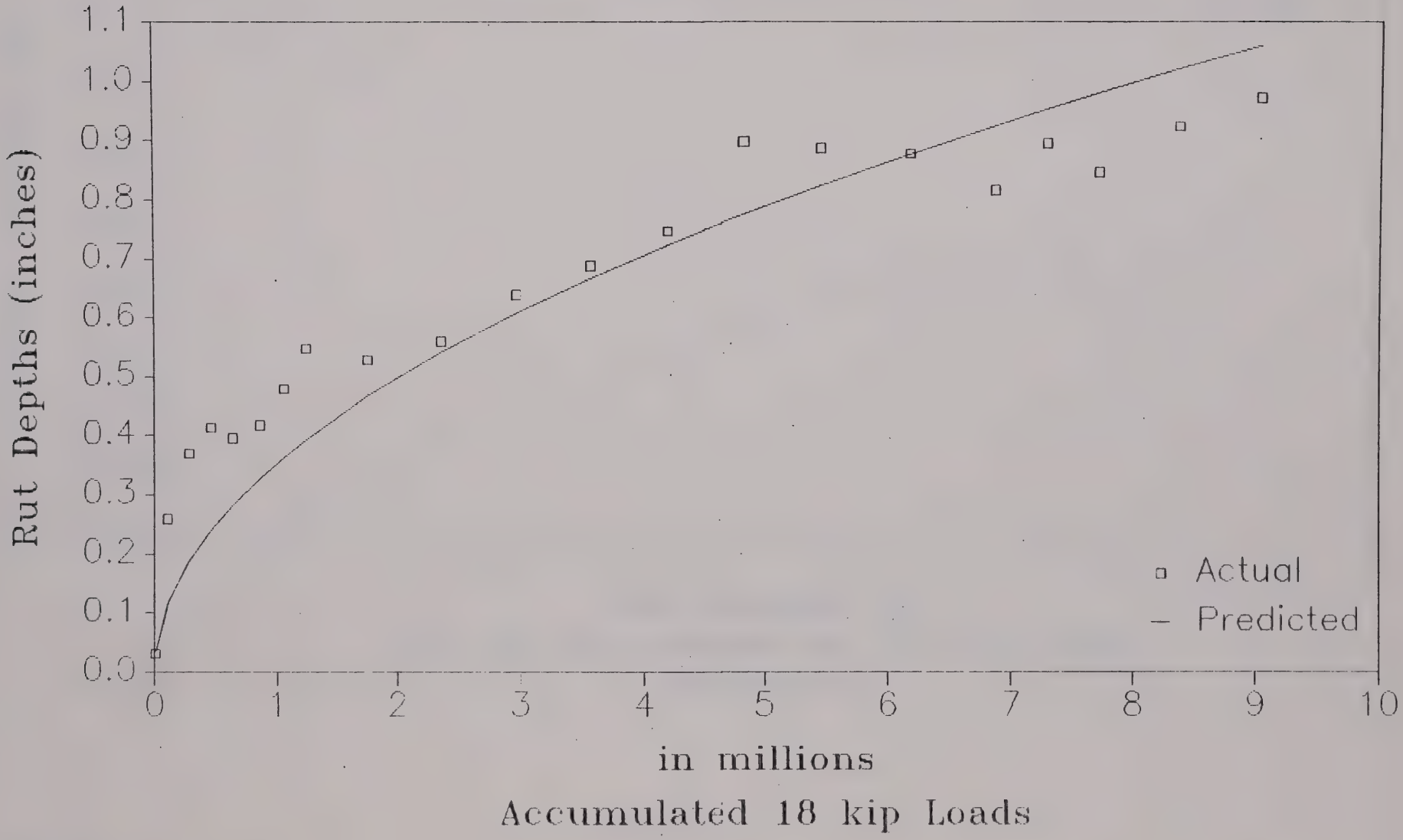

FIGURE C9
Plot of Rut Depths and 18 kip Loads
Test Section 5E

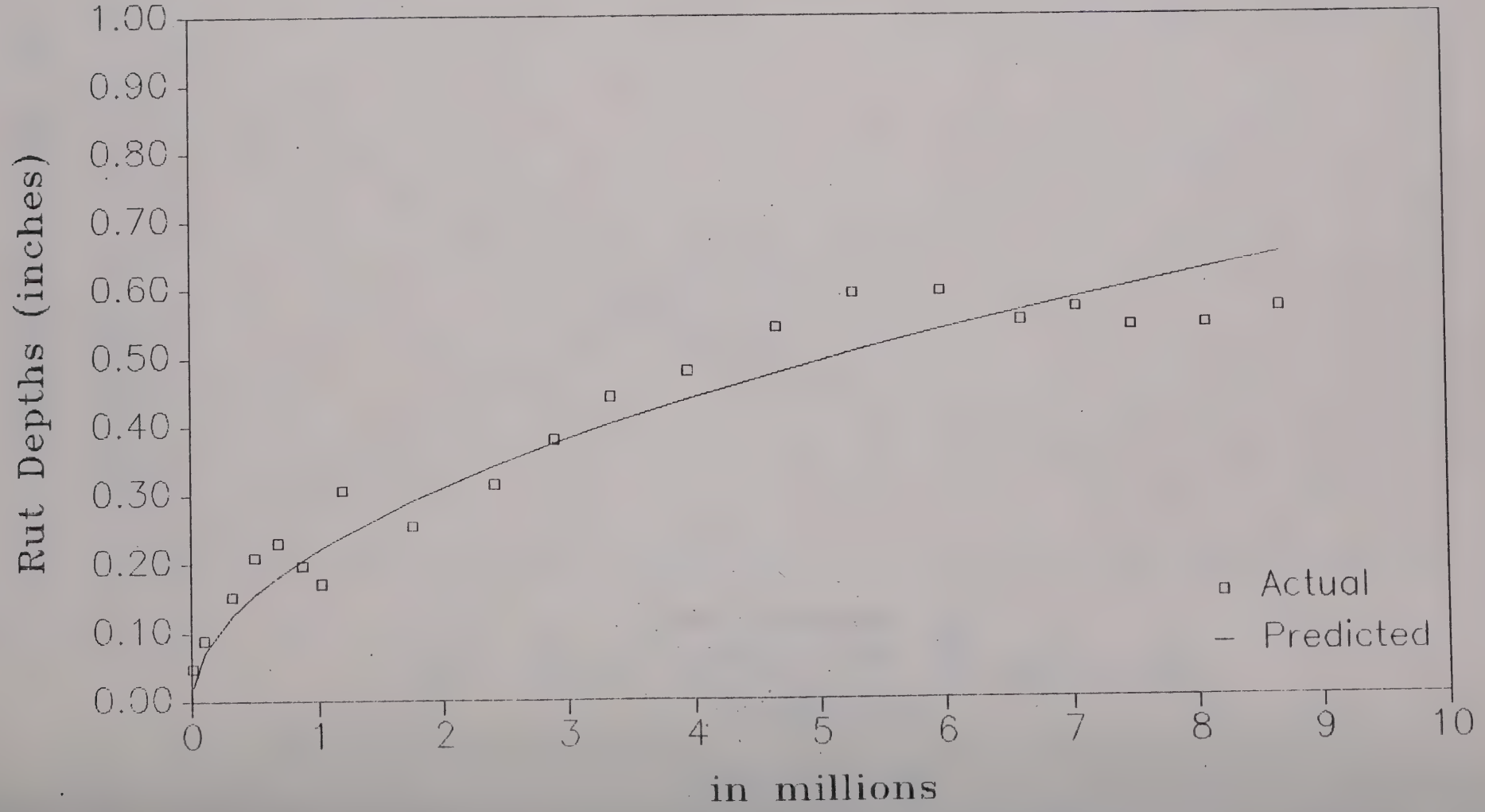

FIGURE C10
Plot of Rut Depths and 18 kip Loads
Test Section 5W

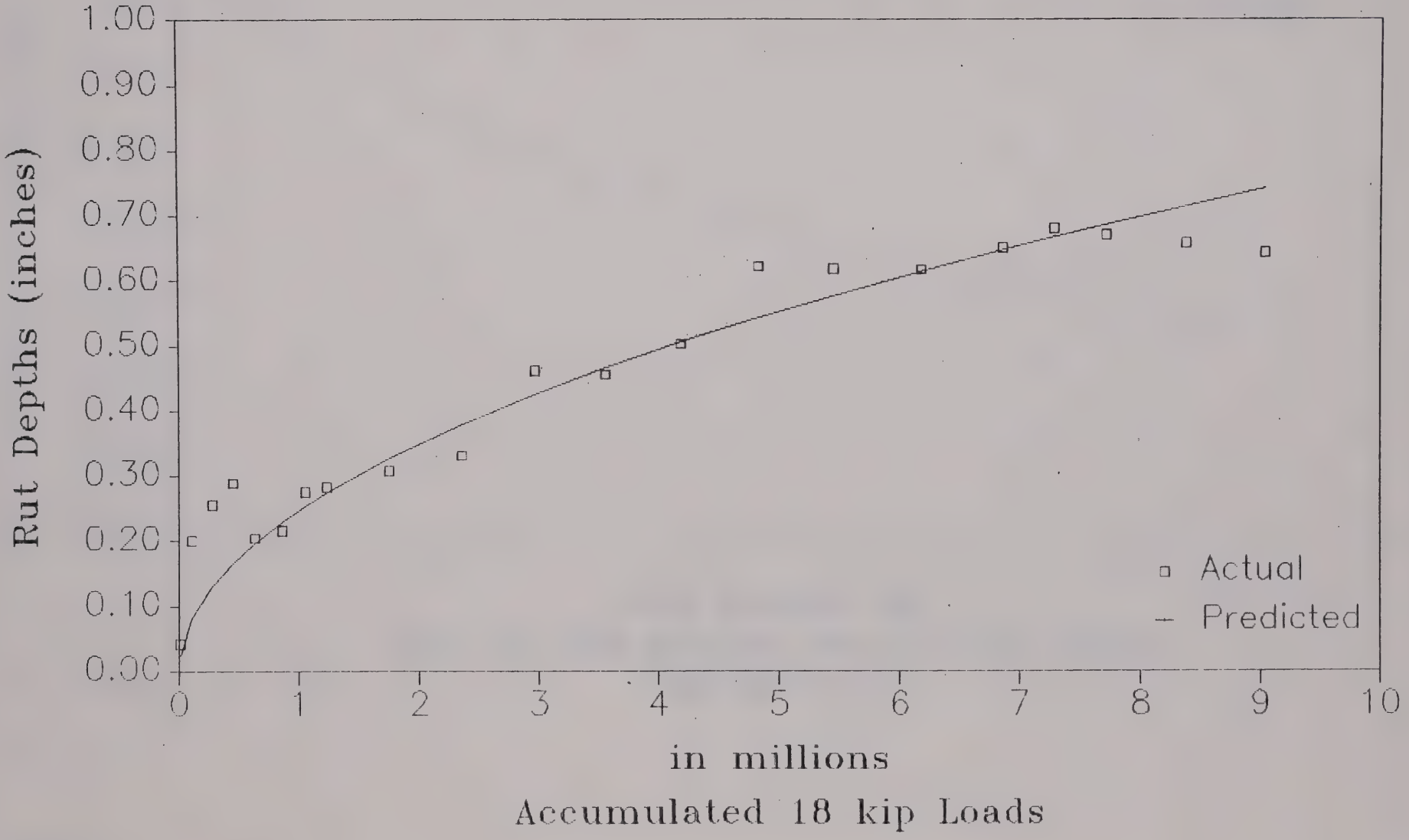

FIGURE C11
Plot of Rut Depths and 18 kip Loads
Test Section 6E

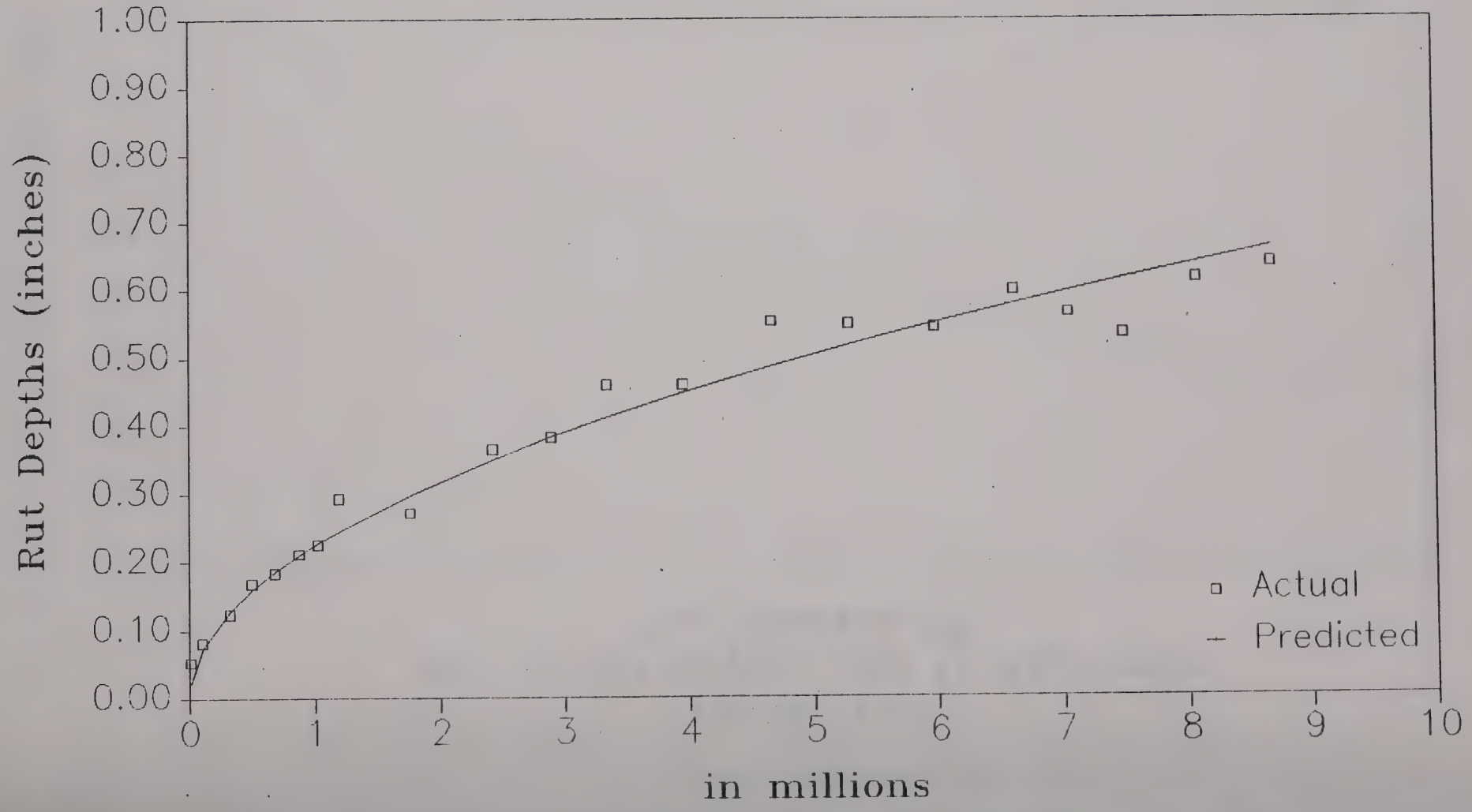

FIGURE C12
Plot of Rut Depths and 18 kip Loads
Test Section 6W

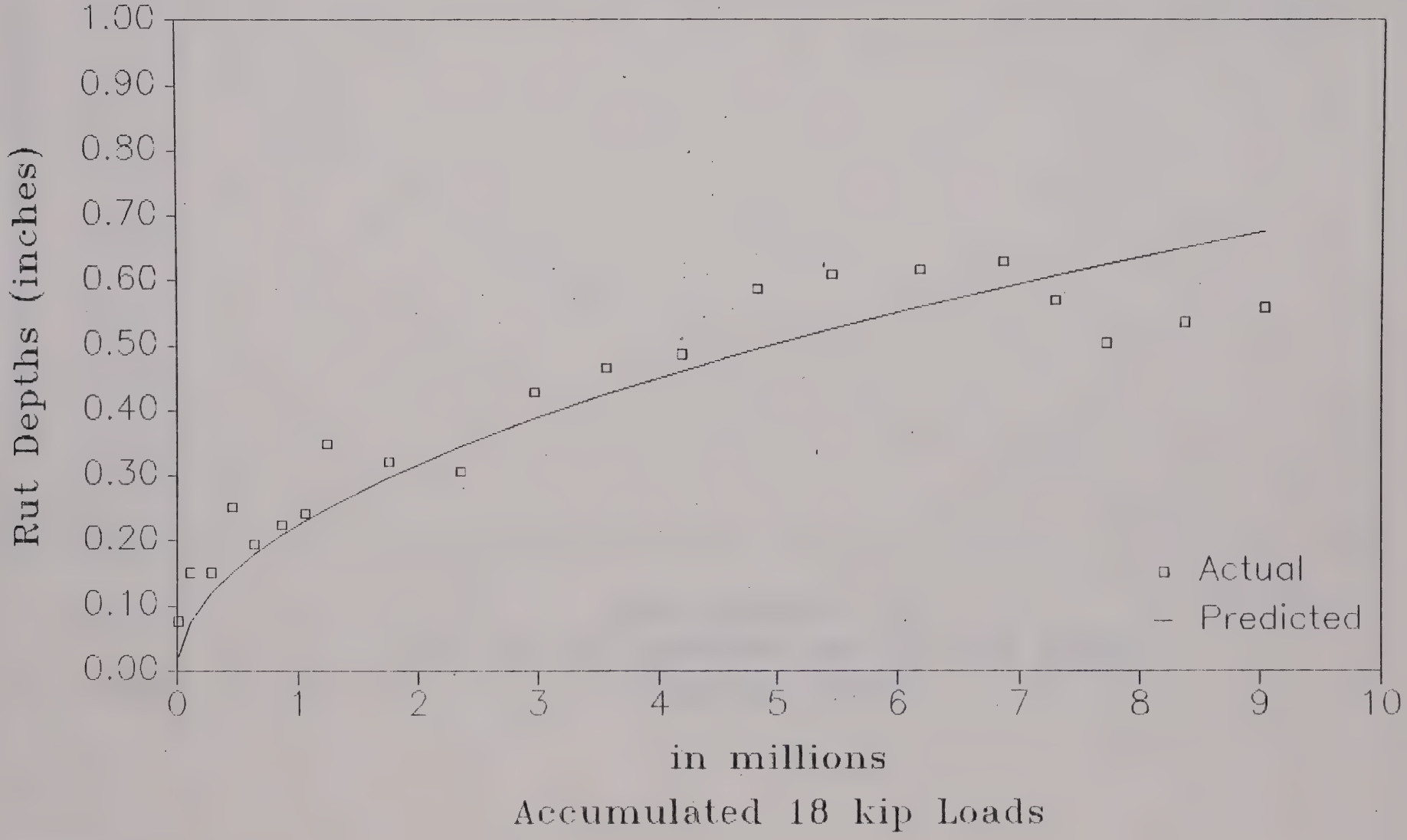

FIGURE C13
Plot of Rut Depths and 18 kip Loads
Test Section 7E

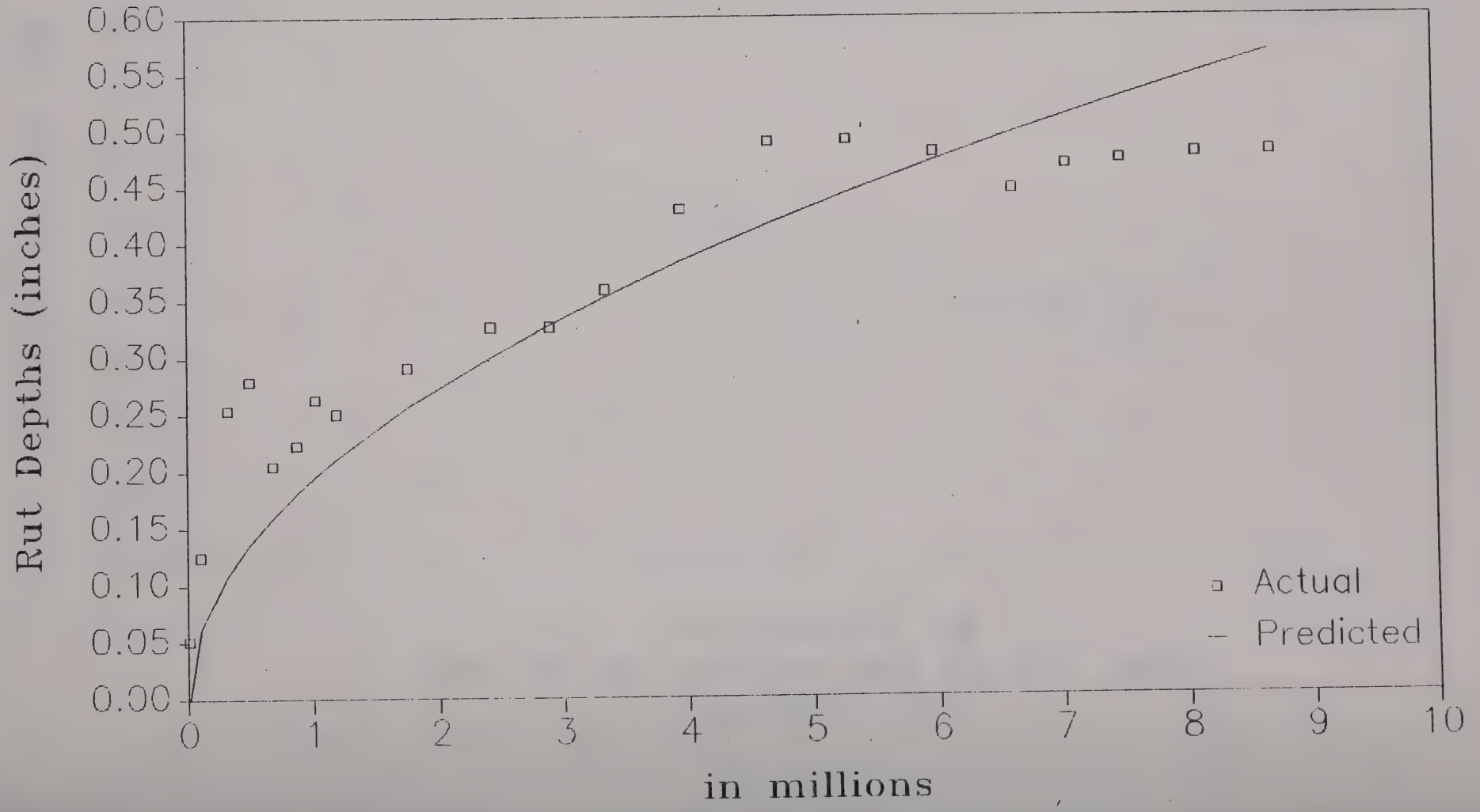

FIGURE C14
Plot of Rut Depths and 18 kip Loads
Test Section 7W

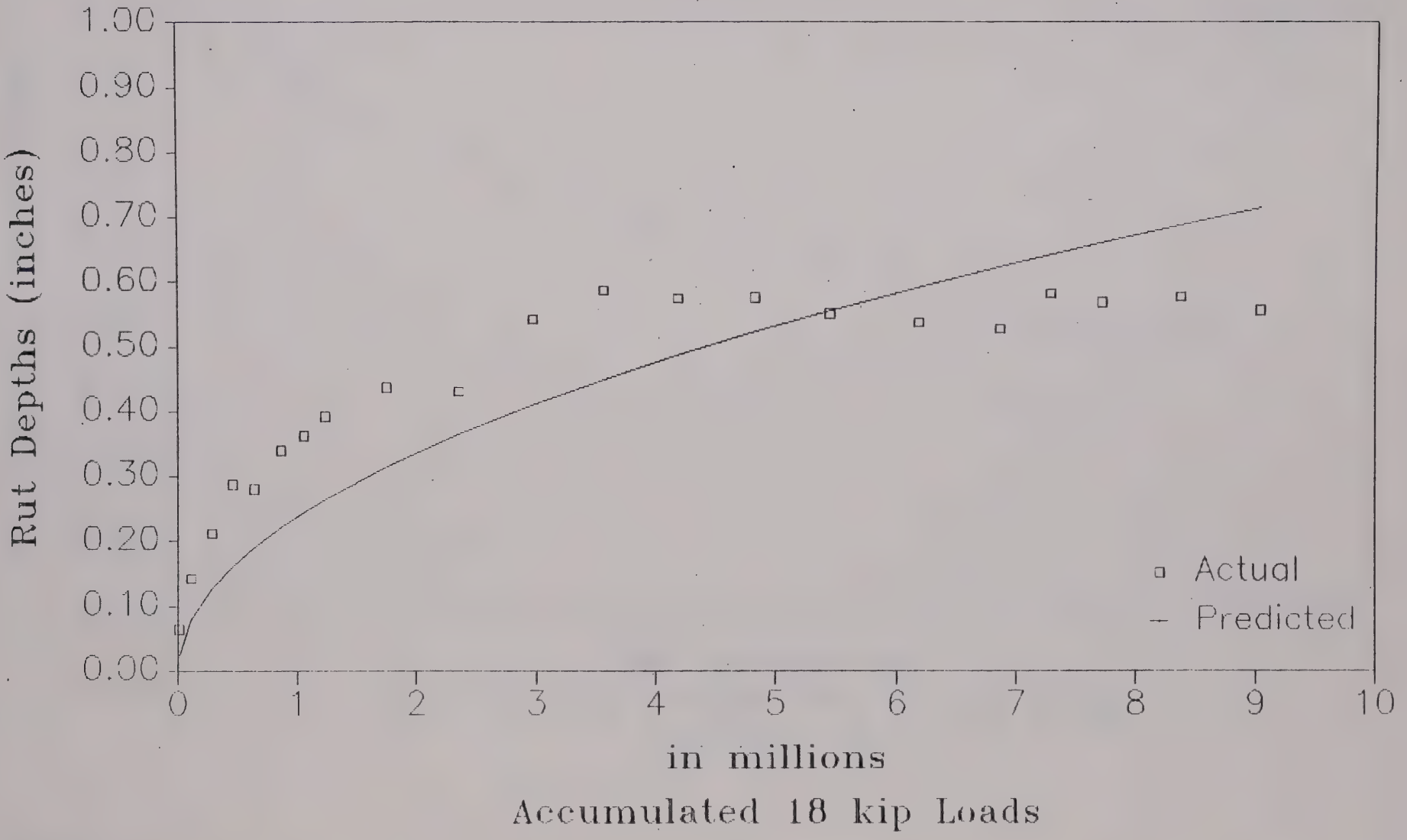

FIGURE C15
Plot of Rut Depths and 18 kip Loads
Test Section 8E

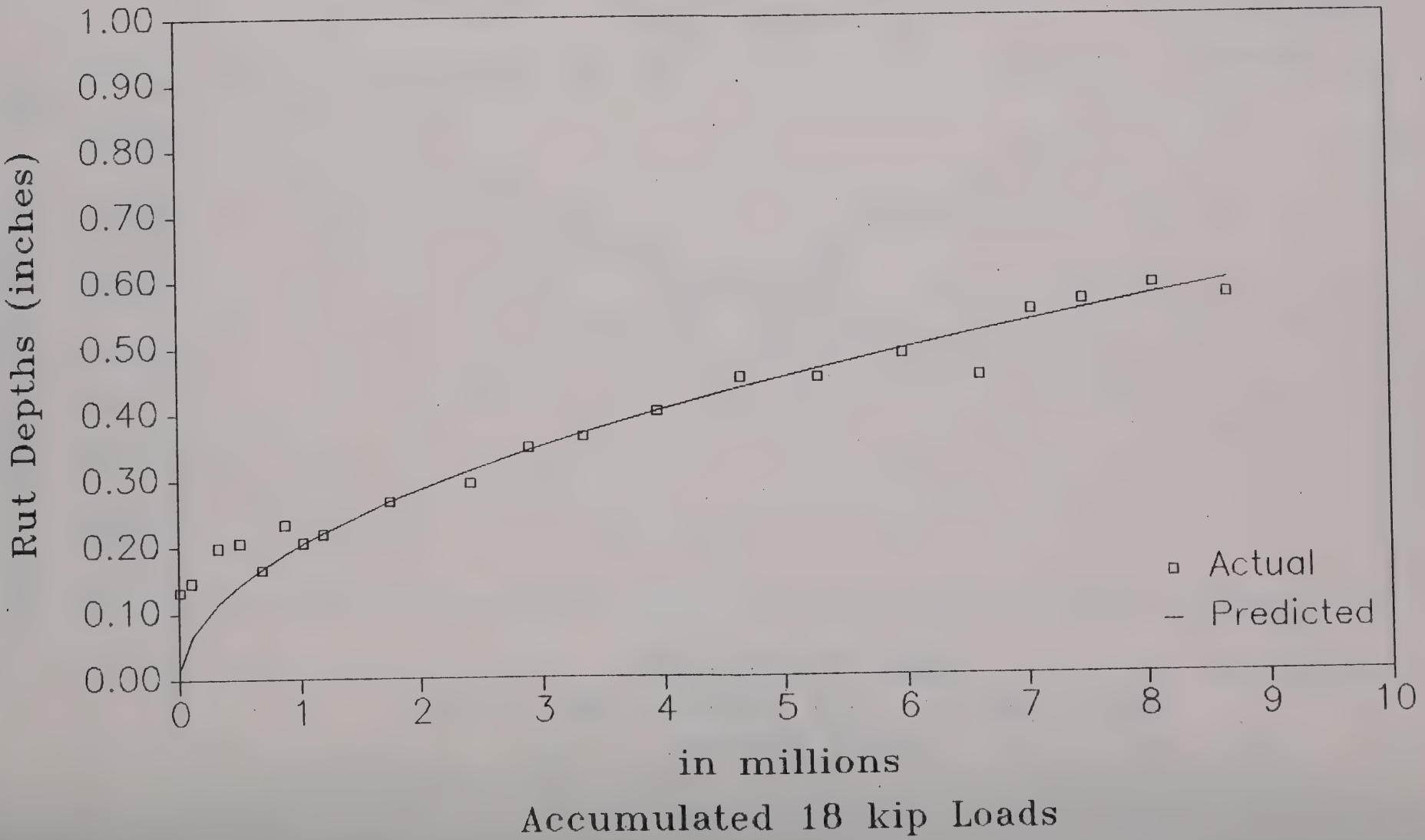

FIGURE C16
Plot of Rut Depths and 18 kip Loads
Test Section 9W

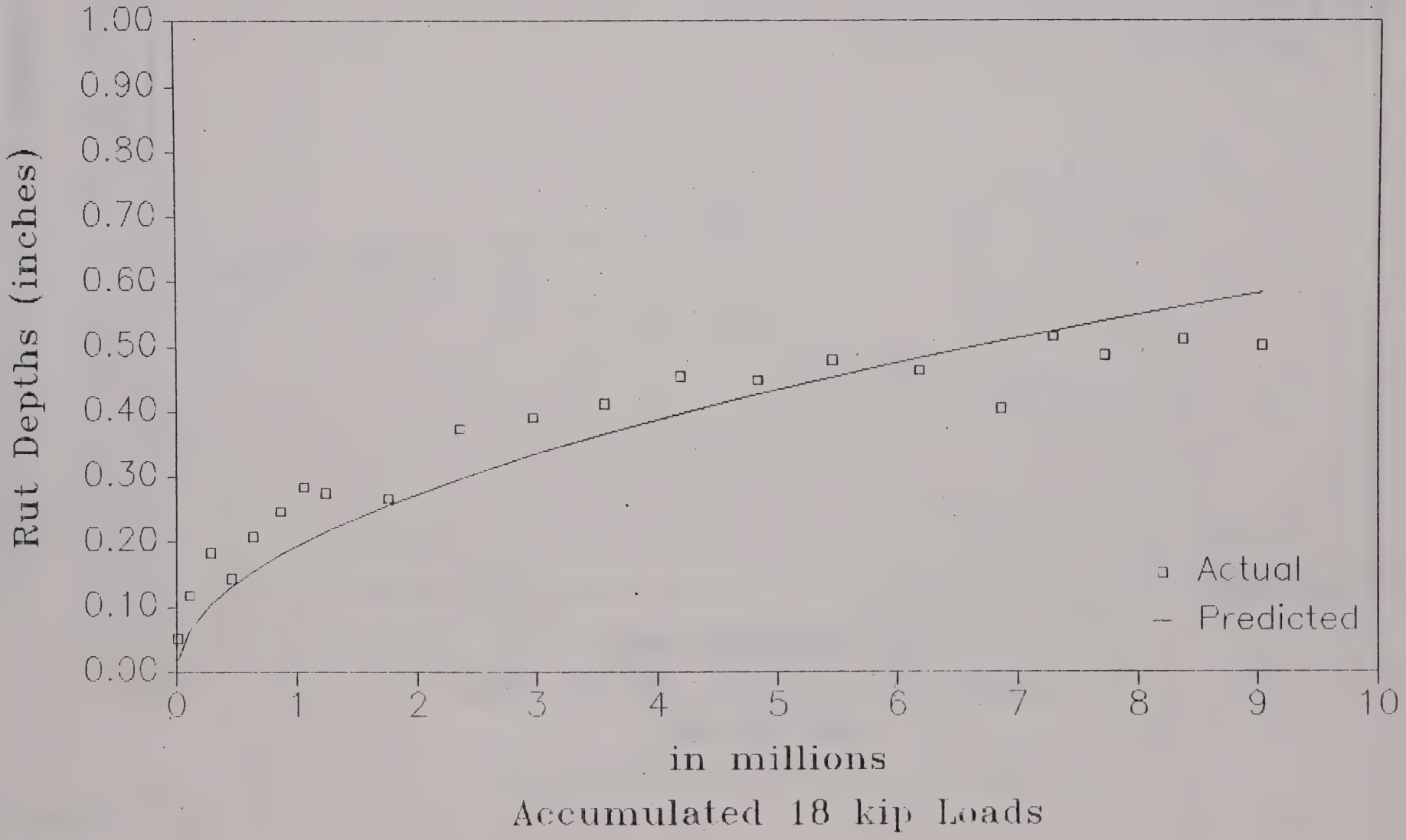

FIGURE D1
Plot of PSI and 18 kip Loads
Test Section 1E

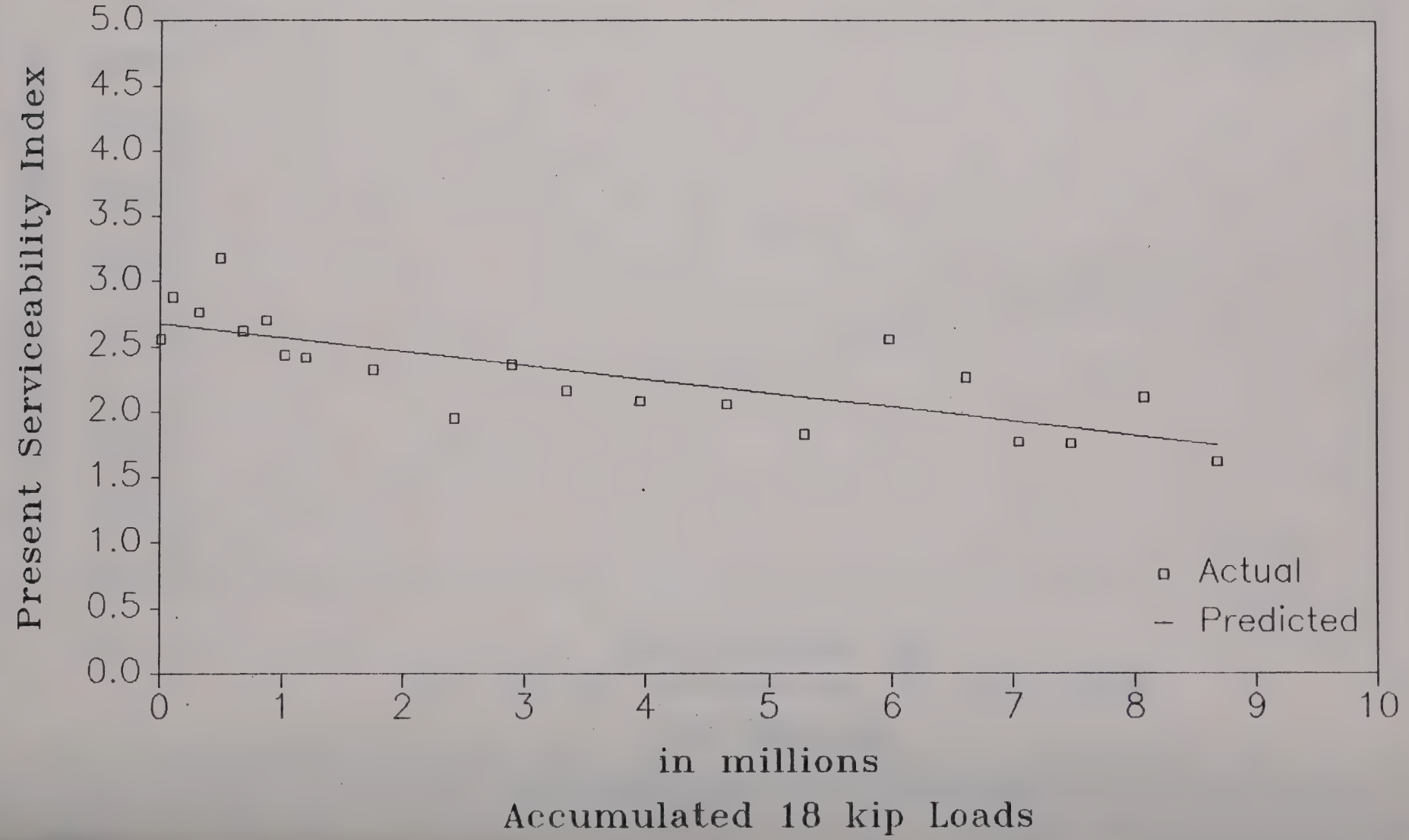

FIGURE D2
Plot of PSI and 18 kip Loads
Test Section 1W

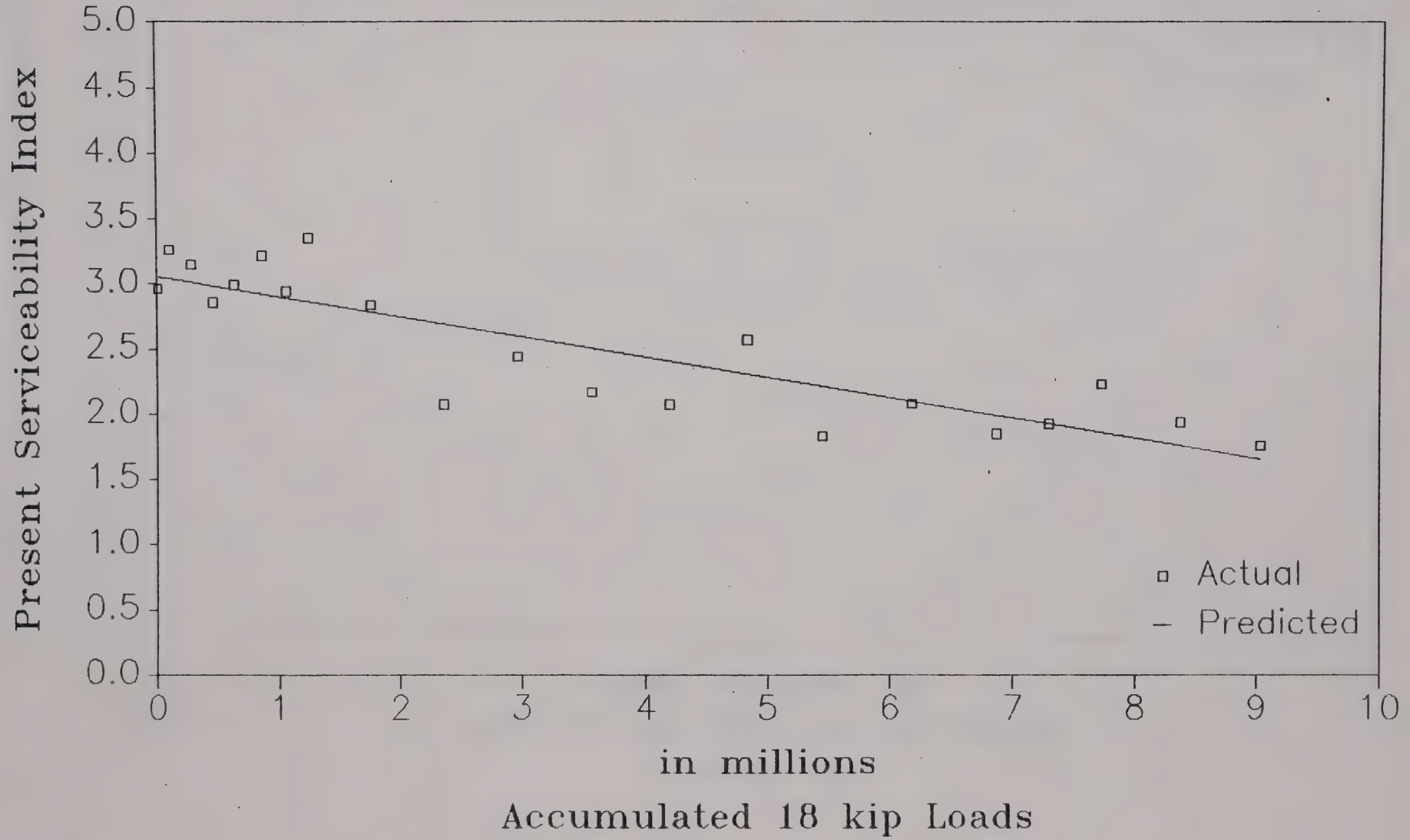

FIGURE D3
Plot of PSI and 18 kip Loads
Test Section 2E

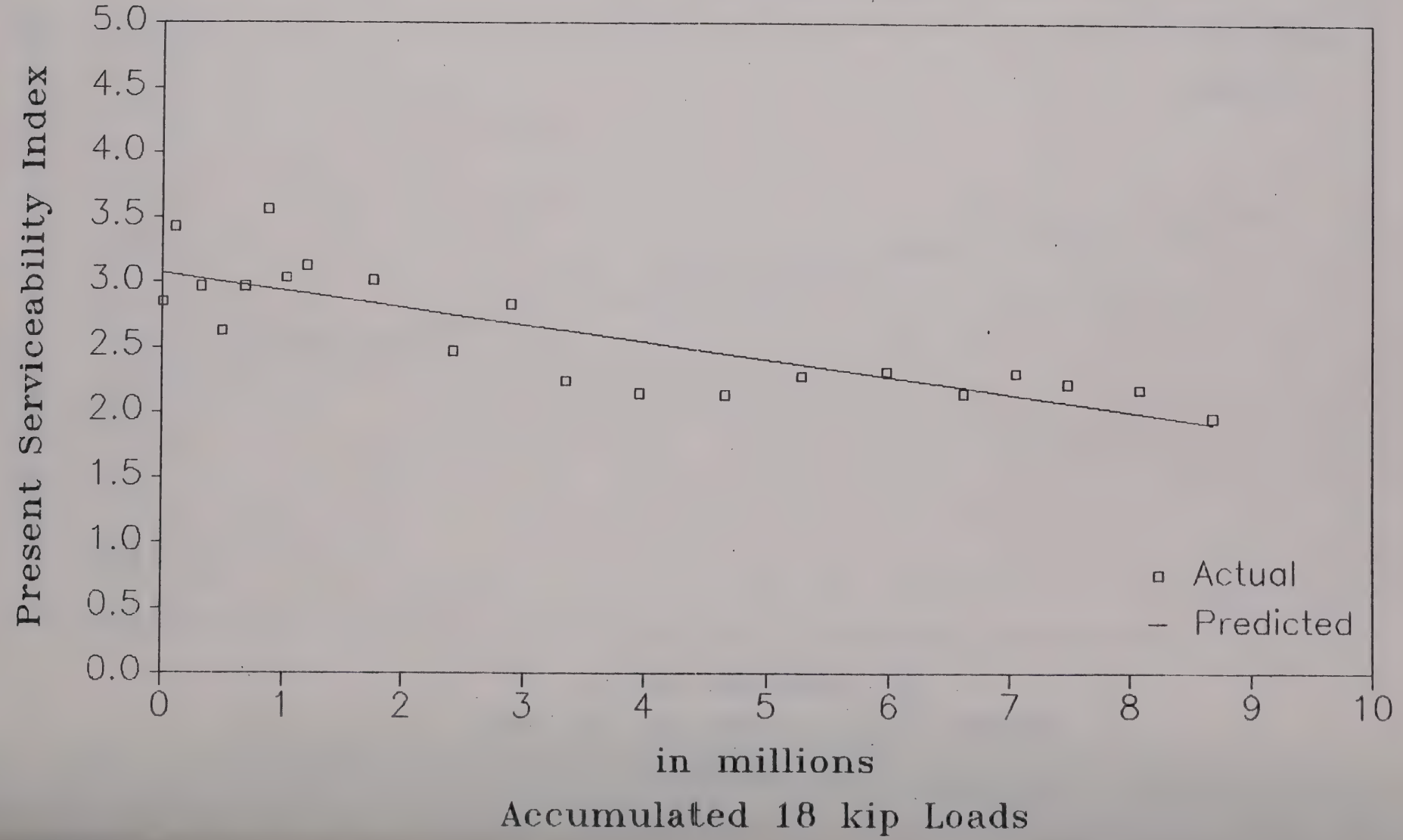

FIGURE D4
Plot of PSI and 18 kip Loads
Test Section 2W

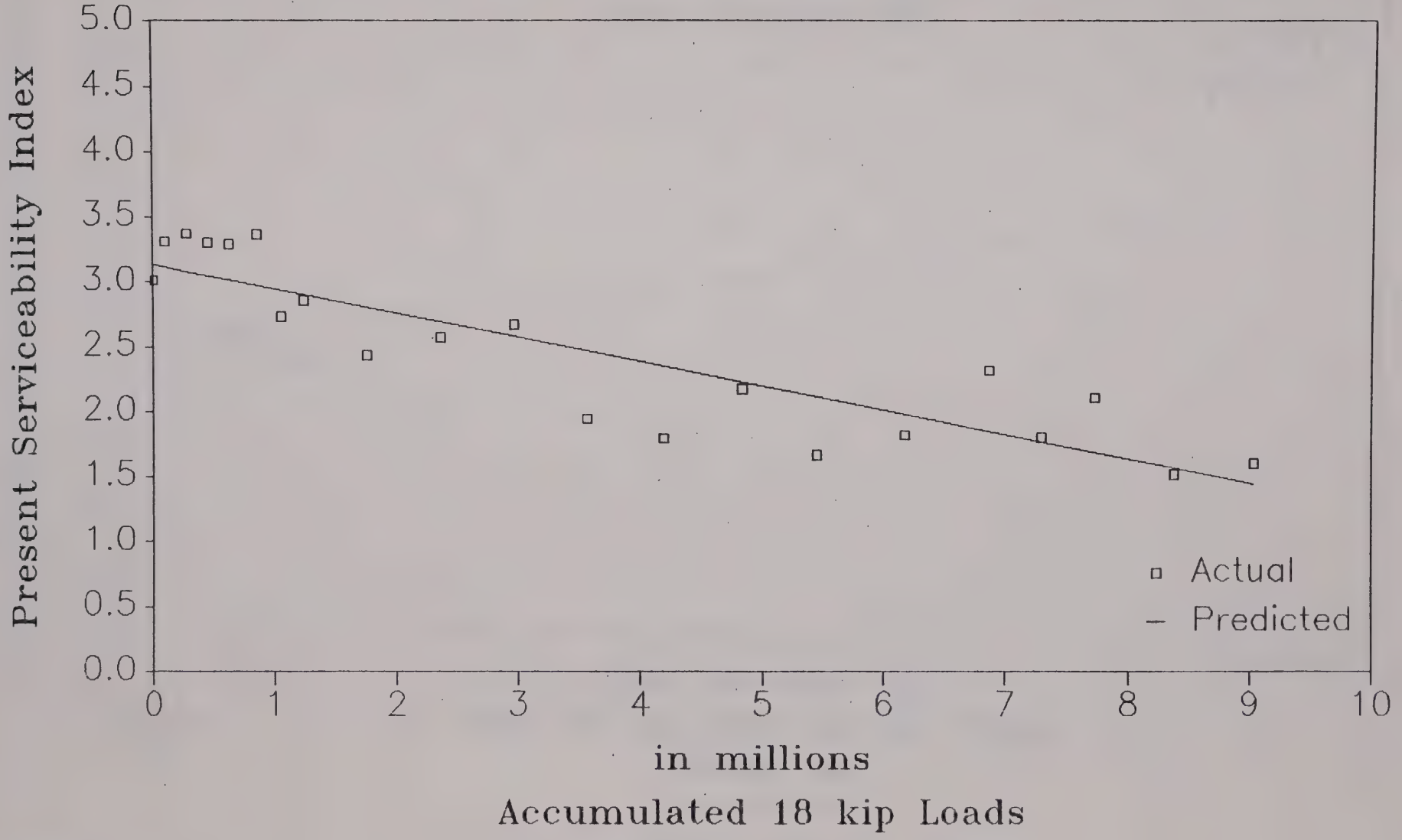

Figure D5
Plot of PSI and 18 kip Loads
Test Location 3E

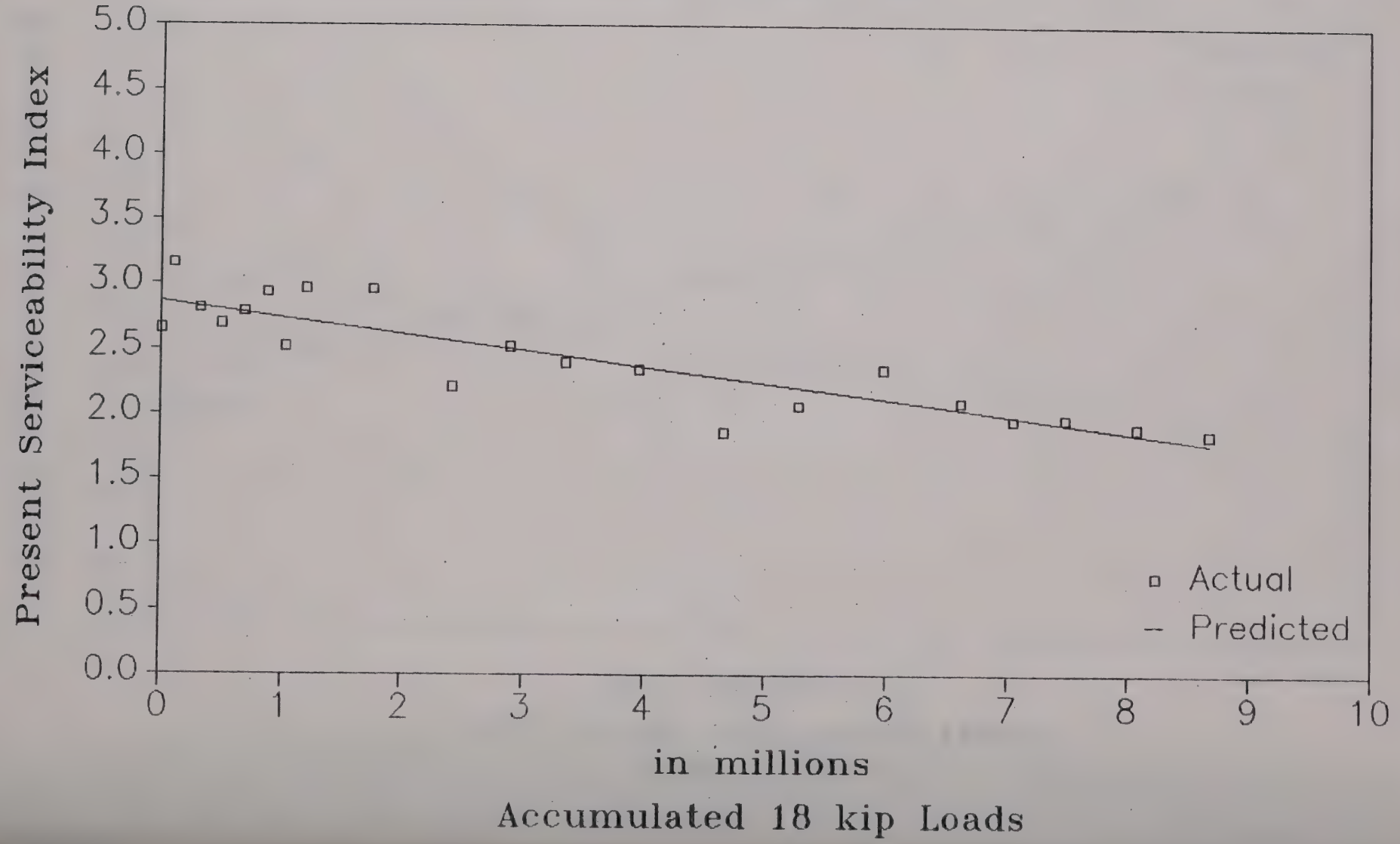

FIGURE D6
Plot of PSI and 18 kip Loads
Test Section 3W

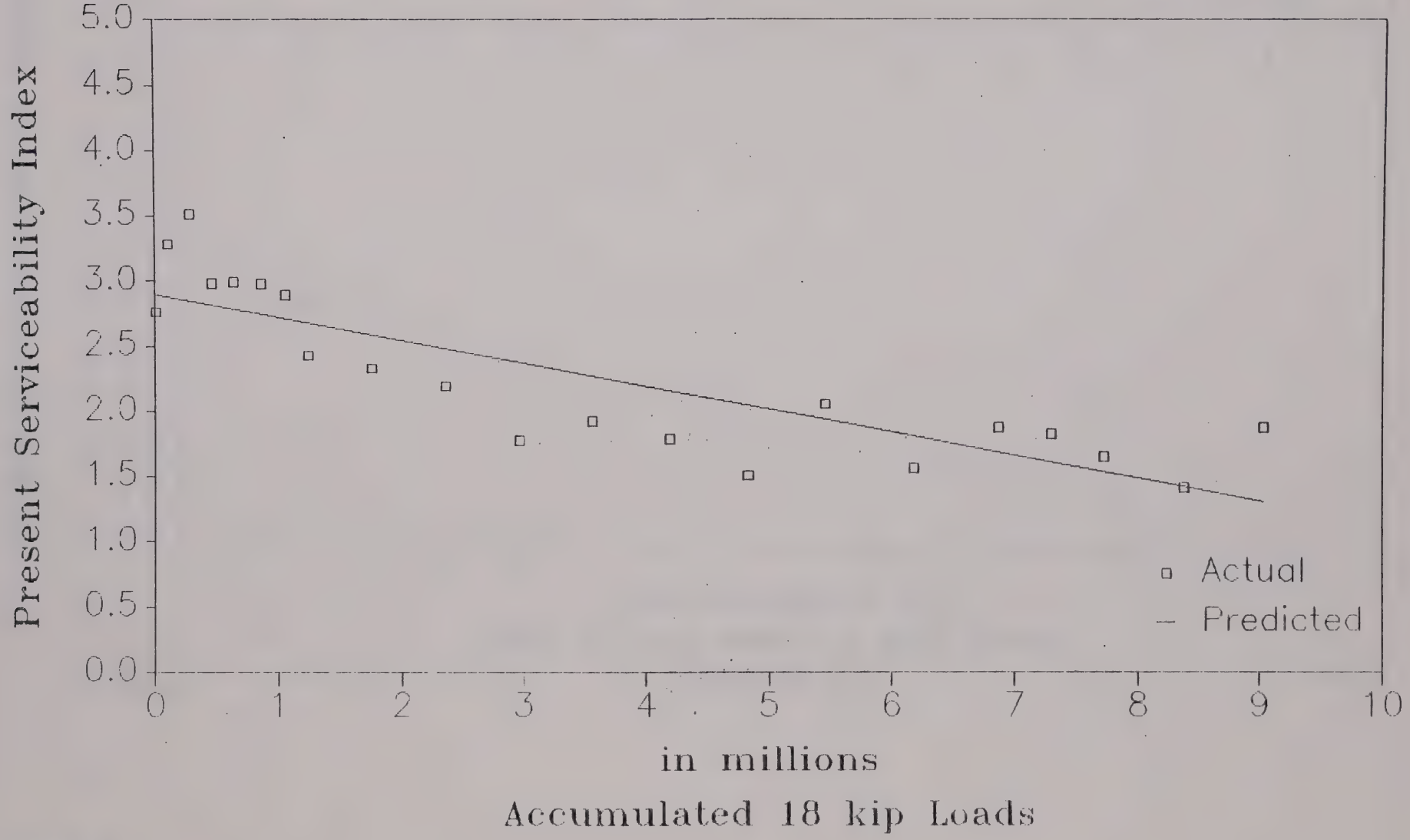

FIGURE D7
Plot of PSI and 18 kip Loads
Test Location 4E

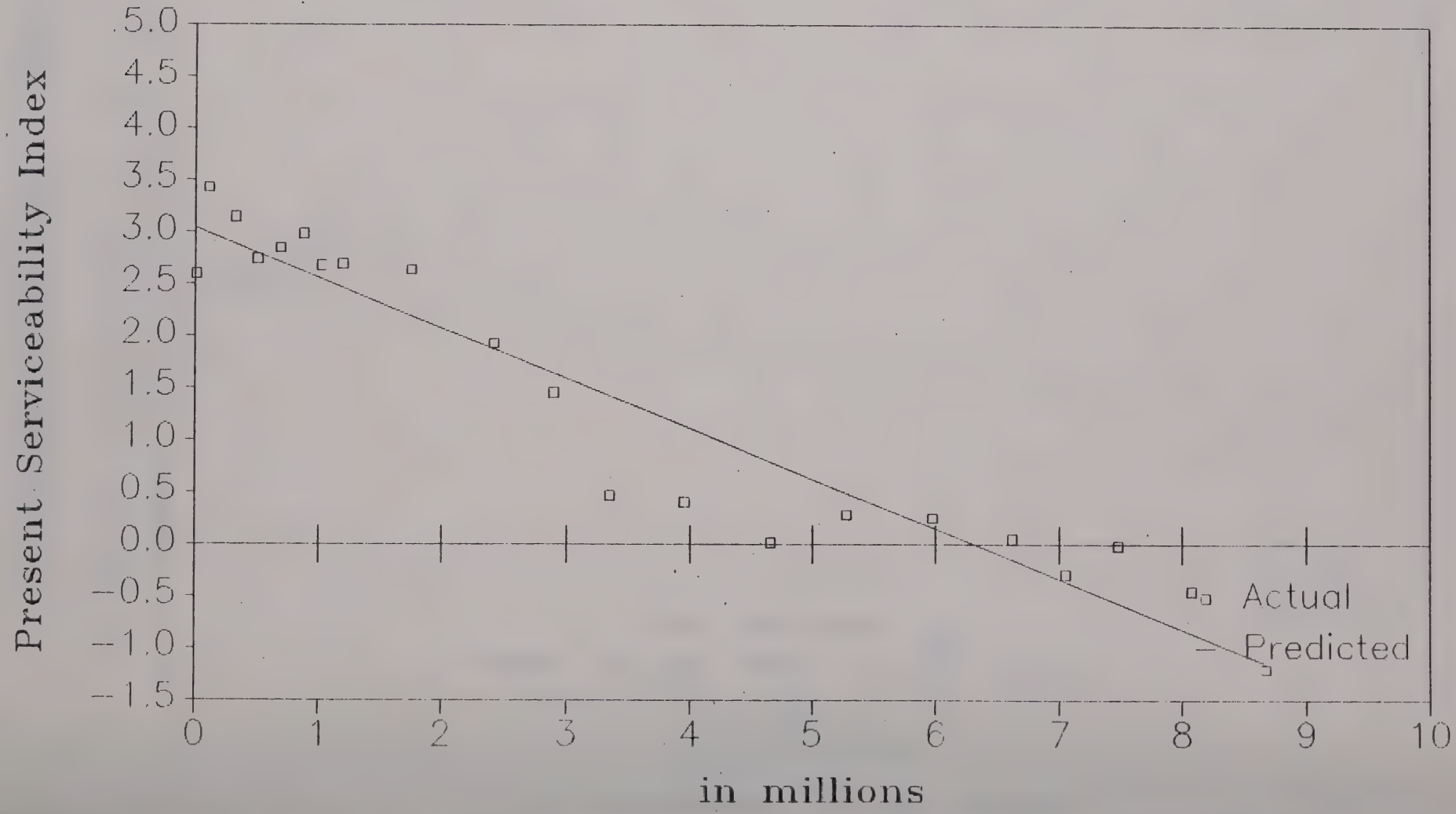

FIGURE D8
Plot of PSI and 18 kip Loads
Test Section 4W

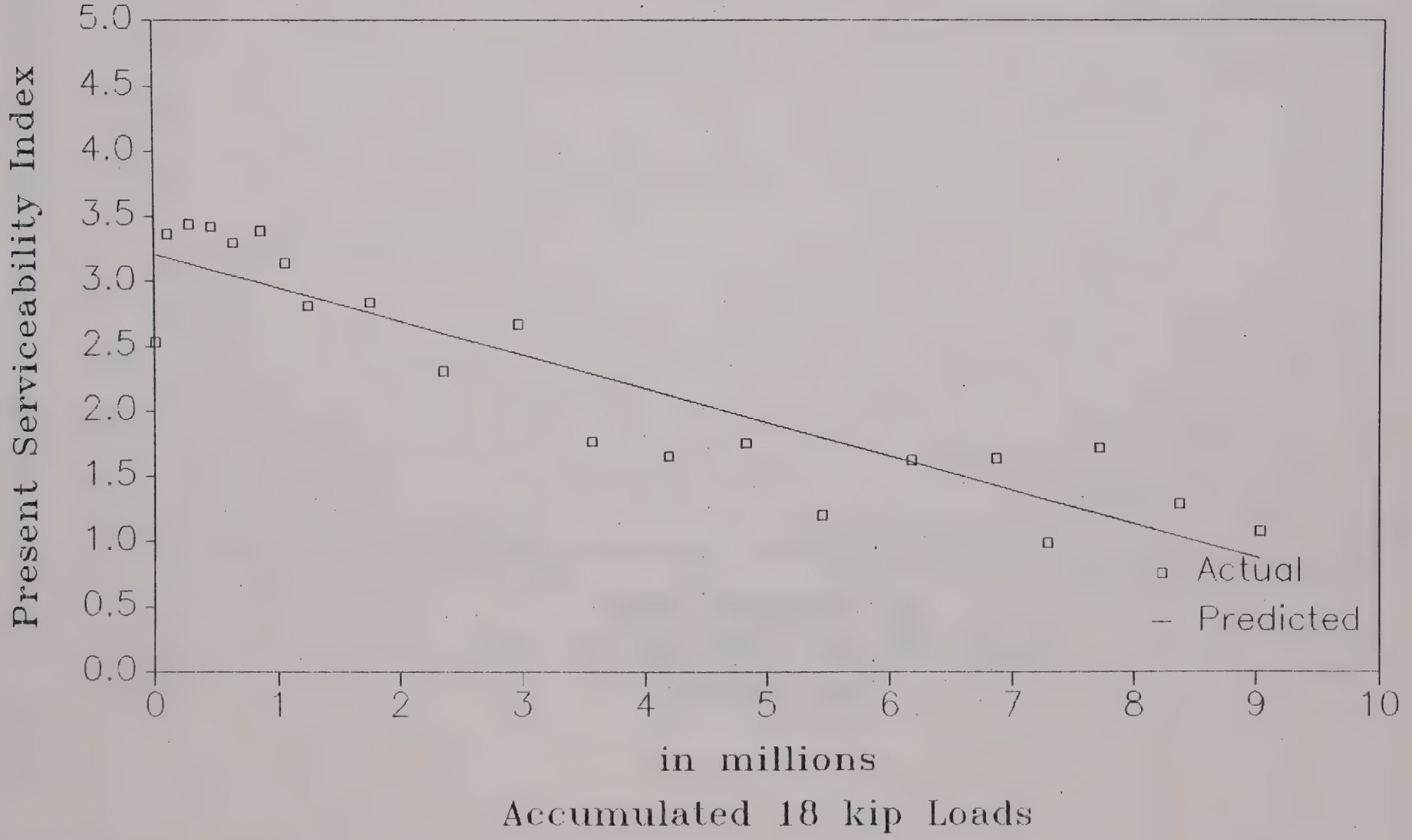

FIGURE D9
Plot of PSI and 18 kip Loads
Test Section 5E

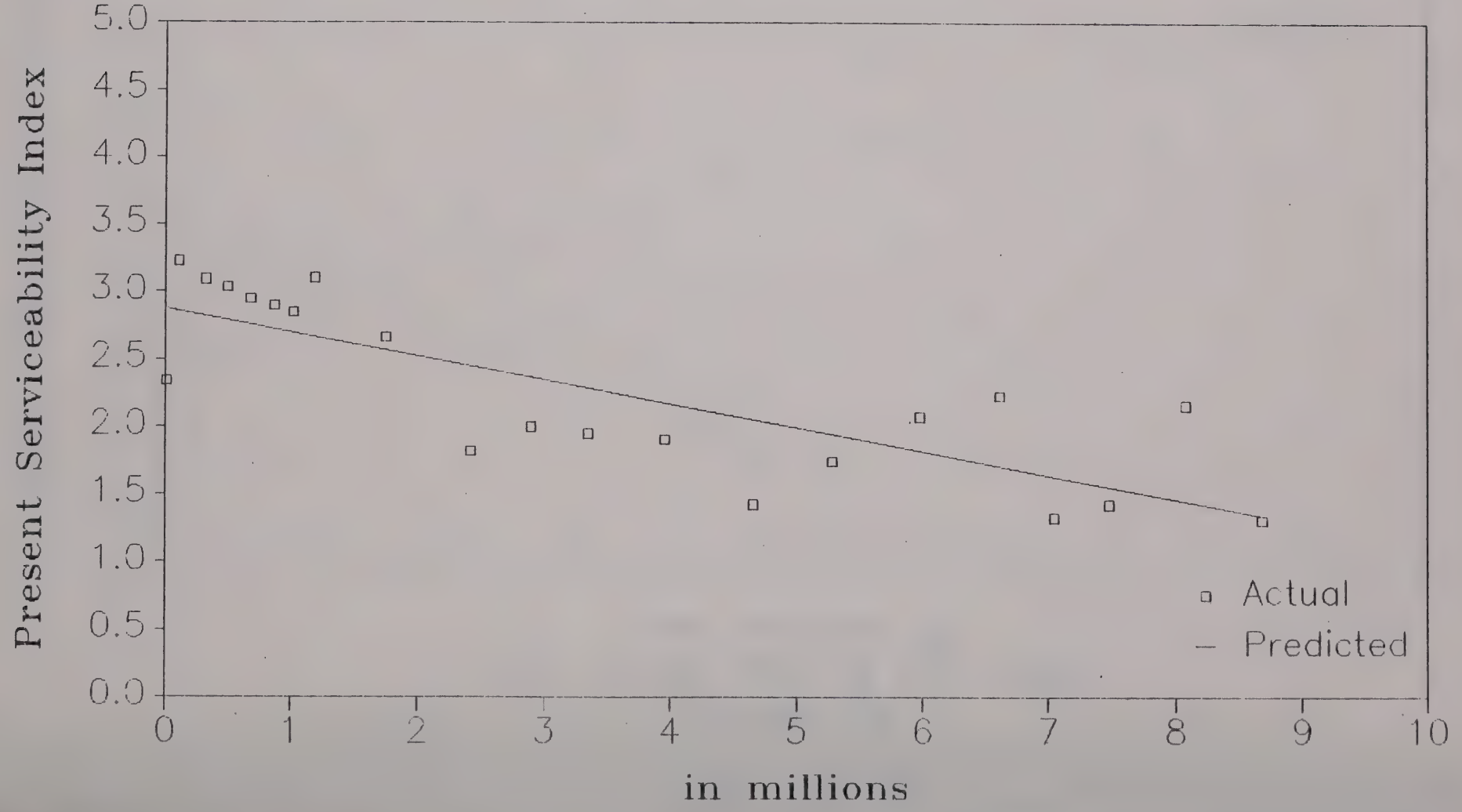

FIGURE D10
Plot of PSI and 18 kip Loads
Test Section 5W

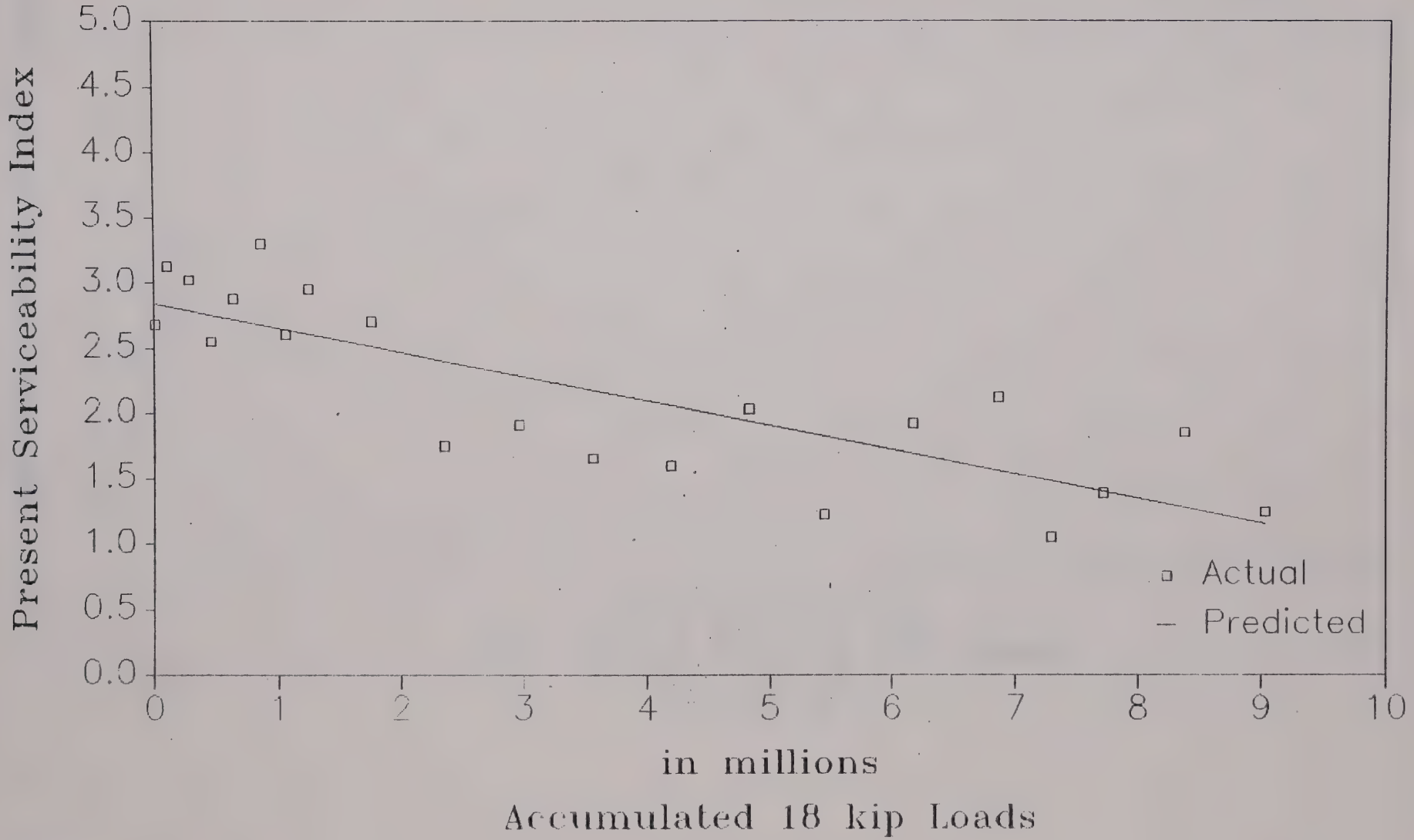

FIGURE D11
Plot of PSI and 18 kip Loads
Test Section 6E

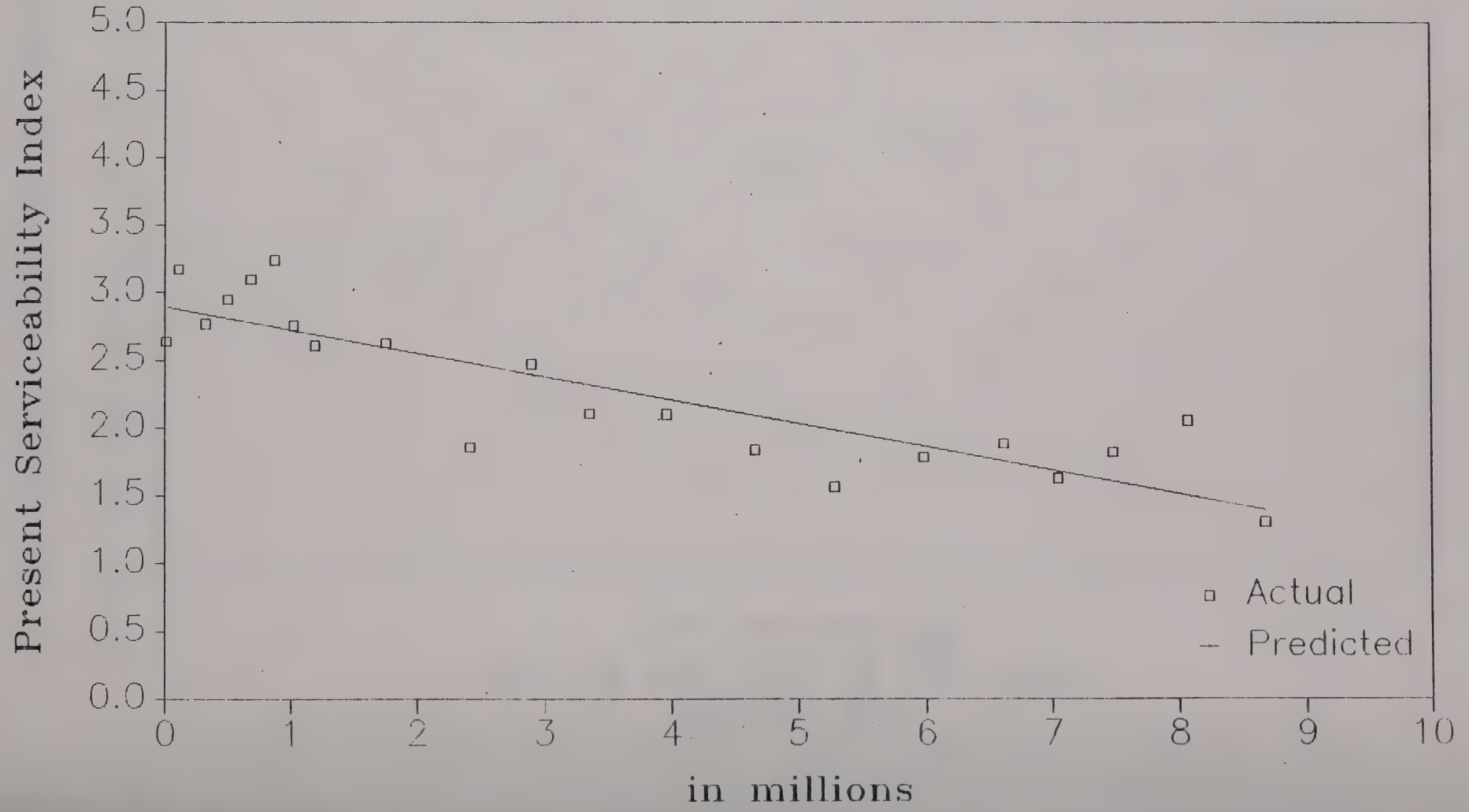

FIGURE D12
Plot of PSI and 18 kip Loads
Test Section 6W

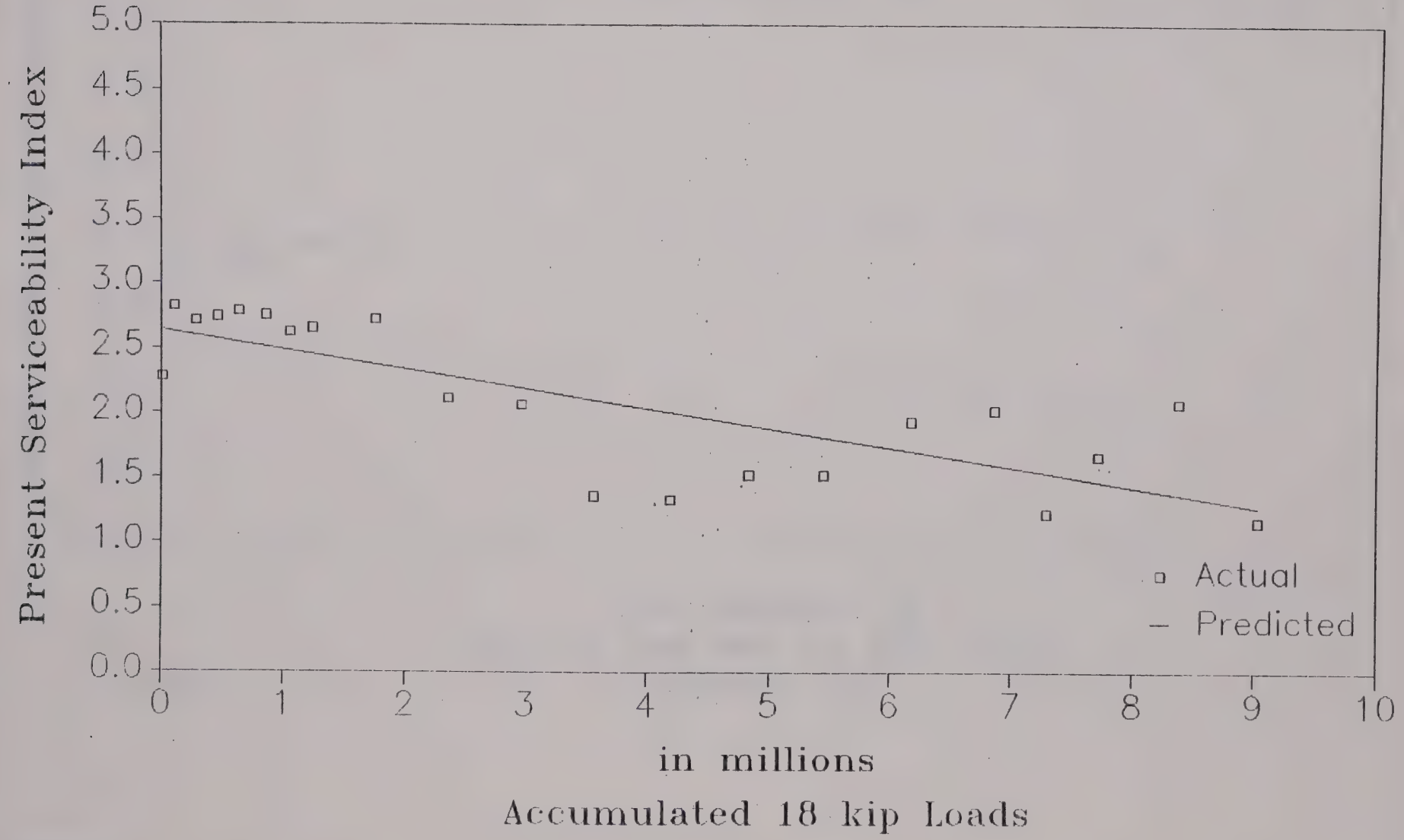

FIGURE D13
Plot of PSI and 18 kip Loads
Test Section 7E

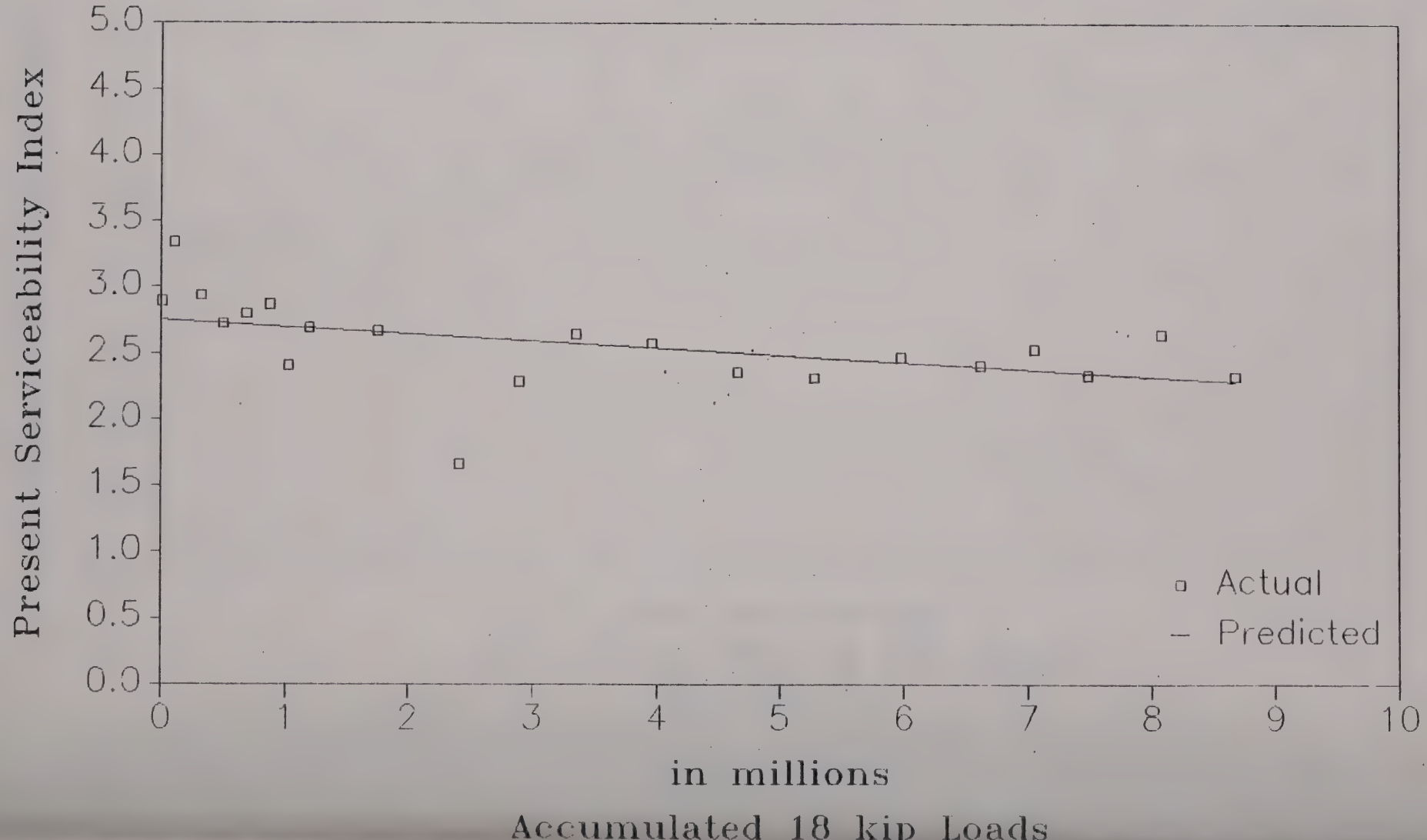

FIGURE D14
Plot of PSI and 18 kip Loads
Test Section 7W

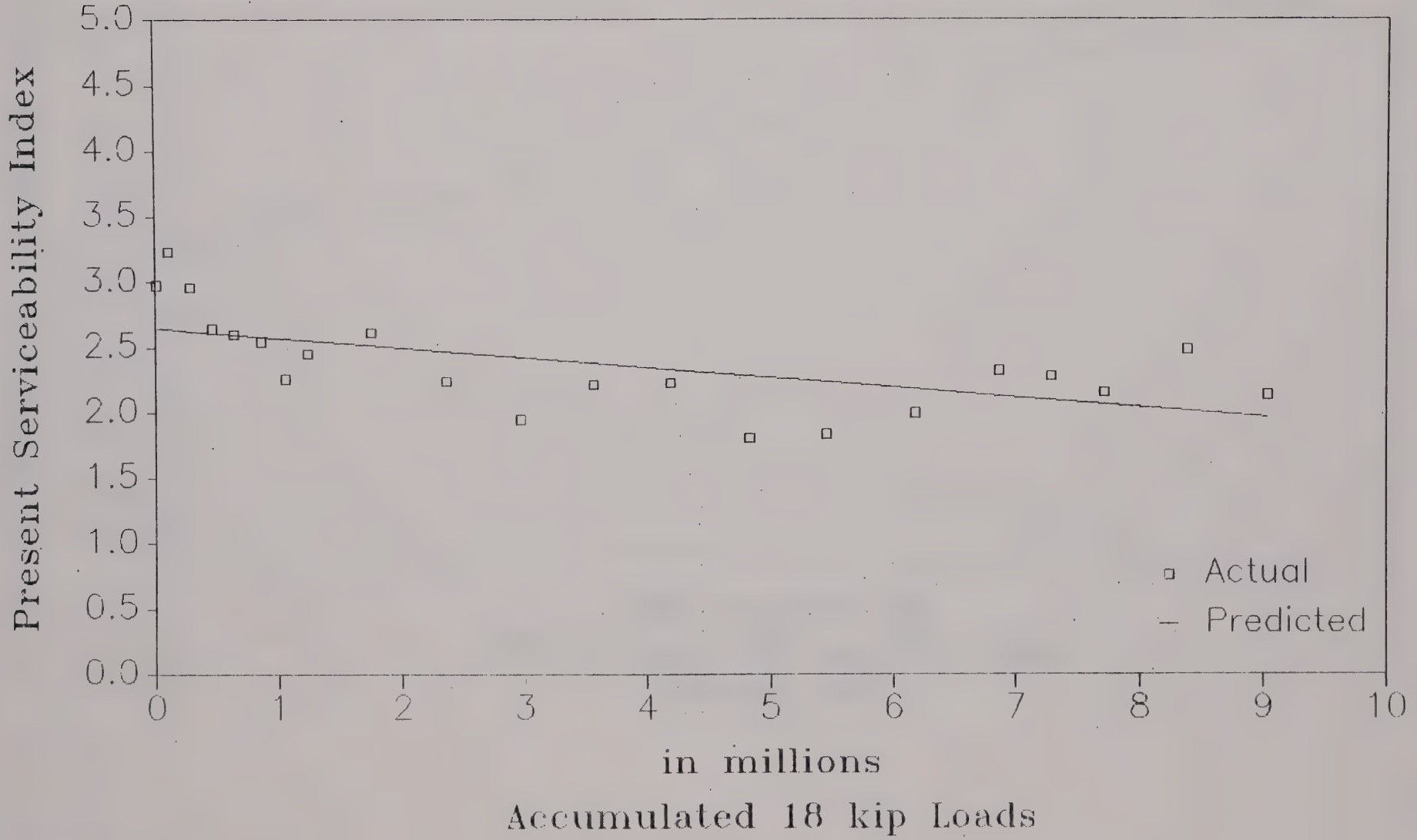

FIGURE D15
Plot of PSI and 18 kip Loads
Test Section 8E

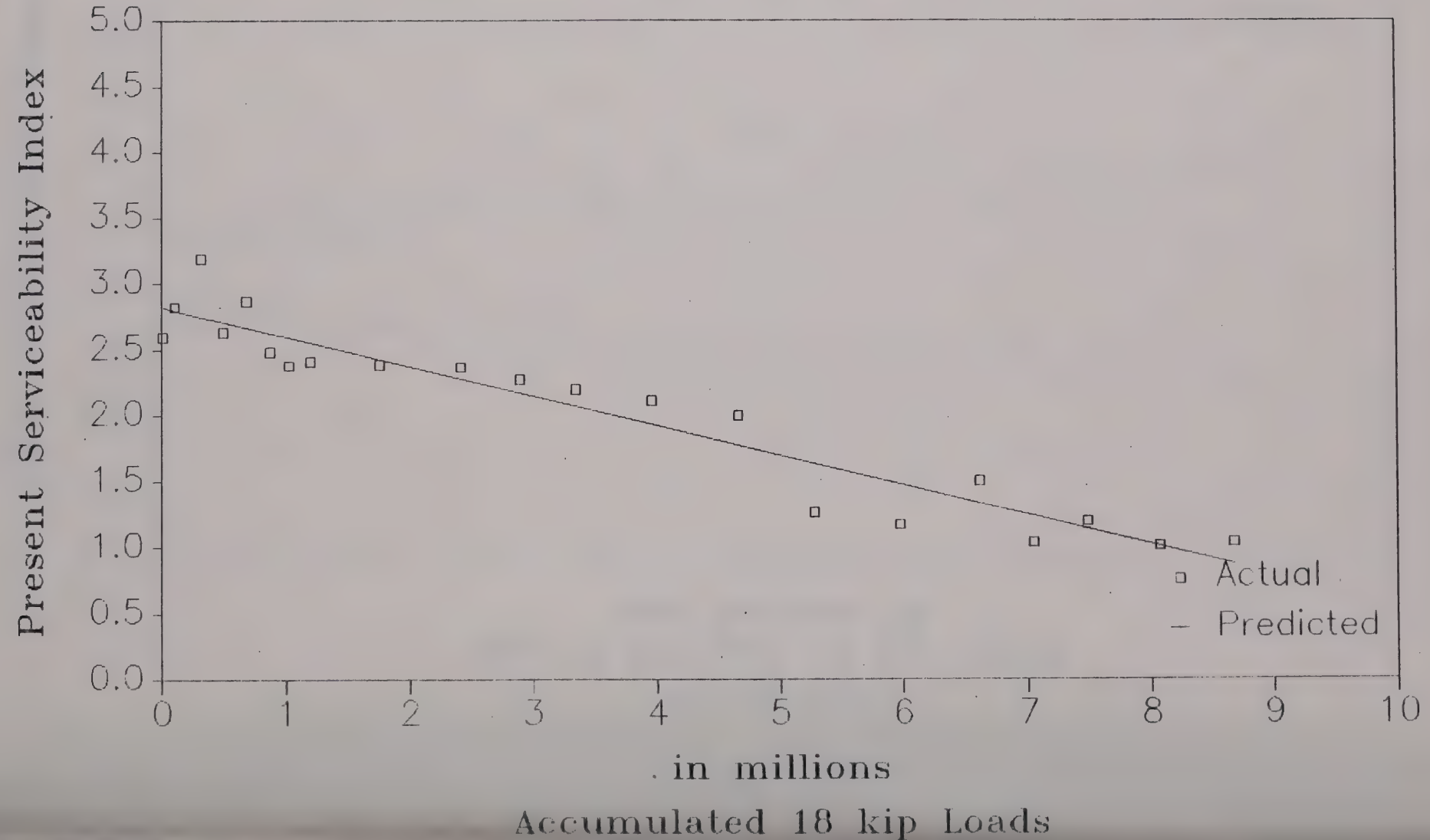

FIGURE D16
Plot of PSI and 18 kip Loads
Test Section 9W

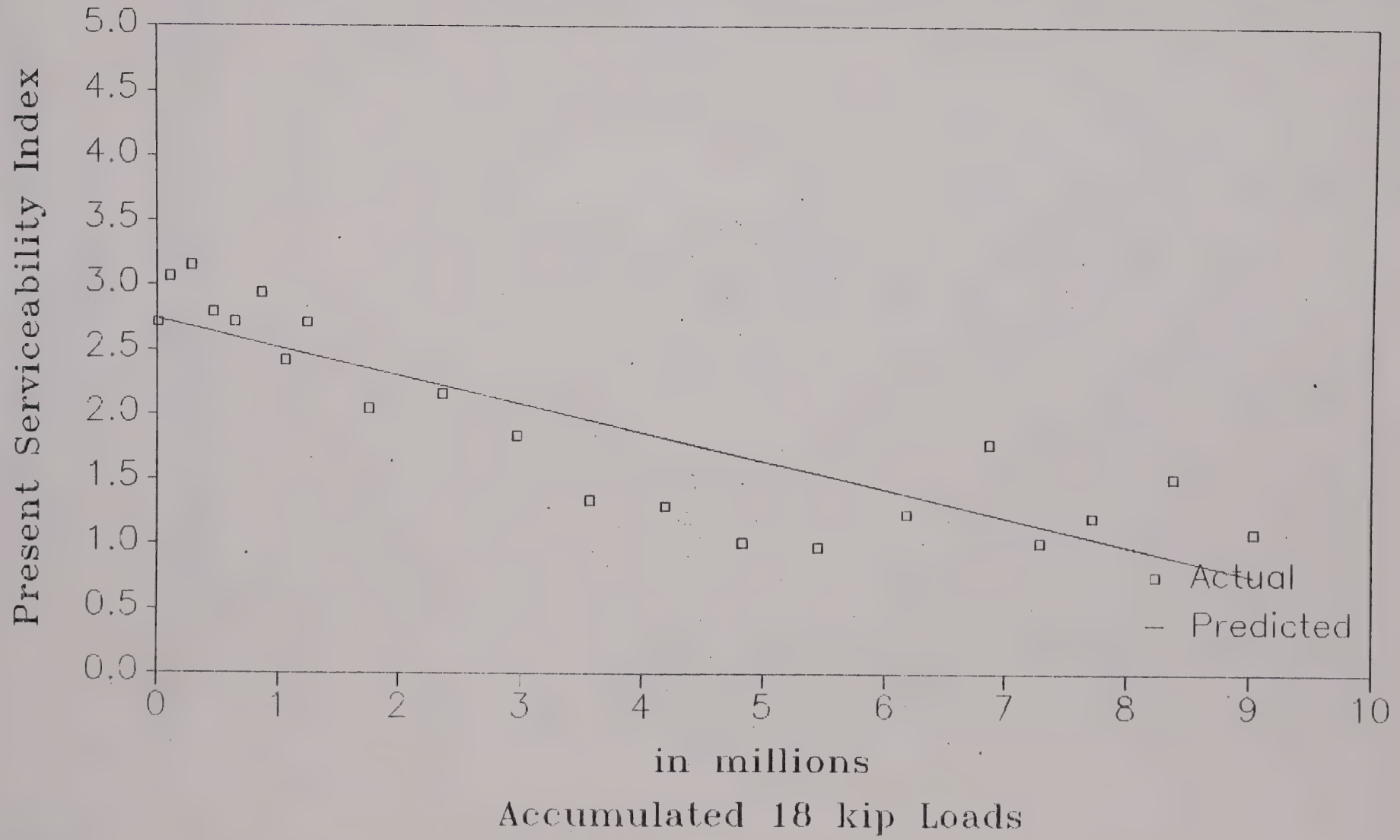

FIGURE E1
Deflection History
Test Section 1E

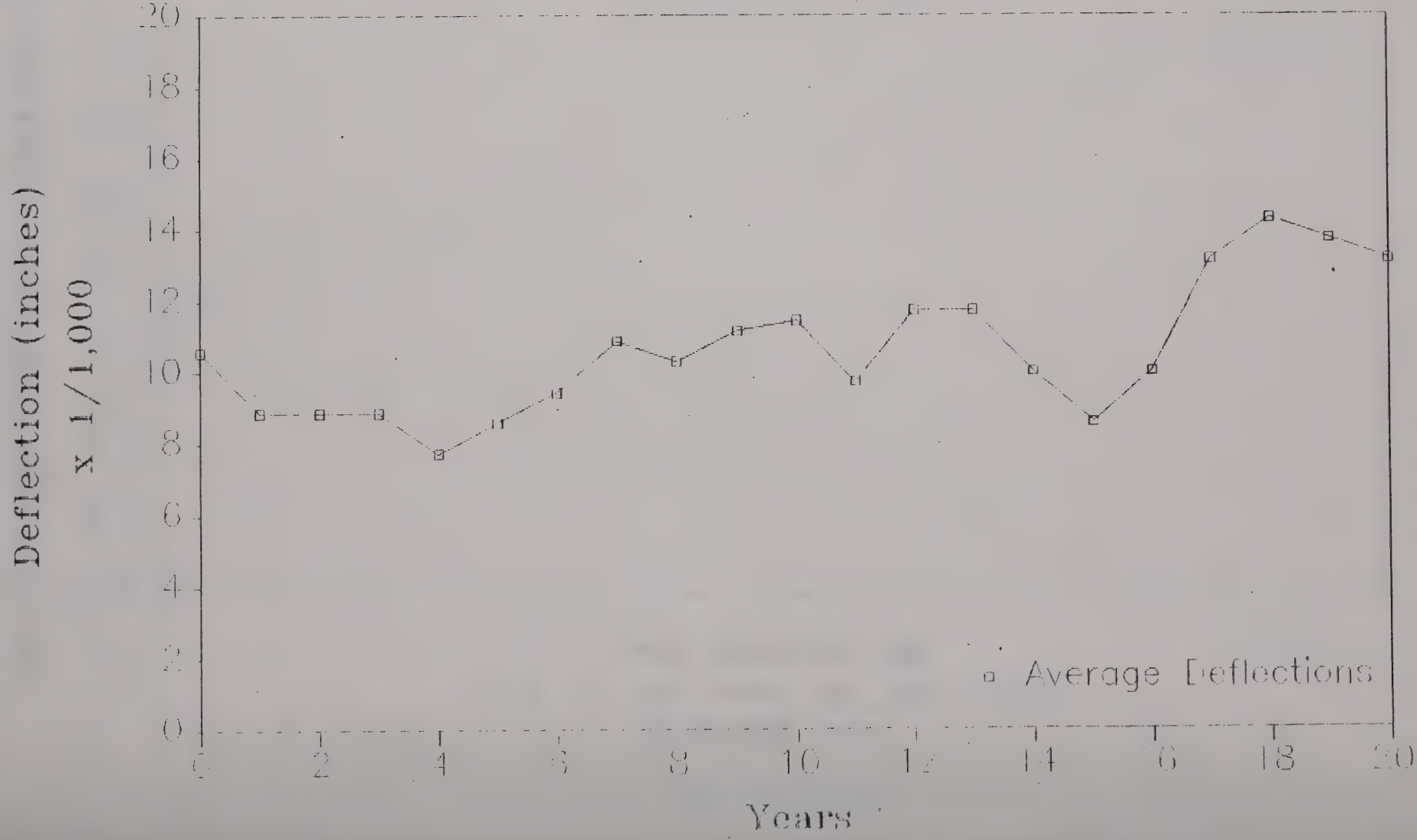

FIGURE E2
Deflection History
Test Section 1W

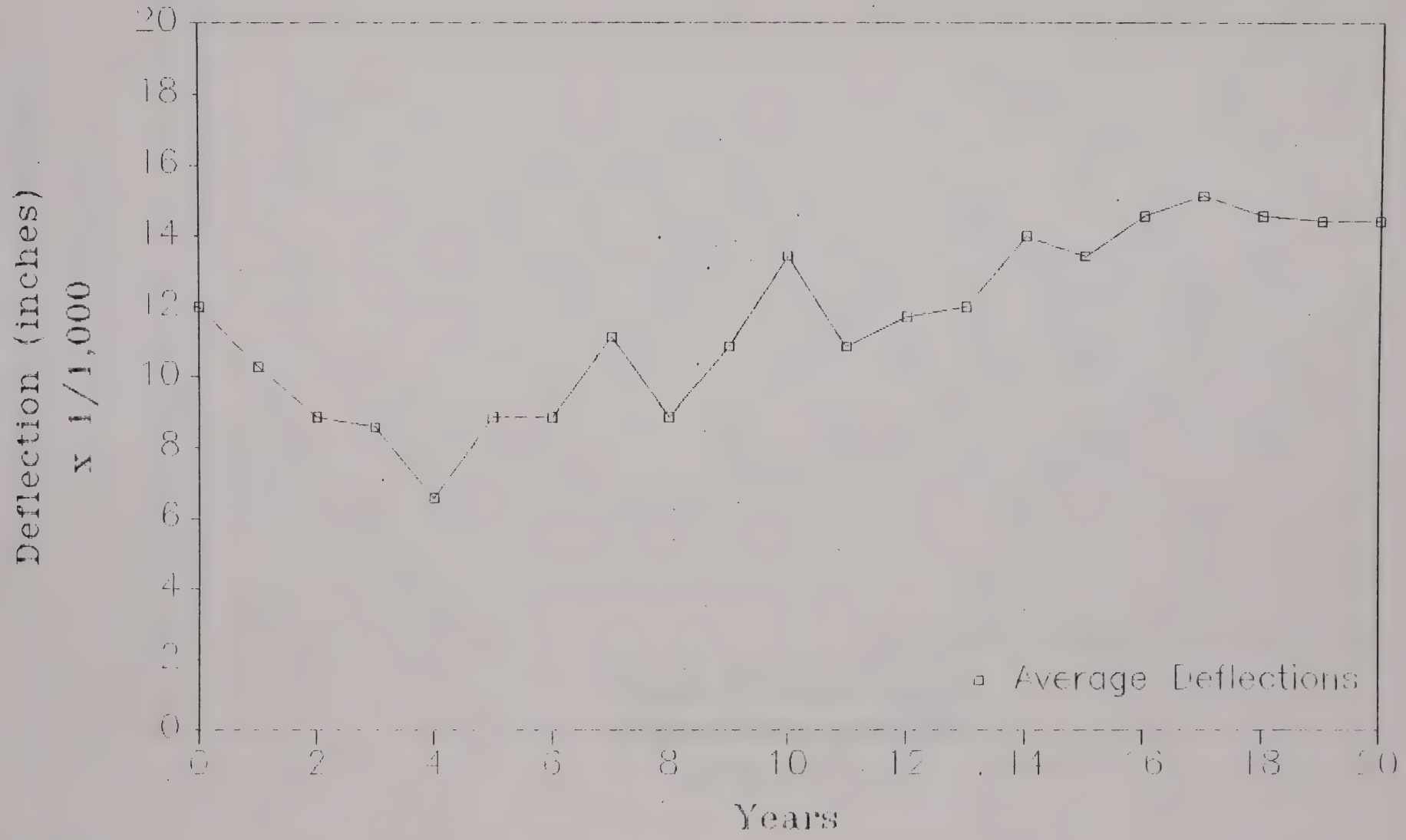

FIGURE E3
Deflection History
Test Section 2E

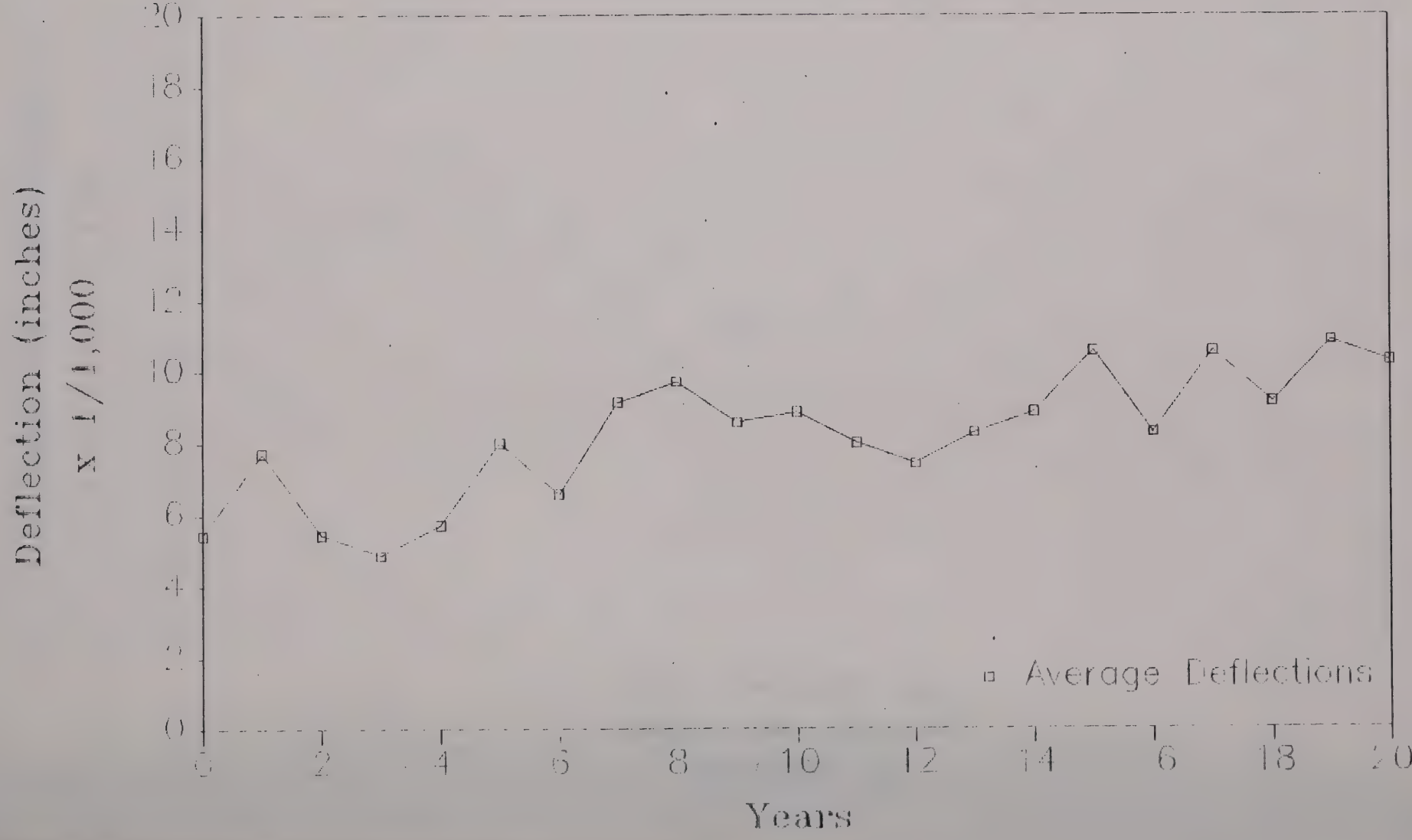

FIGURE E4
Deflection History
Test Section 2W

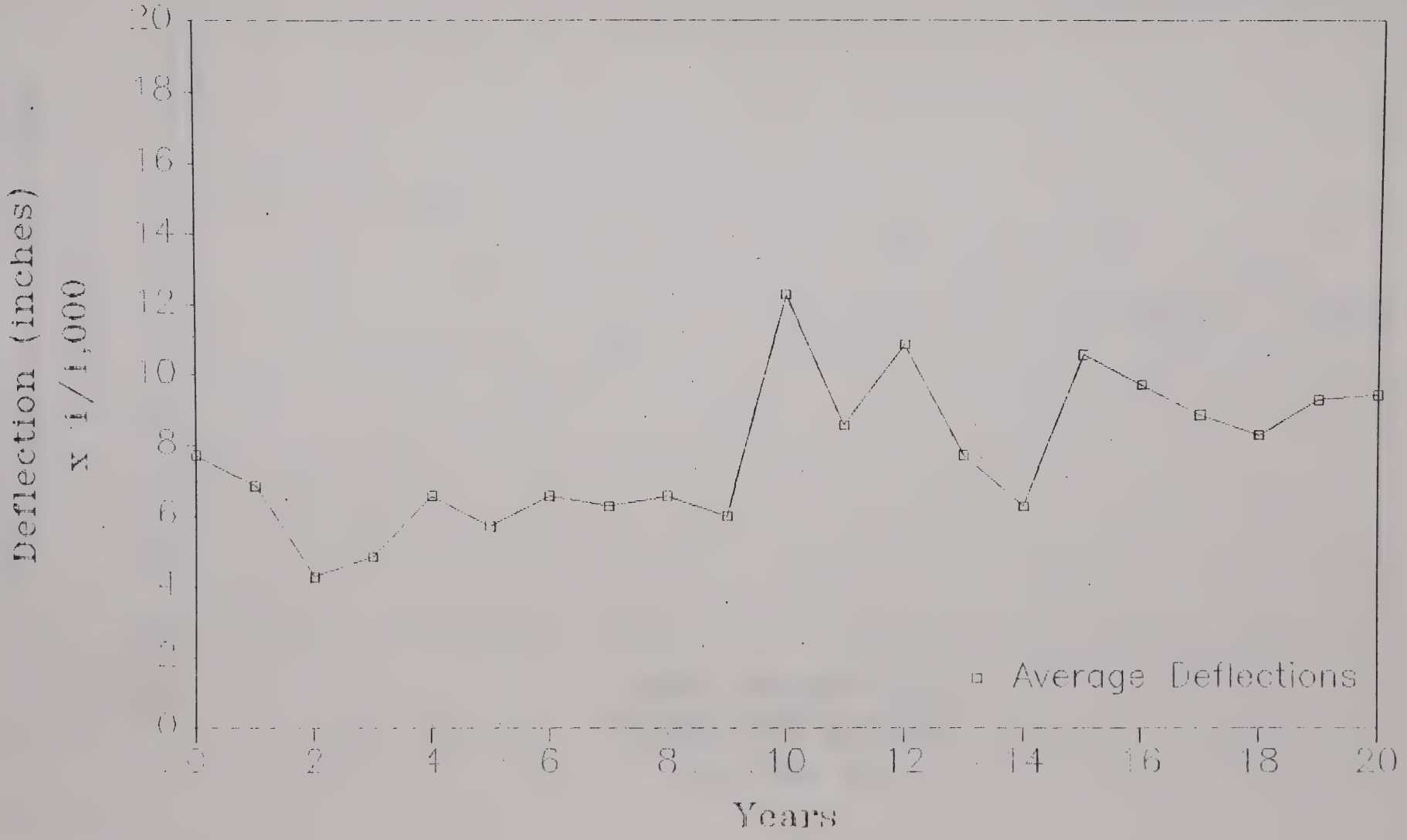

FIGURE E5
Deflection History
Test Section 3E

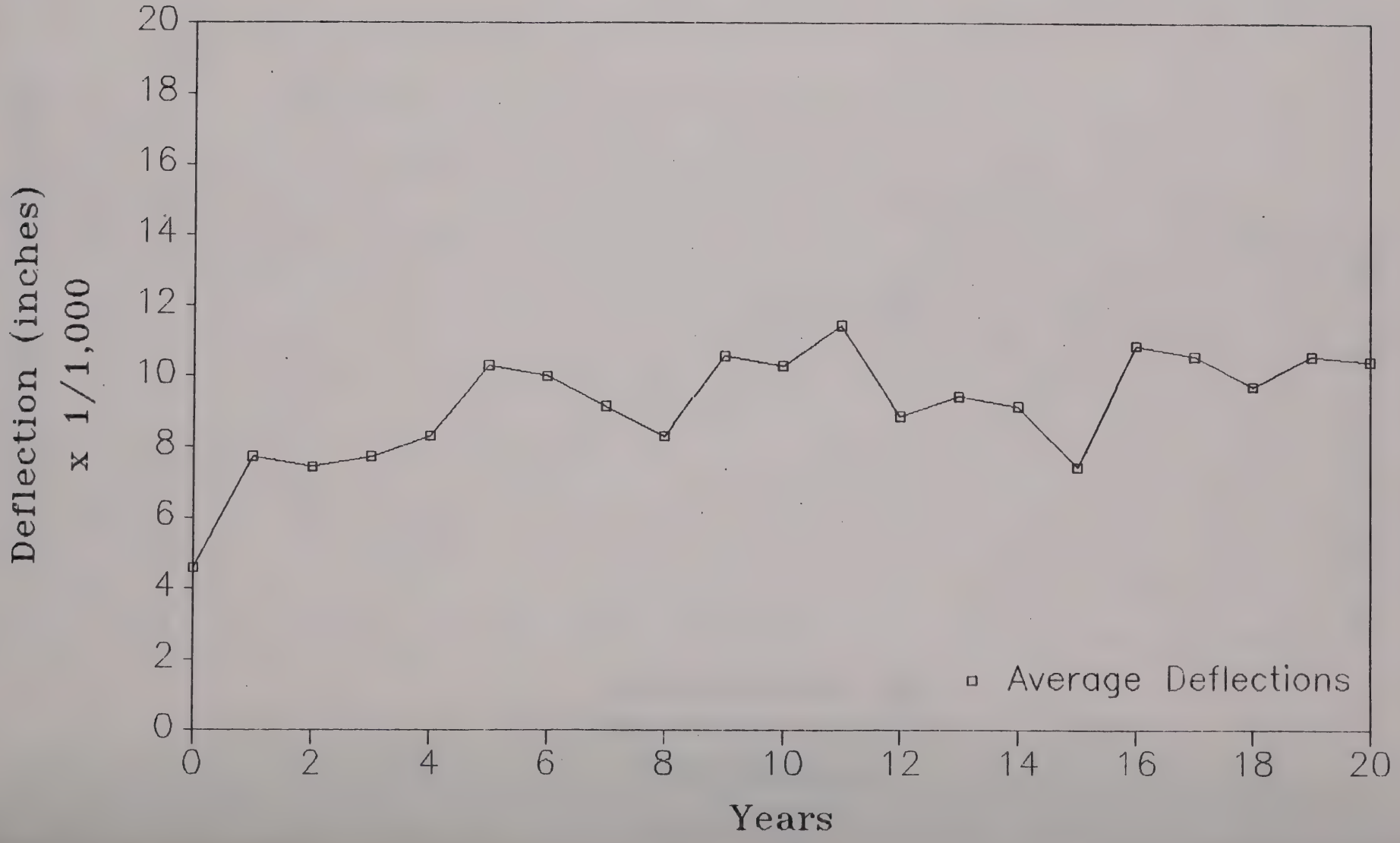

FIGURE E6
Deflection History
Test Section 3W

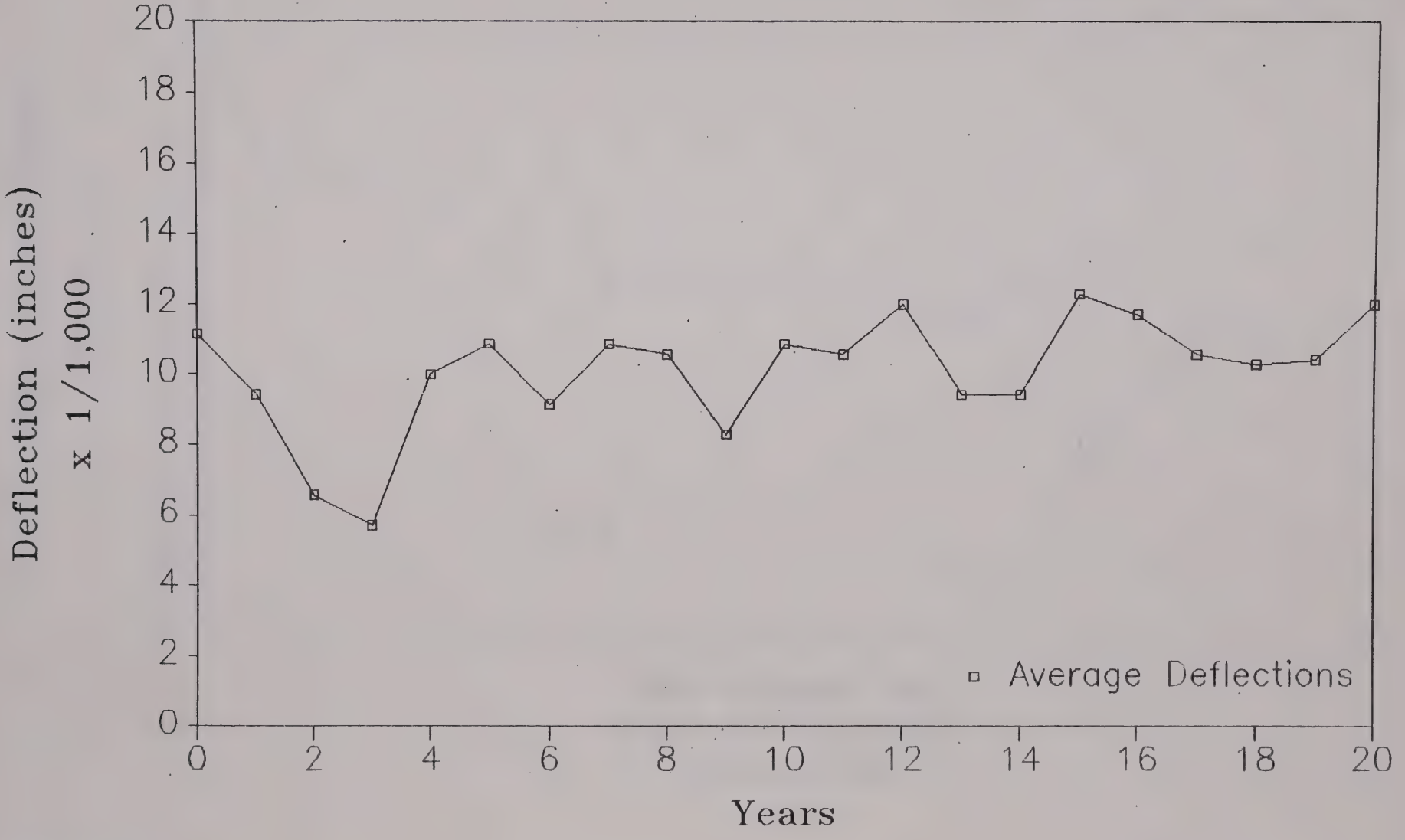

FIGURE E7
Deflection History
Test Section 4E

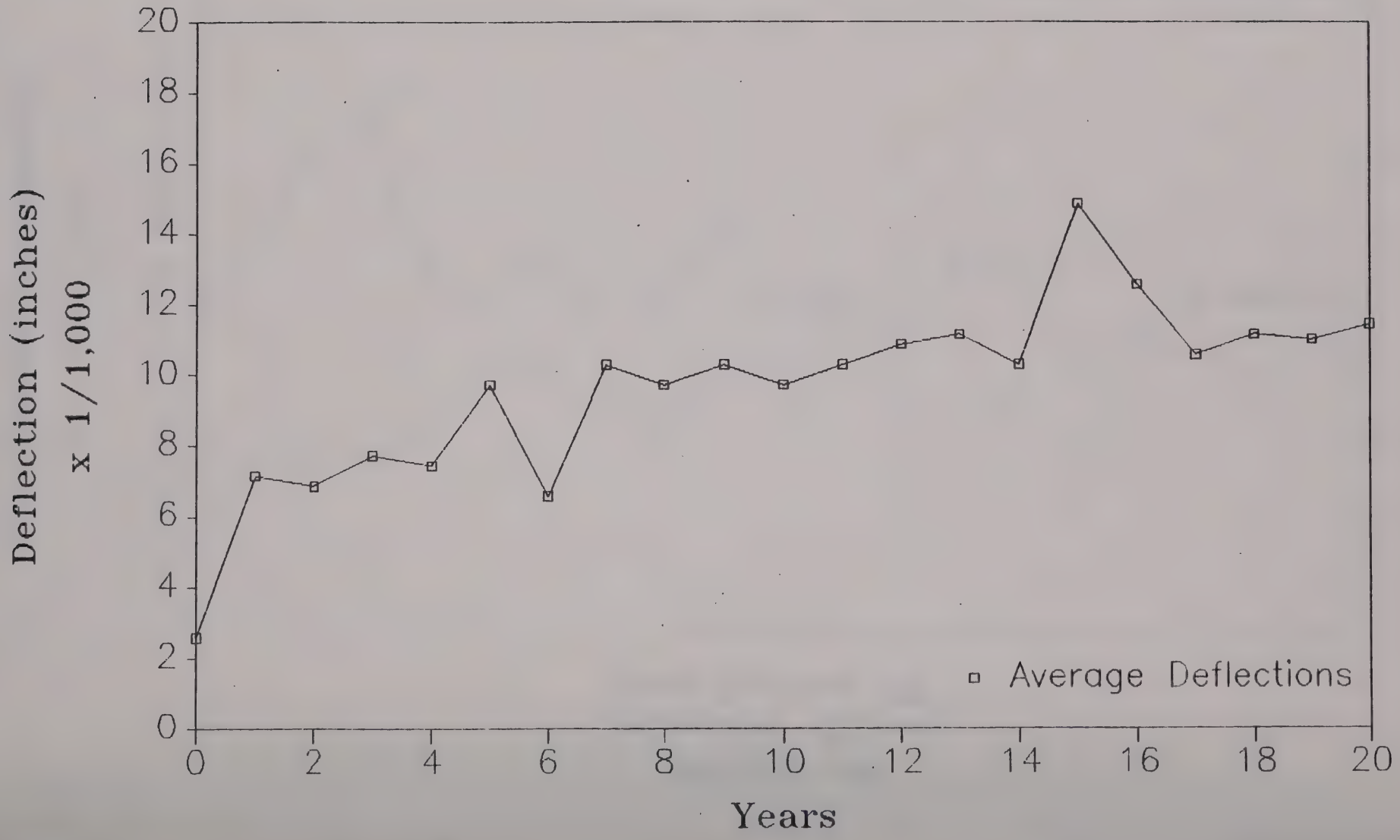

FIGURE E8
Deflection History
Test Section 4W

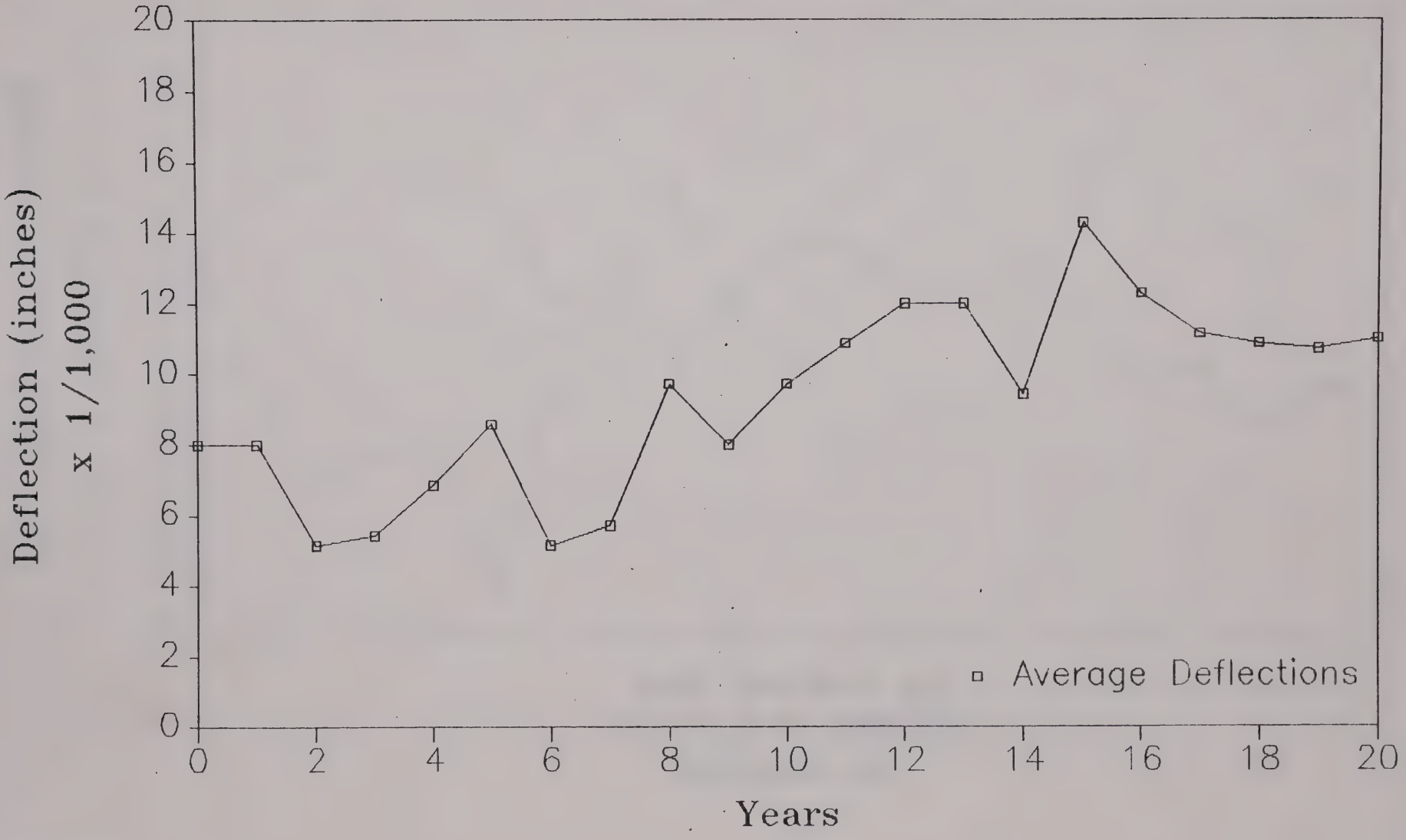

FIGURE E9
Deflection History
Test Section 5E

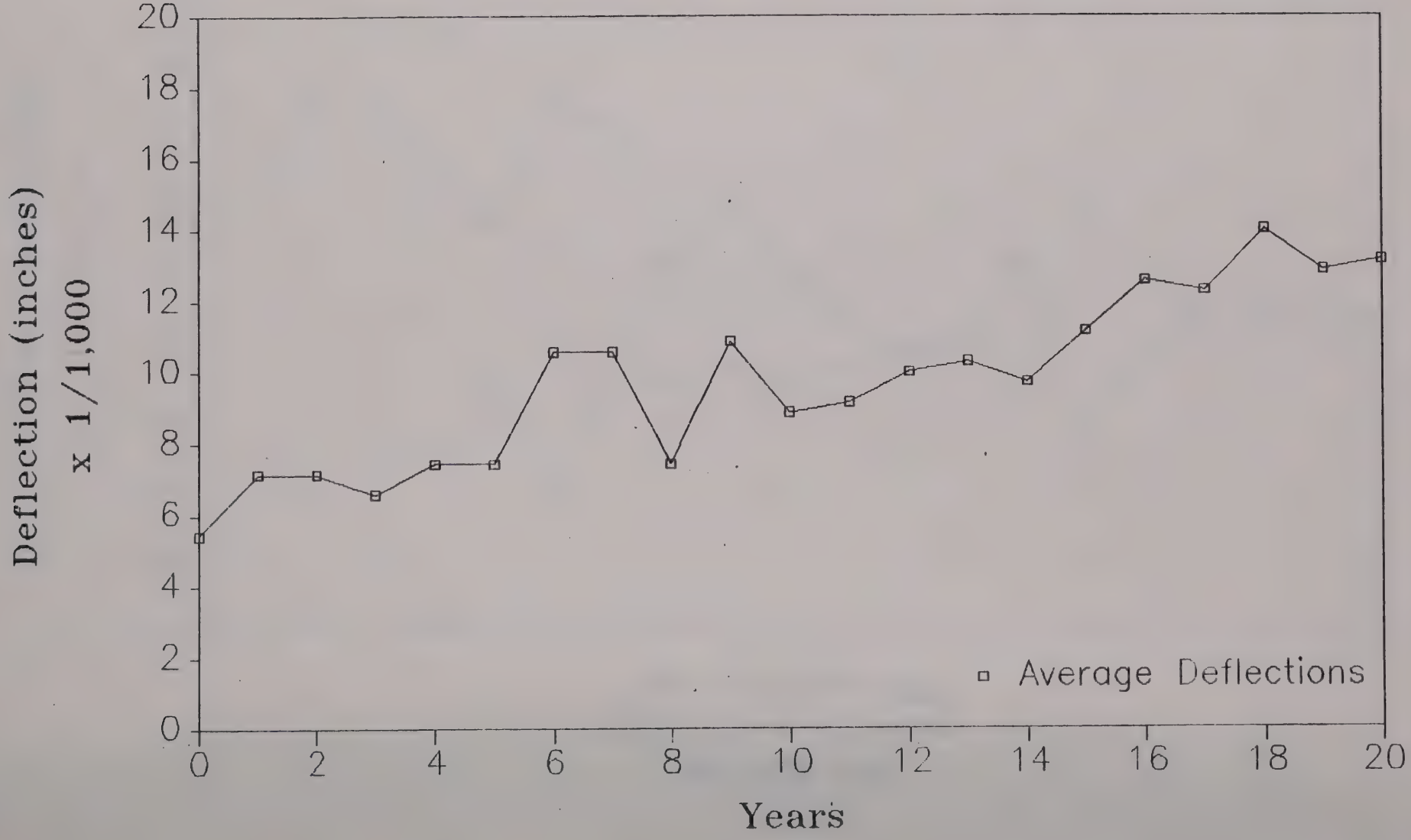

FIGURE E10
Deflection History
Test Section 5W

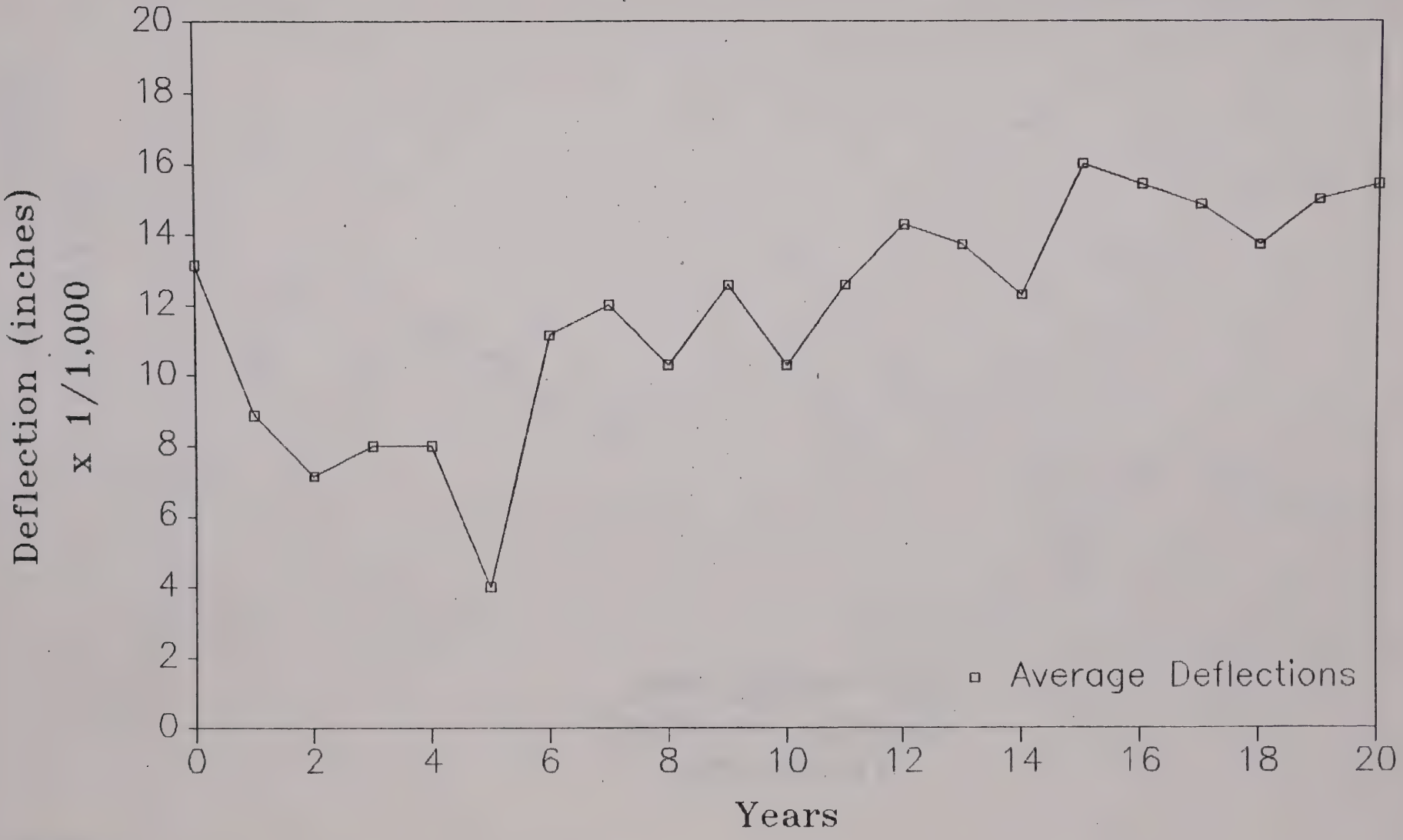

FIGURE E11
Deflection History
Test Section 6E

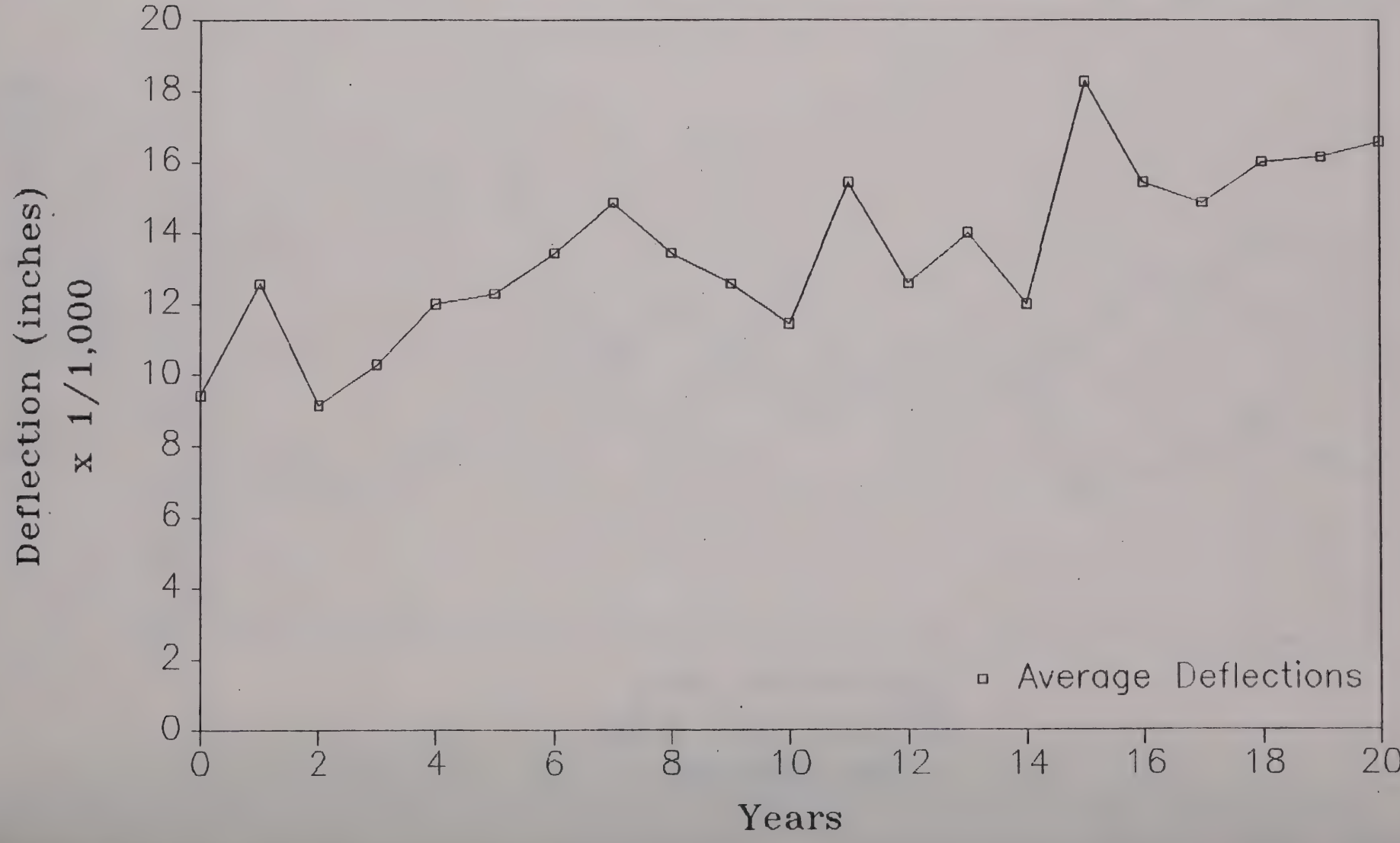

FIGURE E12
Deflection History
Test Section 6W

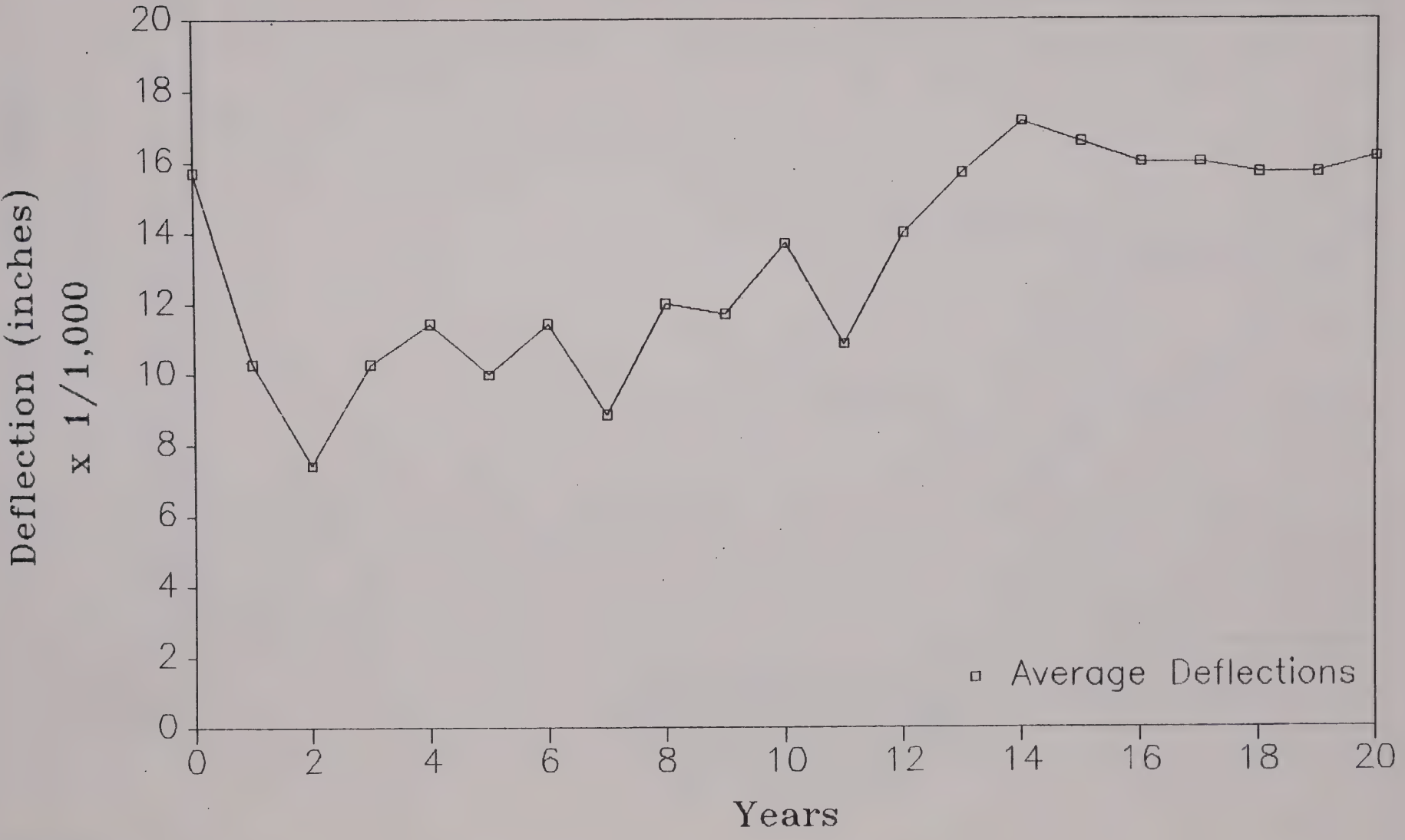

FIGURE E13
Deflection History
Test Section 7E

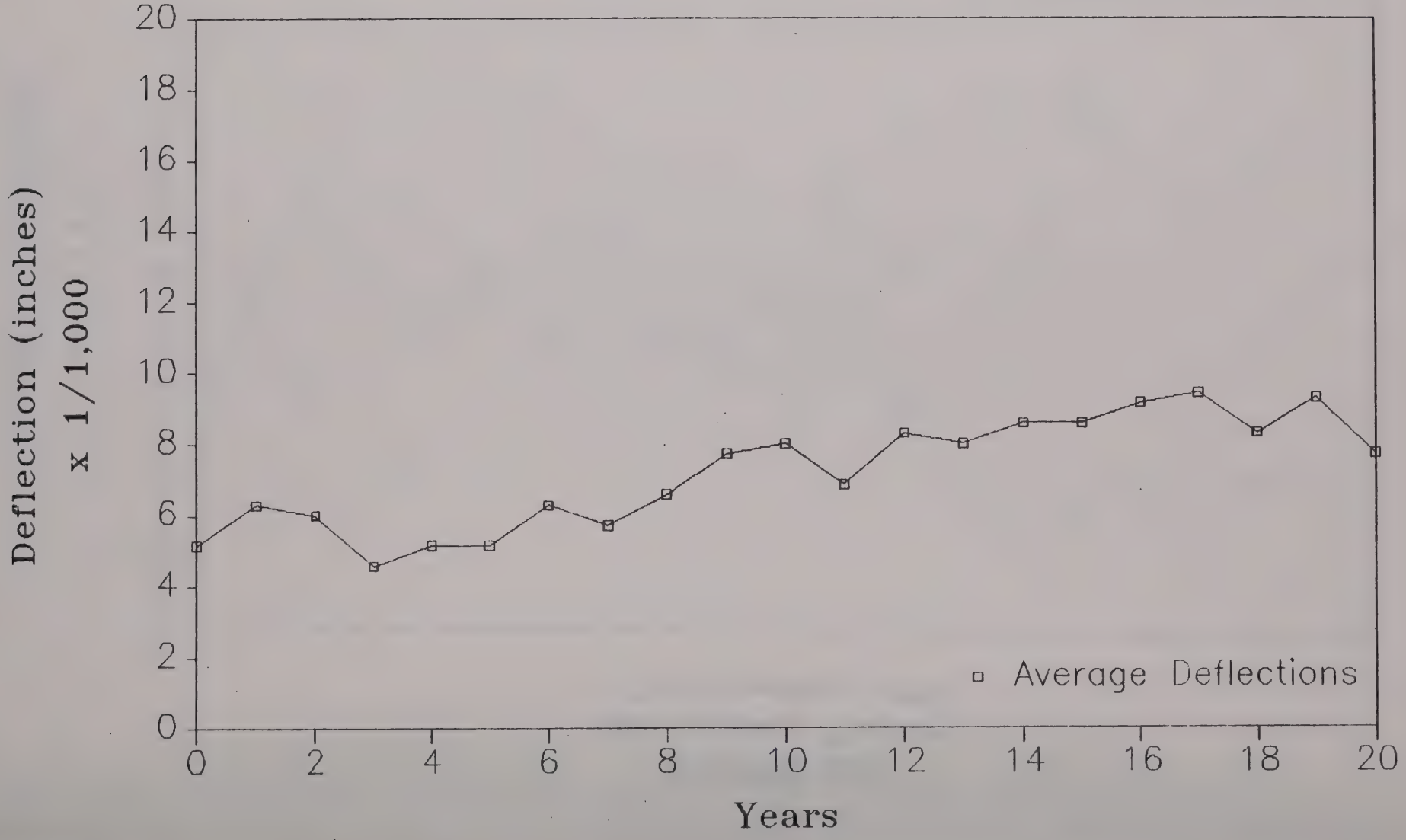

FIGURE E14
Deflection History
Test Section 7W

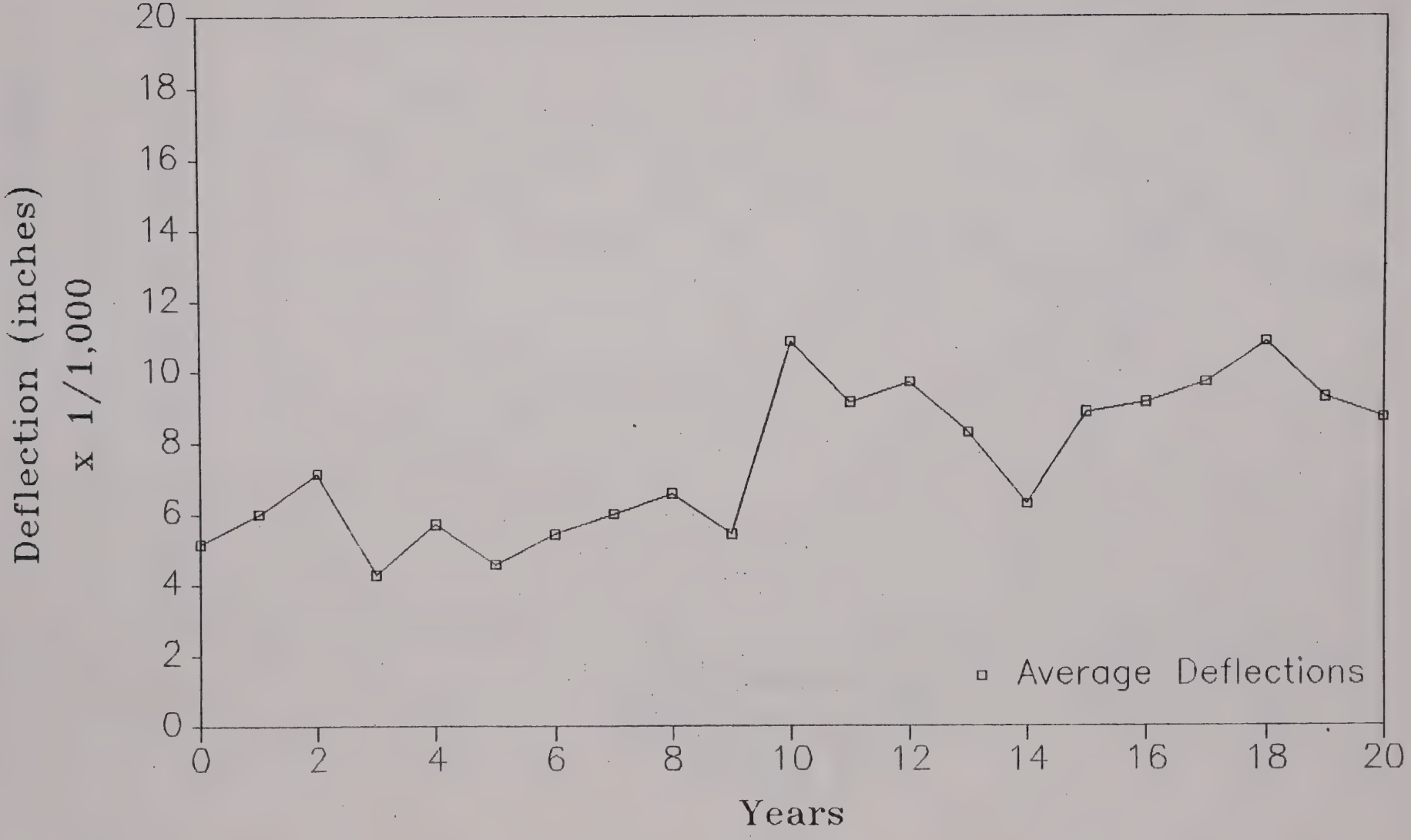

FIGURE E15
Deflection History
Test Section 8E

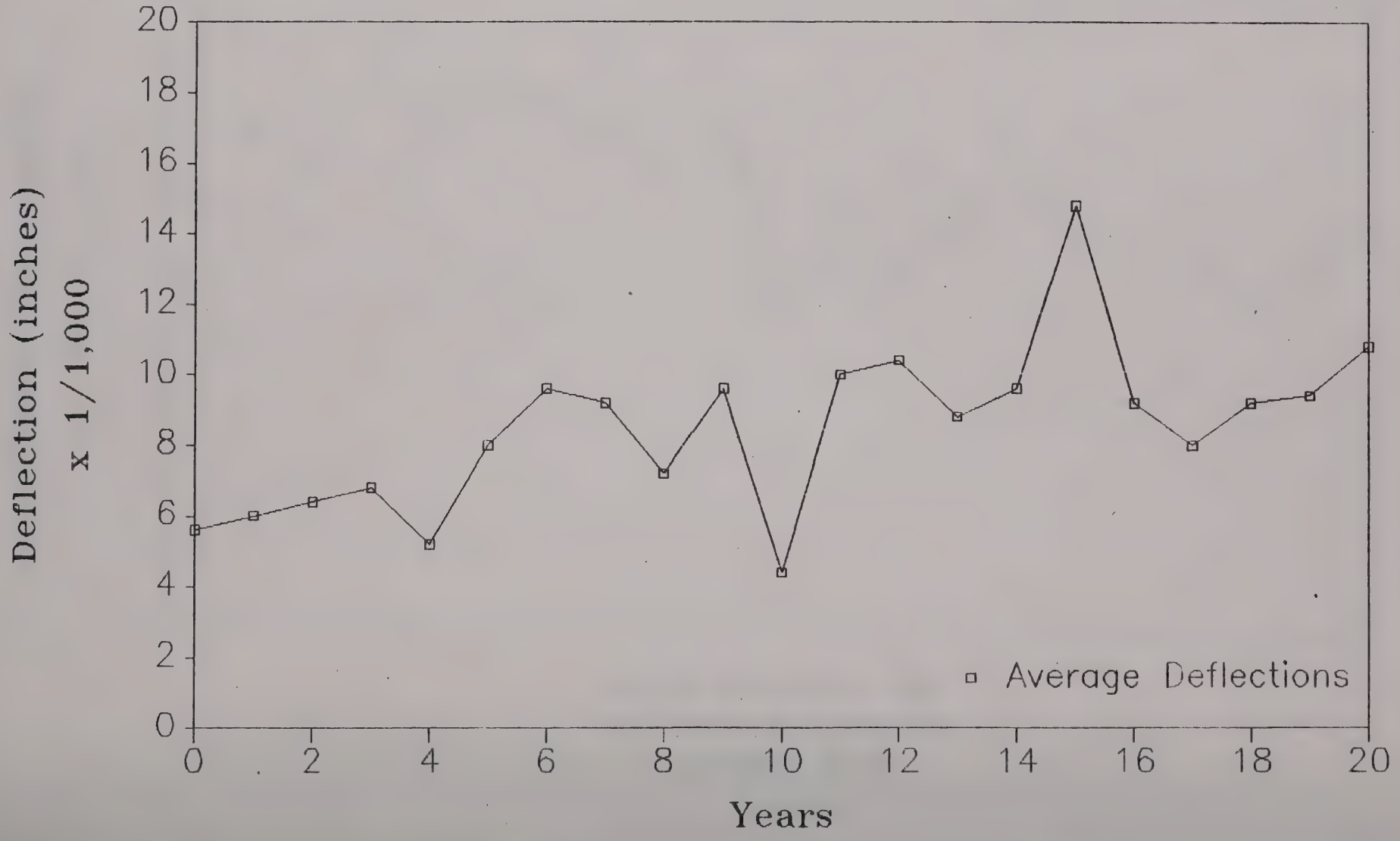

FIGURE E16
Deflection History
Test Section 9W

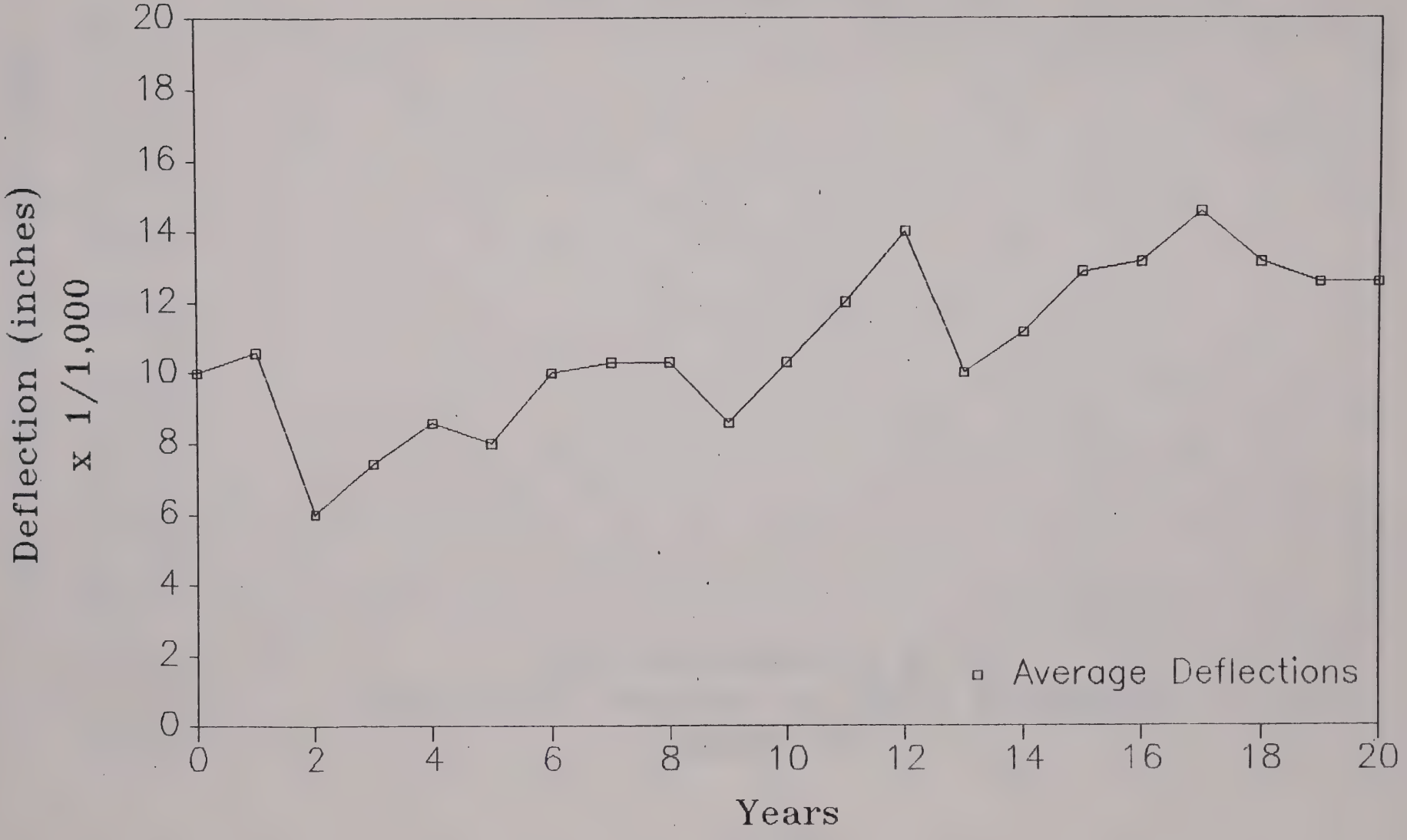

FIGURE F1
Regression Analysis of VESYS Prediction
Test Sections 1E & 1W

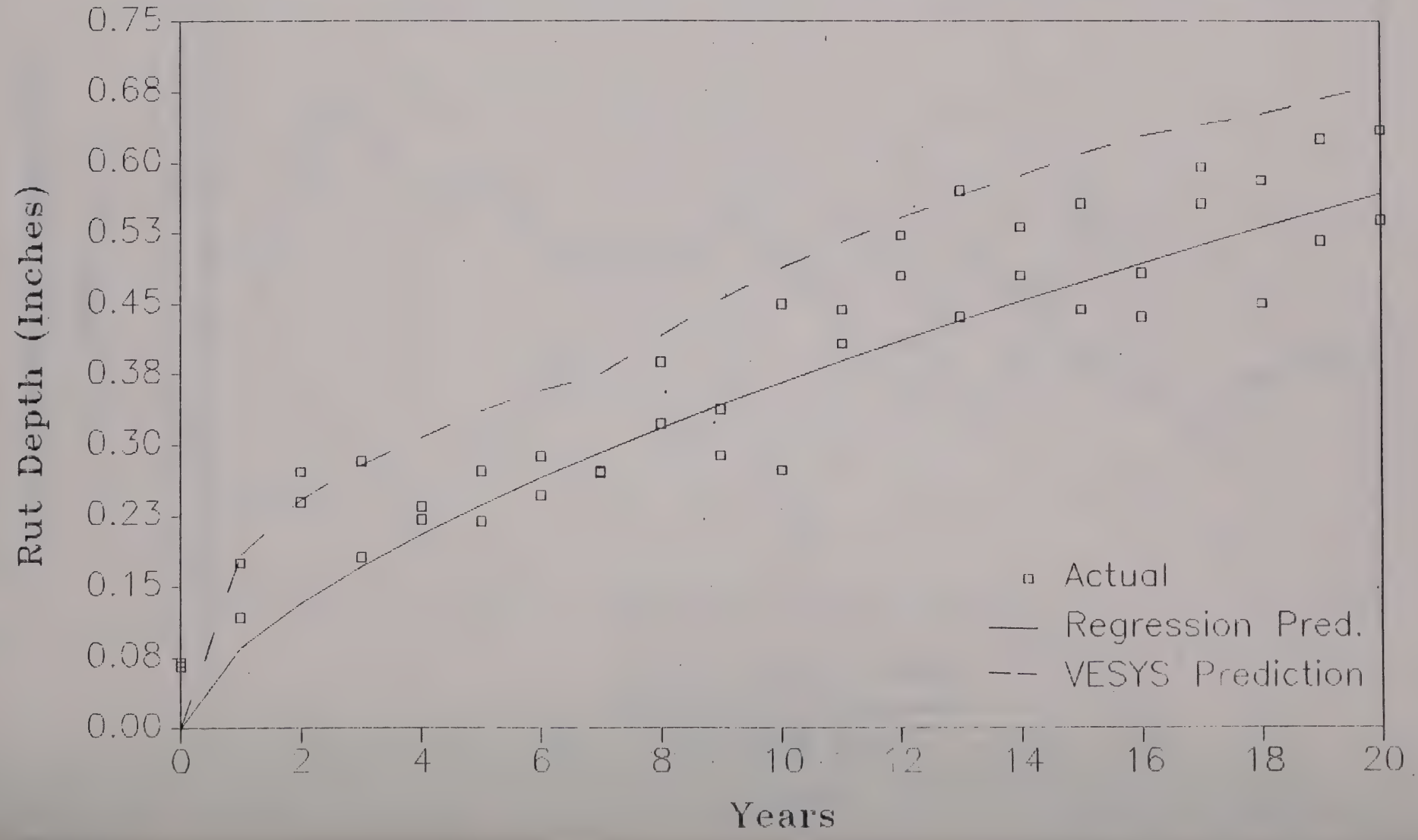

FIGURE F2
Regression Analysis of VESYS Prediction
Test Sections 2W & 2E

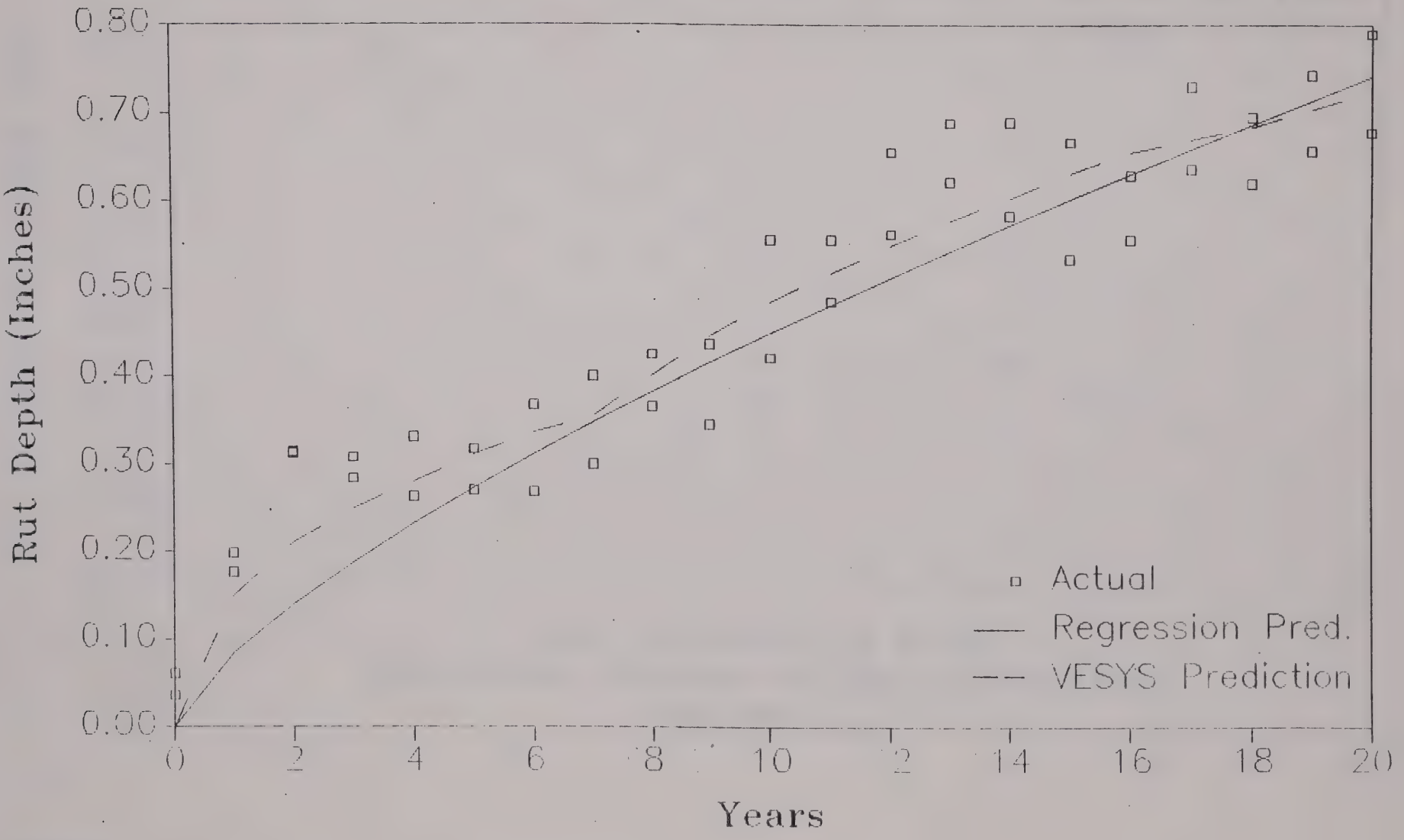

FIGURE F3
Regression Analysis of VESYS Prediction
Test Sections 3W & 3E

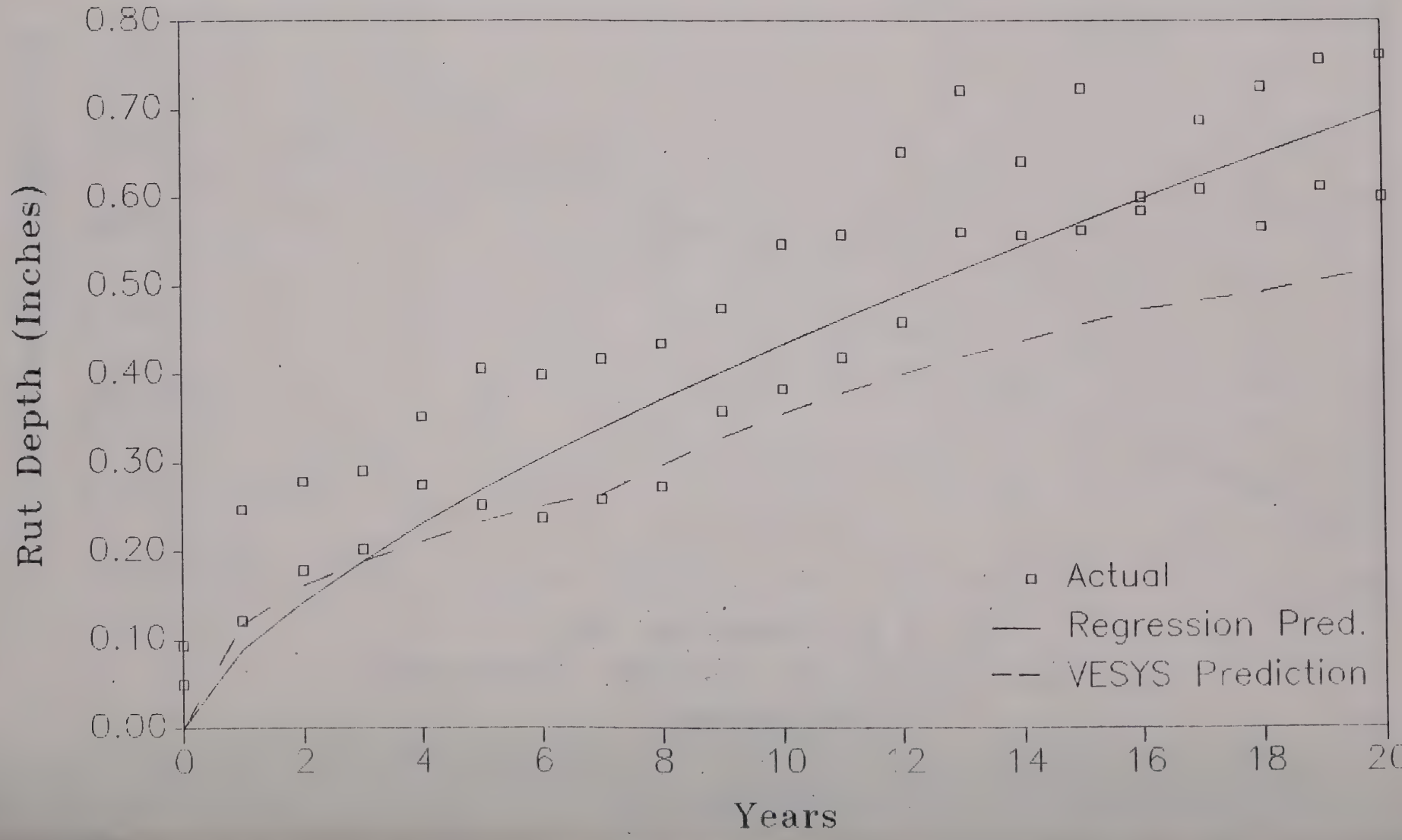

FIGURE F4
Regression Analysis of VESYS Prediction
Test Sections 4W & 4E

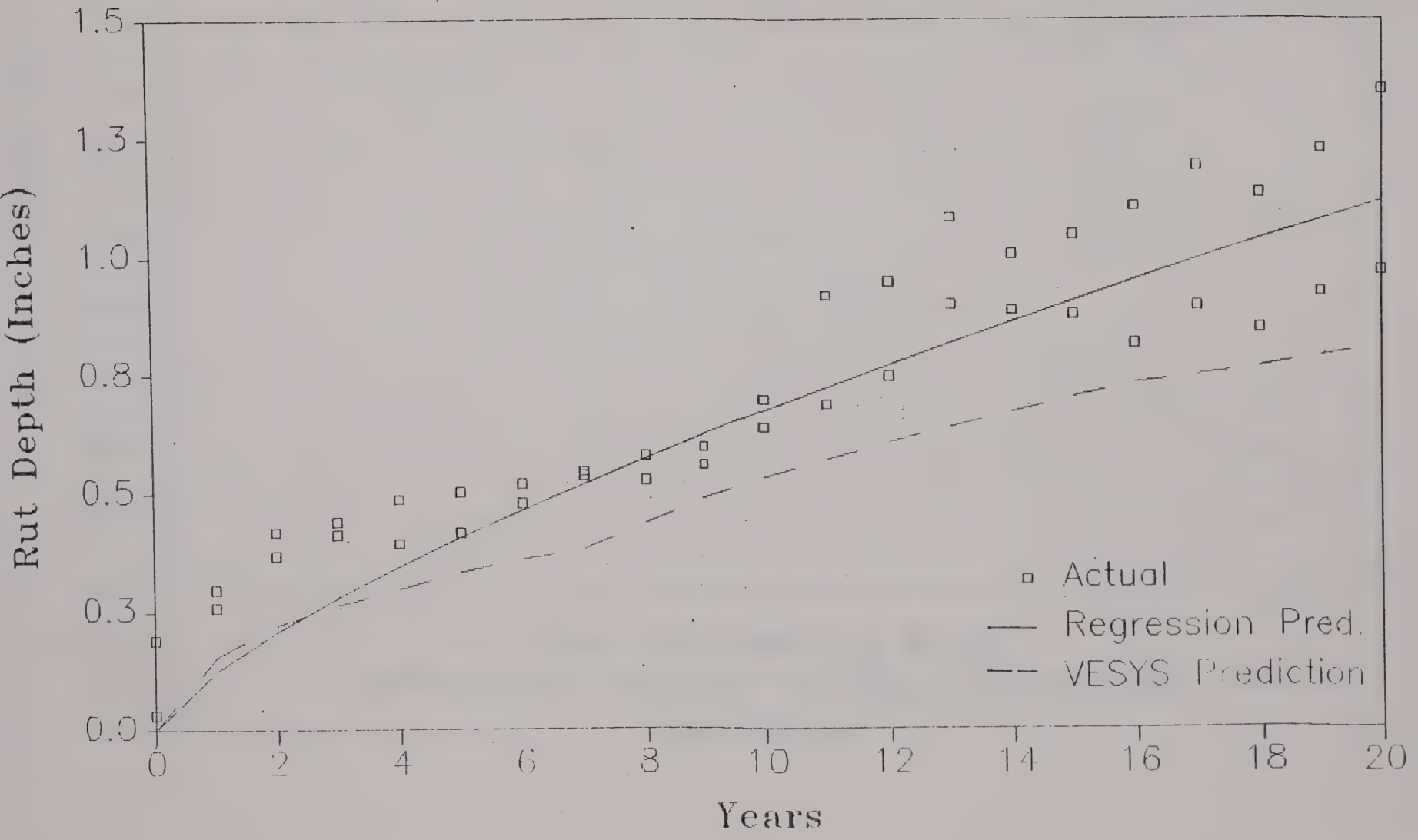

FIGURE F5
Regression Analysis of VESYS Prediction
Test Sections 5W & 5E

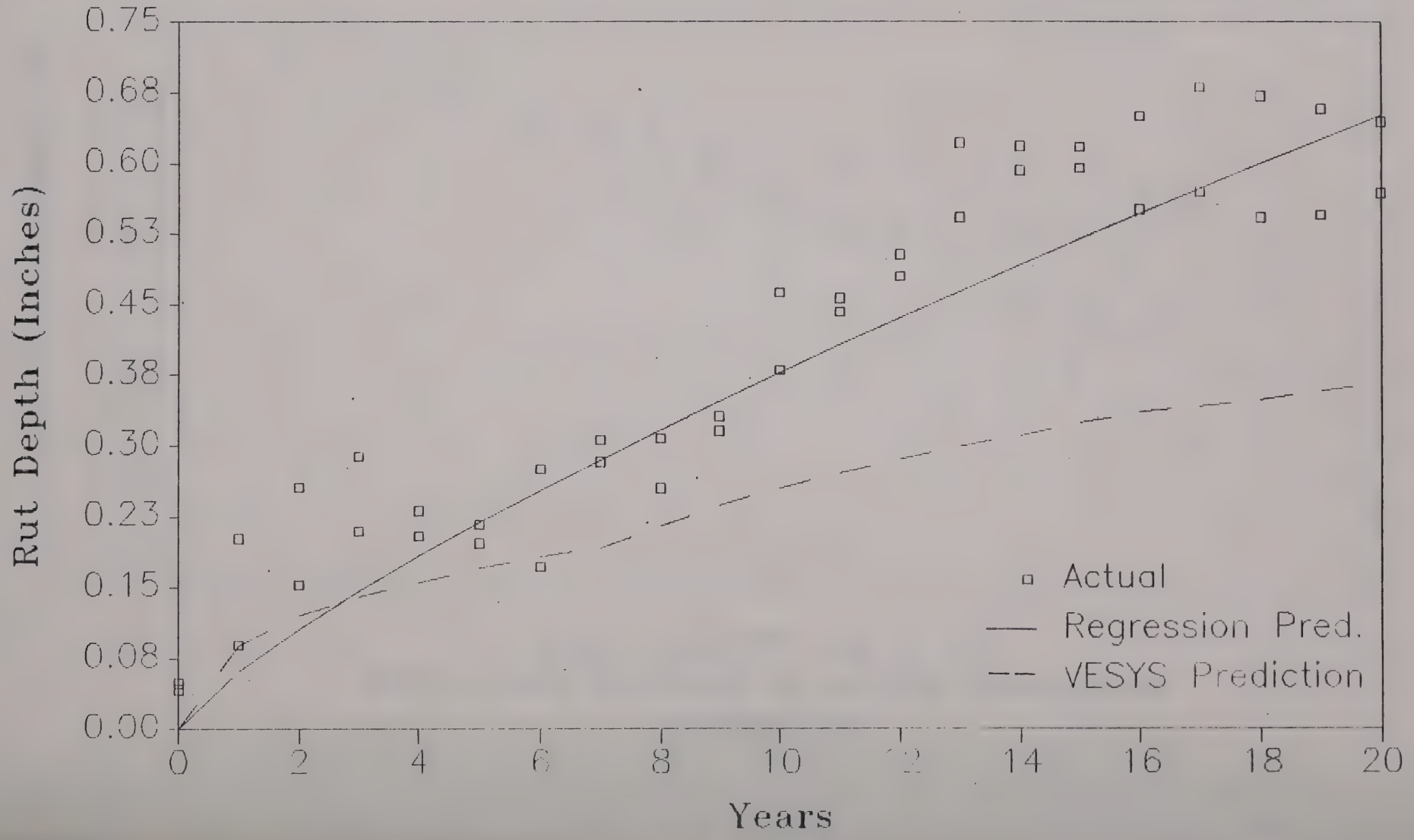

FIGURE F6
Regression Analysis of VESYS Prediction
Test Sections 6W & 6E

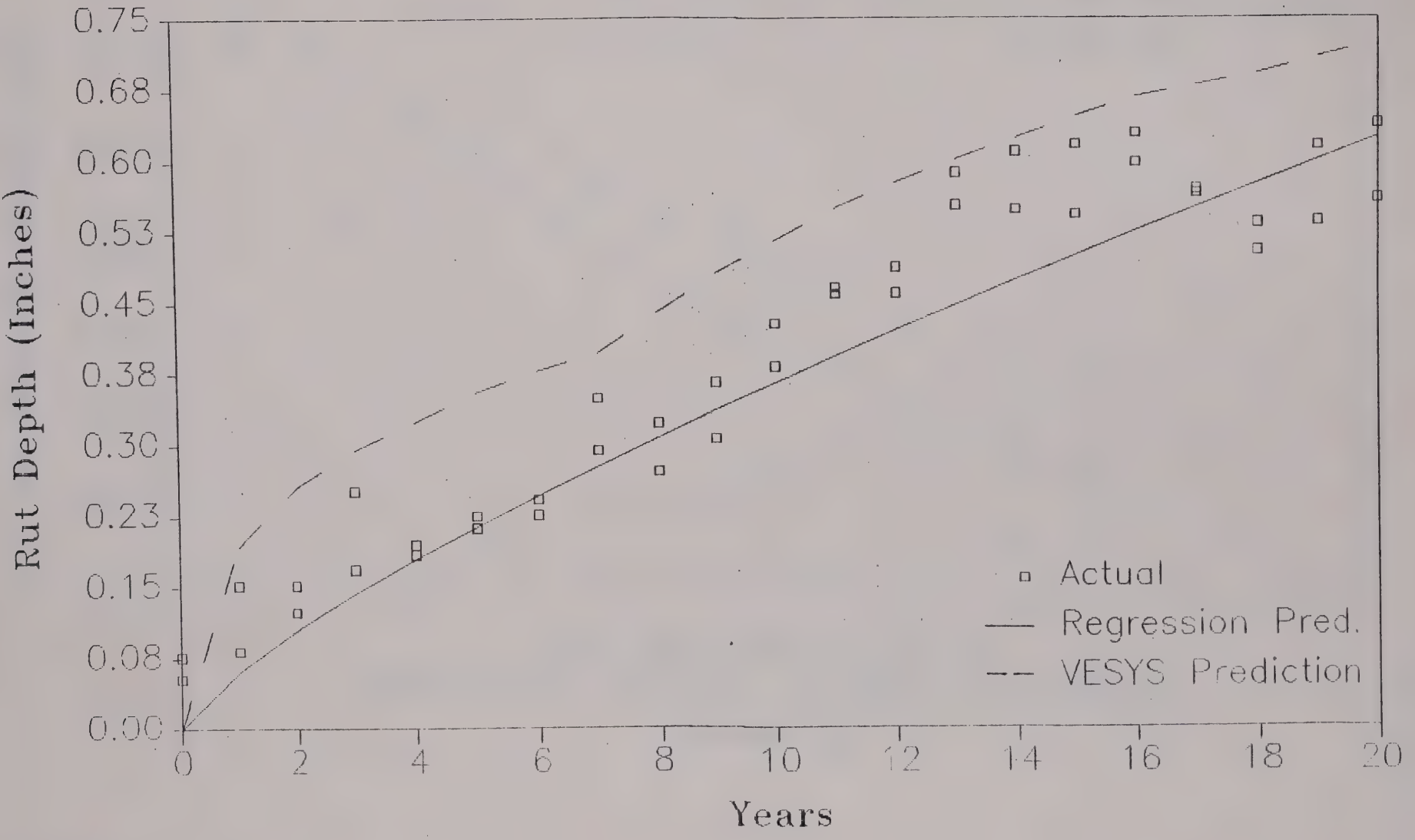

FIGURE F7
Regression Analysis of VESYS Prediction
Test Sections 7W & 7E

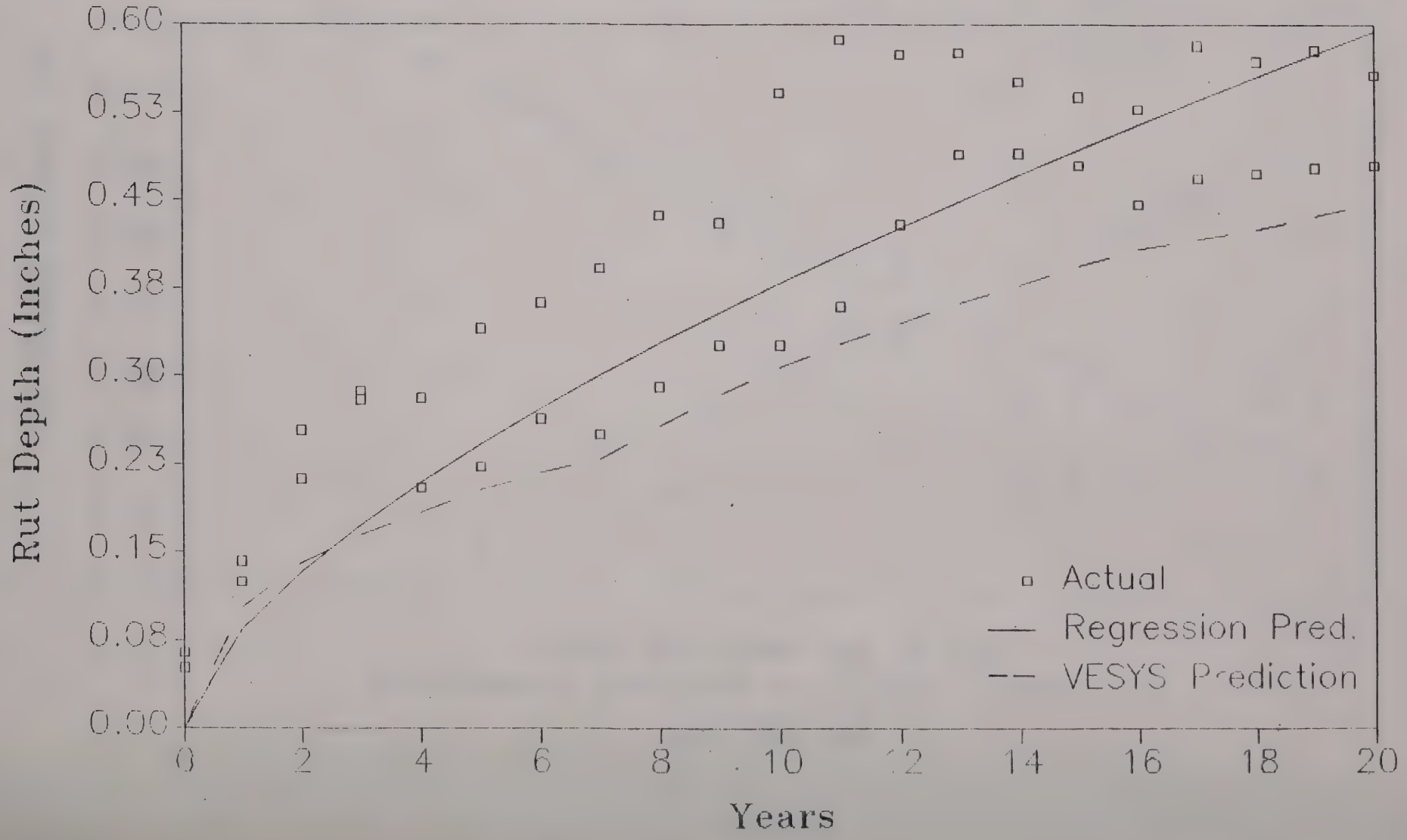

FIGURE F8
Regression Analysis of VESYS Prediction
Test Section 8E

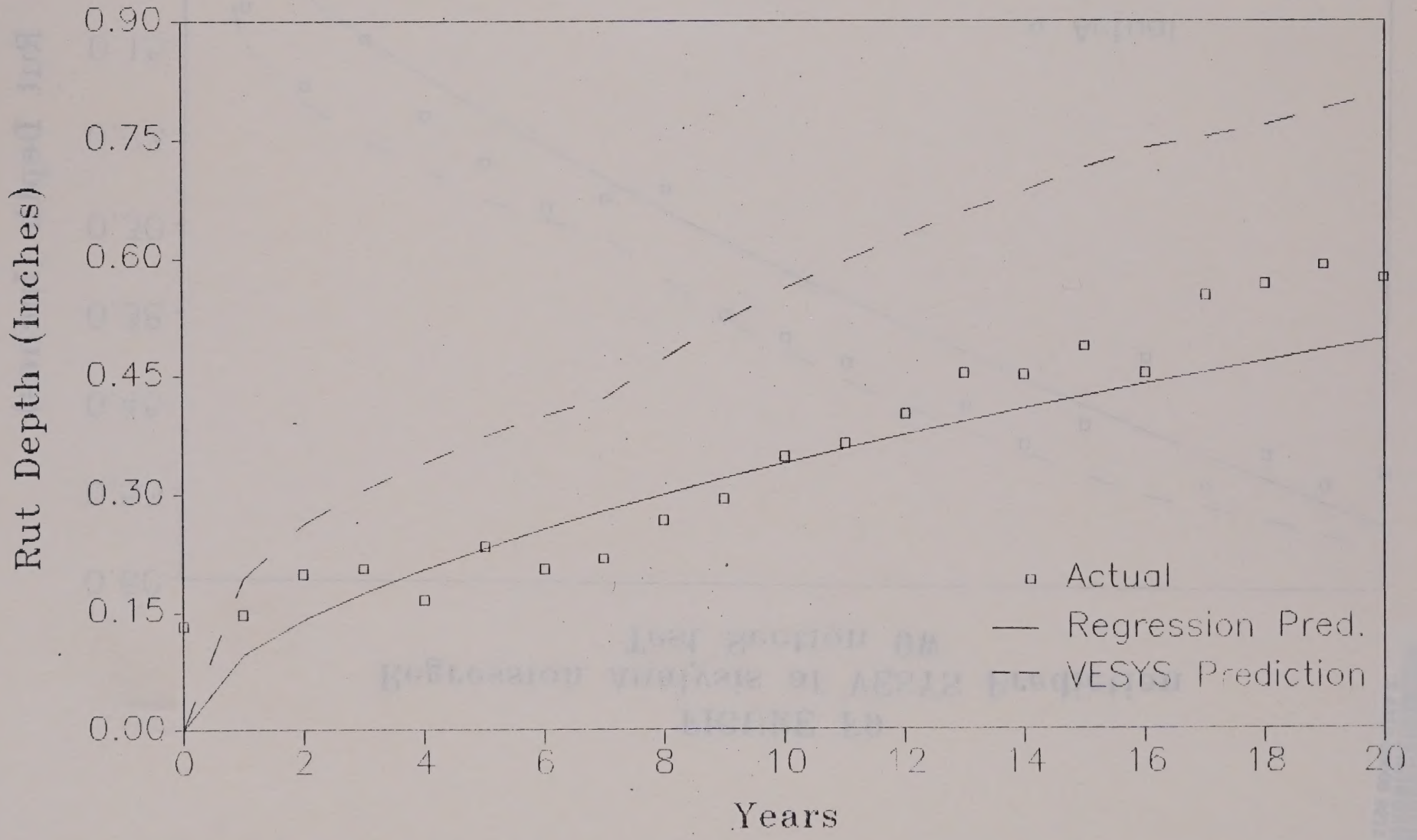

FIGURE F9
Regression Analysis of VESYS Prediction
Test Section 9W

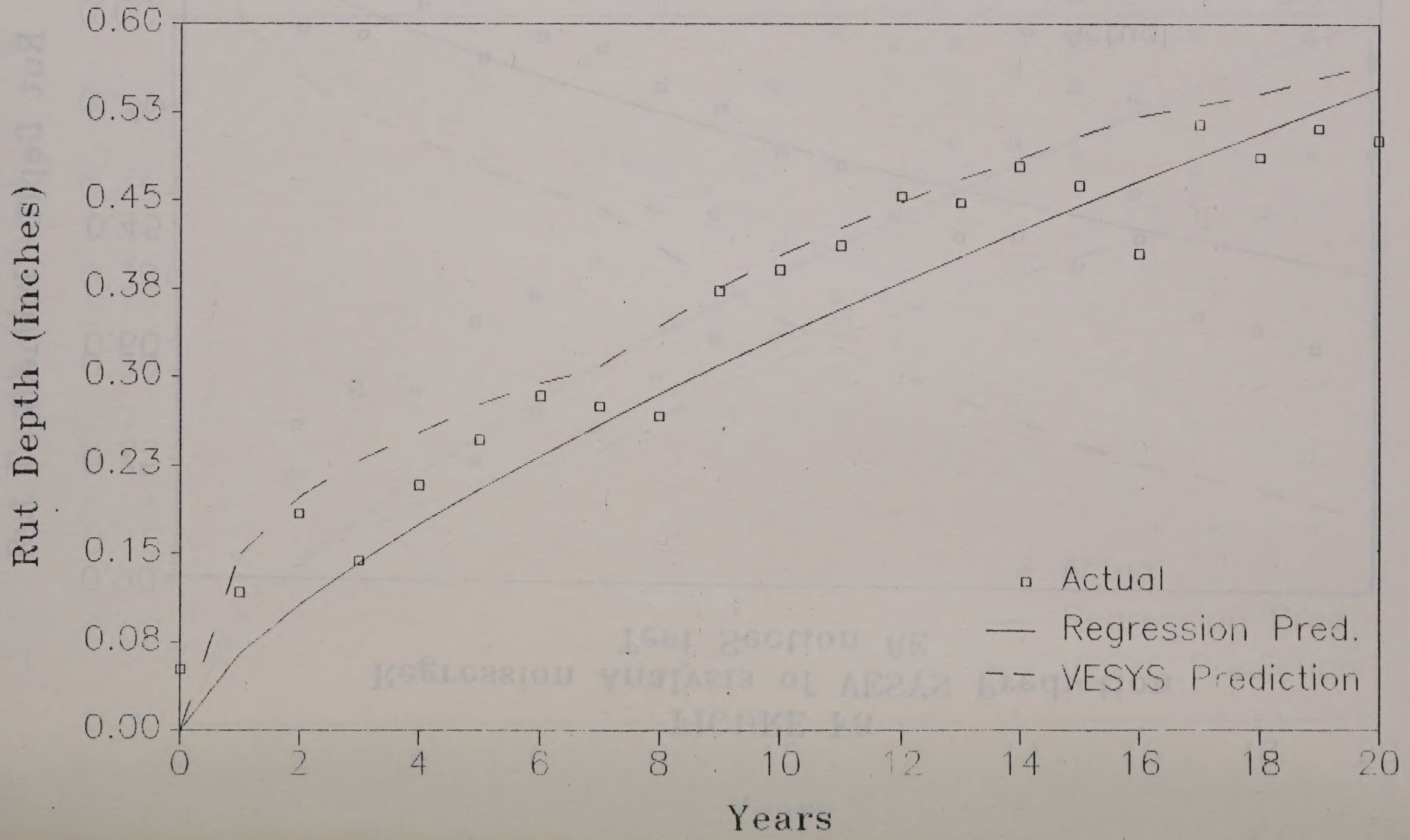

NJDOT RESEARCH LIBRARY
3 4310 00009 9211